

In vivo assessment of changes in bone due to osteoporosis and its possible treatments

Citation for published version (APA):

Brouwers, J. E. M. (2008). *In vivo assessment of changes in bone due to osteoporosis and its possible treatments*. [Phd Thesis 1 (Research TU/e / Graduation TU/e), Biomedical Engineering]. Technische Universiteit Eindhoven. <https://doi.org/10.6100/IR638685>

DOI:

[10.6100/IR638685](https://doi.org/10.6100/IR638685)

Document status and date:

Published: 01/01/2008

Document Version:

Publisher's PDF, also known as Version of Record (includes final page, issue and volume numbers)

Please check the document version of this publication:

- A submitted manuscript is the version of the article upon submission and before peer-review. There can be important differences between the submitted version and the official published version of record. People interested in the research are advised to contact the author for the final version of the publication, or visit the DOI to the publisher's website.
- The final author version and the galley proof are versions of the publication after peer review.
- The final published version features the final layout of the paper including the volume, issue and page numbers.

[Link to publication](#)

General rights

Copyright and moral rights for the publications made accessible in the public portal are retained by the authors and/or other copyright owners and it is a condition of accessing publications that users recognise and abide by the legal requirements associated with these rights.

- Users may download and print one copy of any publication from the public portal for the purpose of private study or research.
- You may not further distribute the material or use it for any profit-making activity or commercial gain
- You may freely distribute the URL identifying the publication in the public portal.

If the publication is distributed under the terms of Article 25fa of the Dutch Copyright Act, indicated by the "Taverne" license above, please follow below link for the End User Agreement:

www.tue.nl/taverne

Take down policy

If you believe that this document breaches copyright please contact us at:

openaccess@tue.nl

providing details and we will investigate your claim.

***In vivo* assessment of changes in bone due to osteoporosis and its possible treatments**

A catalogue record is available from the Eindhoven University of Technology Library

ISBN 978-90-386-1447-2

Copyright ©2008 by J.E.M. Brouwers

All rights reserved. No part of this book may be reproduced, stored in a database or retrieval system, or published, in any form or in any way, electronically, mechanically, by print, photoprint, microfilm or any other means without prior written permission of the author.

Cover design: daphne.van.mourik@gmail.com/ Julienne Brouwers

Printed by the Universiteitsdrukkerij TU Eindhoven, Eindhoven, The Netherlands.

Financial support by de Nederlandse Organisatie voor Wetenschappelijk Onderzoek, Prins Bernard Cultuurfonds, VSB-fonds and SCANCO Medical AG is gratefully acknowledged.



***In vivo* assessment of changes in bone due to osteoporosis and its possible treatments**

PROEFSCHRIFT

ter verkrijging van de graad van doctor aan de Technische Universiteit Eindhoven, op gezag van de Rector Magnificus, prof.dr.ir. C.J. van Duijn, voor een commissie aangewezen door het College voor Promoties in het openbaar te verdedigen op donderdag 27 november 2008 om 16.00 uur

door

Julienne Elisabeth Michaela Brouwers

geboren te Delft

Dit proefschrift is goedgekeurd door de promotoren:

prof.dr.ir. K. Ito

en

prof.dr.ir. H.W.J. Huiskes

Copromotor:

dr.ir. B. van Rietbergen

Contents

Summary	ix
Samenvatting	xi
1 Introduction	1
1.1 Bone	2
1.1.1 Bone cells	3
1.1.2 Estrogen and parathyroid hormone	4
1.1.3 Bone remodeling	4
1.1.4 Mineralization	6
1.1.5 Mechanical usage	6
1.2 Osteoporosis	7
1.2.1 Treatments	8
1.3 Osteoporosis research in humans	10
1.4 Osteoporosis research in animals	11
1.4.1 Animal models	11
1.4.2 Micro-CT	12
1.4.3 Mechanical tests and finite element models	13
1.5 Rationale and outline of the dissertation	14
2 Effects of <i>in vivo</i> micro-CT radiation on bone	17
2.1 Introduction	19
2.2 Materials and methods	19
2.3 Results	22
2.4 Discussion	25
3 Estrogen-deficiency and immobilization induced osteoporosis	29
3.1 Introduction	31
3.2 Materials and methods	32
3.2.1 Animals	32
3.2.2 Micro-CT scanning	32
3.2.3 Finite element model	33
3.2.4 Three-point bending of tibiae	34
3.2.5 Statistics	34
3.3 Results	34
3.3.1 Effects of ovariectomy and neurectomy on metaphyseal, trabecular bone	34
3.3.2 Effects of ovariectomy and neurectomy on epiphyseal, trabecular bone	35

3.3.3	Effects of ovariectomy and neurectomy on FEM derived properties	-	37
3.3.4	Three-point bending of tibiae	-----	37
3.4	Discussion	-----	38
4	Bisphosphonate treatment assessed by <i>in vivo</i> micro-CT		43
4.1	Introduction	-----	45
4.2	Materials and methods	-----	46
4.2.1	Animals	-----	46
4.2.2	Micro-CT scanning	-----	46
4.2.3	Mechanical testing	-----	47
4.2.4	Histomorphometry	-----	48
4.2.5	Statistics	-----	48
4.3	Results	-----	49
4.3.1	Ovariectomy	-----	49
4.3.2	Zoledronic acid treatment	-----	49
4.3.3	Aging	-----	51
4.3.4	Cortical thickness	-----	52
4.3.5	Mechanical testing	-----	53
4.3.6	Histomorphometry	-----	53
4.4	Discussion	-----	54
5	Effects of zoledronic acid on rat vertebrae		59
5.1	Introduction	-----	61
5.2	Materials and methods	-----	61
5.2.1	Assessment of vertebral microarchitecture	-----	62
5.2.2	Static vertebral compression tests	-----	62
5.2.3	Data Analysis	-----	63
5.3	Results	-----	63
5.3.1	Effects of OVX and ZOL on lumbar vertebral microarchitecture	---	63
5.3.2	Effects of OVX and ZOL on vertebral compressive properties	----	63
5.3.3	Comparison between response to OVX and ZOL in lumbar and caudal vertebrae	-----	65
5.4	Discussion	-----	65
6	Rat vertebral compressive fatigue properties		69
6.1	Introduction	-----	71
6.2	Materials and methods	-----	72
6.2.1	Micro-CT scanning	-----	72
6.2.2	Specimen preparation	-----	72
6.2.3	Fatigue compression tests	-----	73
6.2.4	Data analysis	-----	74
6.3	Results	-----	74
6.3.1	Trabecular and cortical microarchitecture	-----	74
6.3.2	Fatigue compression tests	-----	75
6.3.3	Relation between morphology and fatigue properties	-----	76

6.4 Discussion	77
7 PTH treatment of rats assessed by <i>in vivo</i> micro-CT	81
7.1 Introduction	83
7.2 Materials and methods	84
7.2.1 Animals	84
7.2.2 Micro-CT scanning	85
7.2.3 Trabecular tunneling	86
7.2.4 Prediction of gain in bone mass after PTH treatment	86
7.2.5 Three-point bending of tibiae	87
7.2.6 Statistics	87
7.3 Results	87
7.3.1 Metaphyseal, structural parameters	87
7.3.2 Epiphyseal, structural parameters	88
7.3.3 Cortical thickness and polar moment of inertia in the metaphysis and diaphysis	89
7.3.4 Mineralization of meta- and epiphyseal, trabecular bone and meta- and diaphyseal, cortical bone	90
7.3.5 Trabecular tunneling and remodeling	91
7.3.6 Prediction of gain in bone mass after PTH treatment	92
7.3.7 Three-point bending of tibiae	93
7.4 Discussion	93
8 Vibration treatment of rats assessed by <i>in vivo</i> micro-CT	99
8.1 Introduction	101
8.2 Materials and methods	102
8.2.1 Animals	102
8.2.2 Micro-CT scanning	103
8.2.3 Three-point bending of tibiae	104
8.2.4 Statistics	104
8.3 Results	105
8.3.1 Metaphyseal, structural parameters	105
8.3.2 Epiphyseal, structural parameters	106
8.3.3 Cortical thickness and polar moment of inertia in the metaphysis and diaphysis	106
8.3.4 Three-point bending of tibiae	108
8.4 Discussion	108
9 Discussion	111
9.1 Introductory remarks	112
9.2 Main findings and implications	113
9.2.1 Estrogen-deficiency versus immobilization induced osteoporosis	113
9.2.2 Bisphosphonates	114
9.2.3 Anabolic treatments	116
9.3 Ethical considerations	118

9.4 Experimental methods employed; strengths and weaknesses -----	119
9.4.1 <i>In vivo</i> micro-CT -----	119
9.4.2 Animal models -----	120
9.4.3 Mechanical testing -----	121
9.5 Anti-resorptive versus anabolic treatments -----	123
9.6 Clinical considerations -----	124
9.7 Future work, ongoing issues and recommendations -----	125
9.8 Conclusions -----	129
Appendix	131
References	133
Dankwoord	153
Curriculum Vitae	155

Summary

***In vivo* assessment of changes in bone due to osteoporosis and its possible treatments**

Osteoporosis is a skeletal disease characterized by a decrease in bone mass and deterioration of bone microarchitecture, resulting from an unbalance in the amount of bone formed and resorbed during bone remodeling. It often takes place after menopause in women due to estrogen deficiency and results in decreased bone strength and, subsequently, a greater risk of fracture. Pharmaceutical treatments for osteoporosis can roughly be divided into bone resorption inhibitors and bone formation enhancers. To evaluate possible treatments, postmenopausal osteoporosis can be simulated in animals by performing an ovariectomy, which leads to estrogen deficiency and subsequent bone loss. This loss of bone mass and the subsequent microarchitectural deterioration is often analyzed by micro-CT, which until recently was only possible to do *ex vivo*, after sacrifice. Recently, however, *in vivo* micro-CT scanners have become available with which bone in living rats can be scanned. *In vivo* micro-CT, combined with image registration software, offers a potentially more powerful method to identify effects of osteoporosis and treatments over time. Additionally, local changes in bone within the same animal can be monitored over time, which taken together can provide novel and unique information

In this dissertation, we focused on the development of osteoporosis and several treatments in rats. We first concentrated on bone resorption inhibitors and then on bone formation enhancers. Changes over time in bone microstructure were determined as well as mechanical properties after sacrifice using mechanical tests or finite element models.

We first ruled out that radiation damage due to scanning affected our studies. Then two different animal models that simulate bone loss due estrogen-deficiency (i.e. after menopause) and immobilization (e.g. after long bed resting) were compared, as their effects on bone structure and strength may differ. In the metaphysis, the loss of bone volume fraction was found to be similar for both models, while structure and strength were more affected after immobilization. In the epiphysis, changes in bone volume fraction and structure were different. The difference in response between the meta- and epiphysis may be related to different mechanisms underlying the bone loss after estrogen-deficiency and immobilization. These findings offer insight into the aetiology and possible treatment of different types of osteoporosis.

Zoledronic acid (ZOL) is a novel, potent bone resorption inhibitor. In the rat tibia, we found that preventive treatment with ZOL prevented all bone microstructural changes seen after ovariectomy. Recovering treatment significantly improved bone microstructure, though not back to original levels. These results indicate that the time-point of initiation of treatment is important for the final bone microstructure and strength. Both preventive and recovering treatments also led to inhibition of loss of bone mass and static compressive strength in the lumbar vertebra, a clinically relevant site. However, no significant influence of time-point of treatment was found here. Vertebral fractures mostly result from cyclic loading. ZOL may influence mineralization and lead to accumulation of microdamage, possibly affecting fatigue behavior. A method was developed to assess compressive fatigue properties in rat vertebrae. ZOL treated rats were found to have similar fatigue properties as normal rats, indicating that any altered mineralization and accumulated microdamage due to ZOL treatment did not affect fatigue properties.

After exploring the effects of bone resorption inhibitors, we continued with studying the effects of bone formation enhancers. It was found that PTH leads to a linear, constant increase in trabecular and cortical bone mass over time and that mechanical properties improved. Micro-analysis showed that bone was formed on trabeculae, there where most beneficial for structure and strength. This indicates that bone formation resulting from PTH may be mechanically driven. In another study, the effects of a daily period on a vibration platform, which has been described in the literature to increase bone formation, were studied in osteoporotic rats over time. Within six weeks, no significant effects were found to take place. The potential of vibration as treatment for osteoporosis thus could not be established.

Summarizing, for the first time, the comparison between two types of osteoporosis and the effects of several treatments for osteoporosis on bone microstructure were analyzed over time *in vivo*, offering insight into the temporal and spatial effects of bone resorption inhibitors and bone formation enhancers in osteoporotic rats.

Samenvatting

***In vivo* bepaling van veranderingen in bot als gevolg van osteoporose en mogelijke behandelingen**

Osteoporose (botontkalking) is een aandoening van het skelet, die wordt gekenmerkt door een afname in botmassa en beschadiging van de botstructuur, als resultaat van een verstoring van het evenwicht tussen de hoeveelheid botafbraak en -aanmaak. De ziekte komt vaak voor na de overgang bij vrouwen als gevolg van een tekort aan oestrogeen, en resulteert in verminderde botsterkte en vervolgens, een grotere kans op een botbreuk. Farmaceutische behandelingen voor osteoporose kunnen grofweg worden verdeeld in bot afbraak remmers en bot aanmaak stimulators. Om mogelijke behandelingen te evalueren, kan postmenopausale (na de overgang) osteoporose worden gesimuleerd in dieren door een ovariectomie uit te voeren, wat leidt tot een tekort aan oestrogeen en vervolgens verlies van bot. Het verlies van botmassa en structuur kan geanalyseerd worden met behulp van micro-CT, wat tot voor kort echter slechts mogelijk was *ex vivo*, na opofferen. Recentelijk zijn *in vivo* micro-CT scanners beschikbaar gekomen waarmee bot in levende ratten kan worden gescand. Deze *in vivo* scanners bieden, in combinatie met beeld registratie software, een nieuwe methode om de effecten van osteoporose en behandeling daarvan in de tijd te identificeren. Daarbij kunnen lokale veranderingen in het bot binnen hetzelfde dier in de tijd worden gevolgd, wat samengevat, nieuwe en unieke informatie kan opleveren.

In dit proefschrift, richtten we ons op de ontwikkeling van osteoporose en verschillende behandelingen daarvan in ratten. We concentreerden ons eerst op bot afbraak remmers en vervolgens op bot aanmaak stimulators. Veranderingen van de botstructuur werden bepaald in de loop van de tijd met micro-CT *in vivo*, terwijl mechanische eigenschappen werden bepaald aan het einde van een experiment met mechanische testen of eindige elementen modellen.

Het doel van een eerste experiment was om uit te sluiten dat straling van de micro-CT scanner effecten zou hebben op de resultaten, wat inderdaad niet het geval bleek te zijn. Vervolgens hebben we een vergelijking gemaakt tussen diermodellen die botverlies na oestrogeen tekort (na overgang) en na immobilisatie (bv. na een lange periode van bedlegerigheid) simuleren, aangezien effecten op de botsterkte en -sterkte wellicht verschillen. In de metaphyse werd het verlies aan bot volume fractie in beide situaties vergelijkbaar bevonden, terwijl de structuur en sterkte meer aangetast waren na immobilisatie. In de epifyse waren de veranderingen in bot volume fractie en structuur echter verschillend. Het verschil in reactie in de meta- en epifyse zou

gerelateerd kunnen zijn aan een verschil in het mechanisme dat ten grondslag ligt aan botverlies na oestrogeen tekort en na immobilisatie. Deze bevindingen verschaffen inzicht in de etiologie en mogelijke behandelingen van verschillende types van osteoporose.

Zoledronic acid (ZOL) is een nieuwe, krachtige bot afbraak remmer. In de tibia van de rat, vonden we dat preventieve behandeling met ZOL alle veranderingen in bot structuur, die men verwacht na ovariectomie, voorkwam. Een behandeling die werd gestart nadat osteoporose al aanwezig was (herstellende behandeling), verbeterde significant de botstructuur, maar niet terug tot het originele niveau. Deze resultaten laten zien dat het tijdstip waarop de behandeling wordt gestart belangrijk is voor de uiteindelijke botstructuur en -sterkte. Zowel preventieve als herstellende behandeling leidden ook tot een reductie van verlies van botmassa en sterkte in de lendewervels, een klinisch relevante locatie. Echter, hier werd geen significante invloed van het tijdstip van behandeling gevonden. Wervelbreuken zijn meestal het resultaat van cyclische belasting. ZOL zou de mineralisatie kunnen beïnvloeden en tot ophoping van microschade kunnen leiden, waardoor mogelijk het vermoeiingsgedrag wordt beïnvloed. Een nieuwe methode werd ontwikkeld om de compressieve vermoeiings eigenschappen in ratwervels te bepalen. Gevonden werd dat ZOL behandelde ratten dezelfde vermoeiings eigenschappen hadden als normale ratten, wat aangeeft dat een eventuele veranderde mineralisatie en opgehoopte microschade als gevolg van ZOL behandeling niet de vermoeiings eigenschappen beïnvloedt.

Nadat we de effecten van bot afbraak remmers hadden onderzocht, hebben we de effecten van bot aanmaak stimulators bestudeerd. PTH leidde tot een lineaire toename in trabeculaire en corticale botmassa in de tijd, en mechanische eigenschappen verbeterden. Micro-analyse toonde aan dat bot op trabekels werd gevormd, daar waar dit het meest gunstig is voor de structuur en sterkte. Dit geeft aan dat bot aanmaak als gevolg van PTH wellicht mechanisch gestuurd wordt. Vervolgens werden de effecten van dagelijkse perioden op een trilplaat, wat volgens de literatuur kan leiden tot een verhoogde bot aanmaak, in osteoporotische ratten in de tijd bestudeerd. Er werden geen effecten gevonden gedurende de 6 weken dat het experiment duurde. Het was dus niet mogelijk om een positief effect van een behandeling met een trilplaat aan te tonen.

Samengevat, voor de eerste keer werden twee types osteoporose en de effecten van verschillende behandelingen van osteoporose op de bot structuur in de tijd bepaald, *in vivo*. Dit leverde nieuwe inzichten op in de tijds- en plaatsafhankelijke effecten van bot afbraak remmers en bot aanmaak stimulators in osteoporotische ratten.

Chapter 1

Introduction

1.1 Bone

The skeletal system is important for the body both biomechanically and metabolically. It is made up of bones and connective tissue joining them. Bone is the main constituent and is rigid enabling the skeleton to maintain the shape of the body. Bone is a self-repairing structural material, able to adapt its mass, shape and properties to changes in mechanical environment.

A typical long bone (e.g. tibia, femur) consists of a central cylindrical shaft, the diaphysis, and two wider and rounded ends, the epiphyses (figure 1.1). The metaphysis connects the diaphysis with each epiphysis. In a growing human or animal, the growth plate, located in between the epiphysis and metaphysis, ensures continuous growth enlarging the bone while maintaining its shape (117).

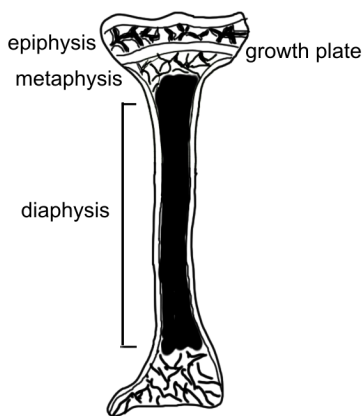


Figure 1.1: Schematic drawing of a tibia in a growing human or animal.

Two types of bone can be distinguished: cortical bone, which is a dense and solid mass and trabecular bone, which is a lattice of small plates and rods known as trabeculae (figure 1.2). Approximately 80% of all skeletal mass in the adult human skeleton is cortical bone (including the diaphysis of long bones), which forms the outer wall of all bones and is largely responsible for the supportive and protective function of the skeleton. Trabecular bone is found in the inner parts of the bone, particularly at the ends of long bones, with bone marrow surrounding it. The outer surface of most bone is covered by the periosteum, a sheet of fibrous connective tissue and an inner cellular layer of undifferentiated cells. The marrow cavity is lined with a thin cellular layer called the endosteum, which is a membrane of bone surface cells.

Bone consists of 65% mineral, 35% organic matrix, cells and water. The bone mineral, which is largely impure hydroxyapatite, is in the form of small crystals between collagen fibers. The organic matrix consists of 90% collagen and about 10% of various noncollagenous proteins (117).

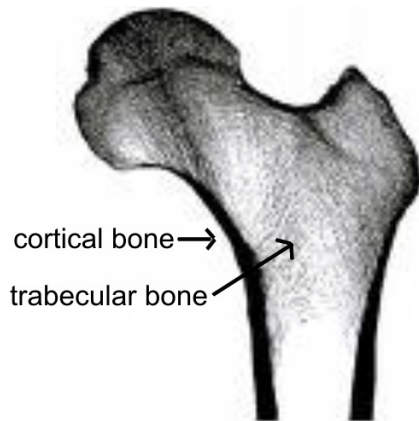


Figure 1.2: Human femur head consisting of cortical and trabecular bone.

1.1.1 Bone cells

The major cellular elements of bone are osteocytes, osteoclasts, osteoblasts and bone-lining cells.

Osteocytes: Osteocytes are the most abundant cell type in mature bone with about ten times more osteocytes than osteoblasts in normal human bone. During bone formation some osteoblasts are left behind in the newly formed osteoid as osteocytes when bone formation moves on. Osteocytes are the cells best placed to sense the magnitude and distribution of strains. They are strategically placed both to respond to changes in mechanical strain and to disseminate fluid flow to transduce information to surface cells of the osteoblastic lineage via their network of canalicular processes and communicating gap junctions. Gap junctions are transmembrane channels, which connect the cytoplasm of two adjacent cells that permit molecules with molecular weights of less than 1 kDa such as small ions and intracellular signalling molecules. Osteocytes may stabilize bone mineral by maintaining an appropriate local ionic milieu, detect microdamage and respond to the amount and distribution of strain within bone tissue that influence adaptive modeling and remodeling. Therefore, osteocytes play a key role in homeostatic, morphogenetic and restructuring process of bone mass that constitute regulation of mineral and architecture (117).

Osteoclasts: Osteoclasts are bone-resorbing cells consisting of 1 to 50 nuclei. Actively resorbing osteoclasts are usually found in cavities on bone surfaces, called resorption cavities. They secrete products that lead to solubilisation of the mineral and organic component of the matrix. Bisphosphonates and estrogen are commonly used to inhibit resorption and are believed to act by inhibiting the formation and activity of osteoclasts and promoting osteoclast apoptosis (117).

Osteoblasts: Osteoblasts are bone-forming cells that synthesize and secrete unmineralized bone matrix (the osteoid) and participate in the calcification. They produce all the constituents of the bone matrix and possess receptors to many bone agents. Bone formation occurs in two phases: matrix formation and mineralization. Matrix formation occurs at the interface between osteoblasts and osteoid. Extracellular mineralization occurs at the junction of osteoid and newly formed bone, the

mineralization front. The rate of bone formation can be determined in humans and animals by administering a fluorescent bone label, which localizes at the mineralization front. The development of osteoblasts and osteoclasts are linked and both are derived from precursors originating in the bone marrow (117).

Bone-lining cells: Bone-lining cells are resting osteoblasts covering quiescent bone surfaces that can return to being active osteoblasts again. They are capable of forming bone without prior resorption in response to anabolic agents such as PTH. They may be influenced by functional strain within bone just like osteocytes (117).

1.1.2 Estrogen and parathyroid hormone

Estrogens are hormones produced by the ovaries in females and play an essential role in maintaining skeletal homeostasis in part by exerting a tonic suppression of cancellous bone remodeling and maintaining remodeling balance between osteoblastic and osteoclastic activity. Many skeletal cells respond to estrogen, among which but not limited to osteoblasts, osteoclasts, chondrocytes and bone marrow progenitors. Estrogens also regulate matrix production, mineralization and growth factor expression. Estrogens inhibit osteoclast differentiation and activity, as well as suppress osteoblast proliferation and control osteoblast apoptosis (149).

During the transition to postmenopause, there is a gradual decrease in estrogen secretion. During and after menopause bone remodeling as well as remodeling imbalance increases resulting in a reduction in bone mass, particularly in trabecular bone, where the surface to volume ratio is significantly greater than in cortical bone (167). The remodeling imbalance is the result of increased osteoclastic activity; the osteoclasts construct deeper resorption spaces and there is some evidence that the ability of the osteoblasts to refill them is also impaired. Moreover, the deeper resorption spaces result in perforation of trabecular plates and loss of architectural elements, weakening the skeleton in regions that contain large amounts of cancellous bone, such as the vertebrae and distal forearm (267).

Parathyroid hormone (PTH) is secreted by the parathyroid gland and acts to maintain normal levels of ionized calcium by acting on the bone and kidney. In bone, PTH leads to bone resorption hereby releasing calcium into the blood. PTH does not directly activate osteoclasts, but possibly does so through osteoblasts. PTH acts directly on cells of the osteoblast lineage, thereby influencing osteoblast differentiation and function, and consequently bone formation. Administration of intermittent PTH to humans or animals elicits skeletal effects in which increased bone formation predominates, whereas continuous treatment with high doses of PTH results in a major increase in bone resorption (198).

1.1.3 Bone remodeling

Bone remodeling is the process of producing and maintaining bone that is biomechanically and metabolically competent. In normal human adults, cortical bone has a mean age of 20 years and trabecular bone 1 to 4 years. The periodic replacement

of bone (bone turnover) helps to maintain optimal load bearing and to repair structural damage. It serves to remove microdamage, replace dead and hypermineralized bone, and adapt microarchitecture to local stresses. Remodeling of trabecular bone may perforate and remove trabeculae, and remodeling of cortical bone increases cortical porosity, decreases cortical width, and hereby possibly reduces bone strength (117). The life cycle of bone remodeling includes six stages: resting, activation, resorption, reversal, formation, mineralization, and back to resting (figure 1.3).

Resting: The resting phase is the time period, in which bone surfaces are quiescent (117).

Activation: The conversion of quiescent bone surface to resorption activity is referred to as activation. Bone-lining cells are believed to digest the endosteal membrane and to retract, thereby exposing the mineralized bone surface, which is chemotactic for osteoclastic precursors (117).

Resorption: Where osteoclasts come in contact with the surface of bone they begin to erode the bone forming resorption cavities (117).

Reversal: This term refers to an interval between the completion of resorption and start of formation (117).

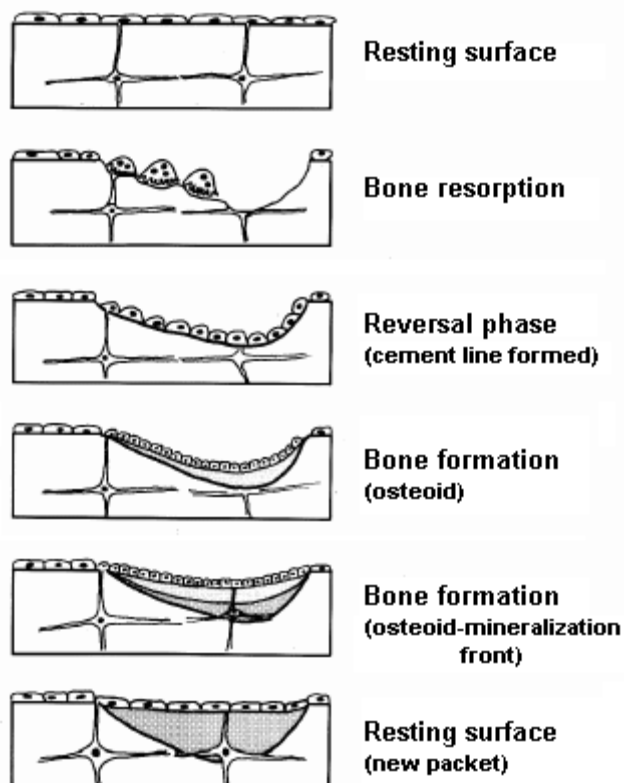


Figure 1.3: Schematic drawing of bone remodeling processes (187).

Formation: The cavity resulting from the actions of the osteoclasts is refilled by osteoblasts via a process that occurs in three distinct phases: initiation, progression and termination (206). During the initiation, osteoblasts start forming bone at the bottom of

the cavity. As bone formation progresses, some osteoblasts are entombed within the matrix as osteocytes but the majority die by apoptosis. Bone formation terminates when the cavity has been refilled, at which point the few osteoblasts that remain become the bone-lining cells covering the quiescent bone surfaces (123).

During bone remodeling, a temporary hole is made, the so called remodeling space. Usually, it equals 2 to 8% of bone volume going up to 20% in trabecular bone due to its large surface to volume ratio. Increased bone turnover increases bone remodeling space. Estrogens and bisphosphonates decrease bone remodeling rates and let the existing remodeling space fill with bone, which causes an increase in bone mass that plateaus. Remodeling rate is dominated by mechanical usage and modulated by PTH, microdamage and other substances (117).

1.1.4 Mineralization

Mineral contributes both to the mechanical strength of bone and to the ability of the skeleton to regulate mineral ion homeostasis (23). The mineral in bone is an analogue of the naturally occurring mineral hydroxyapatite. Bone mineral varies in content, composition and crystal size. Mineralization of bone tissue follows matrix formation by about 15 days and occurs at the interface between mineralized bone and osteoid (117), which is called primary mineral apposition. The newly formed bone will reach a level of approximately 70% of its final mineralization after about 5 to 10 days (117). After full completion of basic structure units, secondary mineralization begins. This process consists of a slow and gradual maturation of the mineral component, including an increase in the number of crystals, a moderate augmentation of crystal size toward their maximum and, to a greater extent, changes in the internal order of the crystals reflecting their degree of perfection (19). Complete mineralization takes about 3 to 6 months (117). Drug therapies for osteoporosis can alter bone mineral properties. Bisphosphonates, which will be explained in the next section, stabilize crystal structure, tend to increase bone mineral crystal size and increase mineral content.

1.1.5 Mechanical usage

Mechanical usage plays an important role in skeletal development and maintenance, starting in prenatal life when muscular contraction modulates bone growth and modeling. Wolff's law was stated in 1892 as follows: "Every change in the form and function of bone or of their function alone is followed by certain definite changes in their internal architecture, and equally definite alteration in their external conformation, in accordance with mathematical laws" (286). Based on this concept, Frost proposed the mechanostat theory stating that bone adapts to mechanical usage (74). The theory is based on the idea that when strains in the bone fall below a threshold value, bone will be resorbed, and when strains are above the threshold value, new bone will be formed. Although this mechanostat is generally held true, limited proof is available on the correlation between *in vivo* strains on a local level and bone resorption and formation.

1.2 Osteoporosis

Osteoporosis is a skeletal disease characterized by a decrease in bone mass and deterioration of bone microarchitecture resulting in decreased bone strength (figure 1.4). This leads to an enhanced fragility of the skeleton and consequently to a greater risk of fracture. The risk of fracture is dependent on the risk of falling and on bone strength. In ageing humans, the number of falls may increase owing to impairments in muscle strength, neuromuscular coordination, balance, vision and hearing (78). Bone strength can be defined by biomechanical parameters, including ultimate force (a measure of strength), ultimate displacement (associated with brittleness) and work to failure (energy absorption) (263). Bone strength is influenced by bone size, shape, architecture and tissue 'quality'. Interestingly, indications have been found that in osteoporotic women, bone that is under low strain is resorbed, while the higher loaded areas are preserved. This leaves the bone still capable of bearing daily loads, but fragile to irregularly oriented or high loads (101;116;259;280). In a study on an osteoporotic femur, however, this was not confirmed (276), although the type of osteoporosis was unknown in this study.

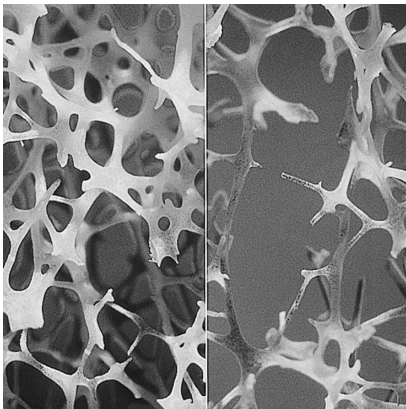


Figure 1.4: Healthy (left) and osteoporotic (right) trabecular bone. (courtesy of the National Osteoporosis Society, UK).

The main cause of osteoporosis is the continuous loss of bone during life starting at about 30 years of age (figure 1.5). An increase in bone loss can take place after a long period of bed rest or reduced physical activity (immobilization). In women, bone loss is exacerbated after menopause due to a decrease in estrogen production (estrogen-deficiency). Therefore, in women, the incidence is much higher than in men. It is currently unknown whether immobilization and estrogen-deficiency induced osteoporosis lead to the same spatial and temporal pattern of bone loss and whether their effects on fractures risk are similar or not. Osteoporosis can also be induced by medications like glucocorticoid, androgen-deprivation therapy, aromatase inhibitors, protease inhibitors, selective serotonin reuptake inhibitors and prolactin-raising antiepileptic agents (4), or induced by pregnancy or lactation (253) although all of these occur much less frequently.

An estimated 10 million people in the US have osteoporosis, of which 80% are women, and almost 34 million more are estimated to have low bone mass, placing them at increased risk for osteoporosis. Osteoporosis is responsible for about 300,000 hip, 700,000 vertebral and 250,000 wrist fractures annually in the US. An average of 24% of hip fracture patients aged 50 and over die in the year following their fracture, mostly due to complications. The estimated direct care expenditures (including hospitals, nursing homes, and outpatient services) in the US for osteoporotic fractures are \$18 billion per year, and costs are rising. Osteoporosis is therefore viewed as a major socio-economic problem (291).

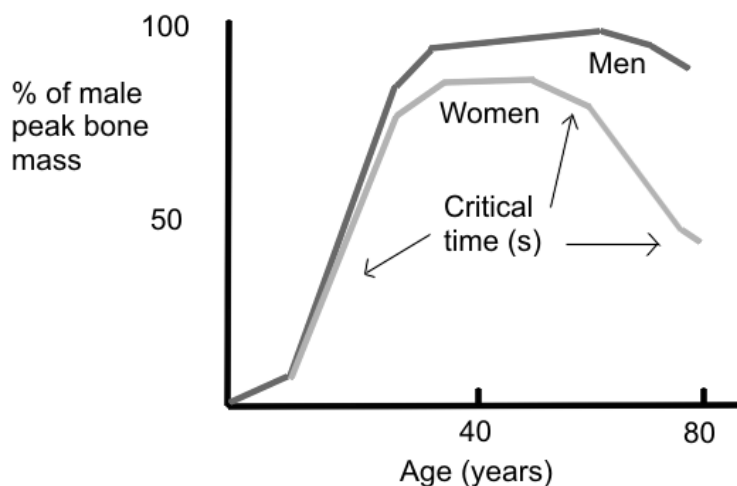


Figure 1.5: Changes in skeletal mass throughout life (197).

1.2.1 Treatments

FDA¹ approved options for osteoporosis prevention or treatment can be largely separated into two categories: anti-resorptive or anti-remodeling agents that target the osteoclast (e.g. hormone replacement therapy [HRT], selective estrogen receptor modulators [SERMs], bisphosphonates and calcitonin), or bone-forming (anabolic) agents such as parathyroid hormone (PTH) and strontium ranelate, which target the osteoblast (78;211). All existing anti-resorptive drug classes reduce, with different efficacy, the activation frequency (i.e. the number of bone remodeling events) in trabecular and cortical bone (78). All approved drugs reduce the risk of vertebral fractures and some the risk of hip and non-vertebral fractures as well. SERMs have modest effects on bone density with the added benefit of reduction of breast cancer risk (211). HRT significantly reduces the rate of osteoporotic fractures and colorectal cancer but increases the odds of the development of breast cancer, deep venous thrombosis, stroke, or cardiovascular disease (211). Also, adequate intake of calcium and vitamin D, has shown to help prevent osteoporosis (161) and increase drug efficacy (160).

¹ FDA: The food and drug administration is an agency of the United States Department of Health and Human Services responsible for the safety regulation of most types of drugs

Vibration treatment, during which a patient is mechanically stimulated daily by standing on a vibrating platform has recently been suggested as interesting addition to drug treatments, although effects of 1 year of treatment in a small cohort of osteoporotic patients merely almost reached significance in the highest quartile of compliance (228). In this dissertation, we will focus on the anti-resorptive bisphosphonates and the anabolic effects of PTH and vibration.

Bisphosphonates

Bisphosphonates are a group of anti-resorptive drugs most commonly used to treat osteoporosis. Among the bisphosphonates that have been given FDA or EMEA² approval for the treatment of osteoporosis are alendronate, etidronate, risedronate, ibandronate and most recently also zoledronic acid (291). These drugs share a common chemical structure and their use has resulted in a reduction of hip and vertebral fractures in patients of about 50% (20;82). While the first bisphosphonates had to be taken once a day orally accompanied by physical discomfort, the latest bisphosphonate, zoledronic acid, only needs to be given intravenously once a year, while maintaining the same antifracture efficacy (17). Bisphosphonates lead to inhibition of osteoclast recruitment, inhibition of osteoclastic adhesion, earlier apoptosis of osteoclasts and inhibition of osteoclast activity (67). This results in reduced bone resorption rates and in part indirectly also to reduced bone formation rates (112;176). Although the loss of bone mass is inhibited by the reduced bone turnover, microdamage repair may be impaired (38;235;252) and may cause increased bone mineralization (236), which can increase the brittleness of bone. In some studies, however, no influence of reduced bone turnover was found on microdamage (2;44). This reduced turnover ultimately may negatively affect bone fragility, although limited proof is available. Also, this indicates that treatment with bisphosphonates should not be initiated in a too early state of the disease, although waiting too long with treatment may lead to fractures. The influence of different starting-points of treatment on the final bone mass, structure and strength is currently unclear.

Anabolic agents

PTH1-34, the active fragment of PTH, is the only FDA-approved anabolic pharmaceutical agent to date for the treatment of postmenopausal osteoporosis and needs to be injected subcutaneously, daily. It exerts potent anabolic effects on bone and increases bone turnover with a net increase in bone mass. It is reserved for patients who have severe postmenopausal osteoporosis with at least two vertebral fractures (251). PTH1-34 reduces non-vertebral fragility fractures by more than 50% and vertebral fracture rates decrease by 65% within 18 months of treatment (196).

While bisphosphonates merely inhibit the loss of bone, PTH actually can increase the bone formation rate, which theoretically offers more potential for the treatment of osteoporosis. Although most increases in trabecular bone mass after PTH treatment

² EMEA: The European Medicines Agency is the European Union body responsible for the evaluation, supervision and pharmacovigilance of medicinal products

have been reported to result from increased trabecular *thickness*, in a few studies an increase in trabecular *number* was reported (31;70;105;120;181;203;237), which is an uncommon feature in itself. It is known that the same increase in bone mass due to trabecular thickness or number has different mechanical implications, with the latter having a higher increase in mechanical performance (90;263). Therefore, it is important to evaluate the changes in both trabecular thickness and number after PTH treatment over time to provide more insight into the potential of increasing mechanical performance.

Cortical porosity, can increase after PTH use (257) and another negative effect of the increased bone turnover is the decreased and altered tissue mineralization (182), which may both negatively affect fracture risk. Also, bone mass may decrease as soon as daily injections are halted (15;97;247). Recent studies focus on the combination of PTH and bisphosphonates, with the concept that PTH first increases bone mass and bisphosphonates then retain it. While bisphosphonates and PTH both are known to reduce fracture risks, many aspects of how they exactly work and what treatment regime is best to follow are still unknown and research is therefore ongoing.

1.3 Osteoporosis research in humans

After new drug treatments for postmenopausal osteoporosis have successfully passed the preclinical phase, clinical trials are conducted. Usually, in phase III clinical trials, which are randomized, double-blind and placebo-controlled, postmenopausal osteoporotic patients are assigned to either placebo or the drug of interest. Treatment is given for three years, after which fracture incidence, the primary outcome, in the hip, vertebra, radius and other sites is compared between drug and placebo treated patients (28). Also, bone turnover markers can be measured in blood or urine and dual energy X-ray absorptiometry (DXA) scans can be made at several time points to assess bone mineral density (BMD). Finally, in a small cohort of patients, iliac crest samples can be removed before and after treatment (left and right) to determine changes in bone turnover rates as well as in bone structure over time.

Bone structure plays an important role in bone strength and thus fracture risk (119;125;263). However, as it is painful to obtain iliac crest biopsies, the number of patients giving consent to this is low, which complicates the interpretation of results. As fracture incidence, which is the primary endpoint, in patient cohorts is relatively low, it takes quite some time to determine significant differences between the number of fractures of the placebo and drug-treated groups resulting in clinical trials that last three years. This not only slows the development of new drugs for treatment of postmenopausal osteoporosis, it also is viewed as unethical to have patients at risk of fracture on placebo treatment for three years (28). The recent development (195) and validation (151;152;154) of high resolution 3-D pQCT instrumentation (HR-pQCT) with a voxel size of <200 μm , and more recently <100 μm , has provided a means for evaluating trabecular microstructure noninvasively at the wrist and tibia. It has been shown to be highly reproducible (26;151), suited to determine changes in bone

microstructure associated with aging (139), to discriminate between men and women (139) and between osteoporotic and osteopenic patients (26). Also, osteoporotic fractures in retrospect have been found to be associated with microstructure (250) and results from finite element analyses (27;179), showing its advantages over DXA. No clinical trials using the HR-pQCT have, however, been reported yet, perhaps as no scans of the hip or vertebra can be made and the predictive value of HR-pQCT for fractures is as yet unestablished.

1.4 Osteoporosis research in animals

1.4.1 Animal models

Before new drug treatments can be tested in humans, they need to be fully analyzed in animals. Even when new drugs are already tested in the clinical phase, researchers often turn to animals to further elucidate aspects of the drugs, because analysis of bone microstructure is limited in humans as described in the previous section. Particularly, small animals like rats are used as their bones respond fast to changes, in a human-like fashion, they are easy to use and inexpensive. There are several animal models, in which an osteoporosis-like state can be induced. This osteoporosis-like state is often referred to as osteopenia, because rats never actually fracture a bone after ovariectomy. To induce immobilization associated osteoporosis, nerve resection (neurectomy), tendon resection, tail suspension, limb casting and limb taping can be performed (118). In this dissertation, we will focus on the neurectomy animal model, which is well-known to simulate immobilization induced osteoporosis. In this model, the nerves controlling the muscles of a lower hind limb are transected, which makes that hind limb unusable. This results in immobilization, which causes bone loss (108;285). The ovariectomized rat model is a widely used animal model to simulate estrogen-deficiency induced bone loss and is commonly used to test potential pharmaceutical agents for the treatment of postmenopausal osteoporosis. The FDA Guidelines For Preclinical and Clinical Evaluation of Agents Used in the Treatment or Prevention of Postmenopausal Osteoporosis (1994) delineate specific preclinical animal models to demonstrate the efficacy and safety of new, potential agents for osteoporosis therapy. The Guidelines in fact recommend that agents be evaluated in two animal species, including the ovariectomized (OVX) rat and in a second non-rodent model (258). In the ovariectomy model, the ovaries of the female rat are removed, resulting in strongly diminished estrogen production, which leads to rapid bone loss (57;153;287;288). In both the neurectomy and ovariectomy model, trabecular bone mass is quickly reduced, while cortical bone responses are less pronounced.

Often, in osteoporotic research, animals are ovariectomized and treated for several weeks or months with a pharmaceutical agent that may serve as potential treatment like e.g. a bisphosphonate. Untreated ovariectomized and control groups are included as well and at the end of the experiment, all animals are sacrificed. Then traditionally, dynamic and static histomorphometry could be performed on bone samples. Dynamic histomorphometry is a commonly used method to determine bone turnover parameters

in bone. It makes use of fluorochromes that are incorporated into the bone at the front of mineralization after subcutaneous injections at two time points (mostly a week is left in between) in a living subject. These labeled sites will fluoresce and can be viewed with ultraviolet microscopy after a bone sample is extracted (i.e. animals are sacrificed or iliac crest biopsy is taken in humans). The rates of formation and mineralization can be calculated from measurements of tissue growth between the labels. Static histomorphometry is a technique where bone structural parameters quantifying the bone microstructure can be calculated by sectioning a bone sample in several slices. One of the major drawbacks of histomorphometry is that it is a destructive technique, which can only be done at one or two time-points. Also, static histomorphometry only gives two-dimensional information on bone structure, just a few sections are analyzed per sample and it is time-consuming.

1.4.2 Micro-CT

Since the nineties, the technique of micro computed tomography (micro-CT) has become available with which the exact 3-D microstructure of small bone samples can be determined with a resolution of up to 10 microns, which allows for the non-destructive analysis of bone microstructure. This has proven to be an indispensable tool to monitor the effects of neurectomy and ovariectomy as well as possible treatments for osteoporosis in rats and other animals and has partly replaced the use of static histomorphometry. From the 3-D scan, several bone structural parameters of trabecular bone can be determined by using the automated scanner software (150). The amount of bone in a selected volume of interest is assessed by calculating the ratio between the amount of bone in the volume (BV) and the total volume (TV) of the volume of interest and is expressed as the bone volume fraction (BV/TV). The mean trabecular number (Tb.N), mean trabecular thickness (Tb.Th.), and mean trabecular separation (Tb.Sp.) are calculated using a direct technique based on distance transformation of the reconstruction. This method estimates a volume-based local thickness by fitting maximal spheres to every point in the structure. The trabecular number is the inverse of the mean distance between the mid axes of the trabecular elements (95). The number of connections between the trabecular elements can be expressed by the connectivity density (Conn.D), which is calculated using the Euler method (200). Bone structure can be characterized by the structure model index (SMI), which is a measure for the ratio of plate- to rod-like bone. For an ideal plate and rod structure, the SMI value is 0 and 3, respectively (96). Finally, cortical thickness, cortical bone mass and moment of inertia can be calculated.

After sacrifice of animals in a study, bone samples are collected and micro-CT scans are made. When comparing the several groups, it can be seen whether the treatment has had an effect on bone structural parameters. Although this method gives valuable information, it does not show how the drug has changed the bone over time, like for example does the effect start right away, does it continue over time or wane, does the time-point of treatment initiation and cessation influence bone microstructure,

what is the temporal and spatial pattern of bone alterations? This information is essential to determine the exact treatment potential for osteoporosis.

Recently, *in vivo* micro-CT scanners have become available with which the exact bone microstructure can be monitored in small, living animals (figure 1.6). Erwin Waarsing was one of the first to conduct several studies during his PhD on methodological issues like segmentation (278;281) and trabecular adaptation and growth after ovariectomy (279;280). This apparatus has several advantages: 1) the amount of animals per study can be reduced as animals only need to be sacrificed at the end of the experiment. This saves the life of many animals and is more time- and cost-efficient. 2) Due to the follow-up nature of the study, different statistical methods can be employed. While in cross-sectional studies, mostly a one-way ANOVA is used to determine differences between groups, in follow-up studies ANOVA with repeated measures can be used, which can compare changes over time between groups and is more sensitive to detect smaller differences. This further reduces the number of animals per groups. 3) Follow-up images of the same animal can be rotated and translated such that they exactly overlap, which is called image registration. By using this image registration, local information can be obtained on changes in bone on a micro-level due to formation or resorption resulting from for example ovariectomy or treatment. The *in vivo* micro-CT is limited mainly by two factors: 1) in mature animals, only a few anatomical sites can be monitored *in vivo*, which are the tibia, the distal femur and the tail. 2) Radiation is used, which may damage the bone or other tissues and this therefore limits the number and frequency of scans.

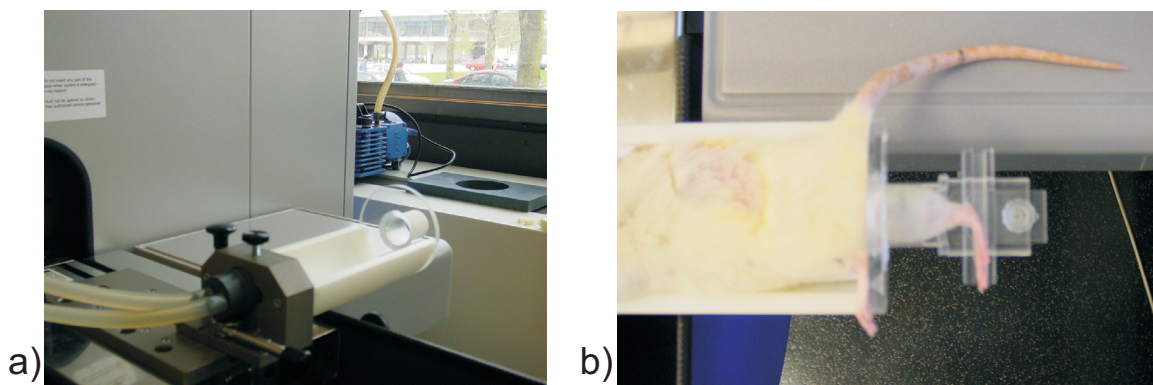


Figure 1.6: a) *In vivo* micro-CT scanner showing rat holder and anesthesia tubes. b) Anesthetized rat lying in the rat holder with one leg fixated for scanning.

1.4.3 Mechanical tests and finite element models

Although bone mass and microstructure have proven to be reasonably good predictors of bone strength (59), an actual measurement of bone strength provides additional insight into the effect of treatments. To this end, mechanical tests are often performed after animals are sacrificed. A commonly used mechanical test is the three-point bending test, which can be done on tibiae and femora. In this test, the bone is placed on the lateral surface on two rounded supporting bars with a certain distance. A preload can be applied at the medial surface of the diaphysis by lowering a third

rounded bar. Then a constant displacement rate is applied until failure. Another possible mechanical test could be done in compression, during which a piece of bone is compressed between two parallel surfaces. For this, a slice of the tibia or femur can be sawed, after which a constant displacement rate is applied until failure. From both tests, stiffness, ultimate force and ultimate displacement can be calculated for each sample.

Besides the monotonic mechanical tests described, dynamic mechanical tests can be performed. Dynamic testing of vertebrae has been extensively done to determine fatigue properties, which resembles the daily life of cyclic loading of the spine (91;178). Tests can be performed either under controlled displacement or load.

Finite element analysis is a well established engineering computational method of strength prediction of complex geometries (217). Finite element models of bone have proven to increase the prediction of bone fracture over that by bone mass (59). They can serve as good replacements for actual mechanical tests when the latter cannot be carried out (e.g. in living animals or humans). Furthermore, they have proven to provide valuable information on strength improvement after drug treatment in osteoporotic patients in clinical trials (135). Also, they can provide additional information on local stresses and strains in the bone, contributions of cortical and trabecular bone to overall strength and influence of tissue properties on strength (222;276).

1.5 Rationale and outline of the dissertation

Although the effects of osteoporosis and several treatments have been thoroughly studied in rats, many aspects are still unknown as they remain unidentifiable in cross-sectional studies for reasons explained above. The *in vivo* micro-CT scanner combined with image registration software offers a potential method to identify effects of osteoporosis and treatments over time. Also, local changes in bone within the same animal can be monitored over time, which taken together can provide novel and relevant information. In this dissertation, we studied the development of two types of osteoporosis in rats and several treatment options for osteoporosis. We first focused on bone resorption inhibitors and then on bone formation enhancers. Changes over time in bone microstructure were determined and in some studies mechanical properties were compared after sacrifice using mechanical tests or finite element models.

Overall, in each animal study of this dissertation, several groups of aged (5.5-8 months old), female Wistar rats were used. The proximal or diaphyseal tibia was scanned in each rat under anesthesia at several time-points to determine changes in bone over time. Every follow-up scan was registered to the baseline scan such that they overlapped. The same volume of interest was analyzed for each measurement and bone structural parameters were determined over time.

As mentioned, possible damaging effects due to radiation when using the *in vivo* micro-CT scanner needed to be determined before any scientific questions could be answered. Therefore, in chapter two, we first studied the effects of radiation. In this study the right tibia of a group of rats was scanned weekly for eight weeks. The left

tibia was only scanned at the first and last time point. Bone structural parameters were compared between both tibiae as well as cell viability, which was determined directly after sacrifice. It was found that eight weekly *in vivo* micro-CT scans did not lead to detectable radiation damage.

Once we established an upper limit of safe usage of the *in vivo* micro-CT, we could address several research questions. Osteoporosis can be caused by estrogen-deficiency and immobilization and may lead to different temporal and spatial patterns of bone loss. This is currently unknown as well as the effects of both types on risk of fracture, which has clinical importance. Therefore, the effects of estrogen-deficiency and immobilization on bone microstructure and strength in mature rats were determined. As mentioned, neurectomy and ovariectomy are two methods to simulate immobilization and estrogen-deficiency induced bone loss in humans. Therefore, in chapter 3 we determined the effects of ovariectomy and neurectomy on bone microstructure in the tibial meta- and epiphysis during four weeks in rats. To determine the effects of both models on mechanical properties, a finite element model of the metaphysis was made and bending properties of the diaphysis were determined with mechanical tests.

Zoledronic acid is the latest bisphosphonate with the highest anti-resorptive potency and has recently been FDA approved for osteoporosis treatment. Weekly injections of zoledronic acid in rats have previously shown to inhibit ovariectomy induced loss of bone mass and strength (85;103). It is unknown how long the effects of a *single* injection last. It is also unknown to what extent bone microstructure and strength can recover after zoledronic acid treatment once osteopenia is already developed, and how this relates to bone that has been *preventively* treated. In chapter four, the effects of a preventive and recovering treatment with a single zoledronic acid injection on bone mass and microstructure were determined over time in the rat tibia.

It is not possible to determine bone microstructure in the vertebra *in vivo*. However, as the vertebra is a clinically relevant site, we also analyzed the vertebrae of the zoledronic acid treated rats after sacrifice in chapter five. As lumbar and caudal vertebrae are loaded differently and have shown to respond differently to ovariectomy (143;162;164;183), we also compared the response to zoledronic acid in both anatomical sites. Finally, the influence of preventive and recovering zoledronic acid treatment on monotonic mechanical properties of lumbar vertebrae was determined.

Vertebral fractures in osteoporotic patients are mostly due to spontaneous fractures, resulting from daily activities or from cyclic loading, rather than from trauma (72;224). Bisphosphonates have shown to influence mineralization (10) and lead to accumulation of microcracks and diffuse damage (38), due to decreased resorption rates. Drug efficacy studies in rats generally focus on changes in bone mass, structure and monotonic mechanical strength, whereas fatigue behavior, which may play an important role in vertebral fractures, may respond differently to pharmacologic intervention than other monotonically-determined mechanical parameters. Therefore, in chapter six, our aim was to develop an experimental approach to determine compressive fatigue mechanical properties in whole rat vertebra, which has not been previously done. This technique then was used to compare fatigue compressive

properties of whole vertebrae in ovariectomized rats treated with zoledronic acid with those of SHAM ovariectomized controls.

After exploring the effects of bone resorption inhibitors we continued with studying the effects of bone formation enhancers. Several aspects of the effects of PTH are still unknown. Therefore, in chapter seven, we aimed to 1) determine the change in trabecular thickness and number after PTH over time, 2) compare the response to PTH between the meta- and epiphysis, 3) determine the effects of PTH on mineralization and mechanical properties, 4) determine the location of new bone formation due to PTH on a micro-level over time and 5) determine predictive value of bone structural properties for gain in bone mass after PTH.

Mechanical stimulation via oscillatory stimulation or vibration plates has been shown to have a potential osteogenic effect on bone, contributing to a bone structure more resistant to habitual loads (75;127-129;201;229;230;294). As such, mechanical stimulation could serve as a potential treatment for osteoporosis, in addition to pharmaceutical intervention. Although the largest increase in bone formation rates have been demonstrated in the tibia of OVX rats, the effects of WBV on bone microstructure are unknown as well as its 3-D effects over time. Therefore, in chapter eight, we analyzed the effects of vibration treatment on tibial bone of ovariectomized, mature rats over time using the *in vivo* micro-CT scanner.

Finally, in chapter nine, an overall conclusion, discussion of results and future work are presented.

Chapter 2

Effects of *in vivo* micro-CT radiation on bone

The contents of this chapter are based on J.E.M.Brouwers, B. van Rietbergen, R. Huiskes, No effects of *in vivo* micro-CT radiation on structural parameters and bone marrow cells in proximal tibia in Wistar rats detected after eight weekly scans, *J Orthop Res.* 2007 Oct;25(10):1325-32

Abstract

Recently developed *in vivo* animal high-resolution micro-CT scanners offer the possibility to monitor longitudinal changes in bone microstructure of small rodents, but may impose high radiation doses that could damage bone tissue. The goal of this study was to determine the effects of 8 weeks *in vivo* scanning of the proximal tibia in female Wistar rats on the bone.

Eight weekly CT scans were made of the right proximal tibia of 9 female, 30-week old, retired-breeder, Wistar rats. Two weeks after the last weekly scan, a final scan was made. Left leg was only scanned during first and final measurements and served as control. A two-way ANOVA with repeated measures was performed on the first and last measurements of left and right tibiae for six bone structural parameters. Bone marrow cells were flushed out and tested for cell viability.

No significant difference was found between left and right for any of the bone structural parameters ($p > 0.05$). Structure model index and trabecular separation significantly changed as a result of aging, while none of the other parameters did. No significant difference was found between left and right in absolute and percentage number of cell viability.

We did not find any indication that the scanning regime applied, in combination with the particular settings used, would affect the results of *in vivo* bone structural measurements in long term studies using aged, female Wistar rats. However, careful consideration should be made when determining the number of scans, particularly when a different experimental design is used.

2.1 Introduction

Recently developed animal high-resolution *in vivo* micro-CT scanners offer the possibility to monitor longitudinal changes in bone microstructure of small rodents (54;278). These scanners, combined with image registration software, provide a promising technique (54;278;279;281) to obtain information regarding changes in bone microstructure due to metabolic diseases such as osteoporosis, metastatic conditions such as bone metastases and bone adaptation resulting from mechanical stimuli. These *in vivo* scanners, however, impose a relatively high ionizing radiation dose, the actual value of which depends on scanning frequency and image resolution.

In typical longitudinal studies the cumulative radiation dose can be on the order of a few gray (Gy), a level at which tissue damage may occur (278). Bone marrow is rather sensitive to radiation: in humans, whole body dosages starting at about 250 mGy lead to reduced lymphocyte counts (39). It was found that a single dose of 5 Gy led to statistically significant changes in bone regeneration, while a 2.5 Gy dose did not (113). Another study found that a 2 Gy dose resulted in alternative growth-plate structures (14). Doses of 400 mGy and lower showed no effects on osteoblast differentiation and activity *in vitro* (53). Bone marrow contains osteogenic progenitor cells, which are closely related to bone formation. Damage to bone marrow cells could lead to changes in bone formation rate and thereby alter bone structure.

Presently, it is not known if tissue damage will affect the results of longitudinal *in vivo* micro-CT studies. In most studies investigating the effects of radiation in animal bone studies, the whole animal was exposed, which is not representative for *in vivo* micro-CT scanning, where typically only a small part of the leg is radiated. In a recent study performed to address this issue, OVX treated mice were used and no effects of radiation were observed (126). In another study, however, in which three weekly *in vivo* micro-CT scans were made of the proximal tibia in three different mouse strains, significant differences were found between the structural bone parameters of the scanned and the control leg for the final measurements of two strains (145). These results suggest that the possible effects of radiation dose on bone structure may depend on the experimental design. Additionally, it is unknown if the results obtained for mice are representative for the rat. The goal of this study was to determine whether an intensive 8 week *in vivo* scanning regime of the rat proximal tibia leads to changes in bone structural parameters and in bone marrow cell viability.

2.2 Materials and methods

Nine female, 30 week-old, retired-breeder, Wistar rats were obtained from Harlan (Horst, The Netherlands) and allowed to acclimatize for 7 days before the start of the experiment. The animals were maintained with a 12:12-hour light-dark cycle and allowed to eat and drink *ad libitum* from a standard laboratory diet. The experiment was approved by the Animals Ethics Committee of the University of Maastricht, the Netherlands.

Weekly *in vivo* CT-scans (Scanco vivaCT 40 scanner, Scanco Medical AG, Bassersdorf, Switzerland) of the right proximal tibia were made during seven weeks at an isotropic resolution of 15 micrometer (figure 2.1). Two weeks after the last weekly scan a final scan was made, since radiation damage was shown to be maximal after that period (61;62). During scanning, the animals were anesthetized with isoflurane for 75 minutes. With the settings chosen, a single scan (70kV, 85 μ A, 1000 projections per 180 degrees, 350 ms integration time), consisting of a stack of 212 images, covers only 3.18 mm axially of the tibia. To include the whole proximal region, two adjacent scans were required, resulting in a total scanning time of about 35 minutes. In the beginning of the experiment, some CT-scans showed movement artifacts due to poor leg fixation. As a result of these artifacts, the two adjacent stacks did not align properly. It was therefore decided to generate two separate stacks of 3.18 mm of the proximal tibia, overlapping 0.3 mm. These stacks were later attached by in-house registration software (275), resulting in a CT-scan that covered 6.06 mm of the proximal tibia. A new leg-fixating device was later developed that solved the movement artifact problem, but the procedure with overlapping stacks was maintained.

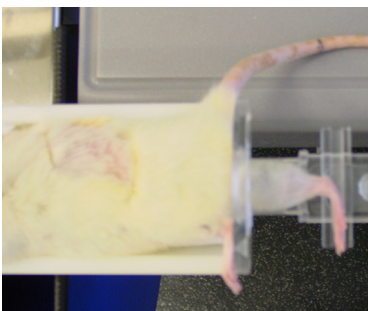


Figure 2.1: Rat lying in the *in vivo* micro CT-scanner with one leg fixated in the developed leg-fixating device.

In order to determine the radiation dose, the local CT dose index (CTDI) was measured for the scanning protocol, to which the animals were subjected, using a dose meter with ionization chamber (Solidose 400, RTI, Mölndal, Sweden). Two different measurements were performed. The first measurement was made in air and resulted in a CTDI value of 939 mGy. The second measurement was made at the center of a 35 mm perspex cylinder that was used as a phantom and resulted in a total dose of 441 mGy. Since soft tissues are surrounding the bone when scanning *in vivo*, the value to which the actual bone is exposed is lower than the value measured in air, although it will be higher than the value measured in the perspex cylinder, which is much larger than soft tissue around the tibia. It should be emphasized here that the CTDI measure takes the actual dose profile into account and will result in a value that can be considerably higher than local dose values measured and thus represents a higher estimate. Although two partly overlapping image stacks were made, the dose in the overlapping region will not be higher than elsewhere. This is due to the fact that the dose profile of the cone beam is such that the dose is maximal at its center and decreases considerably near the sides of the scanned region. Since, by definition, the

overlapping areas are the edges of two scanned regions, the lower radiation dose compensated for the double exposure. Naturally, the whole-body dose does increase when imaging multiple stacks. However, since only a small part of the animal was radiated, the whole-body dose was very small in all cases.

The left tibia, serving as a control, was only scanned at the first and the final time points, and underwent a SHAM-scan for all other measurements. During the SHAM measurements, the animals were put in the micro-CT scanner with their left legs placed in the holder for the same time period as required for a normal measurement, but the legs were not exposed to any radiation. This was done to rule out other possible harmful effects of the procedure, such as stretching of the leg. The design of the rat holder was such that the left leg was not exposed to radiation while scanning the right leg.

Image processing included Gaussian filtering and segmentation. The same filter and segment values were used for every measurement of every animal ($\sigma=0.7$, $\text{support}=1$, $\text{threshold density}=0.504$ g HA/cc). From every baseline and follow-up CT-scan, the metaphyseal area was manually selected by drawing a contour file by the same operator. For each measurement, a new contour file needed to be drawn, because the rats still showed minor growth and remodeling and therefore the previous contour file would not exactly fit. The images were rotated such that each slice showed the bone longitudinally and therefore the whole region below the growth plate could be selected. From the selected region, bone structural parameters were automatically determined: bone volume fraction (BV/TV), connectivity density (Conn.D), structure model index (SMI), trabecular number, thickness and separation (Tb.N, Tb.Th, Tb.Sp). In addition, the average attenuation coefficient of the trabecular bone tissue was determined for all measurements to determine if any changes in bone mineral content could be detected. In our analyses, we focused on the metaphyseal bone, since this part contains newly formed bone from the growth plate and it is known that the growth plate is the most sensitive to radiation. We presumed that if no effects in the metaphysis were found, none would be present in the epiphysis.

The reproducibility of the measurements was investigated in an adjoining pilot study. In this pilot study, the right tibia of a dead rat was measured four times on the same day using the same protocol as used in the radiation effects study. After each measurement, the animal was removed from the holder and repositioned. A contour file was made for the first scan and was applied to the follow-up scans after image registration. Bone structural parameters were determined for all CT-scans according to the method as described earlier. Based on these results, the coefficient of variation (CV) was calculated for each of the investigated parameters. It was found that the CV was less than 1% for all parameters (BV/TV, SMI, Tb.Th, Tb.Sp, Tb.N) with the exception of Conn.D, for which a value of 2% was found.

When two CT-scans of the same animal are made at different time points, the position of the animal in the scanner will not exactly be the same and therefore the CT-scans will also differ in position. In order to detect bone structural changes on a micro-level, one CT-scan needs to be translated and rotated to match the other. We developed image registration software that registers two scans based on minimizing the

correlation coefficient (275). Every weekly scan was registered with the first scan, hereby revealing any possible changes in the microstructure.

It was assumed that any natural changes in the bone structural parameters, throughout the experiment, would be similar in the left and right legs. Furthermore, it was assumed that the effects of the radiation dose on the structural parameters would be negligible if no significant differences in structural parameters after 9 weeks were observed between left and right. Any damaging effect of the first scan on the left tibia was assumed to have been resolved after 9 weeks. A two-way ANOVA with repeated measures was performed on the first and last measurement of the left and the right tibia to determine time effects, group differences and time*group effects. This was done for all structural parameters and the average attenuation coefficient of the trabecular bone tissue. In addition, a regression analysis was performed for the structural parameters of all measurements from the right legs of all rats. For all statistical tests, p-values below 0.05 were considered significant.

The animals were sacrificed after their last scan. To determine cell radiation damage, the scanned parts of both left and right tibiae were sawed off, using an Accutom5 precision cut-off machine (Struers GmbH, Maassluis, Netherlands). A needle filled with α -medium, containing several antibiotics, was placed in the scanned part of both tibiae and released under pressure, flushing out the bone marrow cells. The cell suspensions were incubated at 370⁰ C during 1 to 6 hours for storage, after which a cell viability test was performed with trypan blue. No influence of the storage time was seen in the viability test. The absolute number and the percentage of living and dead cells were determined for both tibiae. A paired student t-test was performed to determine any significant difference in absolute and percentage numbers of viable cells between the left and right tibia.

2.3 Results

All animals showed normal body weight gains. No loss of hair and no skin erosions occurred throughout the experiment, indicating healthy conditions. Figure 2.2 shows the same slice taken from two registered, processed CT-scans of the same rat at weeks 0 and 9. After image registration it can be seen that minimal linear growth has taken place, which can be expected in 30-weeks old rats (280).

With the initial rat holder, movement artifacts were occasionally present in the CT-scans, due to poor leg fixation. Since these artifacts resulted in errors in the determination of bone parameters, they were excluded from further analysis. The criterion for exclusion was based on the blurring of the image and on the correlation coefficient generated by the registration procedure when fitting the overlapping region, as observed by the operator, resulting in the exclusion of eight measurements. Measurements showing only minor movement artifacts were included for analysis, but may have slightly affected the bone parameter values and thus the precision. Figure 2.3 shows the bone structural parameters for all rats longitudinally, where the missing markers indicate excluded measurements. Figure 2.4 shows mean and standard

deviations for all structural parameters for the first and last measurements of both left and right tibia. BV/TV and SMI were found to be significantly different at baseline between left and right.



Figure 2.2: *Left: longitudinal section through CT-scan showing bone at week 0 and 9 of same rat after global registration. Yellow indicates bone at week 0, green indicates bone at week 9, black is overlap. Note that linear growth has taken place, shown by the slight downward movement of the metaphyseal trabeculae. Also, the shape of the bone has slightly changed due to bone remodeling. Middle: longitudinal section showing a typical CT-scan after registration of the two stacks, black is the overlap. Right: Zoomed section of CT-scan showing overlap of two stacks after registration.*

A two-way ANOVA with repeated measures on the first and last measurements of both tibiae revealed no significant differences between left and right for any structural parameter. For SMI and Tb.Sp, significant time effects were determined (Table 2.1). SMI decreased in time and Tb.Sp increased in time. The two-way ANOVA with repeated measures showed no significant differences between left and right, and no significant changes over time for the bone tissue attenuation coefficients ($p=0.10$ and $p=0.48$ respectively).

A regression analysis was performed on all measurements for the right tibia, for all structural parameters of each rat, to determine differences in response between rats. While on average a significant effect of age was found on Tb.Sp and SMI, the regression analyses for all rats individually on Tb.Sp. showed significant increases for some rats, non-significant decreases for other rats and non-significant increases for other rats yet, indicating the diversity. A similar diversity was seen for SMI, where some rats showed significant increases and others showed non-significant increases or decreases. Diversity was also seen for all other structural parameters; significant increases were found in some rats and none significant increases or decreases in other rats.

In the trypan blue test, the percentage dead cells were determined to be on average 6 and 7%, respectively for the right (scanned) and left (control) leg. A paired student t-test revealed no significant difference between the percentage living cells of the right and left tibiae ($p=0.39$). The absolute numbers of living and dead cells were also not significantly different ($p=0.37$, $p=0.47$, respectively). Figure 2.5 is a typical image from trypan blue staining of tibial bone marrow cells, showing mostly living cells.

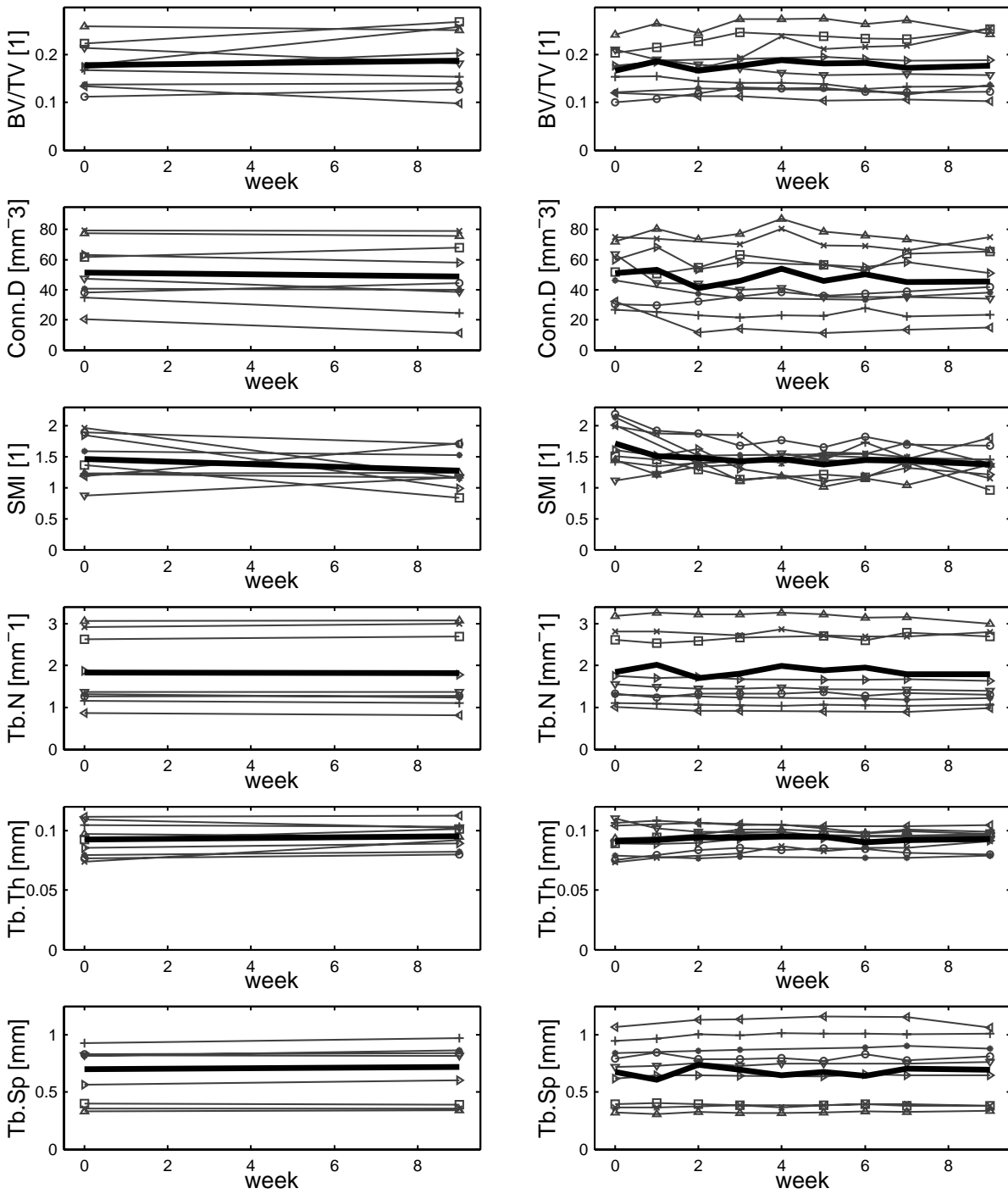


Figure 2.3: Morphological parameters for all animals individually for the left, control tibia (left column) and right, scanned tibia (right column). The same marker is used for every animal in each figure. The thick black line indicates the average value per measurement.

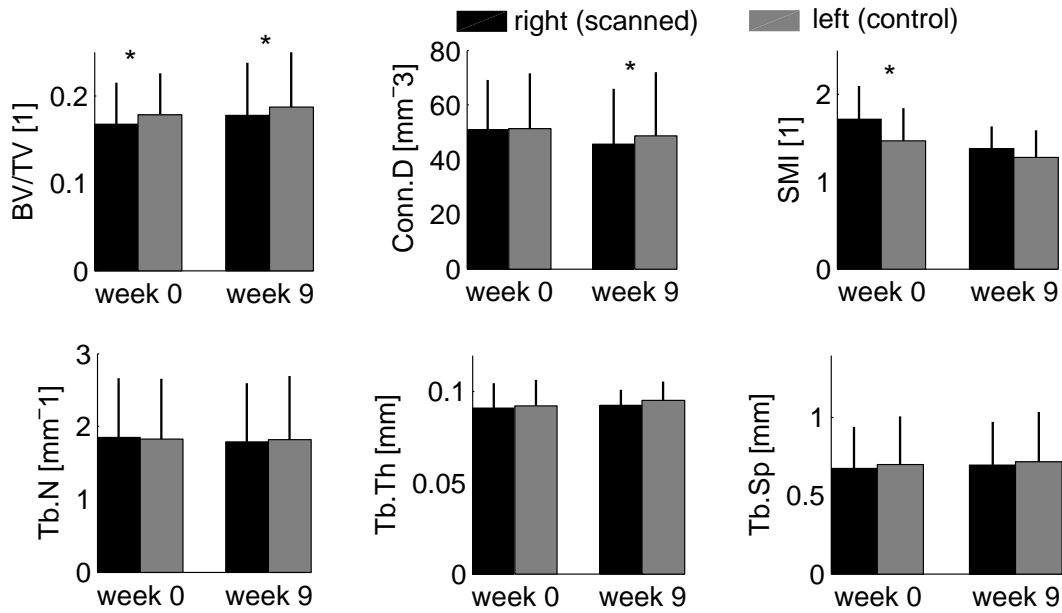


Figure 2.4: Average values and standard deviations for all structural parameters of the first and last measurements in right (scanned) and left (control) legs. Asterisk indicates a significant difference between left and right at that time-point.

Table 2.1: Two-way ANOVA with repeated measures: *p*- and *F*-values

	BV/TV		Conn.D		SMI		Tb.N		Tb.Th		Tb.Sp	
	<i>F</i>	<i>p</i>	<i>F</i>	<i>p</i>	<i>F</i>	<i>p</i>	<i>F</i>	<i>p</i>	<i>F</i>	<i>p</i>	<i>F</i>	<i>p</i>
Time	2.170	0.162	1.16	0.299	10.1	0.007 ^a	3.630	0.077	1.31	0.269	14.6	0.002 ^a
Group	0.207	0.656	0.122	0.732	1.147	0.302	0.003	0.956	0.044	0.836	0.000	0.988
Time*group	0.004	0.952	0.137	0.717	0.171	0.685	3.038	0.103	0.122	0.732	0.762	0.398

BV/TV, bone volume fraction; Conn.D, connectivity density; SMI, structure model index; Tb.N, Tb.Th, Tb.Sp, trabecular number, thickness, and separation.

^a Significant value.

2.4 Discussion

In this study we determined whether an intensive 8 weeks *in vivo* scanning regime of the rat proximal tibia would lead to changes in bone structural parameters or bone marrow cell viability. The scanning frequency was higher than necessary for most studies, thus representing a worst-case scenario. Even then, it was found that no significant changes were determined in bone structural parameters and in bone marrow cell viability as a result of radiation damage.

Our results agree with the work from Judex et al. (126), in which no radiation effects were found in OVX mice. They do, however, seem to contradict the results from a radiation study using a similar radiation dose from Klinck et al. (145), who reported a significant difference between the structural bone parameters of the scanned

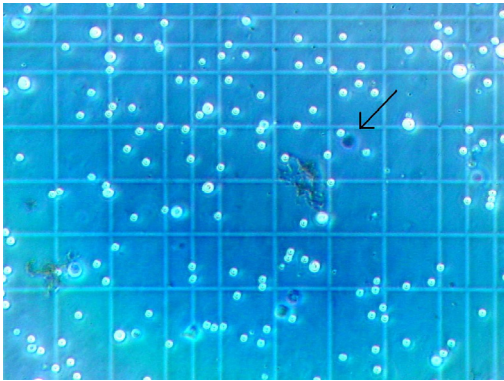


Figure 2.5: A typical image from the trypan blue staining of tibial bone marrow cells. Arrow indicates a dead cell. Mostly living cells can be seen (white dots).

and control leg at the final measurement for two out of three strains of mice used. These mice, however, were between eight and ten weeks old and still had an active growth plate. Our results also do not correspond with observations from Waarsing et al (277;280). Additional dose measurements with the same dose meter using their micro-CT equipment and protocols, however, revealed that the applied CTDI, in air as well as in water, in their studies was twice as high as that in our study, which could explain why effects were seen in their studies and not in our study. In general, results from different studies may be difficult to compare, as some authors report the radiation dose measured in air while others report the dose measured in water or in PMMA. Our findings suggest, however, that the applied radiation dose was close to the maximum acceptable dose and that its effects may depend on the type, age and strain of animal, and on scanning parameters, scanning regime and type of scanner.

Another explanation for the differences between our and earlier studies would be that the stretching and immobilization of the leg that is required to position the leg in the holder on itself could affect the bone structure. During a scan the radiation source needs to be able to rotate around the object to be scanned and therefore, the leg needs to be maximally pulled down, away from the body and fixated. Our fixating device was such that the hip and knee joint were maximally stretched and the ankle joint was kept in a 90 degree angle. It is possible, for example, that the stretching would lead to a period of reduced loading of the bone for some period after the experiment, which could induce bone loss. The design of our study was such that the effect will be the same for left and right and therefore we only determined the effect of the radiation, which was the goal of this study. In these earlier studies that did report effects of radiation, however, no sham scans were made for the contralateral leg.

A significant decrease in SMI, which indicates a change from more rod-like to plate-like bone, and a significant increase in Tb.Sp were found in both tibiae as a result of aging. Although Tb.Sp is expected to increase as a result of aging, SMI is not expected to decrease (32); it might indicate that mostly rod-like trabeculae have disappeared. The fact that changes in SMI and Tb.Sp took place in both tibiae indicates that normal bone remodeling was actually taking place and that bone cell activity was not much affected by the radiation dose. This was also supported by the fact that linear growth and bone remodeling was seen in the CT-scans after global registration (Figure

2.2). No significant overall effect of time was determined in the two-way ANOVA with repeated measures for BV/TV, Conn.D, Tb.Th and Tb.N in the right leg. However, the regression analyses showed significant increases in some rats, significant decreases in others and none significant changes in some rats. This indicates that the individual effects of time varied per rat to some extent.

Figure 2.3 shows there was quite some variability in the follow-up measurements. For each measurement, a new contour file needed to be drawn by the operator to select the region of interest (ROI), because the rats still showed minor growth and remodeling and therefore the previous contour file would not exactly fit. The operator decided manually if newly formed bone was labeled as trabecular bone and therefore included in the ROI or not. Besides this, between each measurement, there was minor linear growth, which means in between two measurements, newly formed bone entered the ROI and some bone exited the ROI on the distal side. Also, minor movement artifacts and experimental variation may have influenced variability.

Since the scanner was calibrated with a hydroxyapatite phantom, a direct, linear relationship exists between the bone tissue attenuation coefficient measured and hydroxyapatite density. We found that the attenuation coefficient did not change significantly over time and did not differ between left and right, indicating that the hydroxyapatite density did not change as a result of aging or radiation. The implications of these results remain limited due to partial volume effects in the scan. However, these results do suggest that bone-tissue mineralization did not change as a result of radiation.

No significant difference was found between the percentage viable cells in right and left tibiae, indicating neither long nor short-term effects on cell viability, which concurs with expectations based on the CTDI (53). Overall effects on all cells were determined and it is possible that certain cell types may have shown relatively large cell deaths. However, since the percentage dead cells was very low, and our aim was to test the legitimacy of using this *in vivo* micro-CT scanning regime, we found it reasonable to determine the overall number of cells. It is also possible that cell damage occurs after several hours, after which it would be repaired again. Such damage would have remained undetected by our methodology. However, it is thought that the most relevant finding for future *in vivo* micro-CT experiments is that no long-term damage was found. The final CT-scan was taken two weeks after the last weekly scan, indicating that any possible undetected cell damage will at least be resolved within two weeks.

A paired student t-test comparing the structural parameters of the left and right leg found a significant difference in BV/TV and SMI. These differences are probably due to natural variance between left and right, but also the region of interest selected from the image by the operator may have been slightly different.

The rats used in this study were retired breeders. Figures 3.3 and 3.4 show that the variation of structural parameters within the group of rats was quite large. They also show that BV/TV and Tb.Th were lower and Tb.Sp was higher than normally seen in 30-week old Wistar rats (110), but are consistent with previous data on retired breeders (140;156). Although structural parameters may differ between normal rats and retired

breeders, it is thought that the rats used were suitable for determining any possible radiation damage in general for female Wistar rats.

Although the left leg was not exposed to radiation when scanning the right leg, systemic radiation effects could have occurred when scanning the right leg, possibly affecting the left leg. However, since the scanned area is relatively small compared to the total body volume, it was assumed that any systemic effect is negligible.

In this study an *in vivo* rodent high-resolution micro-CT scanner was used, suitable to monitor changes in bone microstructure per animal individually, rather than by comparing averages of different groups. This reduces the number of animals needed per experiment by a factor as high as the number of measurements performed. Furthermore, each animal served as its own control, thereby enabling detection of subtle changes in bone structural parameters by paired and repeated measures statistics.

In conclusion, we did not find any indication that the scanning regime applied, in combination with the particular settings used, would affect the results of *in vivo* bone structural measurements in long term studies using aged, female Wistar rats. However, careful consideration should be made when determining the number of scans and the CTDI, particularly when a different experimental design is used.

Acknowledgements

This work was funded by the Netherlands Organisation for Scientific Research.

Chapter 3

Estrogen-deficiency and immobilization induced osteoporosis

The contents of this chapter are based on J.E.M.Brouwers, F.M.Lambers, B.v.Rietbergen, K.Ito, R.Huiskes, Comparison of bone loss induced by ovariectomy and neurectomy in rats analyzed by *in vivo* micro-CT, *J Orthop Res.* 2008, *submitted*

Abstract

Our aim was to test the hypothesis that osteoporosis due to estrogen-deficiency progresses at a faster rate than due to immobilization and that at the same level of bone loss, immobilization-induced bone loss leads to less favorable bone structure and mechanical properties than estrogen-deficiency induced bone loss.

Adult rats were divided into: ovariectomy (OVX) (n=9) and neurectomy (NX) (n=8). At week 0, 1, 2, 3, 4 *in vivo* micro-CT scans were made (vivaCT 40, Scanco Medical AG) of the proximal tibia. Metaphysis of the segmented CT-scans at weeks 0 and 4 were used for a three-dimensional voxel based micro finite element model (FEM). Displacement in the longitudinal direction was prescribed at the proximal end leading to a compression step of 1%. Tibial, mechanical properties were determined in a three-point bending test after sacrifice.

After four weeks, severe deterioration of bone microstructure was seen in the metaphysis in both the OVX and NX groups. Tb.Sp and DA were significantly more deteriorated after OVX. In the epiphysis, bone loss was less severe in both groups, though BV/TV, Conn.D and Tb.N, were significantly lower in the NX compared to the OVX group. Bone in NX rats group appeared more flake-like than in OVX rats and than before surgery. FEM derived stiffness decreased by 29% after OVX and 41% after NX, accompanied by a decrease in bone volume and average von Mises stress. The latter was found to decrease significantly more after NX. No differences were found in bending properties.

Osteoporosis due to estrogen-deficiency progressed at the same rate as that due to immobilization. At the same level of bone loss, immobilization-induced bone loss led to less favorable bone structure and mechanical properties than estrogen-deficiency induced bone loss.

3.1 Introduction

Osteoporosis is a degenerative bone disease that can develop with reduced levels of estrogen during and after menopause. It can also develop after long periods of immobilization or disuse, for example with prolonged bed rest or diminished physical activity. As many postmenopausal women also have limited daily physical activity, they are at increased risk for an osteoporotic fracture.

The rat has been extensively used to study both types of osteoporosis. Estrogen deficiency associated bone loss is induced in these animals by ovariectomy (OVX) (33;57;153;288), while immobilization associated bone loss is induced by sciatic neurectomy, tail suspension or leg taping (270;301). Using such animal models, it has been shown that both types of osteoporosis can severely deteriorate the bone structure. It is known as well, that differences exist between these forms of bone loss. Firstly, it has been established that differences exist in cellular activity (107;148). Whereas ovariectomy leads to an increased bone formation and resorption rate, immobilization leads to decreased turnover rates (7;165;285). This would suggest that bone loss after OVX might proceed faster than that after immobilization.

Secondly, differences exist in the resulting deterioration of bone mass and microstructure (7;43;50;108;159;165;260;285;298). It has been reported that after estrogen-deficiency, bone loss is concentrated in the central part of the metaphysis whereas immobilization leads to an overall loss of bone (7;108;298). This finding supports the hypothesis that ovariectomy induced estrogen-deficiency increases the mechanostat threshold (285), leading to the low loaded regions being resorbed first, whereas the main loaded structures would remain. In the case of immobilization, however, all bone tissue is unloaded and a more random pattern of bone loss would be expected (285). This would suggest that immobilization induced osteoporosis would lead to a more severe loss of the main trabecular structures and thus a more severe loss of stiffness and strength in the main loading direction. It would also suggest that, upon reloading, distribution of loads in immobilized bones would be very inhomogeneous since the adaptation to the loading direction is lost (274).

Based on the results of these previous studies, we hypothesized, first, that bone loss due to estrogen-deficiency would progress at a faster rate than bone loss due to immobilization and, second, that, at the same level of bone loss, immobilization induced bone loss would lead to less favorable bone structures and mechanical properties than estrogen-deficiency induced bone loss. If this hypothesis can be confirmed, this would have consequences for our understanding of bone fracture risk with osteoporosis. When translated to clinical practice, it would, for example, suggest that bone fracture risk of patients that lose bone due to reduced mechanical loading (e.g. bedridden patients or astronauts) would be higher than that of patients with estrogen-deficiency induced osteoporosis, when having the same bone density.

We aimed at testing this hypothesis by studying bone mass and structure over time in the tibia using an *in vivo* micro-CT scanner. The ovariectomized rat was used as a model for estrogen-deficiency and the neurectomized rat was used to model

immobilization. Changes in bone structure were determined in the metaphysis, which is the most common region for structural analysis. For this region, changes in mechanical properties were determined as well using micro- finite element analysis (μ FE). In addition, changes in bone structure in the epiphysis were studied, as differences in mechanical loading between the meta- and epiphysis that have been previously reported (282;285) might result in differences in the response between these sites. Finally, cortical mechanical properties were determined in both groups using a three-point bending test.

3.2 Materials and methods

3.2.1 Animals

Eight 5.5-month old virgin Wistar rats were obtained from Harlan Laboratories (Horst, the Netherlands) and allowed to acclimatize for 7 days before the start of the experiment. These rats were used for a neurectomy experiment (NX). A year later, twelve rats were obtained from the same breeding laboratory, which were also 5.5-month old virgin Wistar rats, to be used for an ovariectomy experiment (OVX). From these rats, 9 were selected based on the first CT-scan to result in a similar distribution in bone mass as in the neurectomy experiment. All rats were maintained with a cycle of 12 hours light and 12 hours darkness and allowed to eat and drink *ad libitum*. The experiment was approved by the Animals Ethics Committee of the University of Maastricht, the Netherlands. At week 0, the OVX rats were ovariectomized and the NX rats underwent a unilateral sciatic neurectomy, while the contralateral leg was SHAM operated. Success of OVX was confirmed at necropsy by determining atrophy of the uterine horns. Rats were sacrificed at 14 weeks under deep anesthesia by cervical dislocation.

3.2.2 Micro-CT scanning

Directly after the operation, a micro CT-scan (70 kV, 114 μ A, 1000 projections per 180 degrees, 261 ms integration time) with an isotropic resolution of 15 microns was made of the proximal tibia (6 mm) using an *in vivo* micro-CT scanner (vivaCT 40, Scanco Medical AG, Brüttsellen, Switzerland). In the OVX group one leg was scanned and in the NX group both the treated and SHAM operated (data not shown but referred to in Discussion) legs were scanned. The CT-scanner was calibrated and a beam-hardening correction algorithm was applied to all scans. Follow-up *in vivo* CT-scans were made after 1, 2, 3 and 4 weeks to monitor bone structure. Every follow-up scan was registered with the first scan by using image registration software that registers two scans based on minimizing the correlation coefficient (275). Total scanning time was 38 minutes for the OVX group and 76 minutes for the NX group, during which the animal was anesthetized with isoflurane and the scanned leg was placed in a custom-made leg-holding device. The design of the rat holder was such that the left leg was not exposed to radiation while scanning the right leg. Radiation

damage to the scanned bone was not expected to occur, based on a previous study, in which 8 weekly CT-scans with the same radiation dose caused no detectable bone damage (36). In that study, we also showed that the reproducibility of all structural parameters was high with a coefficient of variation of about 1%.

From the CT-scans the metaphyseal and epiphyseal trabecular bone was analyzed. Image processing of the metaphyseal and epiphyseal trabecular bone included Gaussian filtering and segmentation and was described elsewhere in detail (36). In brief, the same filtering and segmentation values were used for every measurement of each animal ($\sigma=0.7$, $\text{support}=1$, $\text{threshold density}=0.575$ g HA/cc, equivalent to 24% of maximal grayscale value). From every baseline and follow-up CT-scan, the trabecular bone of the meta- and epiphyseal area was manually selected and bone structural parameters (bone volume fraction (BV/TV), connectivity density (Conn.D), degree of anisotropy (DA), trabecular number, thickness and separation (Tb.N, Tb.Th, Tb.Sp)) were automatically determined.

3.2.3 Finite element model

Segmented CT-scans of the measurements taken at weeks 0 and 4 were used as input for a three-dimensional finite element model. In the first CT-scan of each rat, the tibia-fibula junction was determined. Starting five slices distally to this junction, 100 slices were selected in the first and last CT-scan, which was registered to the first CT-scan, including trabecular and cortical bone of the metaphyseal tibia. Bone voxels were directly converted to equally sized 15- μm brick elements, rendering FE meshes of between 2.6 and 4.4 million elements. Each element was assigned a Poisson's ratio of 0.3 and an isotropic Young's modulus of 10 GPa (the actual value did not influence our results, as our aim was to compare changes in FEM derived properties over time between groups). Displacement in the longitudinal direction was prescribed at the proximal end leading to a compression step of 1%. Displacement in all other directions of the proximal end was suppressed and displacement of the distal end was suppressed in all directions.

The linear-elastic micro-FE models were solved using an iterative element-by-element solver (Scanco Medical AG, Brüttsellen, Switzerland). The computations for all tibiae were sufficiently converged (relative errors in the residual forces and displacements were less than 0.001) (221;223). Several properties were calculated for all samples. Stiffness was computed as the total reaction force needed to achieve 1% compression divided by the displacement. Also, mean von Mises stress as well as coefficient of variation of von Mises stress, defined as the standard deviation divided by the mean times 100%, were determined among all elements per sample. Finally, total bone volume in the model, consisting of trabecular and cortical bone, was determined for each sample.

3.2.4 Three-point bending of tibiae

After sacrifice, all tibiae were dissected and frozen in PBS solution at -20°C . They were thawed prior to three-point bending. The tibia was placed on the lateral surface on two rounded supporting bars with a distance of 2.4 cm. A preload of 1 N was applied (ZWICK, Z020) at the medial surface of the diaphysis by lowering a third rounded bar. A constant displacement rate of 6 mm/min was applied until failure. Displacement was measured from the actuator displacement transducer of the testing machine. From the force-displacement curve, the following mechanical parameters were determined: 1) ultimate load, defined as the maximum load, 2) displacement at ultimate load, which was corrected for the toe region and 3) stiffness, calculated as the slope in the linear region between 40 and 80% of the ultimate load.

3.2.5 Statistics

All parameters were analyzed with an ANOVA with repeated measures using SPSS 15.0 to determine if there was a significant effect of time, group and interaction between time and group. Mauchly's test was first used to verify the assumption of sphericity. If this assumption was not met, a correction was done using the Huynh-Feldt method. All p-values below 0.05 were considered significant. If a p-value was found to be significant in the univariate test, we continued the analysis by looking at the tests of within-subjects contrasts, which was part of the ANOVA with repeated measures, where results using the linear fit were taken. The p-values found here were used to determine whether a result was significant or not. This procedure was performed according to the methods of Field (65) and UCLA Academic Technology Services (290). A paired student's t-test was done within both groups, to determine at what week bone structural parameters were significantly different from week 0.

3.3 Results

3.3.1 Effects of ovariectomy and neurectomy on metaphyseal, trabecular bone

After OVX, all bone structural parameters were already significantly deteriorated at week 1, except for Tb.Sp, which was only significantly increased after week 2 (figure 3.1). After NX, all bone structural parameters were already significantly deteriorated at week 1, except for Tb.N and DA, which were only significantly altered after week 3 and 4, respectively. At week 4, a reduction in BV/TV of 65 % and 69 % in the OVX and NX group, respectively, was found. Bone loss was located in the OVX group mostly in the anterolateral, distal side of the trabecular bone, while bone loss was more uniform in the NX group (figure 3.2). On the lateral side, just below the growth plate, bone loss was more severe in the NX than OVX group. Bone loss was also located centrally in both groups. Bone in NX rats group appeared more flake-like than in OVX rats and than before surgery.

All structural parameters showed a significant effect of time. A significant effect of group was found in Tb.Th, reflecting the small differences that were present between the groups at the start of the experiment. In both groups, bone loss was accompanied by both a decrease in Tb.N and Tb.Th, although the decrease in the latter waned in the OVX group. A significant interaction between group and time was only found for Tb.Sp and DA, interactions for all other structural parameters were not significant.

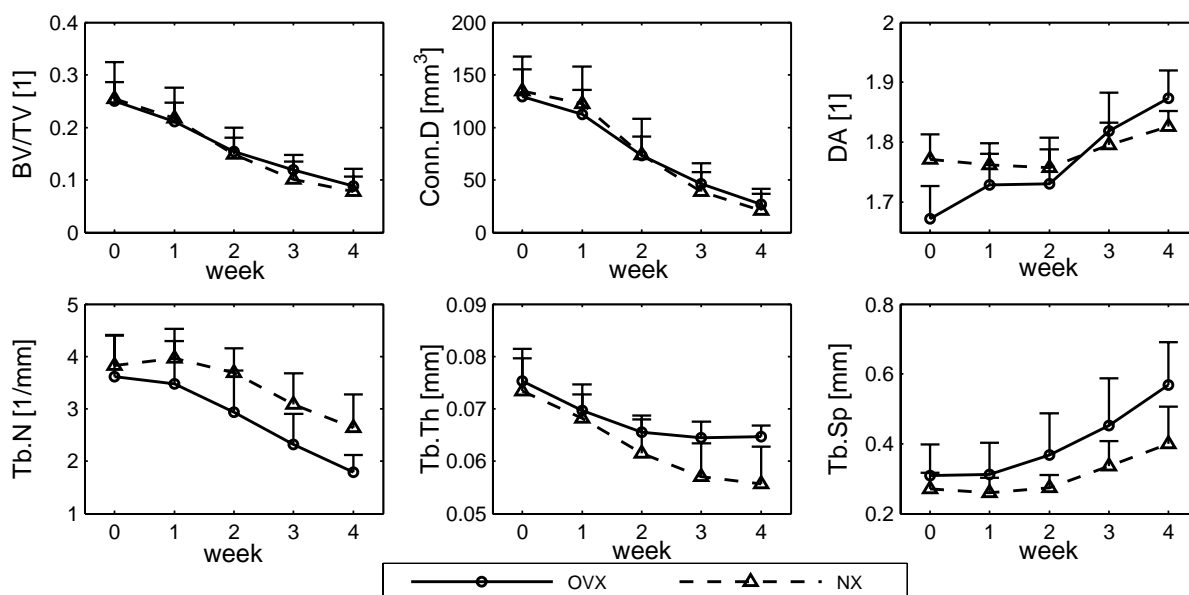


Figure 3.1: Structural parameters in the metaphyseal, proximal tibia for all groups at all time points (mean \pm SD).

3.3.2 Effects of ovariectomy and neurectomy on epiphyseal, trabecular bone

After OVX, all bone structural parameters were already significantly deteriorated at week 1, except for Conn.D and DA, which were only significantly altered after week 2 and 4, respectively (figure 3.3). After NX, all bone structural parameters were already significantly different at week 1, except for Tb.N and Tb.Sp, which were only significantly altered after week 2 and 4, respectively. At week 4, a reduction in BV/TV of 12 % and 20 % in the OVX and NX group respectively was found. Bone loss was most severe just above the growth plate in both groups and no apparent differences were found in the location of bone loss. Bone in NX rats group appeared more flake-like than in OVX rats and than before surgery.

All structural parameters showed a significant effect of time. A significant effect of group was found in Tb.Th, reflecting the small differences that were present between the groups at the start of the experiment. A significant interaction between group and time was found for BV/TV, Conn.D and Tb.Th, interactions for all other structural parameters were not significant.

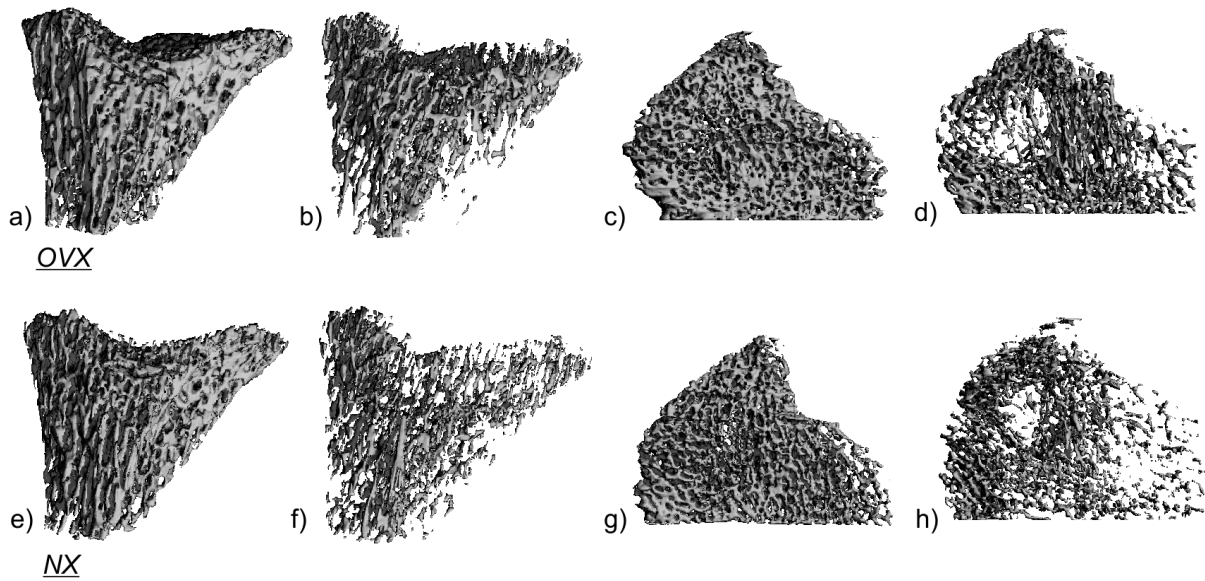


Figure 3.2: 3-D, segmented CT-scans from OVX rat taken at week 0 (a, c) and 4 (b, d), and NX rat at week 0 (e, g) and 4 (f, h). Anterior images (a, b, e, f) show that bone loss was located in the OVX group mostly in the anterolateral, distal side of the trabecular bone, while bone loss in the NX group was more uniform. Top view images (c, d, g, h) show that on the lateral side, just below the growth plate, bone loss was more severe in the NX than OVX group and that bone loss took place centrally in both groups.

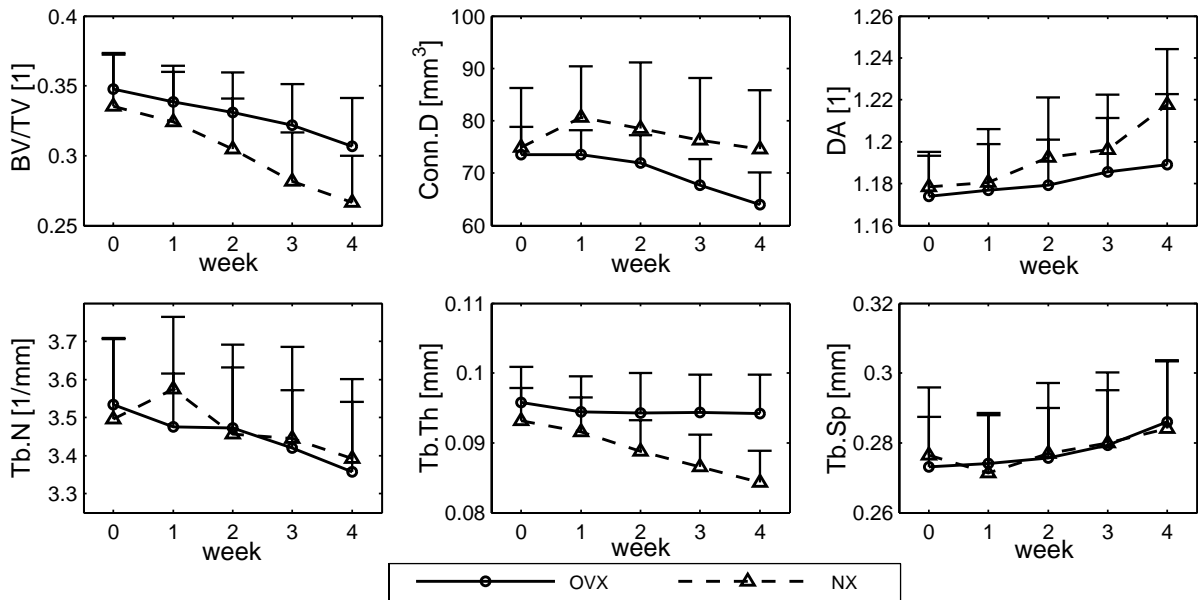


Figure 3.3: Structural parameters in the epiphyseal, proximal tibia for all groups at all time points (mean +/-SD).

3.3.3 Effects of ovariectomy and neurectomy on FEM derived properties

All FEM derived parameters significantly changed over time (figure 3.4 and 3.5). After OVX, stiffness significantly decreased with 29% in four weeks accompanied by a 14% decrease in bone volume and a 12% decrease in average von Mises stress. After NX, stiffness significantly decreased with 41% in four weeks accompanied by a 20% decrease in bone volume and a 19% decrease in average von Mises stress. The interaction between time and group for stiffness almost reached significance ($p=0.056$). The decrease in bone volume was not significantly different between the OVX and NX group, while the decrease in average von Mises stress was significantly different. A significant interaction between time and group was also found for coefficient of variation von Mises stress.

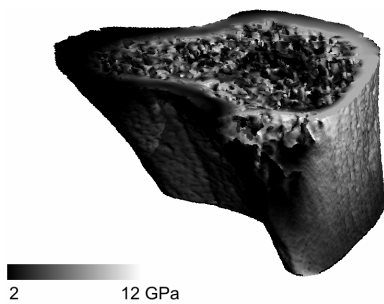


Figure 3.4: Distribution of FEM derived von Mises stress in the metaphysis.

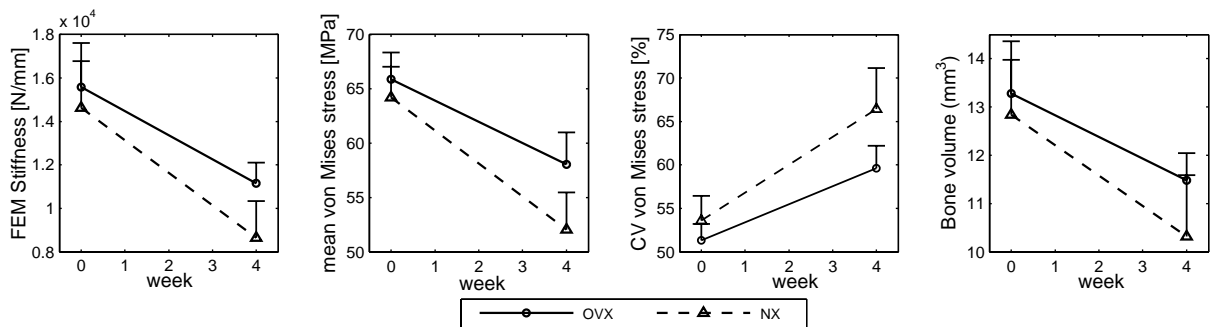


Figure 3.5: FEM derived stiffness, mean von Mises stress, coefficient of variation (CV) in von Mises stress and bone volume in the metaphyseal, proximal tibia in both groups at weeks 0 and 4 (mean \pm SD).

3.3.4 Three-point bending of tibiae

No significant differences were found in all mechanical properties between both groups (figure 3.6).

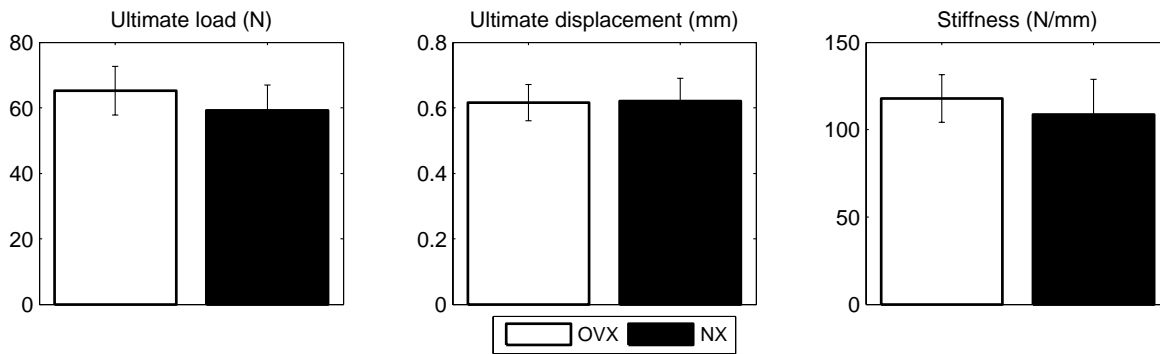


Figure 3.6: *Ultimate load, ultimate displacement and stiffness determined from three-point bending test on tibiae after sacrifice at 4 weeks. No significant differences were found between OVX and NX.*

3.4 Discussion

The rates of bone loss during four weeks of estrogen-deficiency and immobilization in the tibial metaphysis of rats were very similar. In the epiphysis, the rate of bone loss was much lower than in the metaphysis, and some differences were found over time between both groups. This indicates that deterioration of bone mass and structure after estrogen-deficiency and immobilization proceeds at the same rate in the metaphysis only, hence, the first part of our hypothesis was not fully supported. A possible explanation for this finding is that immobilization results in more bone to be resorbed per remodeling cycle such that, although bone turnover rate is lower, bone loss proceeds at the same rate as after estrogen-deficiency.

Changes in bone volume fraction over time and several bone structural parameters in the metaphysis were similar after estrogen-deficiency and immobilization. However, the degree of anisotropy and trabecular separation increased more after estrogen-deficiency than after immobilization. Also, trabecular structure in the NX rats looked more flake-like compared to that in OVX rats and compared to before surgery. Furthermore, results of the micro-FE analyses demonstrated that loss of stiffness in the metaphysis after immobilization was larger than after estrogen-deficiency. In both groups, loss of stiffness was accompanied by a combination of a decrease in bone volume, and a decrease in average von Mises stress per element, with the latter being more reduced after immobilization. Also, variation in bone tissue stresses increased more after immobilization. Taken together, these results support the hypothesis that at the same level of bone loss found in the metaphysis, immobilization-induced bone loss leads to less favorable mechanical properties than estrogen-deficiency induced bone loss. According to this hypothesis, estrogen-deficiency will result in bone loss in the low loaded (transversal) direction while retaining bone in the loaded direction, whereas immobilization will induce bone loss in a more homogeneous manner. This leads to increased anisotropy and less stiffness reduction after estrogen-deficiency compared to immobilization. The larger variation in tissue stresses during simulated compression testing after immobilization is also the result of these differences in structure. Due to

the loss of bone in the loaded direction, the remaining bone would be highly stressed while the bone in transversal direction would be largely unloaded, thus generating large variation in tissue loading. The fact that the average stress was more reduced after immobilization also indicates that larger regions of bone tissue were unloaded with high stresses being very localized.

In this study, it was found that estrogen-deficiency and immobilization led to the same loss of bone volume fraction in the metaphysis. The degree of loss of bone volume fraction was smaller in the epiphysis, however it was significantly more pronounced after immobilization than after estrogen-deficiency. This could be explained by the hypothesis, previously formulated by Westerlind et al (285), that estrogen-deficiency increases the mechanostat threshold leading to low and high strain areas being resorbed and conserved respectively. In contrast, after immobilization an overall reduction in strain would take place resulting in bone loss in all locations. In that study, a finite element model was developed of the tibia, with which strains in the epiphysis indeed were found to be higher than in the metaphysis, which was confirmed in another finite element study (282). In previous studies similar suggestions of higher strains in the epiphysis have been made (8;265). Taken together, this indicates that after estrogen-deficiency, bone loss would be relatively more and less severe in the meta- and epiphysis, where strains are respectively low and high, while after immobilization, bone loss would be more uniform as strains are low in both locations. Another possible explanation for site-dependancy of the difference in response to estrogen-deficiency and immobilization could lie in differences in cell responses, which have shown to vary after ovariectomy between the meta- and epiphysis (107;148). It may also be related to differences in metabolic activity, blood supply, osteoprogenitor cell populations or baseline levels of bone turnover (267).

No significant differences were found for any of the parameters obtained from the 3-point bending tests. Although no comparison can be made to an untreated, control group and no direct measurements for tissue modulus were made, this indicates that the assumption of a unique element modulus for the elements in the FE-model is reasonable. It also indicates that estrogen-deficiency and immobilization most likely lead to similar changes in cortical shape and morphology.

Overall, the severe deterioration of bone microstructure in the metaphysis of estrogen-deficient and immobilized rats found in this study agrees with previous reports (108;165;285), although this is the first *in vivo* study. The lower reduction of bone volume fraction in the epiphysis after estrogen-deficiency concurs with previous reports (108;246). In a study comparing decreases in trabecular bone volume fraction after estrogen-deficiency between the meta- and epiphysis, reductions in bone mass after four weeks were found to be greater in the former, which agrees with our findings (108). The difference in appearance of trabecular structure after estrogen-deficiency and immobilization agrees with other data (108). We also found that bone loss after estrogen-deficiency was located mostly in the anterolateral, distal side of the trabecular bone, while bone loss was more uniform after immobilization. On the lateral side, just below the growth plate, bone loss was more severe after immobilization. This detailed description of differences in locations of bone loss has not been given before.

Previously, however, bone loss has been reported to be located in the central part of the metaphysis after estrogen-deficiency only (7;108;298), while in our study this was also seen after immobilization. Perhaps this is due to differences in duration of study or visualization techniques.

FEM derived stiffness in the metaphysis was found to decrease after estrogen-deficiency and immobilization, though more in the latter, reflecting the loss of bone mass and deterioration of structure. The percent reduction in bone volume of the model, incorporating trabecular and cortical bone, was less than the percent reduction in bone volume fraction calculated for trabecular bone by micro-CT, which indicates that cortical bone mass did not decrease as much as trabecular bone volume fraction. Also, as the decrease in bone volume of the model and bone volume fraction in the metaphysis was not different between the two groups, it can be expected the the reduction in cortical bone mass was similar as well.

The untreated leg of the neurectomy rats was also scanned, of which the data were not shown. As the treated leg of the rats could not be used in locomotion anymore, we expected loads in the untreated leg to be higher and therefore adaptation of bone microstructure of the untreated leg to take place in the form of an increased bone volume fraction. To our surprise, bone structure in the metaphysis deteriorated in the untreated leg as well. After four weeks, bone volume fraction had decreased with 36% accompanied by a decrease in both trabecular number and thickness, although decreases slowed after three weeks. The most likely explanation for this is that overall activity of the rats was severely reduced, leading to less loading of the untreated legs as well. Reduced activity was not seen during the day, however as rats are known to be the most active at night, this may have been apparent at night (240). Bone mass was constant between week 3 and 4, indicating a stabilization of bone loss at that time point. In one pilot rat that was studied for a longer time period, it was found that bone volume fraction in the untreated leg recovered back to 100% of the initial value at eight weeks after surgery, indicating that the reduced activity was probably temporary.

It is clinically relevant to know whether bone loss after estrogen-deficiency and immobilization lead to the same deterioration of bone structure, the loss of bone follows the same time course and the mechanical consequences are the same. If differences are present, then the treatment for patients may be adjusted accordingly. However, as analysis of bone microstructure in living humans is limited, an *in vivo* study in rats serves well as a first predictor. We found few differences in the metaphysis in the first four weeks of osteopenic development after estrogen-deficiency and immobilization, whereas in the epiphysis, deterioration of bone structure was more severe after immobilization. It is, however, in current clinical practice not possible to distinguish between these locations. Possibly, the use of a HR-pQCT scanner in future could enable such a comparison. It would also be interesting to determine the degree of recovery of bone microstructure after the rat is remobilized using an *in vivo* micro-CT scanner. This relates to the situation in which a patient after a long period of bed rest becomes active again or, less frequently occurring, when an astronaut returns to earth from space.

This research was limited by a study period of four weeks, as neurectomy is considered quite harsh for rats. It could be that after four weeks, changes between groups will become different. Also, the time-point at which stabilization of bone structure takes place was not determined. Furthermore, cortical bone was not analyzed in this study. We have previously shown that cortical thickness of the tibia can increase after ovariectomy, which was found to take place after four weeks (34). It could be that this mechanical adaptation after ovariectomy takes place only until after a certain amount of bone is lost. Finally, the FEM employed in this study was quite basic. It only included the metaphysis, a linear compression step was applied, while it is known that the tibia is also subjected to torsion and bending (81) and isotropic material behavior was assumed, while cortical and trabecular bone are known to behave anisotropically (173;243). Despite this, it provided a means to determine whether mechanical properties in this rather simple model were different after estrogen-deficiency and immobilization induced bone loss.

In this study, the exact pattern of bone loss during four weeks after estrogen-deficiency and immobilization induced bone loss was determined in mature rats using an *in vivo* micro-CT scanner. Deterioration of bone volume fraction progressed at the same rate after estrogen-deficiency compared to immobilization in the metaphysis, while in the epiphysis this rate was higher after immobilization. At the same level of bone loss in the metaphysis, immobilization led to less favorable bone structure and mechanical properties than after estrogen-deficiency, which is explained by a lack of adaptation to loading after immobilization.

Acknowledgements

This work was funded by the Netherlands Organisation for Scientific Research (NWO). We thank Leonie Niesen for performing the ovariectomies and the animal care. We thank Anthal Smits for contouring.

Chapter 4

Bisphosphonate treatment assessed by *in vivo* micro-CT

The contents of this chapter are based on J.E.M.Brouwers, F.M.Lambers, J.A.Gasser, B.v.Rietbergen, R.Huiskes, Bone degeneration and recovery after early and late bisphosphonate treatment of ovariectomized Wistar rats assessed by *in vivo* micro-CT, *Calcif Tissue Int.* 2008 Mar;82(3):202-11.

Abstract

Bisphosphonates are anti-resorptive drugs commonly used to treat osteoporosis. It is not clear, however, what the influence of the time-point of treatment is. Recently developed *in vivo* micro-CT scanners offer the possibility to study such effects on bone microstructure in rats. The aim of this study was to determine the influence of early and late zoledronic acid treatment on bone in ovariectomized rats, using *in vivo* micro-CT.

29 female, Wistar rats were divided into an ovariectomy (OVX) (n=5), OVX and zoledronic acid (ZOL) at week 0 (n=8), OVX and ZOL at week 8 (n=7) and a SHAM group (n=9). CT-scans were made of the proximal tibia at weeks 0, 2, 4, 8, 12 and 16 and bone structural parameters were determined in the metaphysis. Two fluorescent labels were administered to calculate dynamic histomorphometric parameters.

At week 16, all groups were significantly different from each other in BV/TV, Conn.D and Tb.N, except for the early ZOL and control groups, which were not significantly different for any structural parameter. After ZOL treatment at week 8, BV/TV, SMI, Tb.N and Tb.Th significantly improved in the late ZOL group. OVX and ZOL groups showed respectively higher and lower bone formation rates than the control group.

Early ZOL treatment inhibited all bone microstructural changes seen after OVX. Late ZOL treatment significantly improved bone microstructure, although the structure did not recover to original levels. Early ZOL treatment resulted in a significantly better microstructure than late treatment. However, late treatment was still significantly better than no treatment.

4.1 Introduction

Postmenopausal osteoporosis affects millions of women world-wide and results in loss of bone mass and bone microstructural changes, which lead to reduced bone strength. It remains unknown how exactly the microstructure is affected over the time-course of osteoporosis development and to what extent this structure can be recovered by drug treatment. Since the assessment of bone structure in humans is still limited to a few peripheral sites, the ovariectomized rat is used in many studies as an animal model for osteoporosis in cross-sectional evaluations. Numerous cross-sectional studies have determined the loss of trabecular bone in the proximal tibia in rats following ovariectomy (OVX) at different time points by measuring bone structural parameters (57;153;288). Ovariectomy has shown to decrease bone volume fraction, connectivity and trabecular number, and to increase trabecular separation and structure model index, which indicates that trabecular bone changes from plate-like to more rod-like, in the proximal tibial metaphysis of the female rat. However, conflicting results were found for the effects of ovariectomy on trabecular thickness, showing increases, decreases or no response at all (157;280;295). These cross-sectional studies are limited to comparing averages per group only, which provides a reduced sensitivity for detection of differences. In addition, no information is obtained regarding the specific locations of bone changes.

Recently, however, *in vivo* micro-CT scanners became available, which can monitor the process of bone loss and microstructural changes in small, living animals. So far, two studies have been reported in which this equipment was used to monitor changes in rat bones after OVX. Interestingly, these studies reported respectively significant increases (280) and decreases (32) in trabecular thickness after ovariectomy, indicating that the response may vary. While the process of bone degeneration after OVX is not fully understood, even less information is available for the process of recovery after drug treatment. The most widely used drugs for treatment of diseases associated with increased bone resorption, such as postmenopausal osteoporosis, are now bisphosphonates.

Many cross-sectional studies have determined the effects of bisphosphonates in rats either as a preventive treatment, before development of ovariectomy-induced bone loss or as a recovering treatment after development of bone loss. Although the results of different experimental designs are difficult to compare directly due to differences in experimental design, preventive treatment in animals may lead to the same the amount of final bone mass as recovering treatment. The associated microstructure in terms of number and thickness of trabeculae, however, can be different. While the influence of the time-point of treatment is highly relevant clinically, no studies were found that directly compared the effects of a preventive and a recovering treatment on final bone mass and associated microstructure. In addition, the fact that only results of cross-sectional studies have been reported complicates the comparison of the final and original bone structure and provides little or no information on the changes in structure over time. Here also, we expect that longitudinal *in vivo* micro-CT imaging will

potentially provide more information about the specific changes in the bone, both spatially and temporally.

For the present study we had two goals: 1) determine the process of bone loss and bone microstructural changes in ovariectomized rats and 2) determine the effects of early and late treatment of osteoporotic rats with a bisphosphonate. We used an *in vivo* high-resolution micro-CT scanner to image the proximal tibia of female, adult Wistar rats. For the treatment, zoledronic acid was used, since this is a third-generation bisphosphonate that proved a potent osteoclast inhibitor. It has shown to be effective in cancer patients with bone metastases and is currently tested in clinical trials as a promising therapeutic agent for osteoporotic patients (103;256).

4.2 Materials and methods

4.2.1 Animals

Thirty-six female, 30 weeks-old, retired breeding Wistar rats were obtained from Harlan Laboratories (Horst, The Netherlands) and allowed to acclimatize for 7 days before the start of the experiment. The rats were maintained with a cycle of 12 hours light and 12 hours darkness and allowed to eat and drink *ad libitum*. The experiment was approved by the Animals Ethics Committee of the University of Maastricht, the Netherlands. The rats were weight-based divided into four groups: control (n=9), ovariectomy (OVX) (n=9), OVX and early zoledronic acid (ZOL) (n=9), OVX and late ZOL (n=9). All rats were ovariectomized at week 0 and the control group underwent a SHAM ovariectomy. Success of OVX was confirmed at necropsy by determining atrophy of the uterine horns. Zoledronic acid was kindly donated by Novartis Pharmaceutical (Basel, Switzerland) and was dissolved in a saline vehicle. The early ZOL group was administered ZOL at a single dose of 20 µg/kg body weight s.c. at OVX (comparable to the phase III clinical trial dose used in osteoporotic patients). The late ZOL group was administered the same single dose eight weeks after OVX. Eleven and four days before necropsy, the fluorescent labels calcein (Fluka, Buchs, Switzerland) and alizarin (Merck, Dietikon, Switzerland) were administered s.c. in a saline vehicle to all rats at a dose of 30 mg/kg and 20 mg/kg body weight respectively, to evaluate bone formation dynamics in the proximal tibial metaphysis. Rats were sacrificed at 16 weeks by exsanguination.

4.2.2 Micro-CT scanning

Directly after the operation, a 6 mm micro CT-scan (70kV, 85 µA, 1000 projections per 180 degrees, 350 ms integration time) with an isotropic resolution of 15 microns was made of the proximal tibia using an *in vivo* micro-CT scanner (vivaCT 40, Scanco Medical AG, Bassersdorf, Switzerland). The CT-scanner was calibrated and a beam-hardening correction algorithm was applied to all scans. Follow-up *in vivo* CT-scans were made after 2, 4, 8, 12 and 16 weeks to monitor bone structure. One CT-scan took

35 minutes, during which the animal was anesthetized with isoflurane and the scanned leg was placed in a custom-made leg-fixating device. The design of the rat holder was such that the left leg was not exposed to radiation while scanning the right leg. Radiation damage to the scanned bone was not expected to occur, based on a previous study, in which 8 weekly CT-scans with the same radiation dose caused no detected bone damage (36). In that study, we also showed that the reproducibility of all structural parameters was high with a coefficient of variation of about 1%.

Image processing included Gaussian filtering and segmentation and was described elsewhere in detail (36). In brief, the same filtering and segmentation values were used for every measurement of each animal ($\sigma=0.7$, support=1, threshold density=0.504 g HA/cc, equivalent to 22% of maximal grayscale value). From every baseline and follow-up CT-scan, the metaphyseal trabecular bone was manually selected and bone structural parameters (bone volume fraction (BV/TV), connectivity density (Conn.D), structure model index (SMI), trabecular number, thickness and separation (Tb.N, Tb.Th, Tb.Sp)) were automatically determined. The average attenuation coefficient of the trabecular bone tissue was determined for all measurements using a protocol provided by the manufacturer of the micro-CT scanner. With this protocol the grey-level of voxels near the trabecular surfaces are not included to ensure that the measurements are not affected by partial volume effects. Also, cortical thickness of the metaphysis was analyzed. The cortical bone starting from the tibia-fibula junction was manually selected for each measurement resulting in a region of approximately 1.8 mm long. The same filtering and segmentation values were used as for the trabecular analysis. Cortical thickness was automatically determined from the selected region.

When two CT-scans of the same animal are made at different time points, the position of the animal in the scanner will not be exactly the same and therefore the CT-scans will also differ. In order to detect bone structural changes on a micro-level, one CT-scan needs to be translated and rotated to match the other. We developed image registration software that registers two scans based on minimizing the correlation coefficient (275). Every follow-up scan was registered with the first scan, hereby revealing any possible changes in the microstructure and minimizing errors in the region of interest for the structural parameters.

4.2.3 Mechanical testing

After sacrifice, all left tibiae were dissected and used for two different mechanical tests. First, a standard three-point bending test was applied. The tibiae were placed on the lateral surface on two rounded supporting bars with a distance of 2.4 cm. A preload of 1 N was applied (ZWICK, Z020) at the medial surface of the diaphysis by lowering a third rounded bar. A constant displacement rate of 6 mm/min was applied until failure. Displacement was measured from the actuator displacement transducer of the testing machine. Stiffness, ultimate force and ultimate displacement were calculated for each sample.

To assess the mechanical properties of the proximal tibia, a proximal tibia compression test was performed similar to the method of Hogan et al (100). A 4 mm

slice of the proximal metaphysis including both cortical and trabecular bone, was sawed below the growth plate using a diamond saw (Struers, Accutom-5). This slice was axially compressed (ZWICK, Z020) during 5 preconditioning cycles between 1 N and 70 N. After the last preconditioning cycle, axial compressive load was applied at 0.5 mm/min until failure while axial displacement was measured using an extensometer. Stiffness, ultimate force and ultimate displacement were determined for all samples.

4.2.4 Histomorphometry

At necropsy, all right tibiae were fixed in 70% ethanol and embedded in methylmetacrylate (Technovit 9100, Heraeus Kulzer, Wehrheim/Ts., Germany). Five μm thin sections were cut to determine fluorochrome-based dynamic histomorphometric parameters of bone formation using an Axiophot photomicroscope (Zeiss, Oberkochen, Germany) linked to a camera (CF 15/4 MC, Kappa, Gleichen, Germany), and a QUANTIMET 600 image analysis system was used to calculate the amount of mineralized surface per bone surface (BS) (percentage), corrected mineral apposition rate (micrometers per day) and bone formation rate (BFR) per BS (micrometers per day). The calculations of the dynamic parameters were performed as recommended previously (207).

4.2.5 Statistics

Since this experiment concerned repeated measures in multiple groups, several statistical tests were performed to reveal changes in parameter values over time and between groups. For all structural parameters, the percentage change at different time intervals was calculated for each animal individually. A one-way ANOVA test with repeated measures was performed on the percentage change for all structural parameters and all groups. Furthermore, a one-way ANOVA with a Bonferroni post-hoc test was used to determine differences between the groups at all time points, for each structural parameter. Also, a one-way ANOVA with a Bonferroni post-hoc test was used to determine differences between the groups in cortical thickness, histomorphometric and mechanical results. For each group, a paired student t-test was performed on the absolute values of the structural parameters of each time point compared to baseline values, to determine the earliest point at which a detectable change was found. A paired student t-test was used to determine late ZOL treatment effects within this group. Finally, a paired-student t-test was performed on the absolute values between each measurement for each group and structural parameter. All p-values below 0.05 were considered significant.

4.3 Results

4.3.1 Ovariectomy

Based on the uterine weight, we determined seven unsuccessful ovariectomies. The rats concerned were removed from further analyses, which left 9 rats in the control group, 5 in the OVX group, 7 in the OVX and late zoledronic acid group and 8 in the OVX and early zoledronic acid group. For each animal, we determined the percentage change in structural parameters compared to the values at week 0. Figure 4.1 shows the average percentage change and upper standard deviation for all groups for BV/TV, Conn.D, SMI, Tb.N, Tb.Th, Tb.Sp. The OVX group without treatment showed large changes in structural parameters, indicating the development of ovariectomy-induced bone loss (figures 4.1 and 4.2). The paired student t-test indicated significant changes within two weeks after ovariectomy for all structural parameters. BV/TV, Conn.D and Tb.N decreased during the experiment and SMI and Tb.Sp increased. Both trabecular thickness and number decreased within two weeks, indicating that both thinning and complete resorption of trabeculae started directly after ovariectomy. The initial rapid loss of bone and connectivity was largely accompanied by trabecular thinning while secondary, slower loss of bone was concomitant with a decrease in trabecular number. While BV/TV, Conn.D, SMI, Tb.N and Tb.Sp showed continuous changes in the same direction throughout the experiment, Tb.Th initially decreased significantly until four weeks after ovariectomy, and then increased again until after 16 weeks Tb.Th was significantly higher than in the control group.

The absolute average values and standard deviations for all structural parameters of all measurements are shown in table 4.1. At the starting point, some differences in the values between the groups were present. This was due to the fact that some animals, which mostly had a relatively low BV/TV, were removed from the study, because they did not respond to the ovariectomy. However, since we compared the relative changes in each animal, the results were most likely not affected by the difference in absolute values.

4.3.2 Zoledronic acid treatment

The early zoledronic acid treatment group and the control group were not significantly different at all time points for all structural parameters.

Up until 8 weeks after ovariectomy, when zoledronic acid was administered to the rats in the late treatment group, the ovariectomy group and the late treatment group were not significantly different for all structural parameters. BV/TV, SMI, Tb.Th and Tb.N were significantly improved in the late ZOL group after four weeks after the single zoledronic acid injection (table 4.2). In addition, Tb.Sp significantly improved within eight weeks after injection, while Conn.D showed no significant response. Between week 12 and 16, all structural parameters stayed constant.

At week 16, BV/TV, Conn.D and Tb.N were significantly different between all groups except for the early treatment and the control group (table 4.3). Tb.Th was only

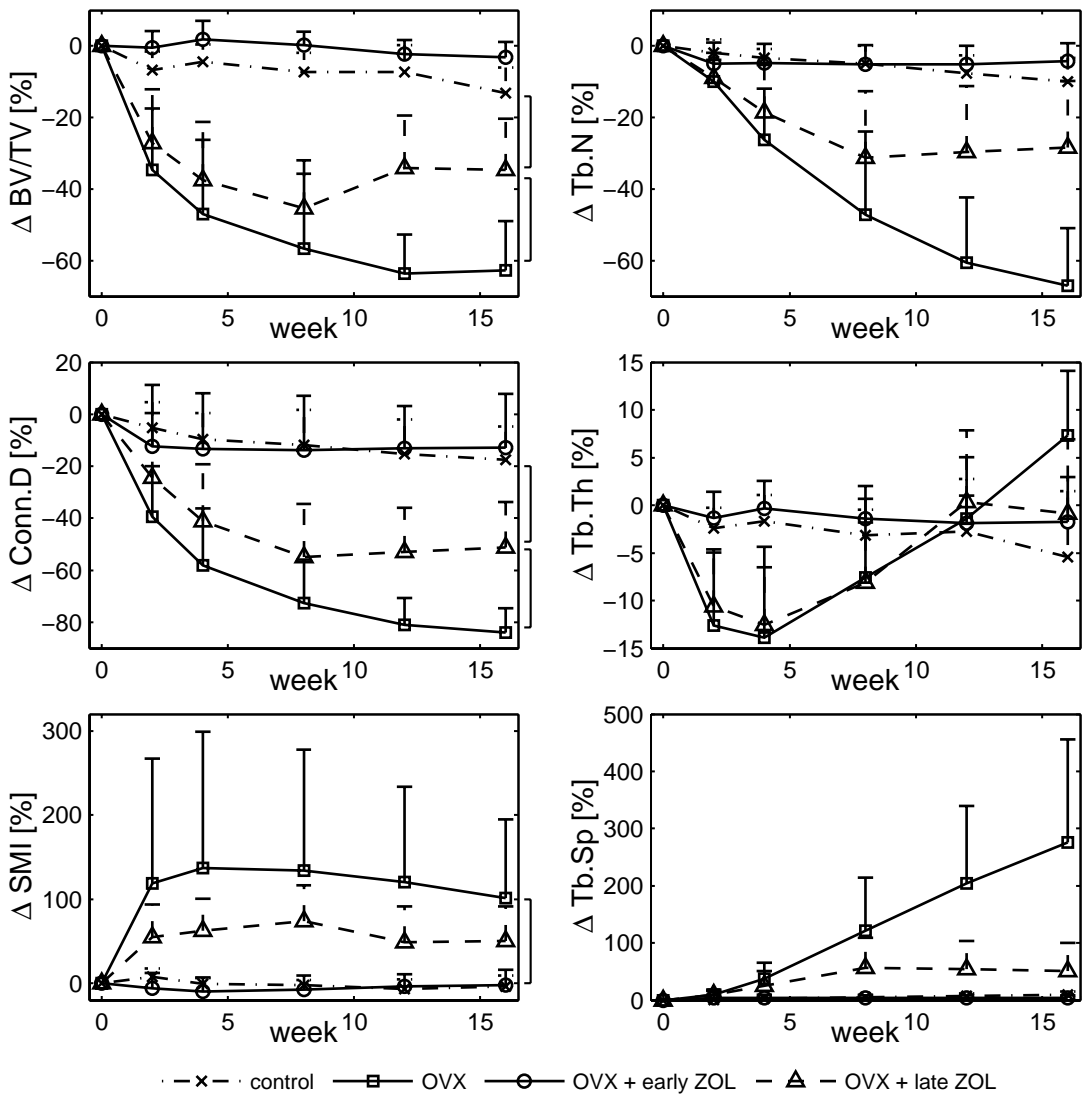


Figure 4.1: Average percentage change in structural parameter in the metaphyseal, proximal tibia and upper standard deviation for all groups at all time points. Brackets indicate $p < 0.05$ at week 16.

Table 4.1 Mean values and standard deviation of all structural parameters of all groups at the start of the experiment.

Group	BV/TV [1]	Conn.D [1/mm]	SMI [1]	Tb.N [1/mm]	Tb.Th [μ m]	Tb.Sp [μ m]
Control	0.17 (0.056)	41 (47)	1.52 (0.53)	1.89 (1.38)	105 (49)	613 (368)
OVX	0.26 (0.055)	141 (76)	1.22 (0.39)	3.77 (1.66)	84 (10)	335 (174)
OVX+ late ZOL	0.23 (0.062)	86 (66)	1.23 (0.34)	2.77 (1.55)	89 (13)	482 (227)
OVX + early ZOL	0.17 (0.056)	38 (21)	1.70 (0.39)	1.86 (0.80)	95 (7)	647 (207)

significantly different between the control and ovariectomy group. Although substantial differences in Tb.Sp and SMI were seen between all groups, except for the early treatment and control group, significant differences were only found between the ovariectomy and control group and between the ovariectomy and early treatment group.

CT-derived mineralization values in all groups did not change over time and did not differ between groups at all time points.

4.3.3 Aging

An ANOVA with repeated measures on all structural parameters of the control group was performed to determine if there was a significant effect of aging. BV/TV and Tb.N were found to significantly decrease and Tb.Sp was found to significantly increase due to aging. All other structural parameters did not change significantly in 16 weeks.

An ANOVA with repeated measures was performed on the percentage change in structural parameters comparing the control and early treatment group to determine any significant differences. BV/TV and Tb.N showed a significant effect of age, treatment and age*treatment and Tb.Sp showed a significant effect of age and age*treatment. While BV/TV decreased significantly over time in both the early treatment and the control groups, the latter of which was found to decrease at a higher rate. Tb.N significantly decreased over time in the control group, however it did not significantly change in the early treatment group as a net result of the ovariectomy, aging and zoledronic acid treatment. Tb.Sp significantly increased in the control group due to aging, while it did not in the early treatment group.

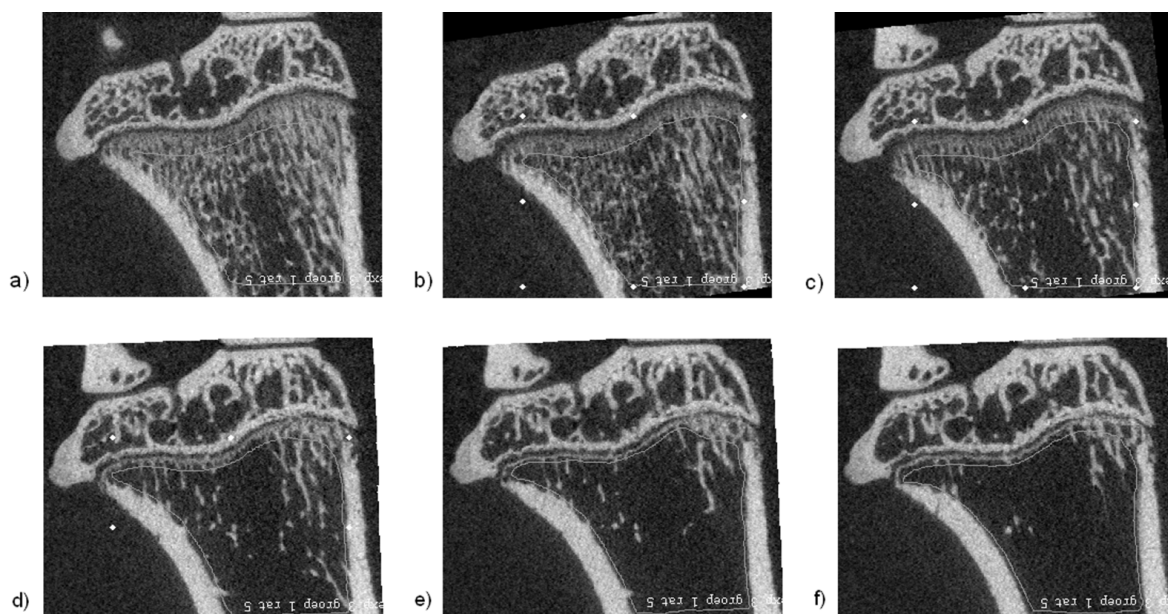


Figure 4.2: Same slice of an unprocessed CT-scan of the same rat in the ovariectomy group taken at week 0 (a), 2 (b), 4 (c), 8 (d), 12 (e), 16 (f). The images show typical trabecular bone loss due to ovariectomy in the metaphysis. White line shows the analyzed metaphyseal bone.

Table 4.2: P-values of paired student's t-test in the late ZOL group after ZOL treatment.

Structural parameter	P-value for weeks 8-12	P-value for weeks 8-16
BV/TV	0.001 *	0.004 *
Conn.D	0.249	0.181
SMI	0.003 *	0.004 *
Tb.N	0.041 *	0.005 *
Tb.Th	0.000 *	0.000 *
Tb.Sp	0.344	0.008 *

* Significant (P<0.05)

Table 4.3: P-values of ANOVA plus Bonferroni post-hoc test comparing all groups at all time points for all structural parameters.

Group	Δ BV/TV					Δ Conn.D					Δ SMI				
	2	4	8	12	16	2	4	8	12	16	2	4	8	12	16
1 vs. 2	0.010*	0.000	0.000*	0.000*	0.000*	0.025*	0.001*	0.000*	0.000*	0.000*	0.027*	0.008*	0.004*	0.001*	0.003*
1 vs. 3	0.005*	0.000	0.000*	0.000*	0.000*	0.341	0.021*	0.001*	0.000*	0.005*	0.929	0.473	0.141	0.305	0.24
1 vs. 4	0.999	0.999	0.999	0.999	0.322	0.999	0.999	0.999	0.999	0.999	0.999	0.999	0.999	0.999	0.999
2 vs. 3	0.999	0.999	0.579	0.000*	0.000*	0.999	0.906	0.811	0.042*	0.027*	0.598	0.443	0.667	0.148	0.37
2 vs. 4	0.000*	0.000*	0.000*	0.000*	0.000*	0.079	0.001*	0.000*	0.000*	0.000*	0.011*	0.005*	0.003*	0.001*	0.003*
3 vs. 4	0.000*	0.000*	0.000*	0.000*	0.000*	0.9	0.023*	0.001*	0.000*	0.000*	0.421	0.29	0.104	0.331	0.206

Group	Δ Tb.N					Δ Tb.Th					Δ Tb.Sp				
	2	4	8	12	16	2	4	8	12	16	2	4	8	12	16
1 vs. 2	0.088	0.001*	0.000*	0.000*	0.000*	0.003*	0.002*	0.673	0.999	0.013*	0.21	0.006*	0.001*	0.000*	0.000*
1 vs. 3	0.108	0.019*	0.005*	0.007*	0.018*	0.008*	0.002*	0.325	0.999	0.999	0.099	0.072	0.2	0.802	0.999
1 vs. 4	0.999	0.999	0.999	0.999	0.999	0.999	0.999	0.999	0.999	0.999	0.999	0.999	0.999	0.999	0.999
2 vs. 3	0.999	0.999	0.353	0.001*	0.000*	0.999	0.999	0.999	0.999	0.152	0.999	0.999	0.128	0.001*	0.000*
2 vs. 4	0.45	0.001*	0.000*	0.000*	0.000*	0.001*	0.001*	0.265	0.999	0.06 *	0.492	0.007*	0.001*	0.000*	0.000*
3 vs. 4	0.623	0.027*	0.004*	0.003*	0.002*	0.003*	0.001*	0.109	0.999	0.999	0.279	0.084	0.187	0.667	0.999

Groups: 1, control; 2, OVX; 3, late ZOL; 4, early ZOL

* Significant (P<0.05)

4.3.4 Cortical thickness

Ovariectomy initially led to a decrease in metaphyseal cortical thickness and at 4 weeks both the ovariectomy and the late ZOL group were significantly lower than the early ZOL group (figure 4.3). However, after 4 weeks it increased again in the ovariectomy group and at 16 weeks cortical thickness was significantly higher than in the control group. Early ZOL treatment inhibited the changes in cortical thickness. The late ZOL group, just like the ovariectomy group, showed an increase in cortical thickness between 4 and 16 weeks, although this was less pronounced.

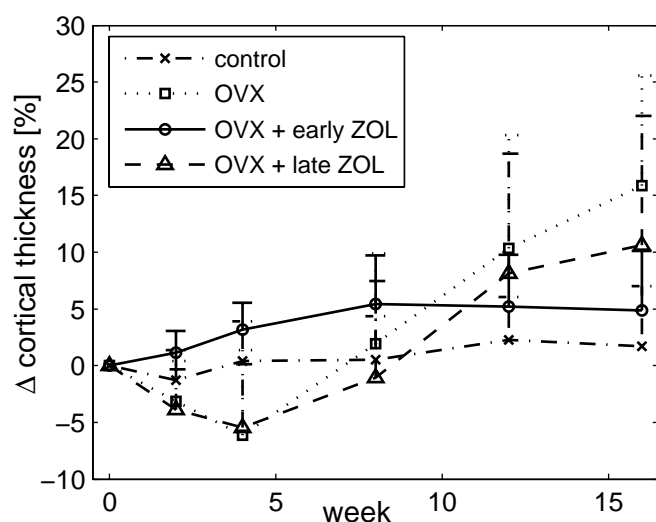


Figure 4.3: Average percentage change in cortical thickness in the metaphyseal, proximal tibia and upper standard deviation for all groups at all time points. At week 4, the ovariectomy and the late ZOL group were significantly lower than the early ZOL group and at week 16 the ovariectomy group was significantly higher than the control group.

4.3.5 Mechanical testing

Experimental test results were obtained for 7 (control), 5 (OVX), 6 (OVX and late ZOL) and 7 (OVX and early ZOL) tibiae. No significant differences were found between all parameters determined in the three-point bending test (figure 4.4a).

For the results from the proximal tibia compression test a significant difference in ultimate displacement was found between the ovariectomy group and the early ZOL group and between the ovariectomy and the control group (figure 4.4b). Although not significantly determined, a trend was observed in which OVX resulted in a lower stiffness and ultimate force, while late ZOL treatment partially recovered these values and early ZOL treatment did to a larger extent.

4.3.6 Histomorphometry

Histomorphometry results were obtained for 5 (control), 5 (OVX), 6 (OVX and late ZOL), 5 (OVX and early ZOL) rats. The OVX group showed a significantly higher mineralizing surface (MS/BS) and bone formation rate (BFR), and a substantially higher mineral apposition rate (MAR) than the control group (figure 4.5). Both ZOL groups showed a significantly lower MS/BS and BFR than the OVX group and control group, while MAR was significantly lower than only the OVX group. Additionally, the late ZOL group had a significantly lower MS/BS and a non-significantly lower BFR than the early ZOL group.

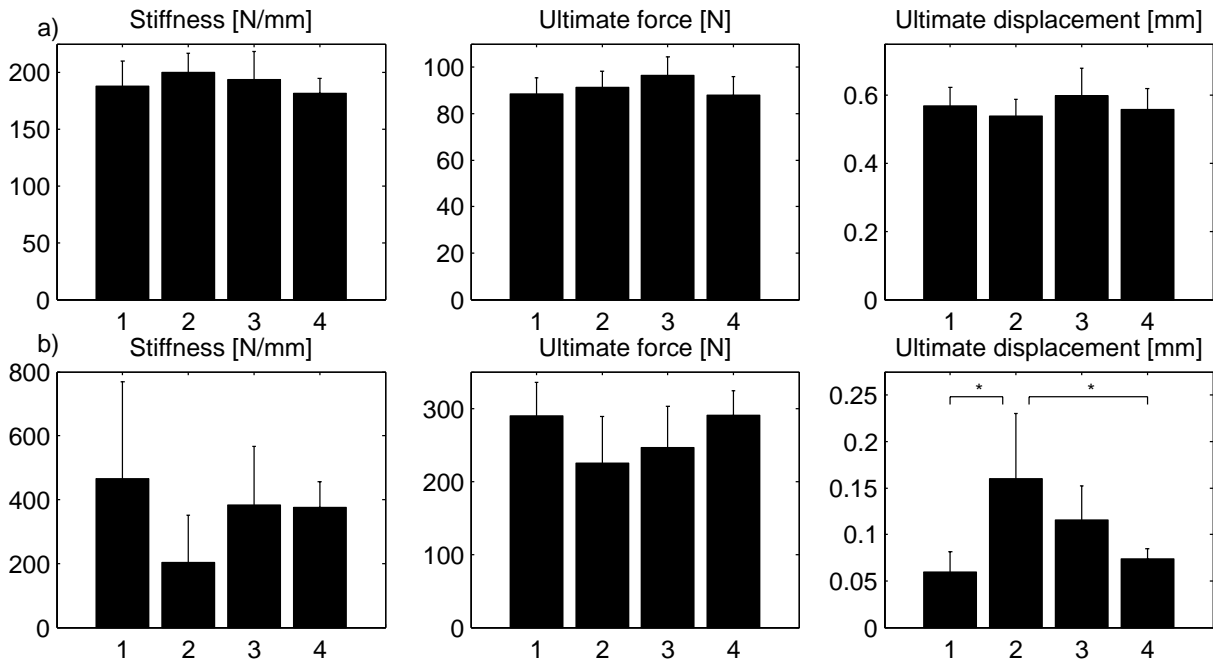


Figure 4.4: Stiffness, ultimate force and ultimate strain determined from 3-point bending test on diaphyseal tibia (a) and axial compression test (b) on the metaphyseal bone. 1= control, 2= OVX, 3= late ZOL, 4= early ZOL group. Asterisk indicates significant difference between groups based on ANOVA and Bonferroni post-hoc test ($p < 0.05$).

4.4 Discussion

In this study we assessed the effects of ovariectomy and of early and late zoledronic acid treatment of ovariectomized rats on the microstructure of metaphyseal bone in the proximal tibia of aged, female Wistar rats over a 16-week time course, using *in vivo* high-resolution micro-CT.

Ovariectomy induced significant changes in all structural parameters within two weeks, indicating the rapid development of ovariectomy-induced bone loss. An initial phase of rapid decreases in bone volume fraction and connectivity was seen, followed by a second phase in which changes took place at lower rates. The initial, rapid loss of bone and connectivity was largely caused by trabecular thinning, while the secondary, slower loss of bone was accompanied by a decrease in trabecular number. Ovariectomy induced large decreases in bone volume fraction, connectivity and trabecular number, and large increases in trabecular separation and structural model index, indicating the change of more plate- to rod-like bone, which agrees with literature on the effects of ovariectomy in rat tibiae (153;278;279;287). A different response was, however seen in trabecular thickness, which initially decreased until four weeks after ovariectomy, and then increased until at the end-point of the experiment it was higher than in the control group. A possible explanation for this response could be that due to an increased osteoclast activity, initially most trabeculae will become thinner, while only few are completely resorbed. After a certain period of resorption, the thinner trabeculae will be

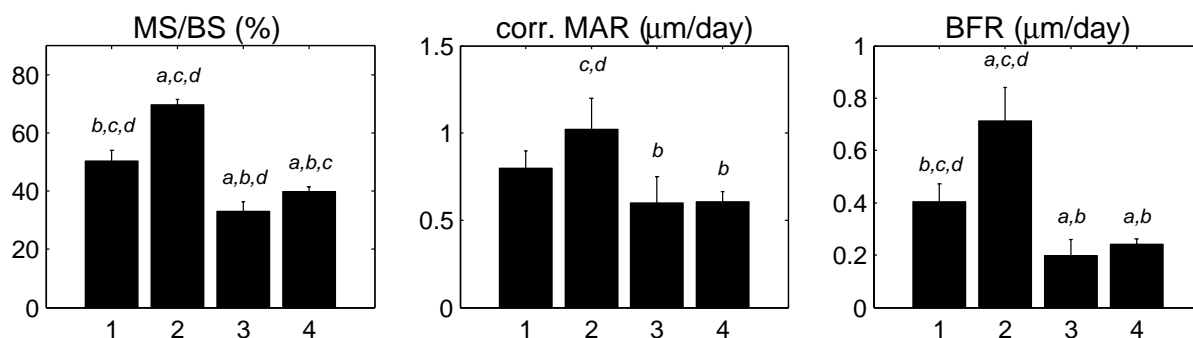


Figure 4.5: Dynamic bone histomorphometric parameters for all groups in the metaphyseal, proximal tibia. 1= control, 2= OVX, 3= late ZOL, 4= early ZOL group. Based on an ANOVA and Bonferroni test, a=significantly different from group 1, b=significantly different from group 2, c=significantly different from group 3, d=significantly different from group 4 ($p < 0.05$).

perforated and will be completely resorbed. Since the thicker trabeculae remain present, the average trabecular thickness will increase. Another possible explanation would be that mechanical adaptation takes place. Since much bone is lost after ovariectomy and the number and thickness of trabeculae decreases, all load-bearing goes through the remaining trabeculae. Therefore, the stress increases in these trabeculae, which stimulates bone formation and would lead to an increased trabecular thickness. It is also possible that a combination of these mechanisms actually takes place. In the two studies published to date regarding *in vivo* micro-CT monitoring of the effects of ovariectomy on the metaphyseal, proximal tibia in rats, the loss of trabecular bone was similar to what was seen here (32;280). However, in these studies, trabecular thickness significantly increased in one study and decreased in the other directly after ovariectomy. Although the same rat strain was used and the same anatomical location was studied, it could be that differences such as the use of retired breeders versus virgin rats, differences in age or differences in type of data analysis led to variable results.

Early zoledronic acid injection at the time of ovariectomy completely prevented all changes in structural parameters and thus the development of ovariectomy-induced bone loss. Aging caused a significant decrease in bone volume fraction, connectivity and trabecular number, and an increase in trabecular separation in the control group, which agrees with the literature (32). However, a significant decrease was merely seen in bone volume fraction in the early zoledronic acid group and at a significantly lower rate than in the control group. This indicates that a single injection of zoledronic acid was powerful enough to inhibit even natural deterioration of bone volume and microstructure due to aging. One year of weekly zoledronic acid injections of a concentration as low as 0.3 µg/kg has shown to completely suppress the effects of ovariectomy in vertebrae of Sprague-Dawley rats and 1.5 µg/kg dose was needed to retain all structural parameters and mechanical properties in the femora (85;103). Similarly, 69 weeks of weekly zoledronic acid injections in ovariectomized rhesus monkeys reduced bone loss in a dose-dependent manner (13). In a phase 2 study both a yearly and a quarterly zoledronic acid dose increased spinal and femoral bone mineral

density in post-menopausal women (219). In the current study, we have shown the long-term, potent inhibiting effects of zoledronic acid on both the bone volume fraction and the microstructure in rats.

While the preventive effects of zoledronic acid have previously been studied in rats (85;103), the effect of zoledronic acid treatment after the development of ovariectomy-induced bone loss on the microstructure, which more closely resembles the clinical situation, is new. Late zoledronic acid injection after eight weeks of bone loss development inhibited further bone loss. Possibly as a result of the filling of resorption cavities (88), a temporary but significant increase in bone volume fraction and thickness, and a significant decrease in the structure model index was seen directly after the administration of zoledronic acid. Four weeks later, however, all structural parameters stayed constant. This is in contrast with the ovariectomy group, which still showed deterioration of bone structure after 8 weeks. Overall taken, bisphosphonate treatment after the onset of osteoporosis is known to stabilize or increase bone volume fraction and trabecular thickness in both humans and animals, which agrees with the data presented here (22;109;215). It is generally thought that the underlying mechanism for an increase in bone volume fraction and trabecular thickness is the inhibiting effect of bisphosphonates on bone resorption preventing further thinning of trabeculae and the reduction of remodeling space by filling of resorption cavities leading to increased bone mass (78;88).

Cortical thickness first decreased as a result of ovariectomy and later increased again, and finally was higher than the control group. Both increases and decreases in metaphyseal, tibial cortical thickness have been reported in cross-sectional studies, which may be due to different analyzing methods or different time points of sacrifice (24;122). Early ZOL treatment resulted in a similar cortical thickness as seen in the control groups, which was fairly constant. Late ZOL treatment resulted in a similar pattern as in the ovariectomy group, although less pronounced, which may be explained by the inhibiting effect of zoledronic acid on bone remodeling rate. Cortical thickness profiles in all groups were similar to those in trabecular thickness, which may be interpreted as an indication that mechanical adaptation takes place in both cortical and trabecular bone after sustained bone loss.

No significant differences were found in mechanical properties determined in the three-point bending test between the ovariectomy and control group, which agrees with the literature (142;202). Also, no significant influence of ZOL treatment was found on the mechanical properties determined in the three-point bending test, which may be expected as zoledronic acid inhibits bone resorption and does not increase formation. In the proximal tibia compression test, ultimate displacement was found to be higher in the ovariectomy group than in the other groups. ZOL treatment partially recovered this increase in ultimate displacement. Although not significantly, ultimate force and stiffness tended to be lower in the ovariectomy group, while ZOL treatment inhibited this. The low number of animals per group and variability in the data unfortunately limits the interpretation of the results. It is known that while endosteal bone resorption takes place during aging and is increased as a result of ovariectomy, periosteal apposition increases as well (1;52;56;133;205;268), which was also seen in our CT-

scans (data not shown), hereby compensating for the loss of endocortical and trabecular bone (225). Therefore, loss of trabecular and endocortical bone may not necessarily mean loss of strength. While first-generation bisphosphonates, such as etidronate, have shown to directly decrease mineralization of bone (144;256), it is thought that zoledronic acid may increase mineralization by inhibiting resorption and thereby allowing longer mineralization (171;204). Furthermore, microdamage could accumulate and both of these effects could alter the mechanical properties of the bone tissue. Nonetheless, the trends in the mechanical properties resembled the trends in bone volume fraction and showed that zoledronic acid inhibited the changes resulting from OVX.

Bone forming activity was slightly higher in the ovariectomy compared to the control group, reflecting an increased turnover rate. Both ZOL groups displayed lower bone forming parameters compared to the control and ovariectomy groups, probably due to suppression of bone formation and resorption. Additionally, the late ZOL group tended to show slightly less bone forming activity than the early ZOL group, possibly due to the later time point of treatment. These results agree with previous reports of decreased osteoblast and osteoclast number after zoledronic acid injection and decreased number of resorption lacunae (88;94). CT-derived estimates of mineralization of metaphyseal trabecular bone were however not significantly increased in ZOL treated rats. This would indicate that ZOL treatment did not influence mineralization in this time frame.

As previously mentioned, at times, substantial differences were found between groups, however, due to a relatively high standard deviation no significant differences unfortunately were detected. This high standard deviation was mostly seen in the ovariectomy and the late treatment group. This was most likely caused by the fact that retired-breeders were used, which are known to show a variable response to ovariectomy. Due to an unsuccessful ovariectomy, seven animals were removed from the study. This decreased the number of animals used in the data analysis and also, since these were mostly animals with a relatively low bone volume fraction, the average bone volume fraction at the start of the study was higher in the ovariectomy and late treatment groups. Therefore, we performed statistical tests on percentage changes in structural parameters rather than on the absolute values. The trend for the percentage and absolute changes looked similar and the p-values were similar for most cases. However, when an ANOVA was performed on the absolute values comparing all groups at week 16, less significant differences in structural parameters were found, indicating the more sensitive approach of the *in vivo* experimental design.

Another limitation to this study was the fact that on average, at eight weeks in the study, the ovariectomy group was in a more deteriorated condition than the late treatment group, while there was no demonstrable explanation for this. Although the ANOVA test showed no significant differences between the groups, the treatment group still had a more favorable start-point to begin with when zoledronic acid was administered. However, because after zoledronic acid injection significant improvement took place while the ovariectomy group still deteriorated, it is shown that this will not have affected the final conclusions.

The method of *in vivo* CT-scans combined with image registration software presented here has enabled us to study our goals in a more efficient way in terms of number of animals needed in the experiment. Follow-up micro-CT scans were made of the same animals enabling us to use paired statistics and relative percentage changes in structural parameters. By registering all CT-scans, we were able to select the same part of the metaphyseal trabecular bone for every measurement, hereby decreasing the variation in structural parameters due to a varying selected region of interest.

In conclusion, ovariectomy induced rapid changes in trabecular bone mass and structure. A single injection of zoledronic acid at ovariectomy completely inhibited these changes in bone mass and structure seen in osteoporotic rats. A single zoledronic acid injection after ovariectomy-induced bone loss was well established, improved bone mass and structure, per group and compared to the control group. Bone volume fraction and the associated bone microstructure at the end-point of this study was, however, significantly less favorable than in the early treatment group.

Acknowledgements

This work was funded by the Netherlands Organisation for Scientific Research, Prins Bernard Cultuurfonds and a VSB-beurs. We thank Jo Habets for performing the ovariectomies and the animal care.

Chapter 5

Effects of zoledronic acid on rat vertebrae

The contents of this chapter are based on J.E.M.Brouwers, B.v.Rietbergen, M.L.Bouxsein, Influence of early and late zoledronic acid administration on vertebral structure and strength in ovariectomized rats, *Calcif Tissue Int.* 2008 Sept; 83(3):186-91.

Abstract

An annual infusion of zoledronic acid (ZOL) reduces fracture risk in osteoporotic patients. Previously, we showed that a single ZOL injection inhibited changes in bone microstructure and strength in rat tibiae after ovariectomy (Brouwers et al., *Calcif. Tissue Int.*, 2008). Here, we determined the effects of a single ZOL injection as preventive and restorative treatment on the bone microstructure and strength in lumbar and caudal vertebrae of ovariectomized (OVX) rats.

Twenty-nine female 35-week old Wistar rats were divided into four groups: SHAM-OVX (n=9), OVX (n=5), OVX and early ZOL (n=8) and OVX and late ZOL (n=7). ZOL was given once (20 µg/kg b.w. s.c.) at OVX in the early ZOL, and eight weeks later in the late ZOL group; rats were sacrificed 16 weeks after OVX. Trabecular and cortical bone microarchitecture were measured in lumbar (L3) and caudal (Cd6) vertebrae using micro-CT and compressive mechanical properties were determined in L3 vertebrae.

Compared to SHAM-OVX, OVX rats had significantly lower BV/TV and SMI, Tb.N, Tb.Sp and Conn.D tended to be deteriorated in lumbar vertebrae, while both ZOL groups did not differ from the SHAM-OVX group. Both ZOL groups had significantly higher BV/TV than OVX; the early ZOL group also had significantly lower SMI and higher Tb.Th. OVX tended to decrease mechanical properties, while early and late ZOL treatment inhibited OVX-induced degeneration. Neither OVX nor ZOL induced changes in trabecular microarchitecture of caudal vertebrae. Summarized, in adult rats a single ZOL injection inhibited OVX-induced changes in lumbar vertebral bone microarchitecture and strength.

5.1 Introduction

Bisphosphonates inhibit bone resorption and are commonly used to treat osteoporotic patients. They slow the process of bone loss and reduce the risk of fracture by maintaining bone mass and microstructure (22;102;234). Zoledronic acid is a potent bisphosphonate that has recently been shown to significantly reduce fracture risk in osteoporotic patients who received once-yearly doses (17;174). As the number and depth of *in vivo* analyses in patients is limited, animal research is ongoing to further elucidate the effects of zoledronic acid on skeletal fragility (79;85;86;103). Previously, we showed in a longitudinal study of adult rats that a single injection of zoledronic acid at the time of ovariectomy (OVX) inhibited OVX-induced deterioration of bone microstructure and strength in the proximal tibiae for up to 16 weeks (33). Furthermore, a single injection of zoledronic acid eight weeks after OVX inhibited further deterioration of the bone microstructure and strength in rat tibiae compared to untreated, OVX rats. Other studies have shown that weekly injections of zoledronic acid inhibit changes in bone microstructure and strength in rat vertebrae after OVX (85;103). However, it is not known to what extent a *single* dose of zoledronic acid is able to inhibit and restore ovariectomy-induced loss of bone mass, structure and strength in rat vertebrae.

Most studies in rats conducted to determine bone changes induced by OVX and/or the efficacy of pharmacologic intervention evaluate skeletal sites with red (haematopoietic) marrow, such as the proximal tibia and lumbar vertebra. Yet, bone sites with yellow (fatty) marrow, such as the distal tibia and the caudal vertebra, are known to have different cell composition than red marrow bone sites, and may respond differently to estrogen depletion (164). Also, caudal vertebrae in rats are subject to a different loading environment than other vertebrae, which may also affect the response to ovariectomy and/or drug intervention.

The goal of this study was to determine the effects of a single zoledronic acid injection as a preventive and restorative treatment on the bone microstructure and strength in lumbar vertebrae of ovariectomized rats. Additionally, we assessed whether lumbar and caudal vertebrae respond similarly to ovariectomy and/or zoledronic acid treatment in terms of bone microarchitecture.

5.2 Materials and methods

Twenty-nine female 35-week old Wistar rats were used from a previous study (33). In brief, rats were weight-based divided into four groups: SHAM-OVX (n=9), ovariectomy (OVX) (n=5), OVX and early zoledronic acid (ZOL) (n=8) and OVX and late ZOL (n=7). Sample size was calculated for the previously conducted longitudinal study and was nine per group. However, the number of animals was lowered and differed between groups due to nonsuccessful ovariectomies, determined after sacrifice based on uterine weight. All rats were ovariectomized at week 0, the SHAM-OVX group underwent a SHAM ovariectomy. The early ZOL group received ZOL at a

single dose of 20 µg/kg body weight s.c. at the time of OVX. The dose was chosen based on a dose-response study in rats, in which 20 µg/kg body weight was found to be most effective (80). The late ZOL group received the same single dose eight weeks after OVX. Rats were sacrificed 16 weeks after OVX by exsanguination.

After sacrifice, whole lumbar (L3) and caudal (Cd6) vertebrae were dissected, soaked in 0.9% saline solution gauze and frozen at -20 °C. This study was approved by the Animals Ethics Committee of the University of Maastricht, the Netherlands. Zoledronic acid was kindly provided as the disodium salt hydrate by Novartis Pharma AG (Basel, Switzerland) and was dissolved in a saline vehicle prior to injection.

5.2.1 Assessment of vertebral microarchitecture

L3 and Cd6-vertebrae were thawed to room temperature and scanned using a high-resolution desktop microtomographic imaging system (microCT40 Scanco Medical AG, Bruetisellen, Switzerland) at an isotropic voxel size of 16 micrometer (55 kV, 145 µA, 500 projections per 180 degrees, 200 ms integration time) and 12 micrometer (55 kV, 145 µA, 500 projections per 180 degrees, 200 ms integration time), respectively. A smaller voxel size was chosen for the caudal vertebrae as their size and therefore volume of interest is smaller than lumbar vertebrae. After scanning, samples were frozen again until mechanical testing. Images were subjected to a Gaussian filter and binarized (sigma=0.8, support=1, threshold = 32% of maximal grayscale value) to separate bone from background (195).

For the L3-vertebrae, the trabecular region was manually selected starting ten slices below the cranial growth plate and ending ten slices above the caudal growth plate, resulting in a trabecular region of approximately 5 mm in axial direction. From this region, six bone structural parameters (bone volume fraction (BV/TV), connectivity density (Conn.D), structure model index (SMI), trabecular number (Tb.N), trabecular thickness (Tb.Th) and separation (Tb.Sp) were automatically determined. The cortical bone was semi-automatically selected from the CT-scans, using the same set of slices as used when selecting the trabecular bone, from which the average cortical thickness was determined. Because the caudal vertebrae had shown to be symmetrical in the cranial-caudal direction, the top half of trabecular bone was manually selected in the CT-scans of the Cd6-vertebrae, starting ten slices below the cranial growth plate. From this region, the same structural parameters were determined as in the L3-vertebrae.

5.2.2 Static vertebral compression tests

All L3-vertebrae were thawed to room temperature prior to mechanical testing. To achieve plano-parallel ends, vertebrae were fixed in a custom-made jig. A double-blade, low-speed diamond saw (Isomet, Buehler, Lake Bluff, IL) was used under constant saline irrigation to remove cranial and caudal ends including the growth plate, resulting in a vertebral height of about 4.2 mm. A single-blade, wafering, low-speed diamond saw was used under constant saline irrigation to remove all posterior pedicles and processes. Anterior elements were clipped off resulting in an isolated vertebral

body. After sawing, the exact vertebral height was measured using a caliper. Vertebrae were kept frozen in a 0.9% saline solution until mechanical testing.

After thawing, vertebrae were compressed at a constant displacement rate (3 mm/min) until failure (Synergie 100, MTS Systems, Eden Prairie, MN). Displacement was measured from the actuator displacement transducer of the testing machine and was corrected for stiffness of the testing system. From the force-displacement curve, the following mechanical parameters were determined: 1) stiffness, calculated as the slope in the linear region between 40 and 80% of the maximum force, 2) ultimate load, defined as the maximum load, 3) displacement at ultimate load and 4) energy to ultimate load, defined as the area under the curve until ultimate load.

5.2.3 Data Analysis

All parameters were compared between groups using an ANOVA with Bonferroni post-hoc test comparing all groups with each other. A two-way ANOVA was done to determine whether the response to ovariectomy and ZOL was different between the L3- and Cd6-vertebrae. P-values less than 0.05 were considered significant.

5.3 Results

5.3.1 Effects of OVX and ZOL on lumbar vertebral microarchitecture

Compared to SHAM, OVX rats had a significantly lower BV/TV in L3 vertebrae (figure 5.1). SMI, Tb.N, Tb.Sp and Conn.D were also substantially deteriorated in the OVX group, however, these differences did not reach significance. Both ZOL groups had significantly higher BV/TV than OVX; the early ZOL group also had significantly lower SMI and higher Tb.Th compared to OVX. Trabecular microarchitecture did not differ between SHAM-OVX and ZOL-treated groups, except for Tb.Th, which was significantly higher in the early ZOL group than in the SHAM-OVX group. Trabecular architecture did not differ between the early and late ZOL groups. Cortical thickness also did not differ between groups.

5.3.2 Effects of OVX and ZOL on vertebral compressive properties

Compressive stiffness and ultimate load were lower in OVX compared to other groups, though this did not reach statistical significance (figure 5.2). There was a trend for both the early and late ZOL groups to have slightly higher stiffness and failure load than the SHAM-OVX group. Displacement at ultimate load was similar in OVX and SHAM groups, while it tended to be lower in both ZOL groups. No differences were observed in energy to failure.

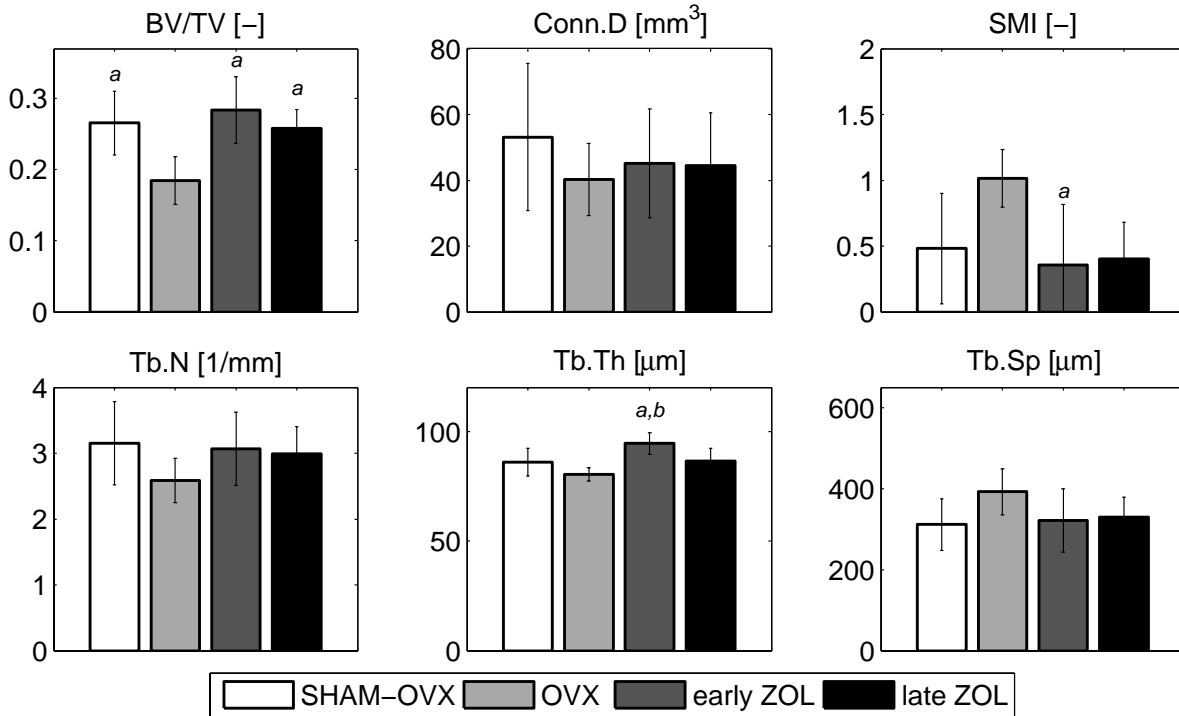


Figure 5.1: Effect of OVX and ZOL treatment on trabecular microarchitecture of lumbar (L3) vertebrae (mean ± SD). a) significantly different from OVX, b) significantly different from OVX-SHAM.

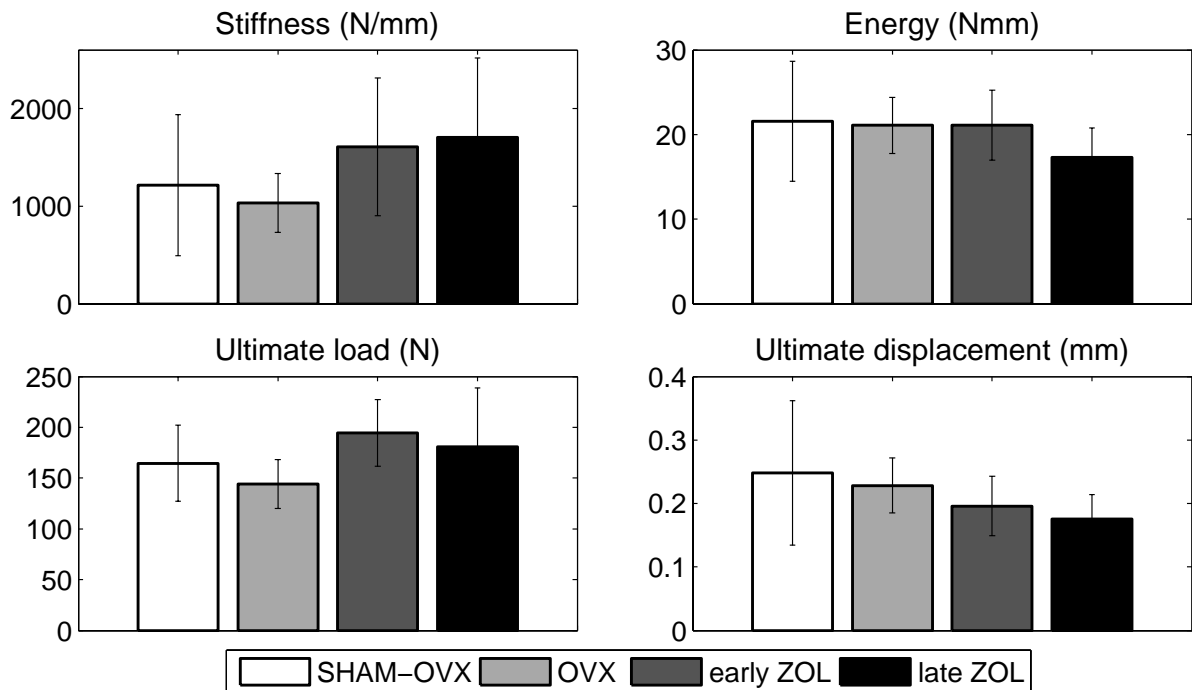


Figure 5.2: Effect of OVX and ZOL treatment on monotonic compressive mechanical properties of lumbar vertebrae (mean ± SD).

5.3.3 Comparison between response to OVX and ZOL in lumbar and caudal vertebrae

In the Cd6-vertebrae, trabecular architecture did not differ between groups (figure 5.3). The response to ovariectomy was significantly different between caudal and lumbar vertebrae for BV/TV and SMI (p-interaction = 0.010 and 0.012, respectively). Zoledronic acid treatment did not alter bone microarchitecture, which may be expected since OVX did not lead to trabecular deterioration in the caudal vertebrae.

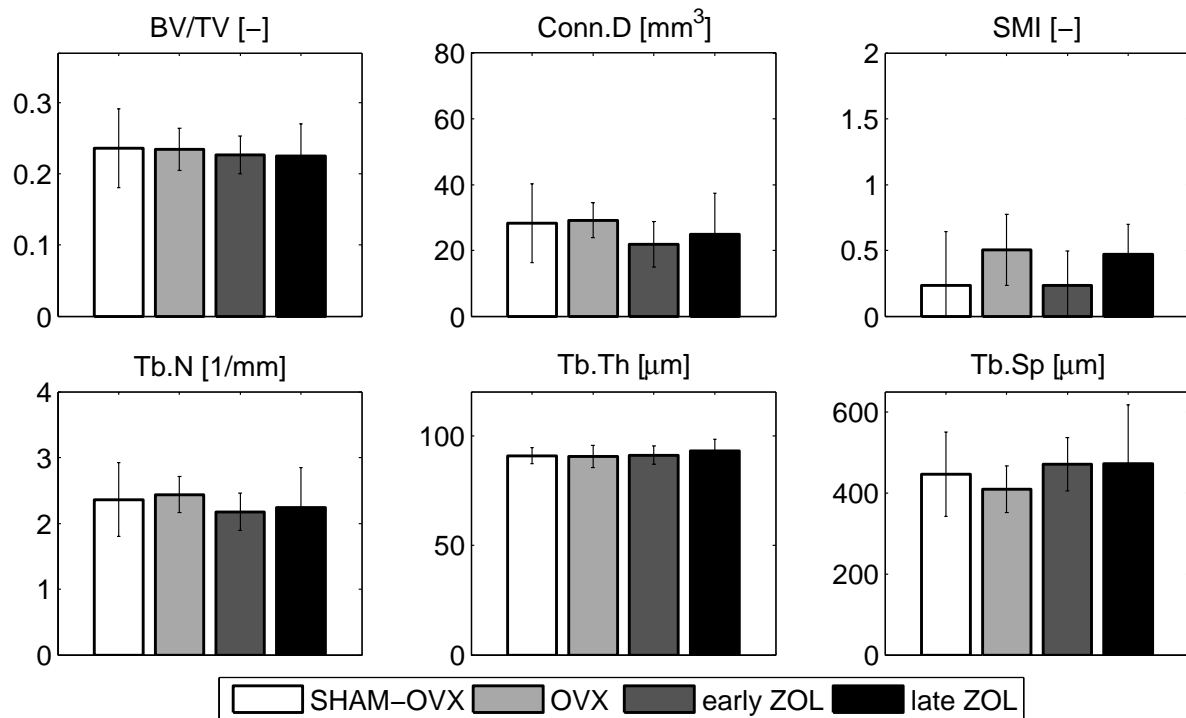


Figure 5.3: Effect of OVX and ZOL treatment on trabecular microarchitecture of caudal (Cd6) vertebra (mean \pm SD).

5.4 Discussion

In this study, we found that 1) a single ZOL injection inhibited deterioration of trabecular bone microarchitecture and strength in lumbar vertebrae of ovariectomized rats, 2) neither ovariectomy nor ZOL treatment influenced microarchitecture in caudal vertebrae and 3) differences between early and late ZOL treatment were not detectable by end-of-study measurements.

Previously, it has been shown that one year of *weekly* injections of zoledronic acid inhibits ovariectomy-induced changes in bone microstructure and bone strength of femora and lumbar vertebrae of rats (85;86;103). Also, it has been shown that, in the same rats as used in this study, a single injection of zoledronic acid prevents deterioration of bone microstructure and strength in tibiae of ovariectomized rats for 16 weeks and a single injection at eight weeks after ovariectomy prevents further deterioration of structure and strength (33). Additionally, in a dose-response study, it

has been shown that a single injection can inhibit structural changes seen after OVX in the tibia and retain mechanical properties in the vertebra (80). In this study, we have determined that a single injection of zoledronic acid can inhibit changes in bone microstructure and strength in vertebrae. Vertebrae present a clinically relevant anatomical site for the treatment of osteoporosis. As such, our study includes novel and relevant information on the effects of a single zoledronic acid injection on trabecular bone microarchitecture and cortical thickness in lumbar as well as in caudal vertebrae. The pattern in bone volume fraction between the four groups in the lumbar vertebrae was exactly the same as that seen in the proximal tibiae (33). Also a significant correlation was found between all individual values for bone volume fraction of the lumbar vertebrae and those of the tibiae ($r^2=0.4$, $p<0.001$, data not shown). This indicates that the response to ovariectomy and zoledronic acid was similar in the tibiae and the lumbar vertebrae.

Mechanical properties of lumbar vertebrae were reduced in ovariectomized versus SHAM-ovariectomized rats, while treatment with zoledronic acid inhibited these losses. Both stiffness and ultimate load in the ZOL treated groups were similar to the SHAM-OVX group. Ultimate displacement tended to be lower in both ZOL groups compared to the SHAM-OVX and OVX groups, which could be an indication of a slightly more brittle tissue due to increased mineralization, although in a recent study no effect of zoledronic acid on mineral crystal size was determined in ZOL treated, ovariectomized rats (296). In general, we conclude that both early and late ZOL treatment resulted in overall, normal mechanical properties.

Unique aspects of our study were that the effect of ovariectomy on caudal vertebrae was analyzed using micro-CT, and that the effect of ZOL treatment on ovariectomized rats was studied in caudal vertebrae. In contrast to the results from lumbar vertebrae, trabecular architecture in caudal vertebrae did not change in response to ovariectomy and zoledronic acid. Our results concur with previous reports on none responsiveness to ovariectomy in caudal vertebrae (143;162;164;183). It has been suggested that differences in marrow composition between lumbar and caudal vertebrae plays a role in responsiveness to ovariectomy (164). Cancellous bone turnover in yellow marrow, such as in the caudal vertebrae, is lower than in red marrow sites, such as in the lumbar vertebra, as evidenced by decreased osteoclast surface, osteoclast number, mineral apposition rate and bone formation rate (164). These differences may be related to the cellular composition and vascularity of bone marrow. Also, it has been shown that the response to PTH is different between caudal and lumbar vertebrae (162). Altogether, this indicates that the response to ovariectomy and to different drug treatments are different in the caudal than in the lumbar vertebra, rendering the caudal vertebra less interesting as a therapeutic testing site.

Differences between early and late ZOL treatment were not detectable by end-of-study measurements, though early ZOL treatment had a slightly better effect on bone morphology compared to late ZOL treatment. The late ZOL group received the ZOL injection eight weeks after ovariectomy. It is known that eight weeks after ovariectomy, bone microarchitecture has significantly deteriorated in the rat vertebra (106). As bone volume fraction was similar in the early and late ZOL groups, we

postulate that after ZOL treatment, bone volume fraction somewhat increased, as seen in the tibiae as well (33), probably due to the filling of resorption cavities (78).

This study had several limitations. The tibiae of the rats used in this study, were previously analyzed by *in vivo* micro-CT and the groups were found to have slightly different baseline values. Since in this study only end-point measurements of the vertebrae were performed, it is possible that there was also a small difference in baseline values in the vertebrae of these rats. Previously, however, we showed in the longitudinal study that these differences did not influence overall trends between groups in the tibiae and therefore it is thought that overall trends in the vertebrae would be similar as well (33). Also, the rats were scanned several times while living, which could have led to radiation damage. However, we showed previously that the design of the rat holder was such that only the scanned leg was exposed to radiation and that no radiation damage was found in the scanned leg after eight weekly scans (36). Therefore, any radiation damage can be ruled out.

Another limitation to this study was the fact that we were unable to detect significant deterioration of mechanical properties resulting from ovariectomy as well as differences between early and late ZOL treatment by end-of-study measurements. This lack of significant effect may relate to the fact that the study was designed for follow-up measurements, which makes the number of samples needed lower than desirable for the present study. For these cross-sectional measurements in the vertebrae, sample sizes were relatively low, reducing the power of the study to detect significant differences. However, it should be noted that our primary question was whether a single injection can prevent OVX induced bone loss. We were able to answer this question with adequate power and statistical significance. In the current study, also a nonsignificant difference of 10% between the early and late ZOL group in bone volume fraction was found. It can be argued whether a study should be designed to detect a small difference of 10% and whether this is scientifically relevant. A power study conducted indicated that with the sample size and variance seen in bone volume fraction of lumbar vertebrae, and a generally assumed power of 80% and α of 0.05, a difference of 20% in mean between the early and late ZOL group would have been detected. Thus, although the study did not have the power to detect a small difference of 10%, it was adequately powered to answer the primary question and to answer secondary questions if the differences were large enough to be clinically relevant (i.e., on the order of 20%). It should also be noted that in previous studies on the effects of weekly ZOL injections on mechanical properties, group sample sizes were between 16-20, offering a higher power to detect differences (86;103). Therefore, further studies with a larger sample size are needed to distinguish between the effects of early and late ZOL treatment on vertebral trabecular microarchitecture and strength.

In conclusion, we showed that a single injection of zoledronic acid inhibits deterioration of bone microstructure and strength in lumbar vertebrae of ovariectomized rats, demonstrating the potent, long-term anti-resorptive effect of this therapy. These data corroborate data from human iliac biopsies taken from osteoporotic patients after three years of ZOL treatment (216). Altogether, these positive effects on

trabecular microarchitecture and strength likely contribute to the anti-fracture efficacy of zoledronic acid.

Acknowledgements

This work was funded by the Netherlands Organisation for Scientific Research (NWO), Prins Bernard Cultuurfonds and a VSBfonds scholarship. We thank John Muller for technical advice and assistance with mechanical testing.

Chapter 6

Rat vertebral compressive fatigue properties

The contents of this chapter are based on J.E.M.Brouwers, M.Ruchelsman, B.v.Rietbergen, M.L.Bouxsein, Determination of rat vertebral bone compressive fatigue properties in untreated intact rats and zoledronic acid treated, ovariectomized rats. *Osteoporosis International*. 2008, *submitted*.

Abstract

Osteoporosis is often treated with bisphosphonates, which reduce fracture risk. The effects of bisphosphonates on fatigue strength, which may be clinically relevant for vertebral fractures, are unknown. We compared vertebral, compressive fatigue properties between normal and zoledronic acid (ZOL) treated, OVX rats.

35-week old Wistar rats were divided into SHAM-OVX (n=7) and OVX with ZOL treatment (n=5) (single injection, 20 µg/kg b.w. s.c.). After 16 weeks, rats were sacrificed and vertebral trabecular microarchitecture and cortical thickness were determined using micro-CT. Vertebral bodies were cyclically compressed in load-control at 2 Hz. For each sample, time to failure, apparent strain at failure, steady-state creep rate, initial stiffness and percent loss of stiffness at failure were calculated. Data were compared using student's t-test.

Morphological parameters were the same in both groups. Samples failed between five minutes and 15 hours. Force displacement curves displayed typical fatigue behavior. Displacement increased over time due to mostly creep and to decreasing secant stiffness. All fatigue properties were similar in both groups.

We established a technique to determine compressive fatigue properties in the rat vertebral body. Our initial results indicate that ZOL-treated OVX rats have similar vertebral fatigue properties as SHAM-OVX controls.

6.1 Introduction

Osteoporosis is a bone disorder that affects millions of people worldwide. It is characterized by an increased bone resorption rate and a decreased bone formation rate, resulting in low bone mass and increased fracture risk. Approximately 50 percent of age-related vertebral fractures are believed to be spontaneous fractures, resulting from daily activities or from cyclic loading, rather than from trauma (72;224).

Bisphosphonates are often used to treat osteoporotic patients. They inhibit bone resorption and thereby slow down the process of bone loss, maintaining bone mass, microstructure and strength in relevant anatomical sites like the femur and vertebra, in animals as well as in humans (22;102;234). Importantly, fracture risk is significantly reduced in osteoporotic patients treated with bisphosphonates (20;83;209;234). Zoledronic acid is a potent, relatively new bisphosphonate that recently has been shown to significantly reduce fracture risk in osteoporotic patients who received once-yearly doses (17). We have previously shown that zoledronic acid both inhibited and recovered loss of bone structure and strength in ovariectomized rat tibiae and vertebrae resulting in values that were similar to control levels (33;34).

Bisphosphonates have also been shown to influence the degree of mineralization of bone tissue due to decreased bone turnover rates and the subsequent prolongation of secondary mineralization (10;18), which may lead to more brittle mechanical behavior (3;11;38;172). Crystallinity of bone tissue has been shown to influence monotonic and fatigue mechanical properties in human cortical bone (297). Microcracks and diffuse damage are commonly seen in human bone (45;64;185) and may act as a stimulus for bone remodeling (184). Studies in dogs have shown that low resorption rates induced by bisphosphonates lead to accumulation of microcracks and diffuse damage (38). It is unknown whether these increases in mineralization and microdamage resulting from bisphosphonates influence the mechanical properties of bone when cyclically loaded.

Compressive and tensile fatigue behavior has been well documented for cortical bone from humans as well as animals (40;42;208;241). More recently, the fatigue behavior of trabecular bone in animals and humans has been found to exhibit similar characteristics as cortical bone (29;30;91;214). Although these studies have provided fundamental information regarding bone fatigue behavior, the integral function of cortical and trabecular bone, which plays an important role in the vertebra, has not been accounted for. Moreover, drug efficacy studies in rats generally focus on changes in bone mass, structure and static mechanical strength, whereas fatigue behavior, which may play an important role in vertebral fractures, may respond differently to pharmacologic intervention than other statically-determined mechanical parameters.

Our aim was to develop an experimental approach to determine compressive fatigue mechanical properties in whole rat vertebra. This technique then was used to compare fatigue compressive properties of whole vertebrae in ovariectomized rats treated with zoledronic acid with those of SHAM ovariectomized controls.

6.2 Materials and methods

Seventeen female 35-week old Wistar rats were used from a previous study described elsewhere (33). At week 0, 8 rats were ovariectomized (OVX-ZOL) and 9 rats were SHAM-ovariectomized (SHAM-OVX). Zoledronic acid was kindly provided as the disodium salt hydrate by Novartis Pharma AG (Basel, Switzerland) and was dissolved in a saline vehicle prior to injection. It was administered at a single dose of 20 µg/kg body weight s.c. at the time of OVX to all rats of the OVX-ZOL group. Rats were sacrificed 16 weeks later by exsanguination and whole L4-vertebrae were dissected, soaked in 0.9% saline solution gauze and frozen at -20⁰ C. This study was approved by the Animals Ethics Committee of the University of Maastricht, the Netherlands.

6.2.1 Micro-CT scanning

Vertebrae were thawed to room temperature and scanned with a desktop micro-CT system (microCT40, Scanco Medical AG, Bruettisellen, Switzerland) at an isotropic resolution of 16 micrometers (55 kV, 145 µA, 500 projections per 180 degrees, 200 ms integration time). After scanning, samples were frozen again until mechanical testing. Images were Gaussian filtered (sigma=0.8, support=1 voxel) and binarized to separate bone from background using a global thresholding procedure (195).

From the CT-scans, the trabecular region was manually selected starting ten slices below the cranial growth plate and ending ten slices above the caudal growth plate, resulting in a trabecular region of approximately 5 mm in axial direction. From this region, six bone structural parameters (bone volume fraction (BV/TV), connectivity density (Conn.D), structure model index (SMI), trabecular number (Tb.N), trabecular thickness (Tb.Th) and separation (Tb.Sp) were automatically determined. Cortical bone was semi-automatically selected from the CT-scans, using the same set of slices as used when selecting the trabecular bone, from which the average cortical thickness was determined.

6.2.2 Specimen preparation

Vertebrae were thawed to room temperature prior to mechanical testing. To achieve plano-parallel ends, vertebrae were fixed in a custom-made jig. A double-blade, wafering, low-speed diamond saw (Isomet, Buehler, Lake Bluff, IL) was used under constant saline irrigation to remove cranial and caudal ends including the growth plate, resulting in a vertebral height of about 4.2 mm. A single-blade, wafering, low-speed diamond saw was used under constant saline irrigation to remove all posterior pedicles and processes. Anterior elements were clipped off using a rongeur resulting in a separated vertebral body. CT-scans taken of pilot-samples had shown no splintering resulted from sawing and clipping. After sawing, the exact vertebral height was measured using a caliper. Vertebrae were kept frozen in a 0.9% saline solution until fatigue testing.

6.2.3 Fatigue compression tests

L4-vertebral bodies were used for fatigue compression tests, which were conducted in load-control at 25⁰ C. A custom-made, steel lower plate was designed in the form of a cup (figure 6.1). The vertebral body was placed with the cranial end facing upwards in the lower cup of the testing machine (Instron 8874, Instron Corp. Canton, MA, USA). The top platen, smaller in diameter than the cup, was lowered onto the vertebra to a compressive preload of 5N, at which point, the displacement was set at zero. Displacement was measured from the actuator displacement transducer of the testing machine. A 0.9% saline solution containing protease inhibitors, was added to the cup to prevent the vertebra from dehydrating and to inhibit micro-organism growth. Since bone is known to fail at a certain strain rather than at a certain load or stress (137;138), and since our aim was to compare the fatigue properties at the tissue rather than structural level between the two groups, all tests were started at the same apparent strain. In a pilot-study, the relation between initial apparent strain and number of cycles to failure was studied. It was found that 0.75% initial apparent strain resulted in a reasonable number of cycles to failure (average number of cycles ~ 40000) and therefore this value was used in all tests. Since the stiffness varied per sample and the test was run in load-control, the load needed to reach the desired initial apparent strain varied as well. Therefore, prior to testing, each sample was cyclically loaded for about 400 cycles with increasing load until the load was reached at which the desired apparent strain was met. The maximum load ranged from 63 to 97 N.

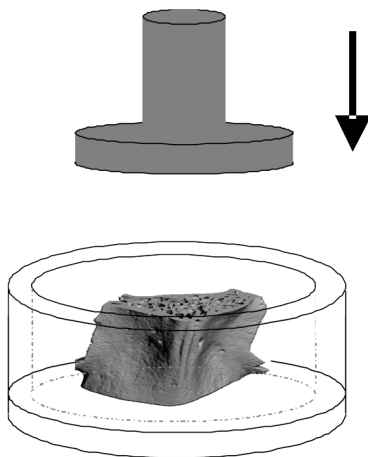


Figure 6.1: Schematic of fatigue loading test. The lower platen, designed as a cup, contained the vertebra. The top platen, smaller in diameter than the cup, was lowered onto the vertebra to a compressive preload of 5N, at which point, the displacement was set at zero. A 0.9% saline solution containing protease inhibitors, was added to the cup to prevent the vertebra from dehydrating and to inhibit micro-organism growth.

During the test, load cycled between 5 N and the determined maximum load in a sinusoidal shape at a frequency of 2 Hz. Failure of the sample was defined as a sudden

increase in displacement. Tests were stopped after 120.000 cycles if failure had not occurred. Every fourth cycle, force and displacement were acquired during one cycle at a sampling frequency of 100 Hz.

For each sample, creep characteristics exhibited three classical phases: an initial phase of high creep rate, a phase of a lower creep rate and a phase in which creep rate was high again, finally resulting in failure (figure 6.2, 6.3) (29;134). From each apparent strain versus time curve, the steady-state creep rate of the secondary phase was determined by fitting a linear line through the central part of the curve. According to the method of Bowman et al (29), a line parallel to this line was drawn at 0.5% higher offset. The intersection of this line with the apparent strain curve was defined as the time to failure and the apparent strain at failure. Secant stiffness was calculated for each recorded cycle by dividing the load range by the displacement range of that cycle. Initial secant stiffness was determined at the start of the experiment and final secant stiffness was determined at the time of failure. For each sample, time to failure, apparent strain at failure, steady-state creep rate, initial stiffness and percent loss of stiffness at failure were calculated.

6.2.4 Data analysis

Pearson correlation coefficients were used to determine the relation between trabecular bone microarchitecture, cortical thickness and compressive fatigue properties. For this, all structural properties were correlated with fatigue properties as well as with log-transformed values of the fatigue properties. Also, all structural and fatigue parameters were compared between the two groups using a Student's t-test. P-values below 0.05 were considered significant.

6.3 Results

During fatigue testing, twelve samples failed between ten minutes and 14.7 hours (1200 and 106000 cycles) and five samples did not fail within the studied period of time. The latter samples showed a decreasing, rather than an increasing, apparent strain range per cycle during the test, accompanied by an increasing secant stiffness suggesting that artifacts were present in these tests (89). These samples were subsequently removed from from all analyses in the study resulting in 7 samples in the SHAM-OVX and 5 in the ZOL group.

6.3.1 Trabecular and cortical microarchitecture

No significant differences were found in trabecular bone microarchitecture and cortical thickness between the SHAM-OVX and the OVX-ZOL treated group except for Tb.Th, which was significantly higher in the ZOL treated group (table 6.1). These data indicate that ZOL treatment inhibited the development of osteopenia expected after ovariectomy.

Table 6.1: Structural parameters and cortical thickness determined in L4 vertebrae (mean \pm SD). Tb.Th was found to be significantly different between groups.

	BV/TV (-)	Conn.D (1/mm ³)	SMI (-)	Tb.N (1/mm)	Tb.Th (μ m)	Tb.Sp (μ m)	Cortical thickness (μ m)
SHAM-OVX N=7	0.288 (\pm 0.034)	60.5 (\pm 25.0)	0.554 (\pm 0.319)	3.27 (\pm 0.583)	89.4 (\pm 5.3)	290 (\pm 46)	174 (\pm 12)
OVX-ZOL N=5	0.285 (\pm 0.043)	43.8 (\pm 11.5)	0.425 (\pm 0.461)	2.91 (\pm 0.500)	95.8 (\pm 1.5)	335 (\pm 70)	183 (\pm 12)

6.3.2 Fatigue compression tests

For all failed samples, force displacement cycles displayed typical fatigue behavior characterized by decreasing secant stiffness, increasing hysteresis and increasing nonlinearity (figure 6.2). Displacement increased over time due to mostly creep and to a lower extent, decreasing secant stiffness. For each sample, the steady-state creep rate was determined from the apparent strain versus time curve, as well as the time to failure and apparent strain at failure (figure 6.3).

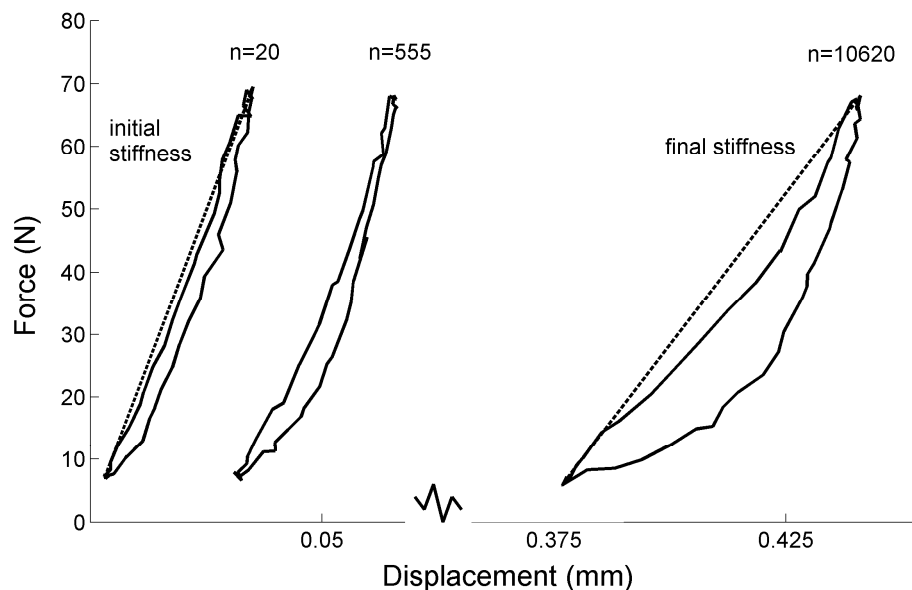


Figure 6.2: Three representative force-displacement cycles throughout the testing period: 20, 55 and 10,620 cycles for a typical sample. Force displacement cycles display typical fatigue behavior characterized by decreasing secant stiffness, increasing hysteresis and increasing nonlinearity. Displacement increases over time due to mostly creep and to a lower extent, a decreasing secant stiffness.

Time to failure, apparent strain at failure, steady-state creep rate, initial stiffness and percent loss of stiffness at failure were not significantly different between the two groups (table 6.2). Steady-state creep rate and log of the time to failure have shown to be inversely linearly correlated in compressive fatigue studies on bovine trabecular

bone (29;30). Here, we also found a strong inverse correlation between log of the steady-state creep rate and log of the time to failure, of all samples taken together ($r^2=0.86$, $p<0.001$, figure 6.4). No difference in this relation was found between SHAM-OVX and OVX-ZOL. Log of the steady-state creep rate and log of the time to failure were similar in the ZOL treated and SHAM-OVX group.

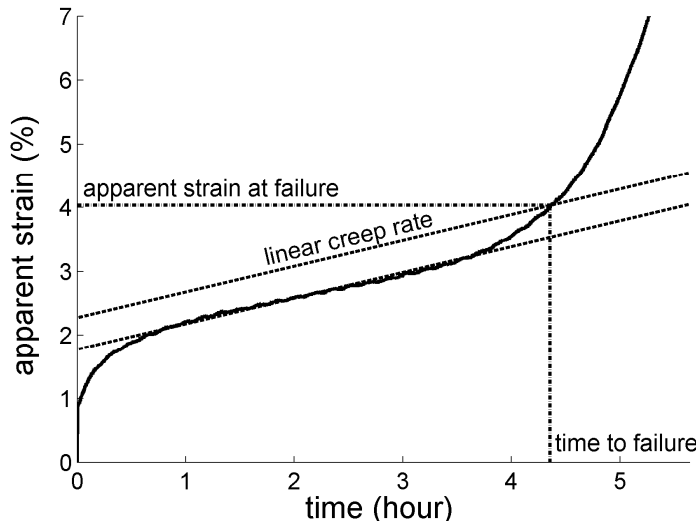


Figure 6.3: Typical sample for which creep characteristics exhibit three typical phases of fatigue: an initial phase of high creep rate, a phase of a steady-state lower creep rate and a phase, in which creep rate is high again, finally resulting in failure [31, 35]. From each apparent strain against time curve, the creep rate of the secondary phase is determined by fitting a linear line. According to the method of Bowman [31] et al., a line parallel to this line is drawn at 0.5% higher offset. The intersection of this line with the apparent strain curve is defined as the time to failure and the strain at failure.

Table 6.2: Fatigue properties determined in L4 vertebrae (mean \pm SD). No significant differences were found.

	Time to failure (hour)	Apparent strain at failure (%)	Linear creep rate (%/hour)	Initial stiffness (N/mm)	Loss of stiffness (%)
SHAM-OVX	5.42 (+-4.67)	4.19 (+-1.52)	0.80 (+-1.25)	2193 (+-285)	20.11 (+-6.68)
OVX-ZOL	5.51 (+-5.80)	4.30 (+-1.50)	0.50 (+-0.37)	2396 (+-191)	16.96 (+-9.59)

6.3.3 Relation between morphology and fatigue properties

BV/TV, Conn.D, Tb.N and Tb.Sp each correlated with apparent strain at failure as well as with log of the apparent strain at failure ($0.31<r^2<0.50$, $p<0.05$). All other correlations between morphologic parameters and fatigue properties were not significant.

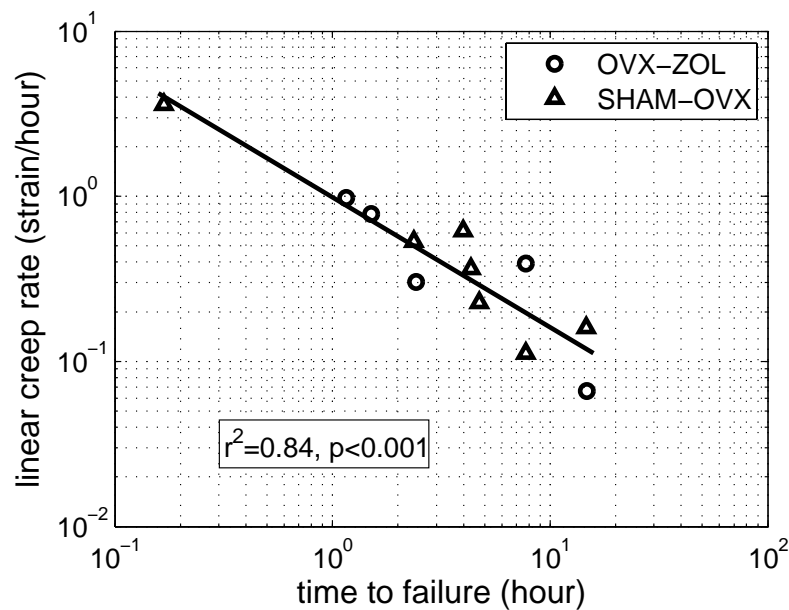


Figure 6.4: Steady-state creep rate plotted against time to failure for all samples on a log-log scale. A significant inverse linear correlation was found between log of the time to failure and log of the steady-state creep rate ($r^2=0.84$, $p<0.001$).

6.4 Discussion

In this study, we developed a method for assessing the fatigue properties of whole rat vertebrae. Typical fatigue behavior was seen in SHAM-OVX as well as in ZOL treated, ovariectomized rats. Fatigue properties were not significantly different between SHAM-OVX and OVX-ZOL rats. Trabecular microarchitecture and cortical thickness were also similar in vertebrae of ZOL treated and SHAM-OVX rats. Previously, we showed that static compressive behavior was similar in L3-vertebrae of the same groups of rats (34). Altogether, this suggests that ZOL treatment of OVX rats results in the same vertebral bone mass and structure as SHAM-OVX rats, as well as the same vertebral static and fatigue properties.

For all vertebrae, force displacement curves displayed typical fatigue behavior characterized by decreasing secant stiffness, increasing hysteresis and increasing non-linearity. This agrees with compressive, fatigue behavior previously reported for cortical and trabecular bone specimens (29;30;40;91). Also, the strong linear correlation between the log steady-state creep rate and the log time to failure agrees with the literature (29;30), which indicates the validity of the test. This also indicates that the integral fatigue behavior of cortical and trabecular bone in rats is similar to the two bone compartments assessed separately. We found an average apparent strain at failure of about 4% for both groups, which is just slightly higher than the 3.4% and 2.8% reported for respectively human and bovine trabecular bone (29;91).

Samples that did not fail during the test were removed from further analysis and showed a decreasing rather than an increasing apparent strain range per cycle during the test accompanied by an increasing secant stiffness. This behavior suggests that

artifacts were present in these tests (89;136), possibly due to vertebral ends that were not perfectly parallel. In this case, when the force range, leading to a 0.75% apparent strain, was determined at the start of the test, the actual area bearing the load would be smaller than the total bone area. During the test, this area would then be compressed, resulting in the load being born by the area of the whole vertebra and thus in lower strains.

The fatigue behavior in these whole vertebrae was comparable to the fatigue behavior found in studies on cortical and trabecular bone, though no fatigue data on rat bone are available. Although not determined in our study, it would be interesting to study whether failure starts in the cortical or trabecular bone.

Few parameters of microarchitecture correlated significantly with fatigue properties or with log of the fatigue properties. The morphology and structural parameters of the vertebrae used in both groups were very similar and any intrinsic variance in bone mass and stiffness was accounted for in the fatigue test by starting all tests at the same apparent strain level. One might therefore expect that trabecular structure does not predict fatigue properties, which needs to be corroborated by additional studies. Notably, in human trabecular bone, bone volume fraction is weakly correlated with strain at failure, which agrees with our findings (214).

Rather than applying the same load, which will result in low bone mass samples failing earlier than high bone mass samples, we applied the same apparent strain in each test. By developing this normalized fatigue test we aimed at determining changes in fatigue properties due to differences at the tissue rather than the structural level. The fact that no difference in fatigue behavior was found between both groups indicates that either no changes occurred in the bone tissue fatigue properties or that we were unable to detect them. Increased microdamage and mineralization that may have taken place in the ZOL group due to lower turnover rate apparently did not lead to detectable changes in fatigue properties of the bone tissue. It may be however, that a longer treatment period would have led to noticeable changes. Also, no untreated OVX group was included in this study and therefore the effects of OVX vs. ZOL treatment cannot be separated. Theoretically, it could be that OVX would lead to altered fatigue properties, which could have then been reversed by ZOL resulting in no differences between SHAM-OVX and ZOL treated OVX rats. This will need to be tested by additional studies.

In our study several samples did not fail during the test, which reduced sample size. Also, between-subject variation was found to be high, which together reduced the power to detect differences between the groups. The sufficient quality of the fatigue test however was reflected in the fact that typical fatigue behavior was seen in terms of force displacement curves and a strong correlation between steady-state creep rate and log of the time to failure. No observation of substantial differences between groups was found, and this study presents therefore the first indication that ZOL treated, ovariectomized rats have similar fatigue properties as control rats. More studies are needed to further elucidate the effects of bisphosphonates on fatigue properties. The gained insight in testing limitations will allow for future study designs to be optimized.

In this study, we developed a method to determine compressive fatigue mechanical behavior of whole vertebrae in rats. Fatigue properties of whole rat vertebra exhibited similar characteristics as isolated cortical and trabecular bone specimens. Vertebral morphology, as well as fatigue properties of ZOL treated ovariectomized rats were similar to SHAM-OVX rats. These findings indicate that ZOL treatment does not have a pronounced negative influence on cyclic mechanical properties, as might be expected if ZOL-treated bone tissue were more brittle or contained excessive microdamage. The development of this methodology will allow further investigation of the effects of osteoporosis treatments on vertebral compressive fatigue behavior.

Acknowledgements

This work was funded by the Netherlands Organisation for Scientific Research, Prins Bernard Cultuurfonds and VSBFonds. We thank Elise Morgan of the Boston University for her advice and for using her fatigue testing equipment. We thank Zackary Mason and John Muller for technical assistance regarding the fatigue testing.

Chapter 7

PTH treatment of rats assessed by *in vivo* micro-CT

The contents of this chapter are based on J.E.M.Brouwers, B.v.Rietbergen, R.Huiskes, K.Ito, Effects of PTH treatment on tibial bone of ovariectomized rats assessed by *in vivo* micro-CT, *Osteoporosis International*. 2008, *submitted*.

Abstract

Our aims were to 1) determine changes in trabecular thickness and number after PTH over time, 2) compare responses to PTH between the meta- and epiphysis, 3) determine effects of PTH on mineralization and mechanical properties, 4) determine locations of new bone formation due to PTH on a micro-level over time and 5) determine the predictive value of bone structural properties for gain in bone mass after PTH.

Adult rats were divided into ovariectomy (OVX) (n=8), SHAM-OVX (n=8), OVX and PTH treatment (n=9). After 8 weeks, rats in the PTH group received daily s.c. injections of PTH (60 µg/kg/day) for 6 weeks. At weeks 0, 8, 10, 12 and 14, *in vivo* micro-CT scans were made (vivaCT 40, Scanco Medical AG) of the proximal and diaphyseal tibia. CT-estimated tissue mineral density was determined. After sacrifice, all tibiae were dissected and used for a three-point bending test.

Effects of six weeks PTH in rats were constant over time in trabecular and cortical bone. PTH increased bone volume fraction linearly over time in meta- and epiphysis, accompanied by increased trabecular thickness in both and increased trabecular number only in the latter. Mineralization increased in trabecular bone and remained constant in cortical bone. Ultimate load, stiffness and energy were increased and ultimate displacement unaltered compared to SHAM rats. Bone was formed on trabeculae there where most beneficial for strength. Bone mass before OVX best predicted bone mass after PTH treatment.

7.1 Introduction

Daily injections of parathyroid hormone (PTH) have anabolic effects on bone and as such offer a potential treatment for osteoporosis. The effects of PTH have been extensively studied in the ovariectomized rat, an animal model that has been shown to be a good first predictor of treatment potential for osteoporosis and as such is commonly used. PTH markedly increases trabecular bone mass in the proximal tibia, femoral neck and lumbar vertebra of ovariectomized, aged and young rats (9;69;111;132;158;163;180;188;189;191;199;202;249;289;302). Additionally, it increases cortical width, cortical bone area and axial moments of inertia as a result of mostly endocortical bone formation, leading to reduced bone marrow cavities, and, to a lesser extent, increased periosteal bone formation (60;77;147;289). Mechanical strength in anatomical sites like the vertebra, femoral neck and femoral diaphysis increases accordingly in rats after PTH treatment (163;188;202;249). Although the effects of PTH have been extensively studied, some aspects are still unclear and need further research.

Although most increases in trabecular bone mass after PTH treatment have been reported to result from increased trabecular *thickness*, in a few studies in dogs, rodents and monkeys, an increase in trabecular *number* was reported after PTH treatment (31;70;105;120;181;203;237), which is an uncommon feature in itself. The suggested mechanism for this was the observation of longitudinal tunneling of thickened trabeculae seen in histological sections as a remodeling mechanism to maintain trabecular thickness within limits. Tunneling of thickened individual trabeculae would convert them into multiple trabeculae, resulting in a normalization of trabecular thickness and an increase in trabecular number. It has been suggested that trabecular thickness will increase until it reaches a maximum, after which intra-trabecular resorption will take place (105). This suggests that changes in trabecular number and thickness may depend on the structure at the start of the treatment and may vary over time depending on dose and duration of treatment, and anatomical site. It is known that the same increase in bone mass due to trabecular thickness or number has different mechanical implications, with the latter having a higher increase in mechanical performance (90;263). Therefore, it is important to evaluate the changes in both trabecular thickness and number after PTH treatment over time to provide more insight into the potential of increasing mechanical performance.

In most studies on PTH in rats, the metaphyseal trabecular bone, often in the tibia, has been analyzed. It is known, however, that even in adult rats, the growth plate is still active, which inherently influences metaphyseal, trabecular bone. As PTH is a naturally occurring hormone that has an essential role in the growth plate, it can be questioned whether the metaphysis would be the best predictor of the effects of PTH in humans, in whom the growth plate closes after adolescence. The neighboring epiphysis, which does not undergo linear bone growth, may offer a more suitable translational site for analyzing PTH effects. Also, loading patterns have shown to be different between the meta- and epiphysis (285), with higher strains occurring in the

latter. Moreover, the response to PTH has shown to be directed towards higher strain areas in a FEM study in osteoporotic patients (87) and has shown to be smaller in the caudal vertebrae, where loads are relatively low, compared to the lumbar vertebrae (162), indicating that PTH effects may be mechanically directed. Taken together, it would be highly relevant to compare the response to PTH between the meta- and epiphysis, which has not previously been done.

Conflicting results have been reported regarding the influence of PTH on the degree and heterogeneity of bone mineralization. In a study in patients, some aspects of mineralization were altered after PTH use in men and women (182). In a study in rats, long-term treatment of rats with PTH resulted in a slightly wider variation in mineralization in the bone reflecting the newly formed bone (147). In two other rat studies, however, no influence of PTH on mineralization was found (249;273). As altered mineralization due to PTH may have detrimental effects on mechanical behavior, in spite of a potentially increased bone mass, it is important to further evaluate the effects of PTH on mineralization and mechanical properties.

Most reported studies on effects of PTH in rats were cross-sectional in design and rats were mostly sacrificed after just one or two different treatment periods providing little information about how exactly microstructure and mineralization evolved over the course of treatment. Additionally, as changes in bone mass and structure could not be monitored in the same animal, no specific knowledge was obtained about how and where new bone is formed on a micro-level. Finally, it could not be determined within a subject how much bone mass had increased after PTH, which is clinically very important as the patient's response to PTH should be monitored and ideally be predicted. Recently, however, *in vivo* micro-CT scanners have become available to monitor bone microstructure in small, living animals. With this tool, combined with image registration software, we were able to analyze changes in bone structure and mineralization over time after PTH treatment in ovariectomized rats and hereby address the following aims: 1) determine changes in trabecular thickness and number after PTH over time, 2) compare responses to PTH between the meta- and epiphysis, 3) determine effects of PTH on mineralization and mechanical properties, 4) determine locations of new bone formation due to PTH on a micro-level over time and 5) determine the predictive value of bone structural properties for gain in bone mass after PTH.

7.2 Materials and methods

7.2.1 Animals

Twenty-five female, 6-month old virgin Wistar rats (Harlan Laboratories, Horst, the Netherlands) were allowed to acclimatize for 7 days before the start of the experiment. The rats were maintained with a cycle of 12 hours light and 12 hours darkness and allowed to eat and drink *ad libitum*. The experiment was approved by the Animals Ethics Committee of the University of Maastricht, the Netherlands. The rats were divided into three groups (with equal weight distributions): control (n=8), ovariectomy

(OVX) (n=8) and OVX and PTH treatment (n=9). All rats were ovariectomized at week 0 and the control group underwent a SHAM ovariectomy. Success of OVX was confirmed at necropsy by determining atrophy of the uterine horns. Rats were left untreated for 8 weeks to allow for osteopenia to develop. After 8 weeks, rats in the PTH group received daily subcutaneous (s.c.) injections of PTH (60 µg/kg/day) for 6 weeks. Synthetic human PTH(1–34) (Bachem, Bubendorf, Switzerland) was dissolved in a vehicle of acidified saline (0.1 N) and 2% rat serum. Body weight was measured weekly, and the PTH dose adjusted accordingly. Rats were sacrificed at 14 weeks by cervical dislocation under deep anesthesia after the final CT-scan.

7.2.2 Micro-CT scanning

Directly after the operation, a 6 mm micro CT-scan (70 kV, 114 µA, 1000 projections per 180 degrees, 261 ms integration time) with an isotropic resolution of 15 microns was made of the proximal tibia using an *in vivo* micro-CT scanner (vivaCT 40, Scanco Medical AG, Brüttsellen, Switzerland). The CT-scanner was calibrated and a beam-hardening correction algorithm was applied to all scans (194). Another 3.15 mm micro CT-scan of the diaphysis was made with an isotropic resolution of 30 microns (70 kV, 114 µA, 250 projections per 180 degrees, 350 ms integration time). Before this measurement, the most distal and proximal point of the tibia was located in a scout-view to ensure that the exact middle of the diaphysis was scanned. Follow-up *in vivo* CT-scans were made after 8, 10, 12 and 14 weeks to monitor bone structure. Every follow-up scan was registered with the first scan by using image registration software that registers two scans based on minimizing the correlation coefficient (275). Total scanning time was 42 minutes, during which the animal was anesthetized with isoflurane and the scanned leg was placed in a custom-made leg-fixating device. The design of the rat holder was such that the left leg was not exposed to radiation while scanning the right leg. Radiation damage to the scanned bone was not expected to occur, based on a previous study, in which 8 weekly CT-scans with the same radiation dose caused no detected bone damage (36). In that study, we also showed that the reproducibility of all structural parameters was high, with a coefficient of variation of about 1%.

From the CT-scans the metaphyseal trabecular bone, epiphyseal trabecular bone, metaphyseal cortical bone and diaphyseal cortical bone were analyzed. For each analysis, the estimated mineral density of the bone tissue was determined based on the linear correlation between CT attenuation coefficient and bone mineral density.

Image processing of all scans included Gaussian filtering and segmentation as described elsewhere in detail (36). In brief, the same filtering and segmentation values were used for every measurement of each animal (trabecular bone: sigma=0.7, support=1, threshold density=0.575 g HA/cc, equivalent to 24% of maximal grayscale value; cortical bone: sigma=0.8, support=1, threshold density=0.642 g HA/cc, equivalent to 26% of maximal grayscale value). From every baseline and follow-up CT-scan, the trabecular bone of the meta- and epiphyseal areas were manually selected and bone structural parameters (bone volume fraction (BV/TV), connectivity density

(Conn.D), structure model index (SMI), trabecular number, thickness and separation (Tb.N, Tb.Th, Tb.Sp)) were automatically determined (figure 7.1). Cortical bone of the metaphysis was manually selected from the hundred most distal slices. From the CT scan of the diaphysis, all slices were manually selected. Cortical thickness and polar moment of inertia were determined. The selected cortical bone in the meta- and diaphysis at week 8 and 14 was registered for all PTH-treated rats to determine to what extent bone formation over 6 weeks was due to endosteal or periosteal apposition.

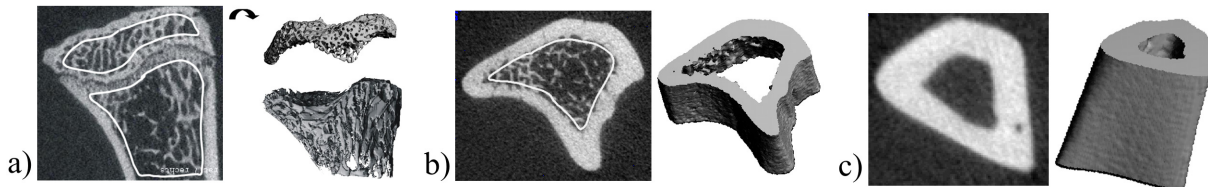


Figure 7.1: CT-scan of a) proximal metaphysis showing hand-drawn contours of the metaphyseal and epiphyseal trabecular bone b) proximal metaphysis showing hand-drawn contours of metaphyseal, cortical bone c) diaphyseal cortical bone.

7.2.3 Trabecular tunneling

We expected trabecular tunneling only to occur, if at all, in the thickest trabeculae, hence for all PTH-treated rats the meta- and epiphyseal, trabecular bone of the CT-scans of week 12 and 14 were registered. After registration, the two CT-scans were overlaid and visually checked for trabecular tunneling. This was done by going through the registered images per five slices, first from proximal to distal end and then from anterior to posterior sides while specifically looking for trabeculae that were thick at week 12 to see whether they were split in two at week 14.

To determine whether there is a maximum trabecular thickness, after which trabecular tunneling takes place, we analyzed the distribution of trabecular thickness in the epiphysis of all rats at all time points. The scanner software provides outputs of counts per bin and trabecular thickness was categorized in bins of 15 microns.

7.2.4 Prediction of gain in bone mass after PTH treatment

We hypothesized that several structural properties may predict the gain in bone mass after PTH, such as bone surface at the start of PTH treatment, bone mass at the start of PTH treatment, bone mass before ovariectomy, amount of bone mass loss after ovariectomy. Therefore, a linear correlation was determined between several structural parameters and the gain in bone mass, gain in bone volume fraction, final bone mass and final bone volume fraction after PTH treatment. This was done for the PTH treated rats only.

7.2.5 Three-point bending of tibiae

After sacrifice, all tibiae were dissected and frozen in PBS solution at -20°C . They were thawed prior to three-point bending. The tibia was placed on the lateral surface on two rounded supporting bars with a distance of 2.4 cm. A preload of 1 N was applied (ZWICK, Z020) at the medial surface of the diaphysis by lowering a third rounded bar. A constant displacement rate of 6 mm/min was applied until failure. Displacement was measured from the actuator displacement transducer of the testing machine. From the force-displacement curve, the following mechanical parameters were determined: 1) ultimate load, defined as the maximum load, 2) displacement at ultimate load, which was corrected for the toe region 3) extrinsic stiffness, calculated as the slope in the linear region between 40 and 80% of the ultimate load and 4) energy to ultimate load, defined as the area under the curve until ultimate load.

7.2.6 Statistics

A one-way ANOVA with repeated measures was performed to compare the PTH treated and OVX groups during treatment between week 8 and 14. A one-way ANOVA with a Bonferroni post-hoc test was used to determine differences between the groups at certain time points, for all parameters. Furthermore, a one-way ANOVA with repeated measures was performed to compare the OVX and SHAM groups between weeks 0 and 8. Finally, an ANOVA with repeated measures was performed in the SHAM group to determine effects of aging. All p-values below 0.05 were considered significant.

7.3 Results

7.3.1 Metaphyseal, structural parameters

At week 8, the ovariectomized groups displayed loss of BV/TV, Conn.D, Tb.N and Tb.Th and an increase in SMI and Tb.Sp, indicating the development of osteopenia (figure 7.2). Beyond 8 weeks, the untreated OVX group showed further deterioration of bone structure except for Tb.Th, which increased.

Daily injections with PTH reversed the effects of OVX and prevented further deterioration of bone structure. PTH treated animals displayed a crude plate-like trabecular bone structure and bone marrow cavity was reduced compared to OVX rats. Over the course of week 8 to 14, a significant effect of time, effect of PTH treatment and an interaction of PTH treatment and time were found for all structural parameters. PTH directly led to an increase in BV/TV accompanied by an increase in Tb.Th and prevention of further loss of Tb.N and further increase of Tb.Sp. This increase in BV/TV and Tb.Th was linear and continued until sacrifice. Loss of Conn.D was prevented and SMI decreased by PTH treatment. In the time frame of week 8 to 10 an interaction of PTH treatment and time was found, indicating that the effects of PTH were present within two weeks. After two weeks of PTH treatment, all structural

parameters were already significantly different from the OVX group. After six weeks of PTH treatment, BV/TV and SMI were not significantly different between the PTH and SHAM groups. Tb.N and Conn.D were significantly lower and Tb.Th and Tb.Sp were significantly higher in the PTH than in the SHAM group. In the SHAM group, BV/TV, Conn.D and Tb.N were significantly decreased and Tb.Sp significantly increased over time as a result of aging.

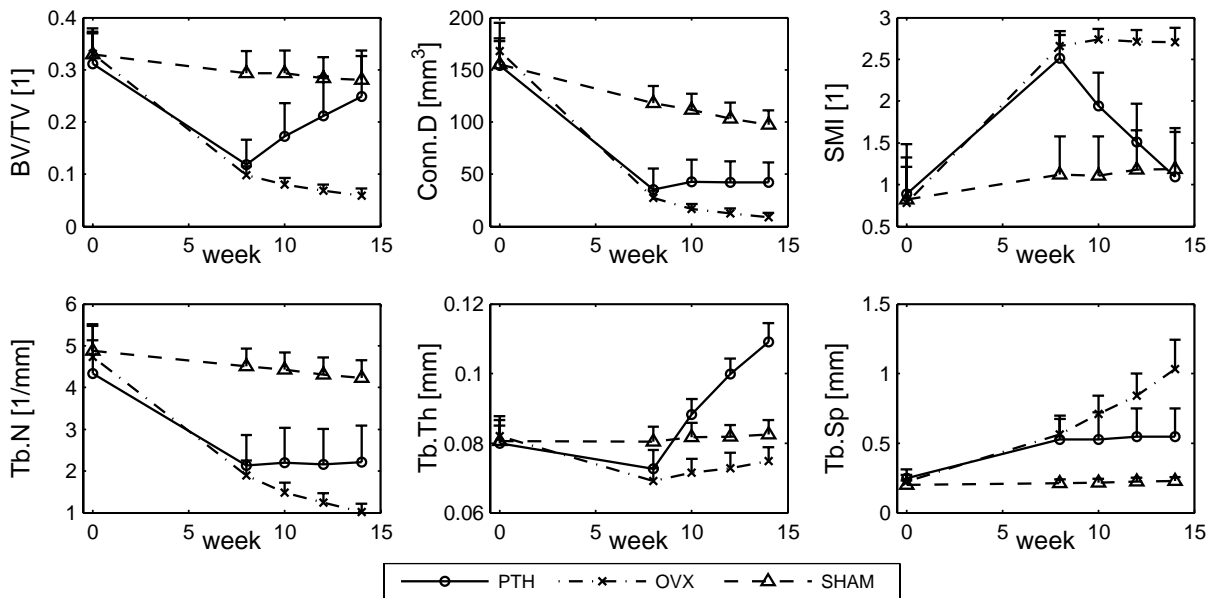


Figure 7.2: Structural parameters in the metaphyseal, proximal tibia for all groups at all time points (mean \pm SD).

7.3.2 Epiphyseal, structural parameters

At week 8, the ovariectomized groups displayed loss of BV/TV, Conn.D and Tb.N and an increase in SMI and Tb.Sp, indicating the development of osteopenia (figure 7.3). Changes in the epiphysis, however, were much smaller than in the metaphysis. Beyond 8 weeks, the untreated OVX group showed further deterioration of bone structure except for Tb.Th, which gradually increased over time.

Over the course of week 8 to 14, a significant interaction of PTH treatment and time was found for all structural parameters except for Conn.D. PTH treatment led to a direct increase in bone volume fraction, accompanied by increases in Tb.N and Tb.Th, while Tb.Sp decreased. This increase in BV/TV and Tb.N was linear and continued until sacrifice, while the increase in Tb.Th waned over time. SMI decreased after PTH treatment, while loss of Conn.D was not prevented. In the time frame of week 8 to 10, a significant interaction of PTH treatment and time was found for all structural parameters except for Conn.D, indicating that the effects of PTH were present within two weeks. After two weeks of PTH treatment, BV/TV and SMI were already significantly different from the OVX group and not significantly different from the SHAM group while Tb.Th was significantly higher in the PTH group than the OVX and SHAM groups. After six weeks of PTH treatment, BV/TV and Tb.Th were

significantly higher than the SHAM group and than baseline values. SMI, Tb.N and Tb.Sp were the same as the SHAM group, while Conn.D remained reduced. In the SHAM group, Conn.D significantly decreased and Tb.Th significantly increased over time as a result of aging.

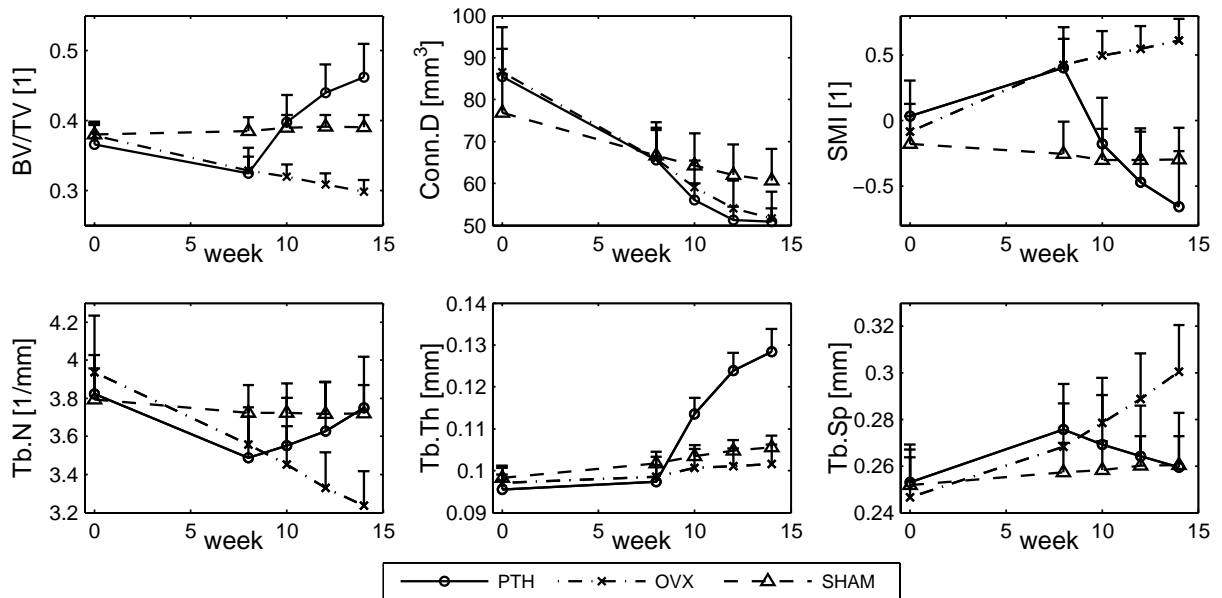


Figure 7.3: Structural parameters in the epiphyseal, proximal tibia for all groups at all time points (mean \pm SD).

7.3.3 Cortical thickness and polar moment of inertia in the metaphysis and diaphysis

Cortical thickness and the polar moment of inertia in the metaphysis did not significantly change within the eight weeks after OVX compared to the SHAM group (figure 7.4). PTH treatment led to a sharp, linear increase in cortical thickness and pMOI, which were both significantly different from the OVX group over time. Visual inspection of registered images of weeks 8 and 14 showed that bone formation was slightly more due to endosteal than periosteal apposition and that bone formation did not take place on all parts of the surface in the same degree (figure 7.5).

Cortical thickness in the diaphysis increased after OVX almost reaching significance ($p=0.07$). PTH treatment led to an even sharper increase, which was linear over time and significantly different from the untreated group. The pMOI increased significantly after OVX in the first 8 weeks. After 8 weeks, this increase waned in the OVX group, while it increased significantly more in the PTH treated group. Visual inspection of registered images of weeks 8 and 14 showed that bone formation was slightly more due to periosteal than endosteal apposition and that bone formation had taken place quite evenly over the whole surface.

Cortical thickness and pMOI significantly, gradually increased over time in the metaphysis and the diaphysis of the SHAM group as a result of aging.

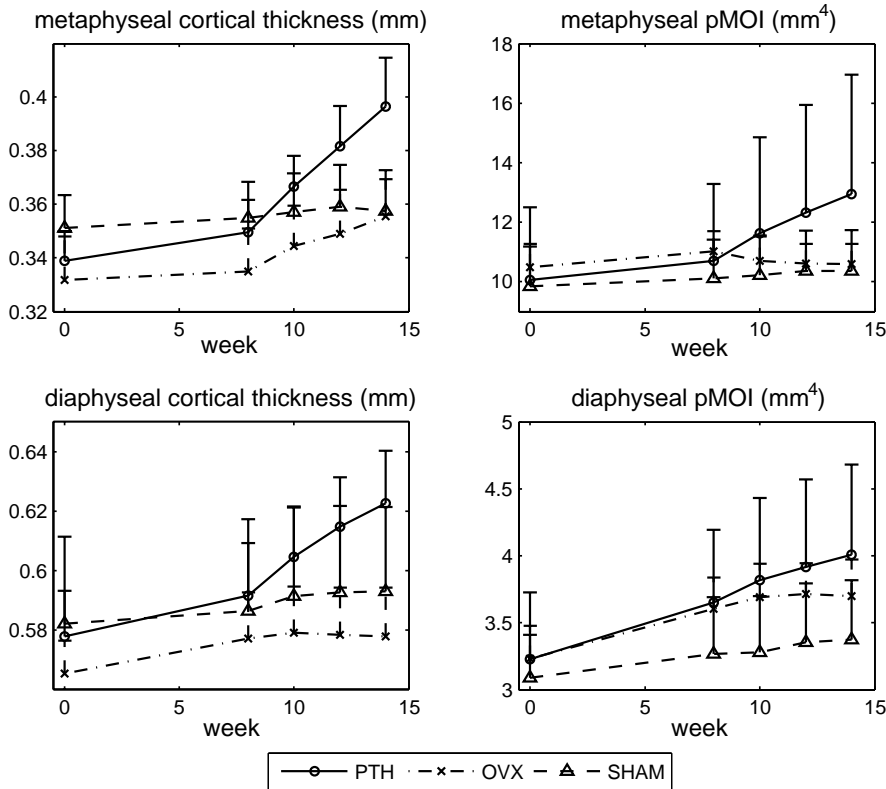


Figure 7.4: Cortical thickness and polar moment of inertia (pMOI) in the meta- and diaphysis of the tibia for all groups at all time points (mean \pm SD).

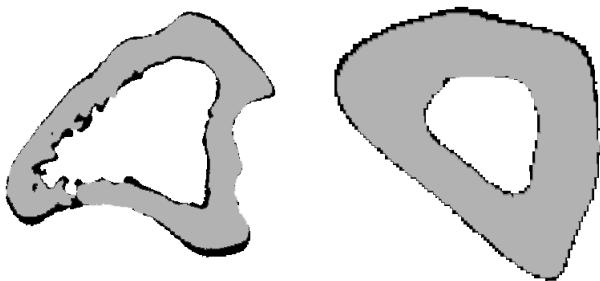


Figure 7.5: Registered images of metaphyseal (left) and diaphyseal (right) cortical bone taken at week 8 and 14 showing bone formation during six weeks in the cortex of a PTH treated rat. Grey is bone at week 8, black is newly formed bone.

7.3.4 Mineralization of meta- and epiphyseal, trabecular bone and meta- and diaphyseal, cortical bone

At the start of the experiment, CT-estimated bone mineral density in the metaphyseal trabecular and cortical bone was significantly higher in the SHAM group than in the other groups. However, because of the use of follow-up data and repeated measures design, we were still able to determine significant effects of OVX and PTH on bone mineral density. Compared to SHAM, OVX was found to lead to a significantly lower increase in mineral density of meta- and diaphyseal, cortical bone

over the first 8 weeks, but did not significantly affect trabecular bone (figure 7.6). Over week 8 to 14, the meta- and epiphyseal trabecular bone of the PTH group was found to have a significantly more increasing bone mineral density than that of the OVX group. Cortical bone mineral density was not affected by PTH treatment. Bone mineral density of all measured bone areas were found to significantly increase over time in the SHAM group.

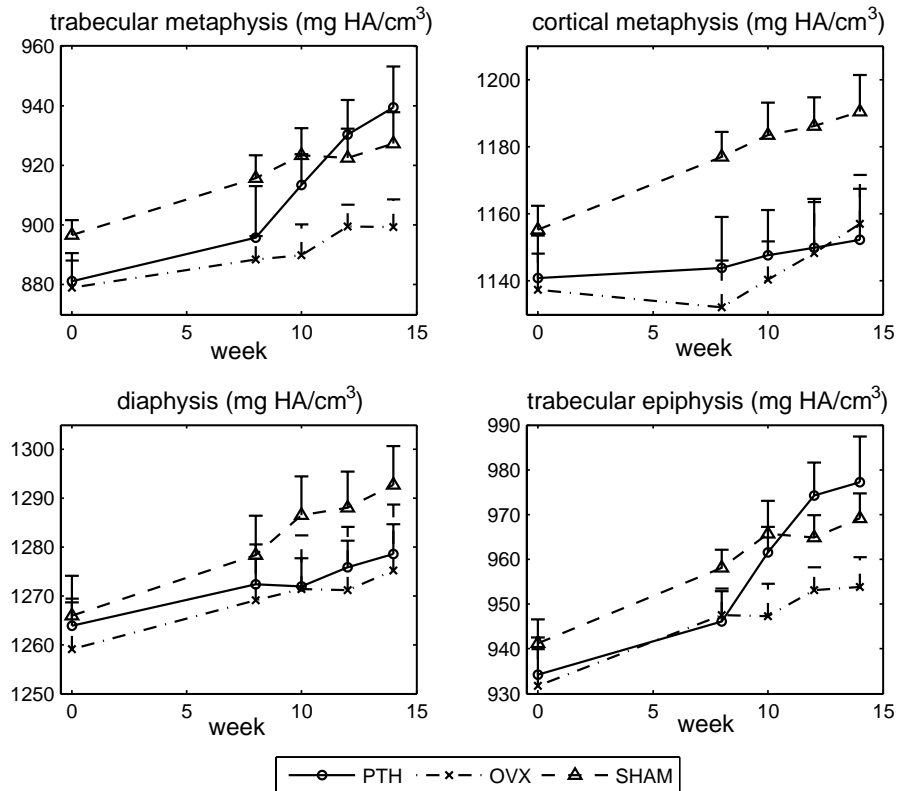


Figure 7.6: CT-estimated bone mineral density of metaphyseal trabecular bone, metaphyseal cortical bone, diaphyseal cortical bone and epiphyseal trabecular bone (mean \pm SD).

7.3.5 Trabecular tunneling and remodeling

For all PTH-treated rats, no cases of trabecular tunneling were detected in metaphyseal trabecular bone between week 12 and 14. For several rats, one trabecula was selected and analyzed as it developed over time after PTH treatment. Figure 7.7 shows how PTH in this particular trabecula first led to filling and overfilling of cavities, while later more bone was added to the surface of the trabecula resulting in a thicker trabecula. Also, resorption still appeared to take place in this trabecula. Another trabecula after segmentation of the image appeared cleaved due to OVX-induced increased resorption. PTH treatment led to bone formation, which took place where it was most beneficial, i.e. at the cleaved site, restoring the trabecula. This indicates that there probably was still a thin line of bone left in the center, which was unaccounted for after segmentation, but large enough for bone formation to take place. It was found

that for all rats, the maximum trabecular thickness continued to increase over time. Therefore, no maximum limit for trabecular thickness appeared to be present.

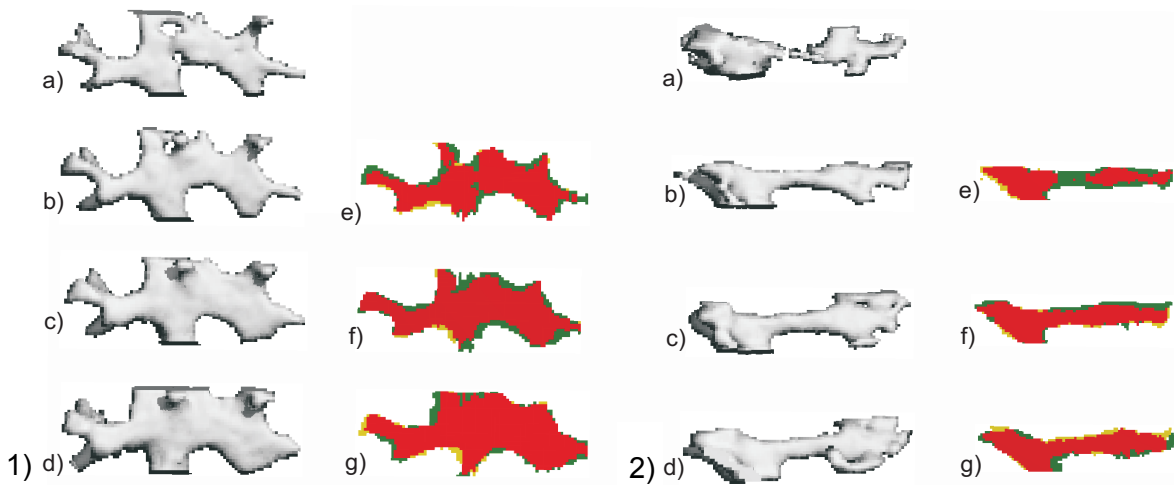


Figure 7.7: A trabecula in two PTH treated, ovariectomized rats was tracked over time to determine the development of bone formation (1 and 2). On the left of figure 1 and 2 you see 3-D segmented images of a trabecula, after PTH treatment is started at week 8, taken at week 8 (a), 10 (b), 12 (c) and 14 (d). On the right you see overlaid 2-D segmented sections comparing week 8 and 10 (e), 10 and 12 (f) and 12 and 14 (g). Yellow indicates resorbed bone, green newly formed bone and red unchanged bone. Bone formation is clearly seen over time in both trabeculae. In trabecula 1, bone is mostly deposited in the cavities in the first two weeks, while later on bone is added to the surface. In trabecula 2, the trabecula appears cleaved after segmentation, although most likely there was still a thin line of bone present. PTH treatment leads to bone formation at the cleaved site, where it is most needed hereby restoring the trabecula.

7.3.6 Prediction of gain in bone mass after PTH treatment

The linear correlations between several structural parameters and the gains in bone mass, gain in bone volume fraction, final bone mass and final bone volume fraction after PTH treatment varied between the specific parameters as well as bone regions (table 7.1). More significant predictions were found for the metaphysis than the epiphysis. Best correlations were found between BV and BV/TV at week 0, and BV and BV/TV at week 14, respectively in both the meta- and epiphysis. Paradoxically, the loss of bone after OVX did not predict the gain of bone after PTH treatment well. From structural parameters evaluated at week 8, bone surface (BS) was the best predictor of the gain in bone after PTH. While BV and BV/TV at week 8 predicted the gain in bone mass over the next 6 weeks quite well, the predictive value of BV and BV/TV at weeks 8, 10 and 12 for the following two weeks was poor to non-significant. Interestingly, in the epiphysis, the slopes of these relations were negative, indicating that the higher BV and BV/TV, the lower the gain. All other significant relations had a positive slope.

Table 7.1: Linear correlation between several structural parameters to predict gain in bone mass, gain in bone volume fraction, final bone mass or final bone volume fraction in PTH treated rats.

Predictive variable	Outcome variable	metaphysis		epiphysis	
		r ²	Slope	r ²	Slope
BS at week 8, 10, 12	ΔBV/TV over week 8-10, 10-12, 12-14	0.42	0.0003	0.23	0.0011
BS at week 8, 10, 12	ΔBV over week 8-10, 10-12, 12-14	0.40	0.0077	n.s.	-
BV/TV at week 8, 10, 12	ΔBV/TV over week 8-10, 10-12, 12-14	n.s.	-	0.41	-0.23
BV at week 8, 10, 12	ΔBV over week 8-10, 10-12, 12-14	0.21	0.13	0.25	-0.21
ΔBV/TV over week 0-8	ΔBV/TV over week 8-14	n.s.	-	n.s.	-
ΔBV over week 0-8	ΔBV over week 8-14	0.48	0.95	n.s.	-
BS at week 8	ΔBV/TV over week 8-14	0.86	0.0012	n.s.	-
BS at week 8	ΔBV over week 8-14	0.77	0.030	n.s.	-
BV/TV at week 8	ΔBV/TV over week 8-14	0.66	0.76	n.s.	-
BV at week 8	ΔBV over week 8-14	0.69	0.88	n.s.	-
BV/TV at week 0	BV/TV at week 14	0.81	1.3	0.85	1.6
BV at week 0	BV at week 14	0.89	1.3	0.93	0.96

7.3.7 Three-point bending of tibiae

Ultimate load and energy in the PTH group were significantly higher than in the SHAM group (figure 7.8). Ultimate load and energy in the OVX group tended to be slightly higher and lower than the SHAM and PTH group respectively, though this did not reach significance. No significant differences were found in extrinsic stiffness and ultimate displacement between all groups, although the trend between groups in extrinsic stiffness was similar to the trend in ultimate load.

7.4 Discussion

For the first time, the effects of PTH treatment on trabecular and cortical bone were analyzed longitudinally with an *in vivo* micro-CT scanner in the same ovariectomized rats for six weeks. It was found that 1) PTH treatment led to constant, linear increases

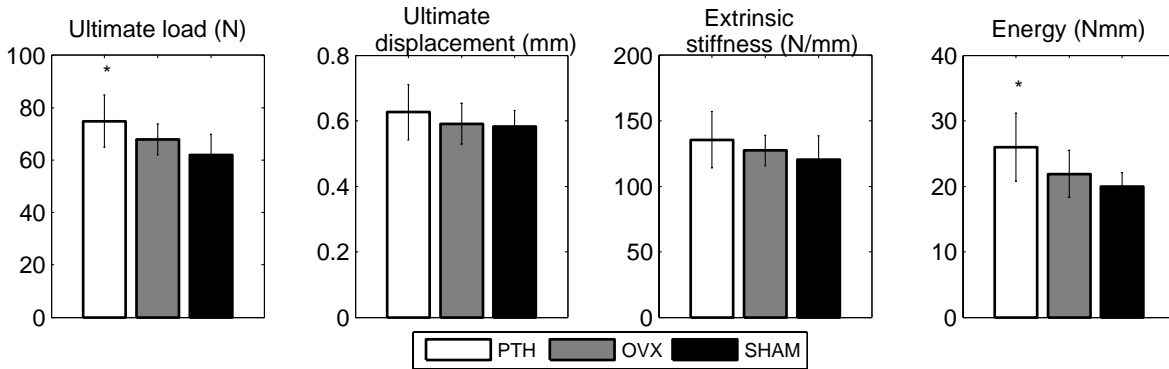


Figure 7.8: Ultimate load, ultimate displacement, extrinsic stiffness and energy determined from three-point bending test on tibiae after sacrifice at 14 weeks. * $p < 0.05$ compared to SHAM.

in trabecular bone mass of the meta- and epiphysis due to linearly increasing trabecular thickness in both regions and linearly increasing trabecular number in the epiphysis 2) a different response to PTH was seen between the meta- and epiphysis in terms of structural parameters 3) PTH resulted in increased trabecular tissue mineralization and unaltered cortical tissue mineralization as well as slightly improved bending properties 4) bone was formed on trabeculae initially there where most beneficial and later on to all surfaces and 5) bone mass after PTH treatment for each rat individually was best predicted by bone mass at the start of the experiment.

In the metaphyseal, trabecular bone, PTH treatment led to a constant, linear increase in bone volume fraction during six weeks accompanied by a constantly increasing trabecular thickness and an inhibition of further loss of trabecular number. Although this is the first *in vivo* report on bone structural parameters, our results agree with previous cross-sectional studies on the eventual effects of PTH on trabecular, metaphyseal bone (69;111;132;158;180;199;203;302) and with an *in vivo* report on changes in bone mineral density (238). In the epiphyseal, trabecular bone, PTH treatment also led to an increasing bone volume fraction, accompanied by a linearly increasing trabecular number while trabecular thickness also increased, which waned over time. Previously, preventive treatment with PTH (at time-point of OVX) in ovariectomized rats led to an increased bone volume fraction, trabecular number and thickness in the tibial epiphysis, compared to untreated OVX and SHAM rats in a cross-sectional study (239), though exact values were not reported. This concurs, however, with the increases that we found after recovering treatment (after osteopenia) with PTH in the epiphysis. For the first time now, bone microstructure in the epiphysis over time was reported after PTH use. The increase in bone volume fraction after PTH treatment over 6 weeks in the meta- and epiphysis was almost exactly the same. This increase resulted in the epiphysis in values that were above SHAM level while in the metaphysis values were still below SHAM. This similar increase suggests that the anabolic response to PTH is comparable in both locations.

Interestingly, the response to PTH treatment was slightly different between the meta- and epiphyseal, trabecular bone, with the most striking difference being an increasing trabecular number in the epiphysis, while it stayed constant in the

metaphysis. There are several possible explanations for this difference between the meta- and epiphysis and for the increase in trabecular number in the epiphysis. The deterioration of bone mass and structure after ovariectomy in the epiphysis was much smaller than in the metaphysis. Therefore, at the start of PTH treatment, the state of the bone was quite different between the meta- and epiphysis, with the latter having a higher trabecular thickness and structure model index. It has been suggested that after PTH treatment, trabeculae will initially become thicker until a certain maximum thickness is reached (105). Trabecular tunneling would then take place, after which thick trabeculae are cleaved into two smaller ones, which has been shown to occur in different species (31;70;105;120;181). This implies that trabeculae will never grow beyond a certain maximum thickness, the value of which may depend on species and anatomical site. As trabecular thickness was higher in the epi- than the metaphysis, this could be an explanation for the increase in trabecular number in the epiphysis and the absence of this in the metaphysis. To test this, we analyzed the distribution of trabecular thickness in the epiphysis of all rats during PTH treatment. It was found that the maximum trabecular thickness continued to increase until week 14. This therefore does not support the idea of a maximum intrinsic trabecular thickness. This is further supported by the fact that trabecular thickness in the metaphysis at the final time point was higher than in the epiphysis, while trabecular number did not increase. Also, no cases of tunneling were seen in the epiphysis after visual inspection. Another explanation could lie in the decrease of total volume of interest over time in the epiphysis seen in the CT-scans due to endosteal apposition. In theory, it could be that the number of trabeculae in the area close to the cortex is lower than average. This would suggest that merely a decrease in total volume would lead to an increase in trabecular number. We analyzed this possibility by using the hand-drawn contour file from week 14 for the CT-scan of week 8, which excludes the outer trabecular region. We then analyzed bone structural parameters again and found that trabecular number was not increased compared to when using the original contour file for week 8 and therefore this possibility is excluded. Another option is that the relatively large amount of the plate-like bone enables trabecular tunneling in a different fashion than previously reported in rod-like bone, which may be difficult to see in the CT-scans. A final possibility is that after 8 weeks, thin trabeculae were removed during segmentation. When these trabeculae increased in thickness, they were included resulting in an increased trabecular number at 14 weeks. This phenomenon is shown in figure 7.7.

Tissue mineral density of meta- and epiphyseal trabecular bone significantly increased over time after PTH treatment, while cortical bone in the meta- and diaphysis was unaffected. It has previously been found that ash density of the vertebral body, including cortical and trabecular bone, was significantly increased in PTH treated, ovariectomized rats compared to untreated, ovariectomized rats already after 5 weeks, while after 16 weeks of PTH treatment, still no effects were found on the femoral, diaphyseal cortical bone (249). In another study, using quantitative backscattered electron imaging to calculate the degree and homogeneity of mineralization, however, no significant effect of 5.5 months of PTH treatment was found on the cortical and

trabecular bone of PTH treated, ovariectomized rats (273). In yet another study on the long-term effects of PTH on mineralization in rats, no significant influences were found, although there was a slightly wider variation in mineralization in the bone reflecting the newly formed bone (147). These differences in results in rats may be due to different methods applied to determine mineralization. Our bending data agree with three-point bending tests in the femur where an increase in ultimate load and extrinsic stiffness after PTH treatment was found in ovariectomized rats (245;283). It can be seen that the trends between groups in ultimate load, extrinsic stiffness and calculated polar moment of inertia are similar, which indicates that the polar moment of inertia was a good predictor of ultimate load and extrinsic stiffness. Ultimate displacement did not differ between all groups, which suggests that the newly formed bone was of similar quality as the old bone and indicates that PTH treatment did not lead to more brittle or ductile mechanical behavior. This is further supported by unaltered tissue mineralization values in the diaphyseal tissue, i.e. cortical bone.

Individual trabeculae were tracked over time during PTH treatment in all rats by using image registration software. With this method, we were able to monitor bone formation after PTH treatment on a micro-level and gather insight into how and where PTH treatment leads to new bone. In many trabeculae, it appeared that in the first two weeks, mostly cavities were filled, while later on bone was added to the outer surface. It has been suggested that increases in bone mass after PTH may occur by remodeling- or modeling-based bone formation (47). Our data suggest that initially remodeling-based bone formation takes place, as cavities are filled with bone, while later modeling-based bone formation is more pronounced as bone is added to the outer surface, which does not appear to have been resorbed first. This will need to be further validated. For several other trabeculae, it was seen that ovariectomy led to severe disruption of the trabecula to the point of almost complete cleavage after segmentation of the images. PTH treatment led to bone deposition there where most beneficial, resulting in full restoral of the trabecula. This could be explained by Frost's mechanostat, which states that bone is deposited where strains and stresses are highest. Since in an almost cleaved trabecula, merely a thin line of bone was present at certain locations, strains and stresses would be highest at these locations leading to bone formation there. This suggests that PTH-induced bone formation is, at least in part, mechanically driven. This agrees with results from two finite element studies on CT-scans of osteoporotic patients treated with teriparatide (rhPTH (1–34)), in which it was found that bone was mostly deposited on locations of high strains (87) and that teriparatide increased vertebral strength by altering the distribution of density within the vertebra (135).

It is clinically relevant to be able to predict to what extent a patient will respond to PTH in order to determine the best treatment. In a clinical study, several characteristics like BMD and age were examined for correlations with the increase in BMD after PTH treatment, however, no strong correlations were found (242). It may be that patients with relatively little bone will respond the most, as they need it most severely or it may just as well be that patients with a relatively large amount of bone will respond the most, as their body already has a more favorable bone turnover. It could be that certain

structural parameters, or their change over time, predict the gain in bone mass after PTH. Since our study was done *in vivo*, it was for the first time possible to determine whether predictions of bone mass can be made. We found that the best predictor of final bone mass and bone volume fraction in both the meta- and epiphysis was bone mass and bone volume fraction at the start of the experiment, before ovariectomy. If these results would be translational to clinical practice, which needs to be tested, this would indicate that bone mineral density before menopause would predict bone mineral density after PTH treatment of osteoporotic patients. Bone surface at the start of treatment was also a good predictor of the gain in bone mass and bone volume fraction over the next 6 weeks, though only in the metaphysis. This may be related to the fact that bone deposition occurs mostly on the surface of trabeculae, which would imply that number and activity of osteoblasts plays less of a role than the amount of bone surface present. In the epiphysis, no other reasonable predictions were found outside bone mass and bone volume fraction at the start of the experiment. This may be related to the fact that bone mass and bone volume fraction were higher than in the metaphysis and were closer to a plateau.

Cortical bone mass increased linearly over time after PTH treatment in the meta- and diaphysis while marrow cavity volume decreased. In several cross-sectional studies, in which the effect of between 8 weeks and 6 months of PTH treatment was evaluated in ovariectomized rats, an increase in cortical bone mass was found (9;111;239). In a study in ovariectomized mice, it was found that within 3 weeks of PTH treatment, cortical thickness was significantly increased in the metaphysis and after 7 weeks, cortical thickness was even higher (303). Diaphyseal cortical thickness was significantly increased only after 7 weeks of treatment. In another study, the effects of PTH treatment on metaphyseal cortical thickness of the tibia in ovariectomized rats was studied *over time* by using pQCT (76). A linear increase in cortical thickness was found until about 6 weeks, after which the effect reached a plateau. Taken together, our linear increase in dia- and metaphyseal cortical bone after PTH treatment agrees with the literature. In the metaphysis, no effect of ovariectomy was found on cortical bone parameters, which agrees with previous studies (24;244). Interestingly, cortical thickness and polar moment of inertia in the diaphysis increased after ovariectomy, which is in contrast to significant decreases (148;237) and no significant changes (93;141) previously reported.

It has previously been found that PTH leads to a predominance of endosteal over periosteal bone apposition in cortical bone (60;77;147;192). Based on registered images of week 8 and 14, before and after PTH treatment, we found that endosteal and periosteal bone apposition both took place in the meta- and diaphysis, with a slight predominance of endosteal formation in the former and a slight predominance of periosteal formation in the latter. We also saw that while the degree of bone apposition was evenly distributed over the endo- and periosteal surface of the diaphysis, it varied quite largely over the endo- and periosteal surface of the metaphysis. This could indicate that bone apposition is stimulated more in certain locations than others, which may also partly be the result of remodeling due to linear growth, which still is present in the adult rat (118;280).

This study was limited by a treatment period with PTH of six weeks. It was found that bone volume fraction in the meta- and epiphyseal trabecular bone and cortical thickness in the meta- and diaphysis continued to increase linearly. It is very likely though that these increases will wane after a longer treatment period. Although no trabecular tunneling was detected, it would be interesting to determine how trabecular structure would develop further over time as bone mass continues to increase. Another limitation lies in the translation of our rat study to clinical practice. It is known that rat cortical bone is not subject to Haversian remodeling (118), which has shown to lead to different responses to PTH compared to species with Haversian remodeling, in which negative (99;248) and no effects (98;218) on cortical thickness were found. Also, rats in our study were subjected to serial radiation resulting from CT-scanning, however, we have previously shown that eight weekly scans do not lead to detectable radiation damage (36). Since the total number of scans in this study was six and the shortest interval between scans was two weeks, we do not expect any radiation damage. Finally, concern has been raised regarding the predictive value of CT-derived tissue mineralization (48;63). It could be that thicker trabeculae after PTH would lead to more beam hardening effects, which would result in a lower average mineralization. The fact that we found an increased mineralization degree indicates that this is most likely not due to beam hardening. It is also possible that the algorithm calculating the mineral density, which peels off two voxels from the outer edge of the bone leaving only a small portion of each trabecula, influences the calculated mineralization values when trabeculae thicken. This is not likely however, as mineralization was not found to decrease when trabecular thickness decreased after ovariectomy. A biological explanation for our results could be that when trabeculae thicken the center is not being remodeled anymore resulting in an increased mineralization.

This study demonstrated that six weeks of PTH treatment of osteopenic rats led to increases in bone volume fraction of the tibial meta- and epiphysis as well as increases in cortical bone mass of the tibial meta- and diaphysis. By using an *in vivo* micro-CT method, it was shown that net bone formation started directly after the onset of treatment, and continued with the same rate for at least six weeks in both trabecular and cortical bone. Deposition of bone appeared to be mechanically driven, resulting in cleaved trabeculae being fully restored again. The increase in bone volume fraction was similar in the meta- and epiphysis, however the resulting changes in microstructure were different, which may have different mechanical implications.

Acknowledgements

This work was funded by the Netherlands Organisation for Scientific Research (NWO). We thank Jo Habets and Leonie Niesen for performing the ovariectomies, giving daily PTH injections and the animal care. We thank Rianne Reinartz and Anthal Smits for contouring.

Chapter 8

Vibration treatment of rats assessed by *in vivo* micro-CT

The contents of this chapter are based on J.E.M.Brouwers, K.Ito, B.v.Rietbergen, R.Huiskes, Effects of vibration treatment on tibial bone of ovariectomized rats analyzed by *in vivo* micro-CT, *J Orthop Res.* 2008, *submitted*.

Abstract

Daily low-amplitude, high-frequency whole body vibration (WBV) treatment can increase bone formation rates and bone volume in rodents. Its effects vary, however, with vibration characteristics and study design, and effects on 3-D bone microstructure of ovariectomized animals over time have not been documented. Our goal was to determine the effects of WBV on tibial bone of ovariectomized, mature rats over time using an *in vivo* micro-CT scanner.

Adult rats were divided into: ovariectomy (OVX) (n=8), SHAM-OVX (n=8), OVX and WBV treatment (n=7). Eight weeks after OVX, rats in the vibration group were placed on a vibrating platform for 20 minutes at 0.3 g and 90 Hertz. This was done 5 days a week for six weeks, twice a day. At week 0, 8, 10, 12 and 14, *in vivo* micro-CT scans were made (vivaCT 40, Scanco Medical AG) of the proximal and diaphyseal tibia. After sacrifice, all tibiae were dissected and tested in three-point bending.

In the metaphysis over week 8 to 12, WBV treatment did not alter structural parameters compared to the OVX group. Between week 12 and 14, BV/TV decreased significantly more in the OVX than the WBV group, which was accompanied by a significantly reduced decrease in Tb.N and increase in Tb.Sp. In the epiphysis, structural parameters were not altered. WBV also did not affect cortical bone and its bending properties.

Summarized, no substantial effects of six weeks of low-magnitude, high-frequency vibration treatment on tibial bone microstructure and strength in ovariectomized rats were found.

8.1 Introduction

Mechanical stimulation of bone by vibration has been shown *in vivo* to have a potential osteogenic effect, contributing to a structure more resistant to habitual loads (51;68;84;114;127-129;201;228-233;294). These mechanical signals are often applied in high-frequency, low acceleration mode and commonly result in small strains (<10 microstrain) in the bone, that are orders of magnitude lower than strains resulting from daily loads (129;231). As they are apparently harmless to the body, they may provide a potential treatment for bone-debilitating diseases like osteoporosis.

In a study performed in sheep, 1 year of daily vibrations resulted in an increase of trabecular bone volume fraction of 32% (230). In a study in which teenagers with low BMD were put on a vibration plate for 10 minutes a day for a year, a small increase in trabecular BMD in lumbar vertebrae was found as well as an increase in femoral cortical bone area (84). However, in the first study on the effects of vibration in a small cohort of osteoporotic women, no significant effect on bone mineral density of the spine, hip or distal radius was found after one year of treatment (228). A significant effect of treatment compliance was shown though in that study and effects in patients of the highest quartile of compliance almost reached significance. These results thus demonstrate the potential osteogenic effect of mechanical vibration, but also suggest that the effects might be site and species dependent.

To further elucidate the effects of low-magnitude, high-frequency whole body vibration (WBV) on bone, several cross-sectional studies have been performed in rodents. It has been shown that WBV in growing, untreated mice can increase bone formation rates (128;293;294), trabecular bone volume and cortical bone area (293), and trabecular bone volume fraction (128) in the tibial metaphysis. Also, the anabolic activity of bone tissue, suppressed by disuse, can be normalized by WBV in adult, female rats (232). To test the potential of WBV for the treatment of postmenopausal osteoporosis, a few studies have been conducted in the ovariectomized (OVX) rat, a commonly used animal model for estrogen-deficiency. In a study testing different parameter settings, a combination of 45 Hz and 3.0 g suppressed the increase in bone remodeling rates and the decline in tibial bending properties (201) seen after OVX. BMD was found to be higher in OVX rats after WBV treatment at 50 Hz and 2 g in a few, but not all, anatomical locations after five weeks (68). However, by week 8 and 12 this was not significant anymore. Finally, in a study by Judex et al. (129), a lower magnitude of vibration was tested. Four weeks of WBV at 90 Hz and 0.15 g for 10 minutes per day in OVX rats led to an increase in bone formation parameters in the tibial metaphysis of 158% in treated compared to control animals. In the femoral epiphysis, trabecular bone volume increased by 22% accompanied by an increased trabecular thickness and decreased connectivity density. However, bone microstructure in the femoral metaphysis interestingly was not improved. These results thus suggest that indeed, WBV can have an osteogenic effect in rodents, but that its effect vary with vibration characteristics and at different anatomical sites. Furthermore, the effect of

WBV on 3-D bone microstructure of ovariectomized animals over time has not been documented.

In this study, we aimed to quantify the effects of WBV on bone structure of ovariectomized rats over time in 3-D. Bone formation rate has been found to respond more in the proximal tibia (128;232) than in the femur (129). This may be caused by damping of the vibrating stimulus by the knee leading to more effectiveness in the tibia than the femur. Hence, in order to get the most pronounced results, we concentrated on the proximal tibia. As in the earlier study by Judex et al. (129), effects in both the epiphysis and metaphysis were determined separately and cortical bone in the meta- and diaphysis was analyzed as well. Furthermore, a novel *in vivo* micro CT device was used which enabled us to track 3-D bone microstructure in the same rats over time in a longitudinal fashion for the first time. Finally, the vibration parameters were selected based on a published study (129), a meeting abstract (292) and a personal communication (210), by and with Judex et al., in an attempt to maximize effects.

8.2 Materials and methods

8.2.1 Animals

Twenty-three female, 6-month old virgin Wistar rats (Harlan Laboratories, Horst, the Netherlands) were allowed to acclimatize for 7 days before the start of the experiment. The rats were maintained with a cycle of 12 hours light and 12 hours darkness and allowed to eat and drink *ad libitum*. The experiment was approved by the Animals Ethics Committee of the University of Maastricht, the Netherlands. The rats were divided into three groups of equal mean weight: control (n=8), ovariectomy (OVX) (n=8), OVX and vibration plate treatment (n=7). Rats were part of a larger study and results of control and OVX groups have been previously described (35). All rats were ovariectomized at week 0 and the control group underwent a SHAM ovariectomy. Success of OVX was confirmed at necropsy by determining atrophy of the uterine horns. After 8 weeks, rats in the vibration group were placed on a vibrating platform for two times 20 minutes per day at 0.3 g and 90 Hertz, once in the morning and once in the afternoon with 8 hours in between. This was done 5 days a week for six weeks. Treatment was based on the settings used in the study by Judex et al. (129), on personal communication (210) and on results reported in an abstract (292). From the latter two, it was apparent that stimulating for 20 instead of 10 minutes, twice instead of once a day, and at 0.3 instead of 0.15 g, would potentially increase bone formation rate in the proximal tibia of OVX rats. Therefore, all three alterations to the settings used in the paper by Judex et al. were based on the concept that a more intense stimulus would increase bone formation rate and therefore increase improvements in structure.

The vibrating platform (Juvent Medical Inc., NJ, USA) was custom made for laboratory animal use, with a cage mounted on to it, in which five animals could be individually placed at the same time (figure 8.1). Acceleration and frequency accuracy

was confirmed using in-house equipment. Rats were sacrificed at 14 weeks under deep anesthesia by cervical dislocation.

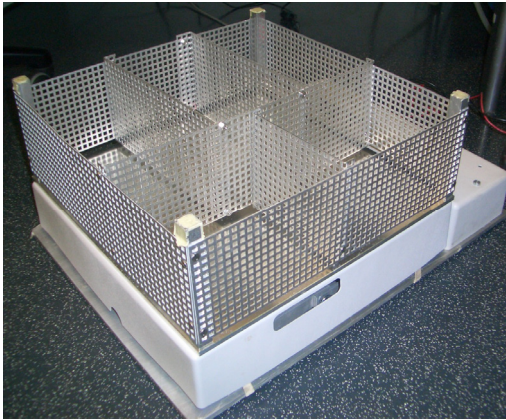


Figure 8.1: A vibrating platform (Juvent Medical Inc., New Jersey, USA) was custom made for laboratory animal use, with a cage mounted on to it, in which five animals could be individually placed at the same time.

8.2.2 Micro-CT scanning

Directly after the operation a 6 mm micro CT-scan (70kV, 114 μ A, 1000 projections per 180 degrees, 261 ms integration time) with an isotropic resolution of 15 microns was made of the proximal tibia using an *in vivo* micro-CT scanner (vivaCT 40, Scanco Medical AG, Switzerland). The CT-scanner was calibrated and a beam-hardening correction algorithm was applied to all scans. Another 3.15 mm micro CT-scan of the diaphysis was made with an isotropic resolution of 30 microns (70kV, 114 μ A, 250 projections per 180 degrees, 350 ms integration time). Before this measurement, the most distal and proximal point of the tibia was located in a scout-view to ensure that exactly the middle of the diaphysis was scanned. Follow-up *in vivo* CT-scans were made after 8, 10, 12 and 14 weeks to monitor bone structure. Body weight was recorded at every measurement. Every follow-up scan was registered with the first scan by using image registration software that registers two scans based on minimizing the correlation coefficient (275). Total scanning time was 42 minutes, during which the animal was anesthetized with isoflurane and the scanned leg was placed in a custom-made leg-fixating device. The design of the rat holder was such that the left leg was not exposed to radiation while scanning the right leg. Radiation damage to the scanned bone was not expected to occur, based on a previous study, in which 8 weekly CT-scans with the same radiation dose caused no detectable bone damage (36). In that study, we also showed that the reproducibility of all structural parameters was high with a coefficient of variation of about 1%.

From the CT-scans the metaphyseal trabecular bone, epiphyseal trabecular bone, metaphyseal cortical bone and diaphyseal cortical bone were analyzed. Image processing of all scans included Gaussian filtering and segmentation and was described elsewhere in detail (36). In brief, the same filtering and segmentation values were used for every measurement of each animal (trabecular bone: sigma=0.7, support=1, threshold density=0.575 g HA/cc, equivalent to 24% of maximal grayscale value;

cortical bone: $\sigma=0.8$, $\text{support}=1$, threshold density= 0.642 g HA/cc , equivalent to 26% of maximal grayscale value). From every baseline and follow-up CT-scan, the trabecular bone of the meta- and epiphyseal area was manually selected and bone structural parameters (bone volume fraction (BV/TV), connectivity density (Conn.D), structure model index (SMI), trabecular number, thickness and separation (Tb.N, Tb.Th, Tb.Sp)) were automatically determined (figure 8.2). Cortical bone of the metaphysis was manually selected from the hundred most distal slices. The tibia was manually selected in the CT scan of the diaphysis, after which cortical thickness and polar moment of inertia were determined.

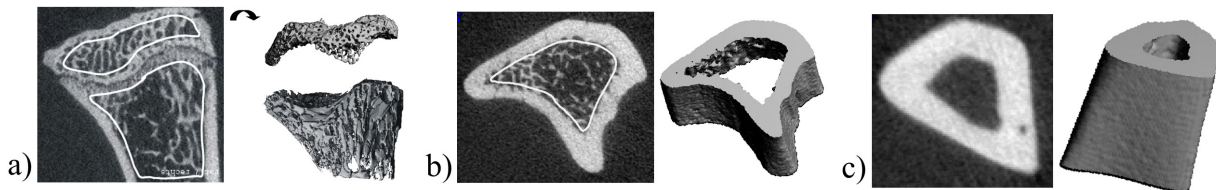


Figure 8.2: CT-scan of a) proximal metaphysis showing hand-drawn contours of the metaphyseal and epiphyseal trabecular bone b) proximal metaphysis showing hand-drawn contours of metaphyseal, cortical bone c) diaphyseal, cortical bone.

8.2.3 Three-point bending of tibiae

After sacrifice, all tibiae were dissected and frozen in PBS solution at -20°C . They were thawed prior to three-point bending. The tibia was placed on the lateral surface on two rounded supporting bars with a distance of 2.4 cm. A preload of 1 N was applied (ZWICK, Z020, Ulm, Germany) at the medial surface of the diaphysis by lowering a third rounded bar. A constant displacement rate of 6 mm/min was applied until failure. Displacement was measured from the actuator displacement transducer of the testing machine. From the force-displacement curve, the following mechanical parameters were determined: 1) ultimate load, defined as the maximum load, 2) displacement at ultimate load, which was corrected for the toe region 3) extrinsic stiffness, calculated as the slope in the linear region between 40 and 80% of the ultimate load and 4) energy to ultimate load, defined as the area under the curve until ultimate load.

8.2.4 Statistics

A one-way ANOVA test with repeated measures was performed to compare the vibration and OVX groups during treatment between week 8 and 14. Also, a one-way ANOVA with a Bonferroni post-hoc test was used to determine differences between the groups at all time points, for all parameters. Furthermore, a one-way ANOVA test with repeated measures was performed to compare the OVX and SHAM groups between week 0 and 8. All p-values below 0.05 were considered significant.

8.3 Results

Body weight of the rats increased significantly after OVX compared to the SHAM group (figure 8.3). After WBV treatment was initiated, body weight initially decreased in the first two weeks, after which it started increasing again at about the same rate as in the OVX group. At the end of the experiment, body weight was significantly lower in the WBV than the OVX group.

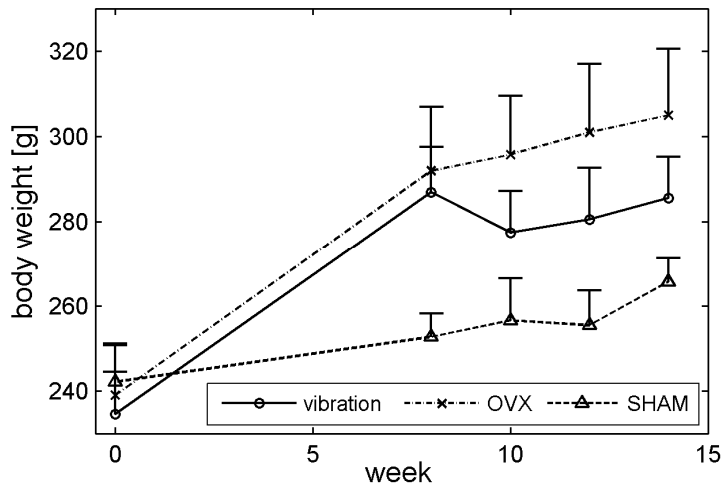


Figure 8.3: Body weight of all rats in all groups at all time points (mean \pm SD).

8.3.1 Metaphyseal, structural parameters

At week 8, the ovariectomized groups displayed loss of BV/TV, Conn.D, Tb.N and Tb.Th and an increase in SMI and Tb.Sp, indicating the development of osteopenia (figure 8.4). Beyond 8 weeks, the untreated OVX group showed further deterioration of bone structure except for Tb.Th, which increased.

WBV treatment did not alter structural parameters compared to the OVX group; in both groups further deterioration of the structure was seen, except for Tb.Th, which significantly increased over time in both groups. Over week 8 to 14, no significant difference between the WBV and OVX group was found for all structural parameters. At all time points, the WBV and OVX groups did not differ in any structural parameter and both groups were significantly different from the SHAM group. Between week 12 and 14 a significant interaction between time and group was found for BV/TV, Tb.N and Tb.Sp. This indicates that BV/TV decreased significantly more in the OVX than the WBV group, which was accompanied by a significantly reduced decrease in Tb.N and reduced increase in Tb.Sp in the WBV group. However, these differences were so small in magnitude that they remained undetected with an ANOVA test with Bonferroni post-hoc test at specific time points.

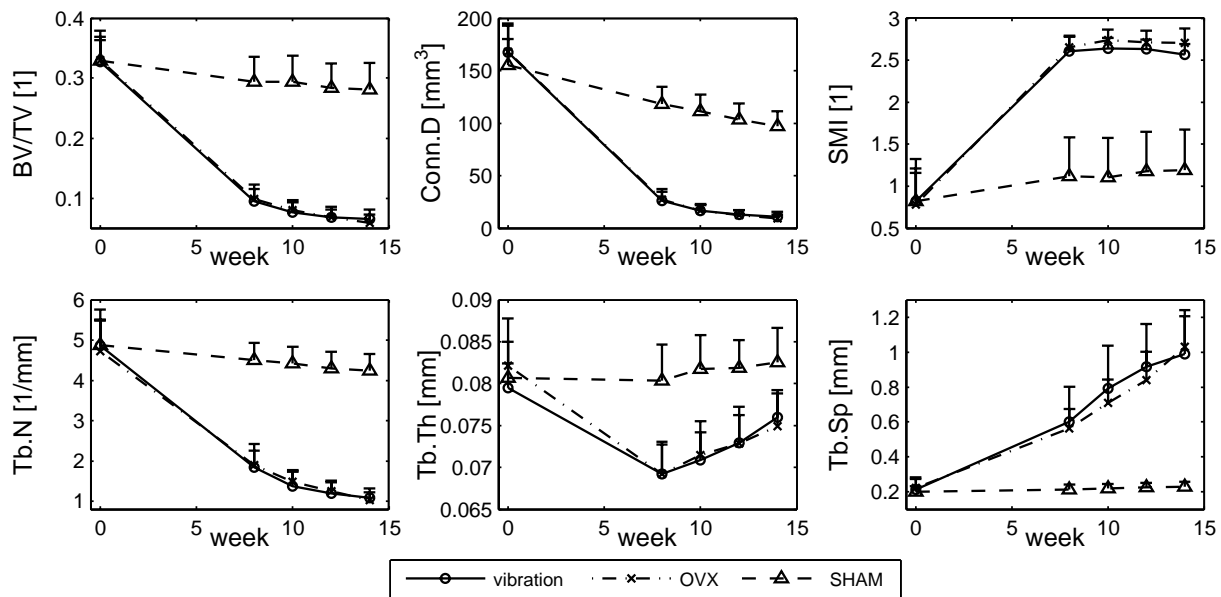


Figure 8.4: Structural parameters in the metaphyseal, proximal tibia for all groups at all time points (mean \pm SD).

8.3.2 Epiphyseal, structural parameters

At week 8, the ovariectomized groups displayed loss of BV/TV, Conn.D and Tb.N and an increase in SMI, Tb.Th and Tb.Sp, indicating the development of osteopenia (figure 8.5). Changes in the epiphysis, however, were much smaller than in the metaphysis. Between week 8 and 14, the WBV and OVX group showed further deterioration of bone structure except for Tb.Th, which gradually increased over time. Over week 8 to 14, no significant interaction between time and group was found for all structural parameters in the WBV and OVX groups, although the pattern of bone loss was slightly different.

8.3.3 Cortical thickness and polar moment of inertia in the metaphysis and diaphysis

In the metaphysis, cortical thickness and the polar moment of inertia did not significantly change within 8 weeks after OVX compared to the SHAM group (figure 8.6). Between week 8 and 14, both the WBV and OVX groups had a significantly increasing cortical thickness and significantly decreasing polar moment of inertia. However, no differences between the WBV and OVX group were found over time. At week 8, pMOI was significantly higher in the WBV than the SHAM group. At all other time points, cortical thickness and pMOI were not significantly different between groups.

In the diaphysis, cortical thickness did not significantly change after OVX compared to the SHAM group, but pMOI significantly increased after OVX in the first 8 weeks. Between week 8 and 14, cortical thickness in the WBV and OVX group did not change

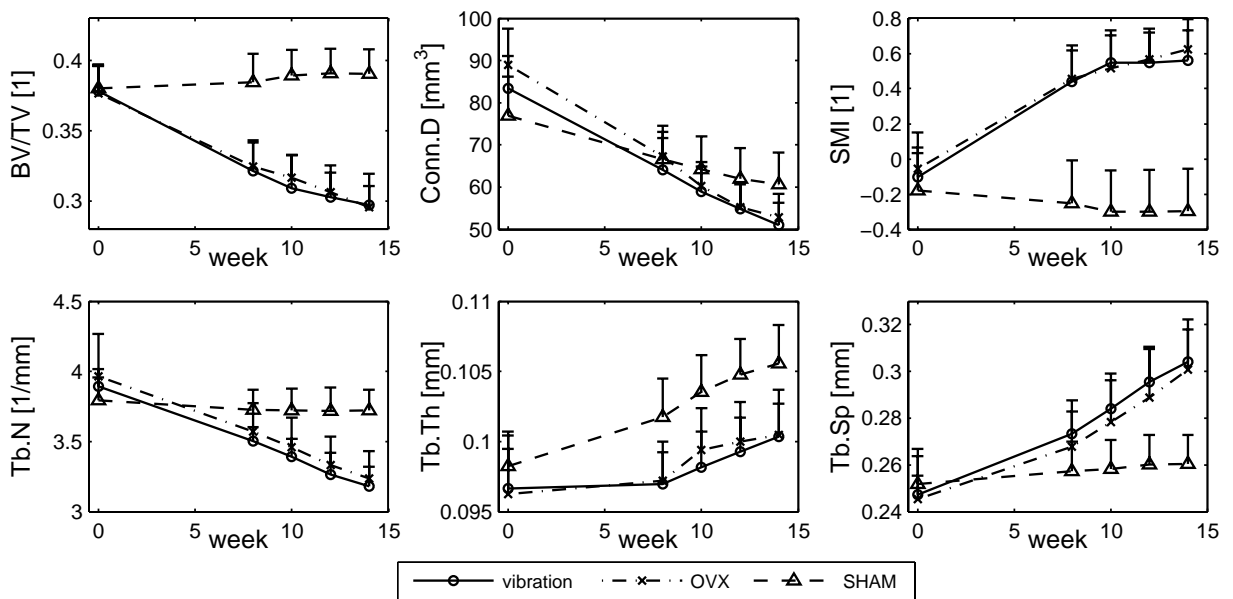


Figure 8.5: Structural parameters in the epiphyseal, proximal tibia for all groups at all time points (mean \pm SD).

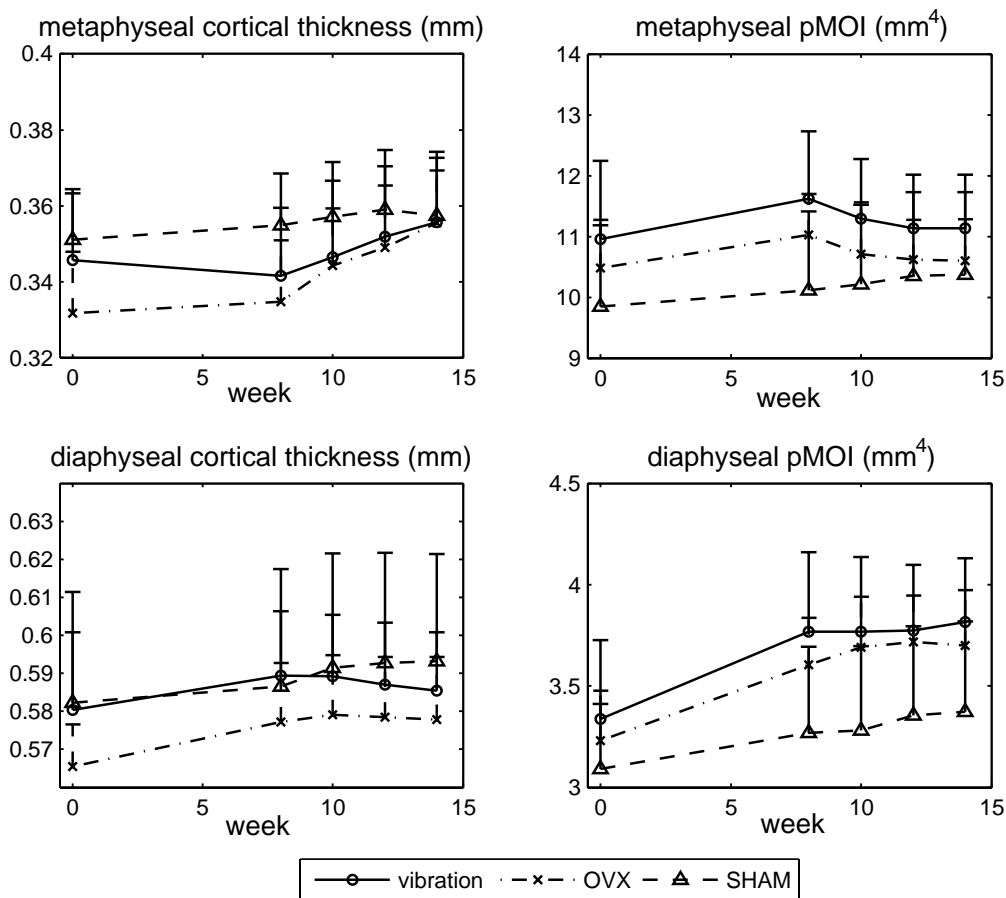


Figure 8.6: Cortical thickness and polar moment of inertia (MOI) in the meta- and diaphysis of the tibia for all groups at all time points (mean \pm SD).

over time, but a significant interaction between group and time was found for the two groups. pMOI significantly increased between week 8 and 14 in both groups, while no difference was found between the WBV and OVX group. At week 8 and 10, pMOI was significantly higher in the WBV than the SHAM group. At all other time points, cortical thickness and pMOI were not significantly different between groups.

8.3.4 Three-point bending of tibiae

No significant differences between all groups were found for all mechanical parameters (figure 8.7). Ultimate load, extrinsic stiffness and energy all showed similar trends, in which the OVX group tended to be respectively slightly higher and lower than the SHAM and WBV group, though this did not reach significance.

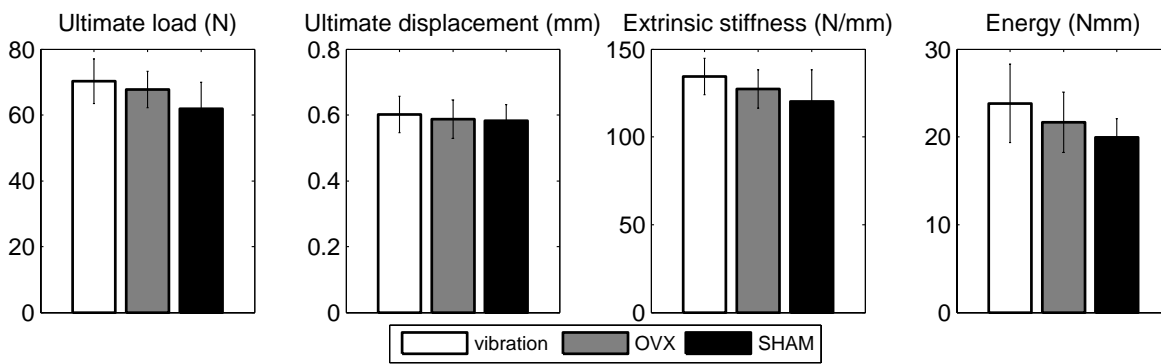


Figure 8.7: Ultimate force, ultimate displacement, extrinsic stiffness and energy determined from three-point bending test on tibia. No significant differences were found between all groups based on ANOVA with Bonferroni post-hoc test.

8.4 Discussion

In this study, the effects of six weeks of vibration treatment on tibial bone were analyzed longitudinally over time in the same ovariectomized rats using an *in vivo* micro CT-scanner. Trabecular bone structure in the proximal meta- and epiphysis did not improve compared to untreated OVX rats, although in the last two weeks, some small inhibitions of deterioration were found. Cortical bone in the metaphysis and diaphysis did not show a significant response to vibration treatment, which was also reflected by unaltered bending properties.

For low-frequency mechanical stimuli, which require a relatively high load, to have an effective anabolic response, strain magnitude and strain-rate have been suggested to be the key modulators (51;129;155;193;233;264). In that kind of mechanical stimulation, resulting fluid flow may mediate bone adaptation (92). The low-magnitude, high-frequency vibration used in our study has previously been shown to lead to strain levels on the order of one microstrain in the proximal tibia in rats (129), which is much smaller than those arising during locomotion (73). As direct strain magnitude or strain-rate are unlikely to play a major role, it has been suggested (231)

that perturbation of intramedullary pressure (213;231) and the resulting intracortical fluid flow (49;284) are the mediators in low-magnitude, high-frequency vibration.

Based on the high bone formation rates reported in the proximal tibia in a similar study in ovariectomized rats after WBV, and the fact that significant improvements were reported earlier in the femoral epiphysis (129), we expected a pronounced effect of WBV in the rat tibia. There are several possible explanations for the fact that this expectation was not met. Firstly, it could be that the results are very sensitive for the actual vibration parameters and experimental design. In our study, these parameters were derived from those used in the previous study, but in order to maximize effects some settings were changed based on a personal communication (210) and a meeting abstract (292). The acceleration used in our study was twice as high as the one used in the earlier study. Also, we used a 20 minute vibrating period, which is twice as long, and rats were vibrated twice a day instead of once. It is possible that this has stressed the rats, which is also suggested by a 6% lower body weight at the end of the study. Perhaps the additional stress of an extra vibration period a day annuls the positive effect on bone formation. Another possibility is that the extra fat mass after ovariectomy would have damped the effect of WBV. However, in the other papers on WBV in ovariectomized rats, there is no mentioning of regulated feeding, which can inhibit an increase in body weight after ovariectomy, while in these studies they did find an effect of WBV (68;129;201). Also, Wistar rats were used instead of Sprague-Dawley rats, which could have led to a different response to WBV due to a different genetic make-up. However, this is not very likely, as both strains are outbred and in the other two studies on WBV treatment of OVX rats, Wistar rats were used as well (68;201). Secondly, it is possible that the response is site-dependent and more pronounced in the femur than in the tibia. We did not study the effects of WBV in the femur and thus can not exclude this possibility. Thirdly, it may be that a marked increase in bone formation rate does not lead to a substantial increase in bone mass perhaps due to an accompanying increased resorption rate. In an earlier study though, actually a decrease in osteoclastic activity was reported (294), although another study did not find a significant effect on osteoclastic activity (293). Fourthly, it could be that changes in bone structure due to WBV were too small to be detected. However, the longitudinal design of our study, allowing for repeated measurements, is a much more sensitive approach than the cross-sectional design used in most earlier studies. Hence, if the effects are too small to be detected in our study, the effect likely is too small to be used as a therapeutic treatment. Finally, it should be noted that although the effects of WBV on femoral, epiphyseal bone microstructure in the study by Judex et al. (129) were considerable, in general the effects of WBV on bone microstructure and BMD have shown to vary per site, species and study design (75;84;114;127-129;228;230;232;293;294).

As no significant effects of vibration therapy on bone structural parameters were determined, it is important to ascertain that the mechanical stimulus was indeed transported from the vibration platform to the rat tibia. The mechanical stimulus used in this study was vertically directed via a ground-based vibration platform. Rats were placed five at a time on the cage, which was divided in five sections and mounted onto

the platform. By separating the rats, we ensured that no mechanical transmission would be lost due to rats climbing on top of each other and hereby damping the signal. By placing accelerometers onto several locations of the cage, we ensured that the frequency and acceleration levels that we used were indeed transferred to the whole surface of the cage. In the vibration study by Judex et al., in which a similar platform was used, it was found that 0.15 g and 90 Hz resulted in strains of 0.74 microstrain (129). As values of 0.3 g and 90 Hz were used in our study, it can be deduced that the microstrain present in the proximal tibia of our rats was about twice as high.

This research was limited by a study period of six weeks. It could be that longer periods of vibration therapy would have induced pronounced effects on bone mass. However, in several rat and mice studies, vibration therapy was only applied during 3 to 4 weeks (129;232;294), after which a marked increase in bone formation rate (129;232;294) and bone volume was found (129). While the WBV rats were put twice daily on special platform cages for treatment, the control groups were not SHAM-treated and remained in their normal cages, because they were also used as control for another study, which was not related to WBV. This is, however, not expected to have affected our results, as the rats did not seem stressed that much by being in a different environment/cage (they were handled almost every day and were used to being in a different environment for a short while), but more so by the actual vibrating motion. Also, rats in our study were subjected to serial radiation resulting from CT-scanning, however, we have previously shown that eight weekly scans does not lead to detectable radiation damage (36).

In summary, in this study, no substantial effects of six weeks of low-magnitude, high-frequency vibration treatment on tibial bone in ovariectomized rats were found. Since there are many factors that may have contributed to this unexpected result, we conclude that further studies are needed to better understand the role of these factors on the effects of WBV in rodents to optimize the potential for treatment of osteoporosis.

Acknowledgements

This work was funded by the Netherlands Organisation for Scientific Research. We thank Jo Habets and Leonie Niesen for performing the ovariectomies and the animal care.

Chapter 9

Discussion

9.1 Introductory remarks

Although the effects of osteoporosis and several treatments have been thoroughly studied in rats, many aspects are still unknown as they remain unidentifiable in cross-sectional studies. *In vivo* micro-CT combined with image registration software offers a potential method to identify effects of osteoporosis and treatments over time. Also, local changes in bone within the same rat can be monitored over time, which taken together can provide novel and relevant information. In this dissertation, we studied the development of osteoporosis in rats and several treatment options for it using *in vivo* micro-CT. We first focused on anti-resorptive and then on anabolic agents, both used in the treatment of osteoporosis. Changes over time in bone microstructure were determined and in some studies mechanical properties were compared after sacrifice using mechanical tests or finite element models.

Overall, in each animal study of this dissertation, several groups of aged, female Wistar rats were used. The proximal or diaphyseal tibia was scanned in each rat under anesthesia at several time-points to determine changes in bone structure over time. Every follow-up scan was registered to the baseline scan such that they overlapped. The same volume of interest was analyzed for each measurement and bone structural parameters were determined over time.

Osteoporosis can be caused by estrogen-deficiency and immobilization and may lead to different temporal and spatial patterns of bone loss, which is currently unknown. As the pattern of bone loss may affect the treatment strategy, this has clinical importance. Also, immobilization-induced osteoporosis, in which mechanical loads are absent or very low, may not result in mechanical adaptation as seen after estrogen-deficiency and therefore may be associated with a different risk of fracture. Therefore, the effects of estrogen-deficiency and immobilization on bone microstructure and strength in mature rats were determined.

Bisphosphonates inhibit bone resorption and are commonly used to treat osteoporotic patients; however, many aspects of their effects are still unclear. It is unknown how long a single injection of zoledronic acid (ZOL), a potent bisphosphonate, can inhibit deterioration of bone structure. The time-point of starting bisphosphonate treatment of osteoporotic patients may influence the resulting bone microstructure and is also unknown. Therefore, we analyzed the effects of preventive (before development of osteoporosis) and recovering (after development of osteoporosis) treatment with ZOL, a potent bisphosphonate, on bone mass and microstructure over time *in vivo* in the rat tibia. Also, bone strength and dynamic histomorphometric measures were studied. Then, the effects of preventive and recovering treatment with ZOL on structure and strength of the vertebra, a clinically relevant site, were analyzed at the end of the experiment. Finally, fatigue properties of the rat vertebra were determined using a newly developed method and compared between control and ZOL treated, ovariectomized rats.

After analyzing the effect of a bone resorption inhibitor, we continued with analyzing the effects of two bone formation stimulators. PTH is known to stimulate bone formation and as such is used in patients with severe osteoporosis. Several aspects

of its use are still unknown, such as the temporal changes in bone microstructure with PTH use, how these may differ between different locations, where new bone is formed locally and how this progresses over time. To address these aspects, we analyzed bone structure in the proximal and diaphyseal tibia during six weeks of PTH treatment in ovariectomized rats. Vibration treatment has shown to have an osteogenic effect in rodents as well, but its effect varies per study design. Therefore, it is essential to further optimize vibration treatment settings to establish the maximum treatment potential for osteoporosis. Bone formation rate has been found to respond the most in the proximal tibia, however, the effects of vibration on bone structure there are unknown. Therefore, we studied the effects of vibration treatment on tibial bone of ovariectomized rats over time.

9.2 Main findings and implications

9.2.1 Estrogen-deficiency versus immobilization induced osteoporosis

Damage due to radiation from the *in vivo* micro-CT scanner was first excluded in chapter two. In chapter three, using this technology, it was found that reductions in bone volume fraction were similarly severe in the metaphysis after estrogen-deficiency and immobilization. Deterioration of bone microstructure in the epiphysis was found to be less prominent than in the metaphysis, though more pronounced in immobilized rats. This may be explained by the hypothesis that estrogen-deficiency increases the mechanostat threshold leading to low (metaphysis) and high (epiphysis) strain areas being resorbed and conserved respectively and in contrast, after immobilization an overall reduction in strain takes place resulting in bone loss in all locations. This implies that bone loss after immobilization can take place anywhere in the body, while after estrogen-deficiency, mostly low strain areas will be resorbed. After estrogen-deficiency, the skeleton is likely to still be able to sustain normal, habitual loads, as it has adapted to those. Once an irregular situation with different loading direction or size takes place, such as an impact fall to the hip, it is possible that fractures occur. After immobilization, however, it is possible that even daily loads may be too large to withstand and fractures could occur more easily, or in anatomical sites that normally do not fracture easily (121).

Secondly, we hypothesized that immobilization accompanied by low or absent mechanical loads, will not result in mechanical adaption, as reported after estrogen-deficiency (101;280) and therefore will be associated with more unfavorable bone structure and mechanical properties than after estrogen-deficiency induced bone loss. In chapter three, we found that mechanical parameters, determined by finite element analysis (FEA), were more deteriorated after immobilization than estrogen-deficiency induced osteoporosis (figure 3.6). Although this analysis was quite basic, we found that the same loss of bone mass resulted in different alterations of mechanical properties. As such, these results provided the first proof for our hypothesis. If similar results are found for humans, it implies that general measures like bone mineral density (BMD) determined by DXA should be differently interpreted depending on the cause of

osteoporosis. Also, physicians may need to respond earlier to reducing bone mineral density values, if they are caused by immobilization.

9.2.2 Bisphosphonates

In chapter four to six, we analyzed the effects of bisphosphonates on bone mass, structure and strength. A single injection of ZOL was given as preventive treatment at the time of ovariectomy, as described in chapter four. Bone microstructure in the proximal tibia was found not to deteriorate during the sixteen weeks of monitoring (figure 4.1). This demonstrates the potent, long-term effects of ZOL, which concurs with recent results from a dose-related study in rats (80) and from a phase III clinical trial, in which patients with postmenopausal osteoporosis received an annual infusion of ZOL for three years (17;216). In another group of rats in our study, osteopenia was first induced and then recovering treatment was started by giving a ZOL injection after eight weeks. Bone volume fraction increased in the next four weeks accompanied by an increasing trabecular thickness and stabilized trabecular number. This opposes the belief, held by some, that bisphosphonates merely inhibit bone loss and do not actually increase bone mass. This is, to the author's knowledge, the first report on a significant increase in bone volume fraction, although nonsignificant increases in bone volume fraction of paired iliac biopsies (before and after treatment) have been reported after one to five years of bisphosphonate treatment of osteoporotic patients (6;21;71). Although a substantial increase in bone volume fraction may have taken place before, it was previously difficult to detect this as *in vivo* analysis of bone structure in animals was limited and paired biopsies in humans is often not performed. It is likely that in our study, bone resorption was initially suppressed after ZOL injection, while bone formation was not yet. This led to a temporary net bone remodeling result, leading to increased bone mass and bone volume fraction. This is schematically shown in figure 9.1 and concurs with previous reports on filling of resorption cavities after bisphosphonate treatment (78). After the rate of bone formation decreased as well, bone remodeling rate was in balance and no net bone formation or loss was found. Bone microstructure in the recovering treatment group did not fully return to baseline values at the end of the study. Therefore, the main conclusion from this study was that bone microstructure after recovering treatment is better than after no treatment at all, however less favorable than after preventive treatment.

In cross-sectional measures taken after sacrifice, a single ZOL injection was also found to inhibit deterioration of bone microstructure and strength in the vertebra, a clinically more relevant site than the tibia (figure 5.1 and 5.2). It was however, not possible to distinguish between preventive and recovering treatment. Differences between these two treatments were often low and not significant. The latter was for the most part due to a different study design in the cross-sectional vertebra and longitudinal tibia study. In the tibia, follow-up measures were available permitting the use of repeated measures and paired statistics, which are more powerful than an ANOVA. Also, follow-up measures enabled the calculation of percent changes over time, hereby

correcting for any differences in groups found at the beginning of the experiment. This clearly illustrates the strengths of *in vivo* over *in vitro* scanning.

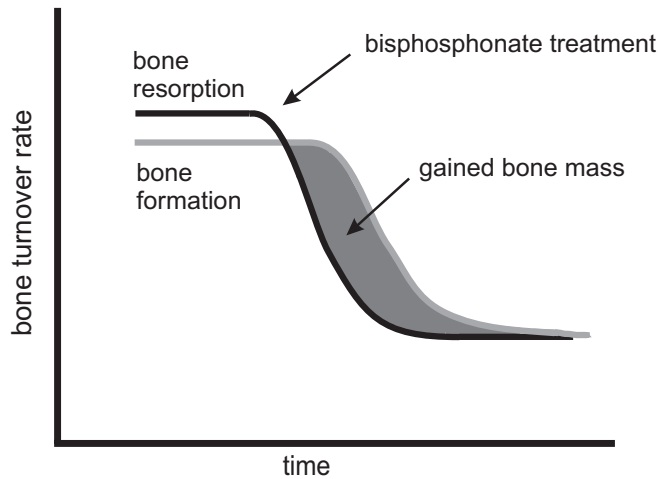


Figure 9.1: *Proposed schematic response to bisphosphonate treatment in bone turnover rates. Prior to bisphosphonate treatment, bone resorption exceeds bone formation rate leading to gradual, net bone loss. After the onset of bisphosphonate treatment, bone resorption first decreases while formation shows a delayed response, which leads to a temporary positive net bone remodeling balance and thus an increase in bone mass. After both bone resorption and formation have reached a new equilibrium, bone resorption and formation rate are equally high, which results in a stable bone mass.*

Vertebral fractures in osteoporotic patients are mostly due to spontaneous fractures, resulting from daily activities or from cyclic loading, rather than from trauma (72;224). Bisphosphonates have shown to influence mineralization (10) and lead to accumulation of microcracks and diffuse damage (38), due to decreased resorption rates. Drug efficacy studies in rats generally focus on changes in bone mass, structure and static mechanical strength, whereas fatigue behavior, which may play an important role in vertebral fractures, may respond differently to pharmacologic intervention than other statically-determined mechanical parameters. Therefore, in chapter six we developed a method to determine fatigue properties in rat vertebral bone. As we used whole vertebral bodies, the interplay between cortical and trabecular bone was taken into account. Yet, fatigue behavior was found to be similar to that seen using only trabecular or cortical bone, and similar to that from other species. Fatigue behavior was similar between control and ZOL treated, ovariectomized rats. Number of samples per group was low however, and the variation high, resulting in a reduced power to detect differences. However, as the mean values for all fatigue properties were very similar, we conclude that this is the first indication that ZOL treated OVX rats have the same fatigue properties as control rats.

9.2.3 Anabolic treatments

After analyzing the effects of a bisphosphonate on bone microstructure *in vivo*, we focused on the effects of anabolic treatments. Daily injections of PTH have shown to increase bone mass in animals (143;162;188;190) and osteoporotic women (196). Several aspects are still unknown, however. In chapter seven, our aims were to 1) determine the change in trabecular thickness and number after PTH over time, 2) compare the response to PTH between the meta- and epiphysis, 3) determine the effects of PTH on mineralization and mechanical properties, 4) determine the location of new bone formation due to PTH on a micro-level over time and 5) determine predictive value of bone structural properties for gain in bone mass after PTH.

Bone volume fraction accompanied by trabecular thickness increased over time after PTH treatment in the meta- and epiphysis, while trabecular number increased only in the epiphysis (figure 7.3). An increase in trabecular number is an uncommon feature that has been reported after PTH use (31;70;105;120;181;203;237;239), and has been attributed to trabecular tunneling. Although we did not find typical examples of trabecular tunneling in our CT-scans, it is possible that this did take place in the epiphysis in a different form. It may also be that after segmentation of the CT-scans, initially thin trabeculae were removed, while after PTH treatment they had thickened enough to be included after segmentation. An increase in trabecular number, is a very promising development that offers more improvement in bone strength and thus fracture risk reduction than an increase in trabecular thickness alone (263). An increased trabecular number has also been demonstrated in primates treated with PTH, which more closely resemble humans (120). Currently, PTH is reserved for patients who have severe postmenopausal osteoporosis with at least two vertebral fractures (251). There has been some concern that PTH first increases bone resorption before formation leading to an initial increased fracture risk (37). However, bone strength has not been found to deteriorate in the early phase of treatment in animals and humans. One of the reasons for this is that bone formation after PTH use can take place on surfaces without prior resorption (170). Taken together, PTH may also be suited for treatment of less severe cases of osteoporosis as bone mass can be improved more than with bisphosphonates, trabecular number may be augmented and negative effects of PTH may play less of a role than thought initially. The comparison between treatment with bisphosphonates and PTH will be elaborated on in paragraph 9.5.

Concern has been raised that PTH alters tissue mineralization due to the high degree of new and therefore low mineralized tissue (182). In our study, CT-derived mineralization in cortical bone did not differ between PTH treated rats and ovariectomized or control rats (figure 7.5). This was also reflected by unaltered ultimate displacement (figure 7.7), which could have been changed if the tissue was more or less brittle due to altered mineralization. Cortical thickness and polar moment of inertia increased directly after PTH treatment. Early findings from clinical studies indicated, however, that increases in trabecular bone mass may be at the expense of cortical bone in osteoporotic patients (37;104), but subsequent studies indicate that at some skeletal sites, beneficial (58;169;272) or no (300) changes occur in cortical bone. The fracture reduction demonstrated in postmenopausal women with osteoporosis

would be consistent with this view (47;196;212). Additionally, interpretation of changes in bone mineral density measures in humans at cortical sites is complex because they are affected by alterations in cortical width, cortical porosity and bone size (47). Increased cortical remodeling leading to an increased porosity may hamper increases in bone mass and oppose the positive effects on bone strength. It should be noted that differences in species may limit the translation from rat to human studies, as remodeling in rat cortical bone is not subject to Haversian remodeling (118).

By generating follow-up *in vivo* micro-CT scans and using image registration software, we were able to track individual trabeculae over time (figure 7.6). We saw several trabeculae that were almost fully cleaved after development of osteopenia at the start of PTH treatment. During treatment, bone was directly deposited in the center of the trabeculae, where most beneficial, hereby restoring the structure and probably increasing strength already after two weeks. Bone formation also took place on the lateral sides of the trabecula though to a lesser extent. Deposition of bone in the center could be explained by Frost's mechanostat, which states that bone is deposited where strains and stresses are the highest. Since in an almost cleaved trabecula, merely a thin line of bone was present at certain locations, strains and stresses would be highest at these locations leading to bone formation there. This suggests that PTH-induced bone formation is, at least in part, mechanically driven. This agrees with results from two finite element studies on CT-scans of osteoporotic patients treated with teriparatide (rhPTH (1–34)), in which it was found that bone was mostly deposited on locations of high strains (87) and that teriparatide increased vertebral strength by altering the distribution of density within the vertebra (135). In our study, other trabeculae were seen in which in the first two weeks mostly cavities were filled, while later on bone was added to the outer surface. It has been suggested that increases in bone mass after PTH may occur by remodeling-based or modeling-based bone formation (47). Our data suggest that initially remodeling-based bone formation takes place, as cavities are filled with bone, while later modeling-based bone formation is more pronounced as bone is added to the outer surface, which does not appear to have been resorbed first. This will need to be further validated. This is, to the author's knowledge, the first report on *in vivo* tracking of individual trabeculae after PTH use and provides novel, unique and relevant information on the location and timeline of bone formation on a micro-level.

It is clinically relevant to be able to predict to what extent a patient will respond to PTH in order to determine the best treatment. This is as yet unknown in patients as well as in animals. Since our study was done *in vivo*, it was for the first time possible to determine whether predictions of bone mass can be made. We found that the best predictor of final bone mass and bone volume fraction after PTH in both the meta- and epiphysis was bone mass and bone volume fraction at the start of the experiment, before ovariectomy (table 7.1). If these results would be translational to clinical practice, which needs to be tested, this would indicate that bone mineral density before menopause would predict bone mineral density after PTH treatment of osteoporotic patients.

In chapter eight, another anabolic treatment was tested in the form of vibration treatment of ovariectomized rats. This has previously been shown to greatly increase

bone formation rates in animals (128;293;294), while effects on bone of osteoporotic, postmenopausal women were only minor (228). Although vibration settings used in our study were extrapolated from a study in which four weeks of vibration led to an increased bone formation rate in the tibia and bone volume in the femur of ovariectomized rats (129), no effects on bone microstructure in the tibial meta- and epiphysis were found in our study. There are several possible explanations for this apparent discrepancy, including but not limited to too much stressing of the rats due to longer vibration periods, different rat strains, anatomical site dependency or an increased resorption rate that annuls the increased formation rate. This discrepancy and the fact that in general, the effects of vibration treatment on bone microstructure and bone mineral density have shown to vary per site, species and study design (75;84;114;127-129;228;230;232;293;294), illustrates that further studies are needed to better understand the role of these factors in order to optimize the potential for treatment of osteoporosis.

9.3 Ethical considerations

Laboratory animals were used for this research. The use of laboratory animals should be carefully weighed and it is the researcher's ethical imperative to always safeguard the so-called three R's:

- Replacement of experimental animals by alternatives.
- Refinement of housing, handling and experimental procedures to reduce discomfort, pain, fear, stress and suffering.
- Reduction of numbers of animals used.

During my PhD, I have tried hard to follow these guidelines to the best of my abilities. During all procedures, all people working with the rats tried their best to reduce the degree of discomfort, pain and suffering, by giving proper anesthesia and analgesia. To establish immobilization induced osteoporosis, we chose the neurectomy instead of tail suspension method to minimize discomfort. Also, housing procedures were made as comfortable as possible. Particularly the last R, reduction of numbers of animals used, has been warranted by the use of the *in vivo* micro-CT scanner, which strongly reduces the number of animals by measuring bone microstructure *in vivo*, and by enabling the use of repeated measures statistics or statistics on absolute or relative changes over time. Traditionally, for each scan, a group of rats would have to be sacrificed. As on average, the number of scans per experiment was six, this has at least reduced the number of rats needed with 83%.

Although the use of laboratory animals should be minimized, it has greatly contributed to the results of this dissertation and provided novel, relevant information on how osteoporosis develops and treatments improve bone microstructure.

9.4 Experimental methods employed; strengths and weaknesses

9.4.1 *In vivo* micro-CT

In this dissertation, we used the recently developed *in vivo* micro-CT scanner. Until now, only a few studies were conducted in osteoporosis research using this scanner. Erwin Waarsing was one of the first to conduct several studies during his PhD on methodological issues like segmentation (278;281) and trabecular adaptation and growth after ovariectomy (279;280). In the last few years, Steven Boyd has analyzed bone structural changes over time after ovariectomy (32;41) as well as the effects of radiation (146). The effects of treatments have however, not been studied yet using *in vivo* micro-CT, in spite of its advantages. These advantages consist first of all of the ability to scan the same animal on several time-points, while in the past, animals needed to be sacrificed in order to be scanned. This results in a lower number of animals needed per experiment, saving the life of many animals and increasing time and cost efficiency. Also, due to the follow-up nature of the study, data can be analyzed using repeated measures or paired statistics, further reducing the number of animals. Finally, animals can be distributed equally into groups, as a baseline scan can be made prior to the start of the study, to determine bone mass and microstructure. This makes the study ‘cleaner’ and clearer conclusions can be drawn.

Furthermore, using image registration, by which follow-up scans can be overlaid, local changes in bone structure can be visualized. Careful considerations should be made though when doing so. In between two or more scans, the bone has inevitably changed in mass and structure. Therefore, assumptions should be made on what part of the bone has not changed and can therefore be used as region for registration. Several choices can be made for this. First of all, overall registration can be done in which the whole scan will be used to overlay with the other scan as best as possible. Also, in the case of a CT-scan of the proximal tibia, the epiphysis can be used to register on, as no growth takes place here anymore. When doing so, the amount of linear growth can be determined qualitatively, and perhaps in future quantitatively as well. Also, changes in the overall shape of the bone can be seen. Finally, one can register on the metaphysis. In this case, local changes at a specific point in the metaphysis can be determined.

The *in vivo* micro-CT scanner used in this dissertation also has several drawbacks and limitations. First of all, the amount of radiation used to obtain high-resolution images is quite high. In chapter two, we established that eight weekly scans does not lead to detectable damage in mature rats. However, it is very well possible that a higher number of scans or a more frequent scanning regime can lead to damage. Also, care should be taken when working with younger animals as they are particularly sensitive to radiation damage, due to their active growth plate. Secondly, in young rats and mice, the whole animal can be scanned, although image resolution then decreases. In mature animals however, only the proximal femur, tibia and tail can be scanned due to a limited field of view, although there are different systems available that are able to scan the whole rat.

9.4.2 Animal models

In this dissertation two commonly used animal models were used, the ovariectomized (OVX) (chapter three to eight) and neurectomized (chapter three) rat. The ovariectomized rat has been used for several decades to simulate postmenopausal osteoporosis. Female rats lose trabecular bone in the proximal tibia and lumbar vertebrae following OVX as a direct result of estrogen deficiency, which is well documented and reviewed (118;130;288). The ovariectomized rat model has several advantages. Its site-specific development of trabecular osteopenia is one of the most reproducible biologic responses in skeletal research (118). Rats are convenient and inexpensive to house. An ovariectomy on a rat is a relatively simple procedure to perform and causes relatively little discomfort to the animal, provided the anesthesia and analgesia are properly maintained. It has been used for several decades and has been shown to be an excellent model in the simulation of osteoporosis. In fact, the FDA Guidelines For Preclinical and Clinical Evaluation of Agents Used in the Treatment or Prevention of Postmenopausal Osteoporosis (1994) recommend that agents be evaluated in two animal species, including the ovariectomized (OVX) rat and in a second non-rodent model (258).

In spite of its advantages, the ovariectomized rat model also has several drawbacks and limitations. The growth plates in the rat skeleton remain opened for quite long after sexual maturation or do not fuse at all (55). Therefore, control groups should always be used to distinguish between changes related to osteopenia, the effect of pharmaceutical agents and normal aging. The slow developing cortical bone loss is another disadvantage as well as the lack of Haversian or intracortical remodeling associated with cortical osteopenia (118). In figure 4.3 and 7.4, we have shown that even an increase in cortical thickness can take place in the tibial meta- and diaphysis after OVX. Most rats used for OVX are outbred, which results in quite large variation in the response to ovariectomy and thus increases the number of animals needed per group to ensure statistical power. To analyze what determines the amount of bone loss after OVX, we explored the relation between bone volume fraction before and after OVX (appendix). It was found that a strong linear correlation exists between bone volume fraction before and after OVX. A final shortcoming is the fact that like other animal models of osteoporosis, the rat has no naturally occurring fragility fractures associated with the osteopenia (118). This has been partially overcome by determining the effects on mechanical properties by mechanically testing various bones such as the vertebral body (chapter five and six), femoral and tibial shaft (chapter four, seven and eight) and proximal femur.

The neurectomized rat is one of several immobilization models, which simulates immobilization induced osteoporosis due to for example a long period of bedrest, reduced activity or space flight. By unilaterally dissecting the sciatic nerve, one leg can not be properly used in locomotion resulting in rapid, local bone loss. As with the OVX model, trabecular bone loss occurs much faster than that in cortical bone after immobilization. More bone loss in the immobilization model is seen in the weight-bearing, lower extremities than the non-weight-bearing, upper extremities (118).

The drawbacks for the neurectomized rat are the same as for the ovariectomized rat model. In addition, the site specificity for the one legged response should be kept in mind. Also, the untreated leg cannot be used as internal control as overall activity can be reduced leading to bone loss there as well (see chapter two).

Retired breeders are rats that have had multiple pregnancies, which reduces plasma levels of estrogen (12). This results in reduced trabecular bone in retired breeders compared to age-matched virgin rats. As their amount of bone is reduced, the amount of bone that is lost after ovariectomy is lower compared to virgin rats, which makes them less suited for experiments with ovariectomy. An advantage of using retired breeders over virgin rats is the easy access to aged animals. Virgin rats can mostly only be obtained in the Netherlands at the maximum age of three months, when their growth plates are still relatively active, while retired breeders are often available at six to eight months. At the start of this PhD study, the reduced bone mass in retired breeders was unknown to us and therefore in chapter three and four retired breeder rats were used, while in chapter two, seven and eight virgin rats were used. In the latter studies, virgin rats were received at about three months and kept in house until they reached the proper age to start the experiment.

In chapter seven it was questioned whether bone changes in the metaphysis would be the best predictor of the effects of drug treatment in humans, in whom the growth plate closes after adolescence. The neighboring epiphysis, which does not undergo linear bone growth, may offer a more suited translational site to analyze these effects. Therefore, it may be useful to analyze effects of drug treatment in both locations to determine whether these are similar or not.

9.4.3 Mechanical testing

Static testing

Three different static mechanical tests were employed in this dissertation. Static compression tests on the proximal tibia and on the vertebral body, and three-point bending tests were conducted. These tests are relatively easy and fast to conduct and provide an estimate of bone strength. Variance on these tests however is quite high due to different kinds of systematic and random errors (166;271), such as not perfectly aligned test platens, not perfectly parallel top and bottom of specimens (in vertebral compression), overestimation of strain due to compliance of the mechanical system. This makes it more difficult to detect significant differences between groups. Although they are relatively easy to conduct, it requires some hands-on experience and precision to reduce errors and maximize reproducibility.

Fatigue testing

As vertebral fractures in patients with postmenopausal osteoporosis are often the result of sustained cyclic loading due to locomotion, it is clinically relevant to assess fatigue compressive properties in addition to static compressive properties. Interestingly, this is not a common procedure in testing of pharmaceutical agents as yet.

In fact, rat bone fatigue behavior has, to the author's knowledge, not been determined at all, while the ovariectomized rat model is recommended by FDA guidelines for testing of new pharmaceutical agents. Therefore, we developed a new method to test fatigue behavior of rat vertebral bone. Although mostly either trabecular cores or cortical bone samples are tested, we tested the whole vertebral body, hereby more closely resembling actual loading conditions and incorporating the integral function of cortical and trabecular bone, which is one of the strengths of the test. In our protocol, a constant loading cycle was applied, while all samples started at the same apparent strain. As stiffness varied per sample, the maximum load corresponding to this apparent strain varied as well and was determined prior to testing. Any intrinsic variance in bone mass and stiffness was hereby accounted for. By developing this normalized fatigue test, we aimed to determine changes in fatigue properties due to differences at the tissue level, rather than at the structural level, which is another strength of the test.

As this was the first attempt to develop a method for determining fatigue behavior in the rat vertebra, there were still issues that need to be resolved or improved. Several samples did not fail in the allotted time period. This was accompanied by a decreasing strain range, which was probably due to end artefacts (89). This means that after preparation of the vertebral body, the top and bottom surfaces were not perfectly smooth. Also, variance in fatigue properties was quite large within the group, which is probably due to both biologic and experimental variance. Although this method can be used for future experiments, it is advised to further develop it and increase the number of samples per group.

Finite element analysis

Finite element analysis is a well established engineering computational method of strength prediction of complex geometries (217). Finite element models of bone have proven to increase the prediction of bone fracture over that by bone mass (59) and can serve as good replacements for actual mechanical tests. Furthermore, they have proven to provide valuable information on strength improvement after drug treatment in osteoporotic patients of clinical trials (135). Also, they can provide additional information on local stresses and strains in the bone, contributions of cortical and trabecular bone to overall strength and influence of tissue properties on strength (222;276). A drawback is that many assumptions need to be made regarding the material behavior and loading conditions, which may limit the interpretation and translational value. Also, consensus needs to be reached between the level of detail, size of modeled bone (mesh) and time needed to solve the analysis. The FEA performed in chapter three were based on a model of the metaphyseal, tibial bone and only included a linear, axial compression analysis assuming isotropic material behavior. As such, it was a simplification of reality as only part of the tibia was included, no torsion and axial loads were analyzed, which are known to be important components of tibial loading (81) and isotropic material behavior was assumed, while cortical and trabecular bone are known to behave anisotropically (173;243). Despite this, these kinds of basic analyses have shown to also have clinical applications (27;179).

9.5 Anti-resorptive versus anabolic treatments

The differences and similarities between the effects of anti-resorptive and anabolic treatments of osteoporosis is the topic of many review papers. In this dissertation both types of treatment were assessed. The effects of zoledronic acid and PTH on bone microstructure in the tibial metaphysis after development of osteopenia (recovering treatment) were analyzed in similar study designs and as such can be appropriately compared. In both studies, ovariectomies were performed to induce osteopenia. Eight weeks later, treatment was initiated when bone microstructure was still deteriorating. Zoledronic acid was only given once subcutaneously, as it has been found to suppress bone resorption rate for several months (80), while PTH needed to be given daily in subcutaneous injections.

Although the magnitude of the effects are likely to be affected by the specific drug dose, the type of response in microstructure can be compared between zoledronic acid and PTH treatment. After zoledronic acid injection, bone volume fraction was found to increase in the next four weeks, accompanied by an increasing trabecular thickness and inhibition of loss of trabeculae as evidenced by a constant trabecular number. It could not be determined whether this increase was linear in these four weeks or whether it only took place in a short amount of time, as only once per four weeks a CT-scan was made. In the following four weeks, no changes in trabecular number and thickness occurred and bone volume fraction consequently stayed constant as well. After PTH treatment was initiated, bone volume fraction as well as trabecular thickness were found to linearly increase over the next six weeks, as shown by two-weekly micro CT-scans. The loss of trabeculae was inhibited as indicated by the constant trabecular number over time. At first sight, it looks like the response to zoledronic acid and PTH is quite similar, as both treatments led to an increased bone volume fraction and trabecular thickness, and a stabilized trabecular number. However, the underlying mechanism for an increase in bone volume fraction and trabecular thickness is quite different. After zoledronic acid treatment, bone resorption was initially suppressed, while bone formation was most likely not yet. This led to a temporary positive net bone remodeling result, leading to increased bone mass and bone volume fraction. After PTH treatment, however, bone formation rate was directly increased, leading to a net increase in bone mass. This is also evidenced by the restoral of almost cleaved trabeculae (figure 7.6), which can only take place if bone formation rate is increased and not if merely resorption cavities are filled. Subsequently, if these studies were continued for a longer period of time, it is likely that bone volume fraction and trabecular thickness in ZOL treated rats would have stayed constant, while PTH treated rats would have displayed increasing bone volume fraction at least until some point in time. In normal rats that were treated with medium and high doses of PTH for two years, bone marrow space of the femoral midshaft was completely filled with bone (238), indicating that bone formation after PTH use can continue for quite some time, even far beyond natural stages.

The increase in bone volume fraction was much larger after PTH than ZOL treatment. It is probable that a lower PTH dose would have resulted in a lower increase

in bone volume fraction and trabecular thickness although the increase could have been linear as well. It is unknown whether at any dose of PTH given daily, eventually a stable state of high bone mass would be reached. The time-point at which this could be reached may depend on the drug dose and the state of bone may be far beyond natural as mentioned before (238). A lower ZOL treatment dose would have led to a shorter period of inhibition of changes in bone structure, as previously shown in a dose-related study, in which preventive ZOL treatments were analyzed over time (80). It is unknown if the initial increase in bone volume fraction and trabecular thickness found in our study is present at all doses. It is possible though that the degree of increase depends on the dose.

9.6 Clinical considerations

In the previous sections, some clinical implications and considerations have arisen and been discussed. In this section, this will be complemented with issues that have not been brought up yet.

It is currently unknown whether estrogen-deficiency and immobilization induced bone loss result in the same structural and mechanical degradation in humans or animals. Therefore, when a female patient has been found to have a low BMD, it is unknown whether the risk of fracture will be different for estrogen-deficiency or immobilization induced osteoporosis. Also, it is unknown whether the time scale on which changes take place are similar between estrogen-deficiency and immobilization induced osteoporosis or not, and therefore it is unknown whether intervention should be started at the same time-point or not. For physicians, it is thus important to be able to distinguish between estrogen-deficiency and immobilization induced osteoporosis in order to optimize the treatment potential and reduce the risk of fracture. In this dissertation, it was found that deterioration of bone microstructure in the metaphysis followed the same pattern in the first four weeks, while in the epiphysis changes in bone microstructure were more severe after immobilization. It is, however, in current clinical practice not possible to distinguish between these locations. Possibly, the use of a HR-pQCT scanner in future could enable such a comparison. Finally, we determined that after estrogen-deficiency and immobilization, mechanical properties of the metaphysis significantly decreased more in the latter while loss of bone volume fraction was the same.

Current treatments for osteoporosis reduce the risk of vertebral fractures by 40 to 70%, some also reduce the risk of non-vertebral fractures by 20 to 35% and/or hip fracture by 40 to 50% (28;227). Although highly efficacious, currently approved therapies do not entirely prevent fractures (28). Moreover, optimal antifracture efficacy may not actually be achieved in clinical practice as treatment compliance is quite low (177). Therefore, research for treatment of osteoporosis is ongoing. The idea has risen to combine an anabolic agent, which stimulates bone growth, together with a bisphosphonate that inhibits resorption and therefore in the past years, combination therapy has been the target of interest. Discontinuation of PTH treatment may result in

loss of gained bone mass (15;97;247), although in some studies a sustained effect of reduced risk of fracture was reported (168;212). Sequential treatment after PTH use with bisphosphonate could prevent loss of bone mass. Animal studies on combination therapy have shown promising results (5;220;254;255). To study combination therapy in osteoporotic patients, several concurrent and sequential studies have been conducted although in none of them fracture reduction was determined as primary endpoint. Bisphosphonates have been found to attenuate the anabolic effects of PTH (16;66;226). Negative effects on BMD have been found for concurrent use (16;66) while sequential use has proved more promising (15;226).

By using the *in vivo* method presented in this study, several combinations of different periods of PTH and sequential bisphosphonate treatment could be time and cost-efficiently studied in animals hereby providing solid data to assist in making choices for clinical studies. Also, by using image registration, local information could be obtained; e.g., it could be determined whether trabeculae, newly formed by trabecular tunneling during PTH treatment, are maintained after bisphosphonate treatment. Also, clinical studies, in which new drug therapies are tested, could be performed using HR-pQCT (high resolution peripheral quantitative computed tomography) to analyze bone microstructure in the radius and tibia, which has been shown to be highly reproducible (26;151;175), suited to determine changes in bone microstructure associated with aging (139), suited to discriminate between men and women (139) and between osteoporotic and osteopenic patients (26). Also, osteoporotic fractures have been found to be associated with microstructure (250) and finite element analyses (27;179) derived from HR-pQCT images, showing its potential advantages over DXA. Using image registration with HR-pQCT images, which has not been done before, would give the opportunity to determine local changes in bone due to for example drug treatment. It could be studied whether the bone formation after PTH use in the center of almost cleaved trabeculae seen in chapter seven of this dissertation, is also found in humans. Furthermore, the question whether bone formation after PTH use is mechanically driven or not, could be investigated.

9.7 Future work, ongoing issues and recommendations

Several possibilities enabled by the use of the *in vivo* micro-CT scanner combined with image registration have arisen during this PhD study, which unfortunately due to limitations of time, were not further explored but are interesting to elaborate on. Currently, dynamic histomorphometry is a commonly used method to determine bone turnover parameters in bone. This technique has been used and performed by Novartis, as part of a collaboration in chapter four, where the effects of early and late ZOL treatment were analyzed *in vivo* in the tibia. There are several drawbacks to this technique. Degree of resorption is based on counting of resorption pits, which only gives limited information. Also, animals need to be sacrificed in order to obtain this information and therefore, bone turnover can only be determined once at the end of the experiment, providing no information on earlier time points. In humans, it involves a

painful procedure of taking a bone biopsy from the iliac crest, which is mostly done only twice (left and right) and at this location only. Finally, it involves a tedious and time-consuming process.

After registration of a follow-up CT-scan with a previous scan, it can be seen in the images where new bone is formed and resorbed in the time between the CT-scans. This could be the basis for a new method to determine bone turnover rates in living patients or animals. Two consecutive CT-scans should be made with some time in between. A week is a suited time period as this is mostly used in dynamic histomorphometry and to ensure that not too many changes in the bone have taken place, which optimizes the quality of registration. Trabecular bone can be selected from the CT-scans, which are then registered. After registration, both images are segmented and combined in one image. By counting the number of voxels of old, new and unchanged bone, the volume percent of bone formation and resorption can be determined. As in dynamic histomorphometry no direct three-dimensional values for bone formation are determined, first a correlation study should be performed in which the steps taken during dynamic histomorphometry are directly simulated to validate the method. It has previously been shown that this is qualitatively possible by Waarsing et al. (280). Once quantitative validation of the method has also taken place, it could in future be an interesting addition to dynamic histomorphometry. This new method would have several advantages: 1) it can be done *in vivo* 2) it can be done at any time point 3) bone resorption can be determined in addition to bone formation 4) less time is needed as many steps can be automated.

A first attempt was made to develop such an *in vivo* method to determine bone turnover rates, which was not published previously. Ovariectomized rats, early treated with ZOL, and SHAM rats of the follow-up study in the tibia described in chapter four, were found to have similar structural parameters over the course of the experiment. Trabecular bone of the metaphysis of CT-scans of all rats of these two groups, taken at week 0 and 16 was registered (figure 9.2). Then volume percent bone resorption and formation was calculated. It was found that the average percent bone formation was 18 and 22% for ZOL treated and SHAM rats respectively, which was not significantly different. Average percent bone resorption was 35 and 48% for ZOL treated and SHAM rats respectively, which was significantly different. Although this method was not fully optimized and validated yet and the values are a first estimate, the fact that bone formation and resorption were lower in ZOL treated rats agrees with the dynamic histomorphometry data (figure 4.5). This method could in future be further optimized to serve as a useful addition to dynamic histomorphometry.

In chapter seven, it was found that during PTH treatment, bone was directly deposited where most beneficial, hereby restoring the structure and probably increasing strength already after two weeks. We suggested that as strains and stresses would be highest there where only a thin line of bone was present, PTH-induced bone formation is, at least in part, mechanically driven. This agrees with results from two finite element studies on CT-scans of osteoporotic patients treated with teriparatide (87;135), where bone formation appeared to be mechanically driven. Also, it has been found that physiological levels of PTH are needed for the mechanical responsiveness of bone in a

mechanical stimulation study in rats (46). This is, however, in contrast with data from several studies, in which immobilized rats were treated with PTH, after which no response should be expected if the effects of PTH were indeed mechanically driven. Trabecular bone loss was, however, found to be completely inhibited by PTH treatment in neurectomized and tail suspended rats and cortical bone loss was attenuated in the former, but not in the latter (186). In a dose-response study in hindlimb unloaded rats, high doses of PTH increased bone formation rates and trabecular thickness to values that exceeded normal values and a therapeutic dose prevented the decrease in bone formation and trabecular thinning (269). In contrast, in other studies in rats treated with PTH, immobilization attenuated the anabolic effects of PTH on trabecular bone and largely prevented them in cortical bone (266). Also, a reduced response to PTH treatment of ovariectomized rats was found in the skull and caudal vertebra, sites known to have reduced loading (143;162). Taken together, it remains unclear whether the anabolic response to PTH is mechanically driven or not. Perhaps, intermittent PTH always leads to bone formation, but becomes more pronounced and mechanically driven, i.e. directed to locations of high strains, when the bone is loaded. More research will need to be done to elucidate this. Currently, PTH is not approved for the treatment of immobilization osteoporosis in patients. It would be interesting to further investigate the role of mechanical loading in the effects of PTH to determine whether it could serve as a potential treatment for immobilized patients.

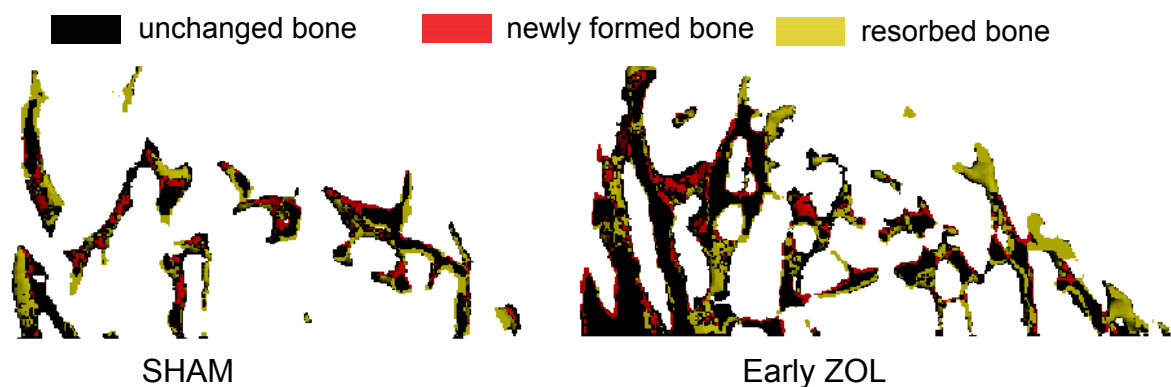


Figure 9.2: *Overlaid registered longitudinal cross sections of trabecular bone in the metaphysis of a SHAM (left) and an OVX rat early treated with ZOL (right) scanned at week 0 and week 16. Unchanged, newly formed and resorbed bone can be seen in both images.*

In chapter three, the effects of neurectomy on bone microstructure were determined over time. It would be interesting to determine the temporal and spatial effects of remobilization over time *in vivo* as well. In several cross-sectional studies the effects of remobilization in rats have been determined. It has mostly been found that remobilization does not lead to full recovery of the bone (115;124;131;261;262), although the severity of alterations most likely depend on the duration of immobilization. It has also been found that remobilization accompanied by physical exercise or PTH treatment increases the degree of recovery (25;115;124;131;299). It

would be interesting to use the developed *in vivo* method from this dissertation to study the influence of different durations of immobilization on the degree of recovery. Also, the duration of recovery of the bone would be interesting to follow over time and to determine whether the recovery is linear over time or gradually wanes. Furthermore, as it is possible to determine changes within a rat, recovery of individual rats and variance therein could be monitored. Finally, it can be studied whether locations of new bone formation coincide with locations of previous bone resorption.

In chapter seven, the effects of six weeks of PTH treatment of ovariectomized rats were studied. At the end of the experiment, bone volume fraction and trabecular thickness in the metaphysis were still increasing, and in the epiphysis trabecular number was increasing as well. Also, cortical thickness was increasing linearly as well. It would be interesting to study longer periods of PTH treatment as well as different starting points of treatment after ovariectomy. For each starting point of treatment, the duration of PTH treatment needed to return to the original bone microstructure as closely as possible, could be determined. The use of an *in vivo* micro-CT scanner enables these types of experiments. Although zoledronic acid treatment of osteopenic rats cannot lead to full restoral of bone microstructure, similar studies could be performed in which the influence of different starting points of treatment on final bone microstructure would be explored.

Currently, in animal testing of drugs for postmenopausal osteoporosis, merely static mechanical tests are performed on the vertebra or femur. However, as vertebral fractures in patients with postmenopausal osteoporosis are often the result of sustained cyclic loading due to locomotion, it is clinically relevant to assess fatigue, compressive properties in addition to static, compressive properties in rats. A method was developed in chapter six to determine fatigue, compressive properties in the rat vertebra. This method needs to be further validated, standardized and optimized, but would be very interesting to incorporate in the procedure of testing new drugs for osteoporosis. Providing information on effects of new drugs on fatigue, compressive properties may better predict their effectiveness in osteoporotic patients, which could reduce costs in the clinical phase of osteoporosis research.

Finally, in chapter three, we determined that after estrogen-deficiency and immobilization, mechanical properties of the metaphysis significantly decreased more in the latter while loss of bone volume fraction was the same. We hypothesized that this was due to the general lack of mechanical adaptation resulting from strongly decreased mechanical loading after immobilization. It would also be interesting to determine locally if low strain areas are indeed resorbed, as stated in Frost's mechanostat. This could be done by registering follow-up scans and determining the bone that has been resorbed in between the scans. By running a FEA on the first CT-scan, strain in the whole bone could be determined. Then the average strain in the resorbed area would be compared with the average strain of the whole bone to determine whether strain is indeed relatively low there. In a finite element study on the proximal tibia of a rat, the relationship between local strains and bone resorption was analyzed, and was however found not to be significant (282).

9.8 Conclusions

In mature, female rats, we have determined that:

- Eight weekly *in vivo* micro-CT scans did not lead to detectable radiation damage in the proximal tibia.
- Deterioration of bone structure was larger in the tibial meta- than epiphysis after immobilization and estrogen-deficiency.
- Immobilization and estrogen-deficiency induced osteoporosis were characterized by the same degree of bone loss in the metaphysis of the proximal tibia, while the epiphysis was affected more after immobilization.
- Our hypothesis that, at the same level of bone loss, immobilization leads to less favorable mechanical properties than estrogen-deficiency, was confirmed by our data.
- A single injection of zoledronic acid before ovariectomy fully inhibited deterioration of bone microstructure and strength in the tibia for sixteen weeks.
- A single injection of zoledronic acid after eight weeks of osteopenic development significantly improved bone microstructure and inhibited reduction in strength in the tibia for eight weeks.
- A single injection of zoledronic acid before and eight weeks after ovariectomy inhibited deterioration of bone microstructure and mechanical properties of the vertebra.
- Rat vertebrae exhibited typical fatigue behavior.
- Vertebral fatigue compressive properties of control rats were similar to those of ZOL treated, ovariectomized rats in a small cohort of rats.
- PTH treatment of ovariectomized rats led to a linear increase in bone volume fraction and trabecular thickness in the tibial metaphysis during six weeks.
- PTH treatment of ovariectomized rats led to a linear increase in bone volume fraction, trabecular number and trabecular thickness in the tibial epiphysis during six weeks.
- Six weeks of PTH treatment of ovariectomized rats led to a linear increase in cortical thickness, constant mineralization values in the cortex and an increased bending stiffness in the tibia.
- PTH induced bone formation was sometimes found to be located in the waisted center of almost fully cleaved trabeculae, hereby restoring them, suggesting that its effect is mechanically driven.
- Bone volume fraction before ovariectomy was correlated with bone volume fraction after PTH treatment of ovariectomized rats.
- No effects of six weeks of vibration treatment were found on tibial bone of ovariectomized rats.

In this dissertation, several scientific contributions have been made to the understanding of bone remodeling in osteoporosis and its treatment, by using an *in vivo* micro-CT scanner combined with image registration. At the same degree of bone loss, reductions in mechanical properties were found to be greater after immobilization than estrogen-deficiency induced osteoporosis due to optimization of bone structure. This finding supports the mechanostat theory of bone remodeling and demonstrates the importance of mechanical loading to bone functionality. Furthermore, it demonstrates that mechanisms of osteoporotic diseases are important in understanding the different effects on fracture risk in patients. Comparison of different treatments for osteoporosis demonstrated their particular interactions with the process of bone remodeling. The anti-resorptive effect of zoledronic acid on bone structure was found to be dependent on the time-point of initiating treatment, and led to a temporary and limited increase in bone mass. In contrast, anabolic PTH led to linear increases in bone mass over time, without limit within the time frame studied. Our findings also suggest that effects of PTH on structure and strength may vary throughout the body and that bone formation with PTH treatment is mechanically modulated. Finally, the absence of effect on bone by vibration further adds to the controversy of this treatment strategy and demonstrates the limited understanding on the basic science level of this intriguing physical effect on bone remodeling.

Appendix

It would be interesting to know whether bone volume fraction in one anatomical site is predictive of bone volume fraction in another one and therefore to know whether if a rat or a human has a high bone volume fraction in one anatomical site, this can be extrapolated to other sites. In chapter five, we found that bone volume fraction in the tibia and L3 vertebra were moderately correlated with each other. Also, it is clinically relevant to be able to predict what the response to a drug would be based on the initial bone volume fraction. In chapter seven, we showed that bone volume fraction before osteopenia was highly predictive of bone volume fraction after PTH treatment of osteopenic rats. Finally, it is currently unknown what determines the degree of bone loss after ovariectomy; possibly, bone volume fraction before ovariectomy determines the degree of bone loss. As in chapter seven and eight bone structure in the meta- and epiphysis were determined over time, we had data available to study the aforementioned relationships. In table 9.1 pearson correlates are shown for several relationships.

Table 9.1: *Linear correlation between bone volume fraction of the epiphysis and metaphysis, and between bone volume fraction before and after ovariectomy.*

Predictive variable	Outcome variable	Rat groups	R ²	Slope
BV/TV week 0 metaphysis	BV/TV week 0 epiphysis	PTH, vibration, OVX, SHAM	0.64	0.36
BV/TV week 0 metaphysis	BV/TV week 8 metaphysis	PTH, vibration, OVX	0.48	0.51
BV/TV week 0 metaphysis	Δ BV/TV week 0-8 metaphysis	PTH, vibration, OVX	0.46	0.49
BV/TV week 0 metaphysis	% Δ BV/TV week 0-8 metaphysis	PTH, vibration, OVX	n.s.	-
BV/TV week 0 epiphysis	Δ BV/TV week 8 epiphysis	PTH, vibration, OVX	0.63	0.92
BV/TV week 0 epiphysis	Δ BV/TV week 0-8 epiphysis	PTH, vibration, OVX	n.s.	-
BV/TV week 0 epiphysis	% Δ BV/TV week 0-8 epiphysis	PTH, vibration, OVX	n.s.	-

A strong, positive linear correlation was found between bone volume fraction in the epiphysis and metaphysis, indicating that when a rat has a relatively high bone volume fraction in the metaphysis, it will also have that in the epiphysis. In the meta- and epiphysis, bone volume fraction before ovariectomy was found to positively correlate most strongly with bone volume fraction eight weeks after ovariectomy. In the metaphysis, bone volume fraction before ovariectomy also correlated with the decrease

in bone volume fraction over eight weeks. This indicates that the higher the bone volume fraction before ovariectomy, the greater the loss.

References

1. Aerssens J, van Audekercke R, Talalaj M, Geusens P, Bramm E, Dequeker J 1996 Effect of 1alpha-vitamin D3 and estrogen therapy on cortical bone mechanical properties in the ovariectomized rat model. *Endocrinology* **137**:1358-1364.
2. Allen MR, Burr DB 2007 Three years of alendronate treatment results in similar levels of vertebral microdamage as after one year of treatment. *J Bone Miner Res* **22**:1759-1765.
3. Allen MR, Iwata K, Phipps R, Burr DB 2006 Alterations in canine vertebral bone turnover, microdamage accumulation, and biomechanical properties following 1-year treatment with clinical treatment doses of risedronate or alendronate. *Bone* **39**:872-879.
4. Allport J 2008 Incidence and prevalence of medication-induced osteoporosis: evidence-based review. *Curr Opin Rheumatol* **20**:435-441.
5. Arends RJ, Chan HN, Van de Klundert TMC, Van Oudheusden H, Langerwerf PEJ, Van Beuningen-de Vaan MJA, Ederveen AG 2005 High dose of bisphosphonate enhances the effect of pth on trabecular bone in ovariectomized rats. in proceedings of 2nd joint meeting of ECTS/IBMS, Geneva, p. P045-Tu.
6. Arlot M, Meunier PJ, Boivin G, Haddock L, Tamayo J, Correa-Rotter R, Jasqui S, Donley DW, Dalsky GP, Martin JS, Eriksen EF 2005 Differential effects of teriparatide and alendronate on bone remodeling in postmenopausal women assessed by histomorphometric parameters. *J Bone Miner Res* **20**:1244-1253.
7. Bagi CM, Miller SC 1994 Comparison of osteopenic changes in cancellous bone induced by ovariectomy and/or immobilization in adult rats. *Anat Rec* **239**:243-254.
8. Baldock PA, Need AG, Moore RJ, Durbridge TC, Morris HA 1999 Discordance between bone turnover and bone loss: effects of aging and ovariectomy in the rat. *J Bone Miner Res* **14**:1442-1448.
9. Baumann BD, Wronski TJ 1995 Response of cortical bone to antiresorptive agents and parathyroid hormone in aged ovariectomized rats. *Bone* **16**:247-253.
10. Bauss F, Dempster DW 2007 Effects of ibandronate on bone quality: Preclinical studies. *Bone* **40**:265-273.
11. Benhamou CL 2007 Effects of osteoporosis medications on bone quality. *Joint Bone Spine* **74**:39-47.
12. Bernstein L, Pike MC, Ross RK, Judd HL, Brown JB, Henderson BE 1985 Estrogen and sex hormone-binding globulin levels in nulliparous and parous women. *J Natl Cancer Inst* **74**:741-745.

13. Binkley N, Kimmel D, Bruner J, Haffa A, Davidowitz B, Meng C, Schaffer V, Green J 1998 Zoledronate prevents the development of absolute osteopenia following ovariectomy in adult rhesus monkeys. *J Bone Miner Res* **13**:1775-1782.
14. Bisgard JD, Hunt HB 1936 Influence of roentgen rays and radium on epiphyseal growth of long bones. *Radiology* **26**:56-68.
15. Black DM, Bilezikian JP, Ensrud KE, Greenspan SL, Palermo L, Hue T, Lang TF, McGowan JA, Rosen CJ 2005 One year of alendronate after one year of parathyroid hormone (1-84) for osteoporosis. *N Engl J Med* **353**:555-565.
16. Black DM, Greenspan SL, Ensrud KE, Palermo L, McGowan JA, Lang TF, Garnero P, Bouxsein ML, Bilezikian JP, Rosen CJ 2003 The effects of parathyroid hormone and alendronate alone or in combination in postmenopausal osteoporosis. *N Engl J Med* **349**:1207-1215.
17. Black DM, Delmas PD, Eastell R, Reid IR, Boonen S, Cauley JA, Cosman F, Lakatos P, Leung PC, Man Z, Mautalen C, Mesenbrink P, Hu H, Caminis J, Tong K, Rosario-Jansen T, Krasnow J, Hue TF, Sellmeyer D, Eriksen EF, Cummings SR, HORIZON Pivotal FT 2007 Once-yearly zoledronic acid for treatment of postmenopausal osteoporosis. *N Engl J Med* **356**:1809-1822.
18. Boivin G, Arlot M, Trechsel U, Meunier PJ 2003 Effects of intravenous zoledronic acid on the degree of mineralization of bone in post-menopausal osteoporosis: a quantitative microradiographic analysis of transiliac biopsies after one year. *J Bone Miner Res* **2(Suppl)**:S261.
19. Boivin G, Meunier PJ 2002 The degree of mineralization of bone tissue measured by computerized quantitative contact microradiography. *Calcif Tissue Int* **70**:503-511.
20. Boonen S 2007 Bisphosphonate efficacy and clinical trials for postmenopausal osteoporosis: Similarities and differences. *Bone* **40**:S26-S31.
21. Borah B, Dufresne TE, Ritman EL, Jorgensen SM, Liu S, Chmielewski PA, Phipps RJ, Zhou X, Sibonga JD, Turner RT 2006 Long-term risedronate treatment normalizes mineralization and continues to preserve trabecular architecture: sequential triple biopsy studies with micro-computed tomography. *Bone* **39**:345-352.
22. Borah B, Dufresne TE, Chmielewski PA, Johnson TD, Chines A, Manhart MD 2004 Risedronate preserves bone architecture in postmenopausal women with osteoporosis as measured by three-dimensional microcomputed tomography. *Bone* **34**:736-746.
23. Boskey AL 2001 Bone mineralization. In: Cowin SC (ed.) *Bone Mechanics Handbook*, second ed. CRC Press, pp. 1-33.
24. Bourrin S, Ammann P, Bonjour JP, Rizzoli R 2002 Recovery of proximal tibia bone mineral density and strength, but not cancellous bone architecture, after long-term bisphosphonate or selective estrogen receptor modulator therapy in aged rats. *Bone* **30**:195-200.
25. Bourrin S, Palle S, Genty C, Alexandre C 1995 Physical exercise during remobilization restores a normal bone trabecular network after tail suspension-induced osteopenia in young rats. *J Bone Miner Res* **10**:820-828.

26. Boutroy S, Bouxsein ML, Munoz F, Delmas PD 2005 In vivo assessment of trabecular bone microarchitecture by high-resolution peripheral quantitative computed tomography. *J Clin Endocrinol Metab* **90**:6508-6515.
27. Boutroy S, van RB, Sornay-Rendu E, Munoz F, Bouxsein ML, Delmas PD 2008 Finite element analysis based on in vivo HR-pQCT images of the distal radius is associated with wrist fracture in postmenopausal women. *J Bone Miner Res* **23**:392-399.
28. Bouxsein M, Delmas P 2008 Considerations for Development of Surrogate Endpoints for Anti-Fracture Efficacy of New Treatments in Osteoporosis: A Perspective. *J Bone Miner Res*.
29. Bowman SM, Guo XE, Cheng DW, Keaveny TM, Gibson LJ, Hayes WC, McMahon TA 1998 Creep contributes to the fatigue behavior of bovine trabecular bone. *J Biomech Eng* **120**:647-654.
30. Bowman SM, Keaveny TM, Gibson LJ, Hayes WC, McMahon TA 1994 Compressive creep behavior of bovine trabecular bone. *J Biomech* **27**:301-305.
31. Boyce RW, Paddock CL, Franks AF, Jankowsky ML, Eriksen EF 1996 Effects of intermittent hPTH (1-34) alone and in combination with 1,25(OH)₂D₃ or risedronate on endosteal bone remodeling in canine cancellous and cortical bone. *J Bone Miner Res* **11**:600-611.
32. Boyd SK, Davison P, Muller R, Gasser JA 2006 Monitoring individual morphological changes over time in ovariectomized rats by in vivo micro-computed tomography. *Bone* **39**:854-862.
33. Brouwers JEM, Lambers JM, Gasser JA, van Rietbergen B, Huiskes R 2008 Bone degeneration and recovery after early and late bisphosphonate treatment of ovariectomized wistar rats assessed by in vivo micro-computed tomography. *Calcif Tissue Int* **82**:202-211.
34. Brouwers JEM, Rietbergen Bv, Bouxsein ML 2008 Influence of early and late zoledronic acid administration on vertebral structure and strength in ovariectomized rats. *Calcif Tissue Int* **83**:186-191.
35. Brouwers JEM, Rietbergen Bv, Huiskes R, Ito M 2008 Effects of PTH treatment on tibial bone of ovariectomized rats assessed by *in vivo* micro-CT. *Osteoporos Int* **submitted**.
36. Brouwers JEM, van Rietbergen B, Huiskes R 2007 No effects of in vivo micro-CT radiation on structural parameters and bone marrow cells in proximal tibia of wistar rats detected after eight weekly scans. *J Orthop Res* **25**:1325-1332.
37. Burr DB 2005 Does early PTH treatment compromise bone strength? The balance between remodeling, porosity, bone mineral, and bone size. *Curr Osteoporos Rep* **3**:19-24.
38. Burr DB, Miller L, Grynblas M, Li J, Boyde A, Mashiba T, Hirano T, Johnston CC 2003 Tissue mineralization is increased following 1-year treatment with high doses of bisphosphonates in dogs. *Bone* **33**:960-969.
39. Bushberg JT, Seibert JA, Leidholdt EM, Boone JM 1994 *The essential physics of medical imaging*, first ed. Williams & Wilkins, Baltimore.
40. Caler WE, Carter DR 1989 Bone creep-fatigue damage accumulation. *J Biomech* **22**:625-635.
41. Campbell GM, Buie HR, Boyd SK 2008 Signs of irreversible architectural changes occur early in the development of experimental osteoporosis as assessed by in vivo micro-CT. *Osteoporos Int*.

42. Carter DR, Caler WE, Spengler DM, Frankel VH 1981 Uniaxial fatigue of human cortical bone. The influence of tissue physical characteristics. *J Biomech* **14**:461-470.
43. Cavolina JM, Evans GL, Harris SA, Zhang M, Westerlind KC, Turner RT 1997 The effects of orbital spaceflight on bone histomorphometry and messenger ribonucleic acid levels for bone matrix proteins and skeletal signaling peptides in ovariectomized growing rats. *Endocrinology* **138**:1567-1576.
44. Chapurlat RD, Arlot M, Burt-Pichat B, Chavassieux P, Roux JP, Portero-Muzy N, Delmas PD 2007 Microcrack frequency and bone remodeling in postmenopausal osteoporotic women on long-term bisphosphonates: a bone biopsy study. *J Bone Miner Res* **22**:1502-1509.
45. Cheng XG, Nicholson PH, Lowet G, Boonen S, Sun Y, Ruegsegger P, Muller R, Dequeker J 1997 Prevalence of trabecular microcallus formation in the vertebral body and the femoral neck. *Calcif Tissue Int* **60**:479-484.
46. Chow JW, Fox S, Jagger CJ, Chambers TJ 1998 Role for parathyroid hormone in mechanical responsiveness of rat bone. *Am J Physiol* **274**:E146-E154.
47. Compston JE 2007 Skeletal actions of intermittent parathyroid hormone: Effects on bone remodelling and structure. *Bone* **40**:1447-1452.
48. Cory E, Patel N, Nazarian A, Snyder B, Bouxsein ML, Fajardo R 2007 Effect of surrounding tissue on density evaluation via microcomputed tomography. in proceedings of the 32th annual meeting of the ORS, San Diego, CA.
49. Cowin SC, Weinbaum S, Zeng Y 1995 A case for bone canaliculi as the anatomical site of strain generated potentials. *J Biomech* **28**:1281-1297.
50. Cui W, Shi Z, Fu H, Zheng Q, Qiu L 1997 Comparison of changes of bone mass, parathyroid hormone and calcitonin between two animal models of bone loss. *Zhongguo Ying Yong Sheng Li Xue Za Zhi* **13**:5-8.
51. Cullen DM, Smith RT, Akhter MP 2001 Bone-loading response varies with strain magnitude and cycle number. *J Appl Physiol* **91**:1971-1976.
52. Danielsen CC, Mosekilde L, Svenstrup B 1993 Cortical bone mass, composition, and mechanical properties in female rats in relation to age, long-term ovariectomy, and estrogen substitution. *Calcif Tissue Int* **52**:26-33.
53. Dare A, Hachisu R, Yamaguchi A, Yokose S, Yoshiki S, Okano T 1997 Effects of ionizing radiation on proliferation and differentiation of osteoblast-like cells. *J Dent Res* **76**:658-664.
54. David V, Laroche N, Boudignon B, Lafage-Proust MH, Alexandre C, Ruegsegger P, Vico L 2003 Noninvasive in vivo monitoring of bone architecture alterations in hindlimb-unloaded female rats using novel three-dimensional microcomputed tomography. *J Bone Miner Res* **18**:1622-1631.
55. Dawson AB 1925 The age order of epiphyseal union in the long bones of the albino rat. *Anat Rec* **31**:1-17.
56. Day CJ, Kim MS, Stephens SRJ, Simcock WE, Aitken CJ, Nicholson GC, Morrison NA 2004 Gene array identification of osteoclast genes: differential inhibition of osteoclastogenesis by cyclosporin A and granulocyte macrophage colony stimulating factor. *J Cell Biochem* **91**:303-315.

57. Dempster DW, Birchman R, Xu R, Lindsay R, Shen V 1995 Temporal changes in cancellous bone structure of rats immediately after ovariectomy. *Bone* **16**:157-161.
58. Dempster DW, Cosman F, Kurland ES, Zhou H, Nieves J, Woelfert L, Shane E, Plavetic K, Muller R, Bilezikian J, Lindsay R 2001 Effects of daily treatment with parathyroid hormone on bone microarchitecture and turnover in patients with osteoporosis: a paired biopsy study. *J Bone Miner Res* **16**:1846-1853.
59. Eckstein F, Kuhn V, Lochmuller EM 2004 Strength prediction of the distal radius by bone densitometry--evaluation using biomechanical tests. *Ann Biomed Eng* **32**:487-503.
60. Ejersted C, Andreassen TT, Hauge E-M, Melsen F, Oxlund H 1995 Parathyroid hormone (1-34) increases vertebral bone mass, compressive strength, and quality in old rats. *Bone* **17**:507-511.
61. Engstrom H 1987 Effects of irradiation on growing bones. *Swed Dent J Suppl* **45**:1-47.
62. Engstrom H, Jansson JO, Engstrom C 1983 Effect of local irradiation on longitudinal bone growth in the rat. A tetracycline labelling investigation. *Acta Radiol Oncol* **22**:129-133.
63. Fajardo R, Cory E, Patel N, Nazarian A, Snyder B, Bouxsein ML 2007 Specimen size and porosity can introduce error into micro-ct-based tissue mineral density measurements. in proceedings of the 32th annual meeting of the ORS, San Diego, CA.
64. Fazzalari NL, Forwood MR, Smith K, Manthey BA, Herreen P 1998 Assessment of cancellous bone quality in severe osteoarthritis: bone mineral density, mechanics, and microdamage. *Bone* **22**:381-388.
65. Field A 2005 Repeated-measures designs (GLM 4). In: Wright DB (ed.) *Discovering statistics using SPSS*, 2 ed. SAGE publications, pp. 427-482.
66. Finkelstein JS, Hayes A, Hunzelman JL, Wyland JJ, Lee H, Neer RM 2003 The effects of parathyroid hormone, alendronate, or both in men with osteoporosis. *N Engl J Med* **349**:1216-1226.
67. Fleisch H 2003 Bisphosphonates in osteoporosis. *Eur Spine J* **12 Suppl 2**:S142-S146.
68. Flieger J, Karachalios T, Khaldi L, Raptou P, Lyritis G 1998 Mechanical stimulation in the form of vibration prevents postmenopausal bone loss in ovariectomized rats. *Calcif Tissue Int* **63**:510-514.
69. Fox J, Miller MA, Newman MK, Metcalfe AF, Turner CH, Recker RR, Smith SY 2007 Daily treatment of aged ovariectomized rats with human parathyroid hormone (1-84) for 12 months reverses bone loss and enhances trabecular and cortical bone strength. *Bone* **41**:321-330.
70. Fox J, Miller MA, Newman MK, Turner CH, Recker RR, Smith SY 2007 Treatment of skeletally mature ovariectomized rhesus monkeys with PTH(1-84) for 16 months increases bone formation and density and improves trabecular architecture and biomechanical properties at the lumbar spine. *J Bone Miner Res* **22**:260-273.
71. Fratzl P, Roschger P, Fratzl-Zelman N, Paschalis EP, Phipps R, Klaushofer K 2007 Evidence that treatment with risedronate in women with postmenopausal osteoporosis affects bone mineralization and bone volume. *Calcif Tissue Int* **81**:73-80.

72. Freeman MA, Todd RC, Pirie CJ 1974 The role of fatigue in the pathogenesis of senile femoral neck fractures. *J Bone Joint Surg Br* **56-B**:698-702.
73. Fritton SP, McLeod KJ, Rubin CT 2000 Quantifying the strain history of bone: spatial uniformity and self-similarity of low-magnitude strains. *J Biomech* **33**:317-325.
74. Frost HM 1987 The mechanostat: a proposed pathogenic mechanism of osteoporoses and the bone mass effects of mechanical and nonmechanical agents. *Bone Miner* **2**:73-85.
75. Garman R, Gaudette G, Donahue LR, Rubin CT, Judex S 2007 Low-level accelerations applied in the absence of weight bearing can enhance trabecular bone formation. *J Orthop Res* **25**:732-740.
76. Gasser JA 1995 Assessing bone quantity by pQCT. *Bone* **17**:S145-S154.
77. Gasser JA 1997 Quantitative assessment of bone mass and geometry by pQCT in rats in vivo and site specificity of changes at different skeletal sites. *J Jpn Soc Bone Morphometry* **7**:107-114.
78. Gasser JA 2006 The relative merits of anabolics versus anti-resorptive compounds: where our targets should be, and whether we are addressing them. *Curr Opin Pharmacol* **6**:313-318.
79. Gasser JA, Green JR, Shen V, Ingold P, Rebmann A, Bhatnagar AS, Evans DB 2006 A single intravenous administration of zoledronic acid prevents the bone loss and mechanical compromise induced by aromatase inhibition in rats. *Bone* **39**:787-795.
80. Gasser JA, Ingold P, Venturiere A, Shen V, Green JR 2008 Long-Term Protective Effects of Zoledronic Acid on Cancellous and Cortical Bone in the Ovariectomized Rat. *Journal of Bone and Mineral Research* **23**:544-551.
81. Gautier E, Perren SM, Cordey J 2000 Strain distribution in plated and unplated sheep tibia an in vivo experiment. *Injury* **31 Suppl 3**:C37-C44.
82. Geusens P, Reid D 2005 Newer drug treatments: their effects on fracture prevention. *Best Pract Res Clin Rheumatol* **19**:983-989.
83. Giavaresi G, Fini M, Gnudi S, Nicoli Aldini N, Rocca M, Carpi A, Giardino R 2001 Comparison of calcitonin, alendronate and fluorophosphate effects on ovariectomized rat bone. *Biomed Pharmacother* **55**:397-403.
84. Gilsanz V, Wren TAL, Sanchez M, Dorey F, Judex S, Rubin C 2006 Low-level, high-frequency mechanical signals enhance musculoskeletal development of young women with low BMD. *J Bone Miner Res* **21**:1464-1474.
85. Glatt M 2001 The bisphosphonate zoledronate prevents vertebral bone loss in mature estrogen-deficient rats as assessed by micro-computed tomography. *Eur Cell Mater* **1**:18-26.
86. Glatt M, Pataki A, Evans GP, Hornby SB, Green JR 2004 Loss of vertebral bone and mechanical strength in estrogen-deficient rats is prevented by long-term administration of zoledronic acid. *Osteoporos Int* **15**:707-715.
87. Graeff C, Zysset PK, Marin F, Gluer CC 2007 Bone apposition in patients on Teriparatide treatment is preferably directed to skeletal regions of local structural weakness: Assessment by high resolution CT based finite element analysis in vivo. in proceedings of the 29th annual meeting of the ASBMR, Honolulu, HI.

88. Greiner S, Kadow-Romacker A, Wildemann B, Schwabe P, Schmidmaier G 2007 Bisphosphonates incorporated in a poly(D,L-lactide) implant coating inhibit osteoclast like cells in vitro. *J Biomed Mater Res A* **83**:1184-1191.
89. Guo XE, Gibson LJ, McMahon TA 1993 Fatigue of trabecular bone: avoiding end-crushing artifacts. *Trans 39th Orthopaedic Research Society* **18**:584.
90. Guo XE, Kim CH 2002 Mechanical consequence of trabecular bone loss and its treatment: a three-dimensional model simulation. *Bone* **30**:404-411.
91. Haddock SM, Yeh OC, Mummaneni PV, Rosenberg WS, Keaveny TM 2004 Similarity in the fatigue behavior of trabecular bone across site and species. *J Biomech* **37**:181-187.
92. Han Y, Cowin SC, Schaffler MB, Weinbaum S 2004 Mechanotransduction and strain amplification in osteocyte cell processes. *Proc Natl Acad Sci U S A* **101**:16689-16694.
93. Hara K, Kobayashi M, Akiyama Y 2007 Influence of bone osteocalcin levels on bone loss induced by ovariectomy in rats. *J Bone Miner Metab* **25**:345-353.
94. Herrak P, Gortz B, Hayer S, Redlich K, Reiter E, Gasser J, Bergmeister H, Kollias G, Smolen JS, Schett G 2004 Zoledronic acid protects against local and systemic bone loss in tumor necrosis factor-mediated arthritis. *Arthritis Rheum* **50**:2327-2337.
95. Hildebrand T, Ruegsegger P 1997 A new method for the model-independent assessment of thickness in three-dimensional images. *J Microsc* **185**:67-75.
96. Hildebrand T, Ruegsegger P 1997 Quantification of Bone Microarchitecture with the Structure Model Index. *Comput Methods Biomech Biomed Engin* **1**:15-23.
97. Hodsmans AB, Fraher LJ, Adachi JD 1995 A clinical trial of cyclical clodronate as maintenance therapy following withdrawal of parathyroid hormone, in the treatment of postmenopausal osteoporosis. *J Bone Miner Res* **10(Suppl 1)**:S175.
98. Hodsmans AB, Fraher LJ, Watson PH, Ostbye T, Stitt LW, Chi JD, Taves DH, Drost D 1997 A randomized controlled trial to compare the efficacy of cyclical parathyroid hormone versus cyclical parathyroid hormone and sequential calcitonin to improve bone mass in postmenopausal women with osteoporosis. *J Clin Endocrinol Metab* **82**:620-628.
99. Hodsmans AB, Steer B.M., Fraher LJ, Drost DJ 1991 Bone densitometric and histomorphometric responses to sequential human parathyroid hormone (1-38) and salmon calcitonin in osteoporotic patients. *Bone Miner* **14**:67-83.
100. Hogan HA, Ruhmann SP, Sampson HW 2000 The mechanical properties of cancellous bone in the proximal tibia of ovariectomized rats. *J Bone Miner Res* **15**:284-292.
101. Homminga J, Van-Rietbergen B, Lochmuller EM, Weinans H, Eckstein F, Huiskes R 2004 The osteoporotic vertebral structure is well adapted to the loads of daily life, but not to infrequent "error" loads. *Bone* **34**:510-516.
102. Hordon LD, Itoda M, Shore PA, Shore RC, Heald M, Brown M, Kanis JA, Rodan GA, Aaron JE 2006 Preservation of thoracic spine microarchitecture by alendronate: Comparison of histology and microCT. *Bone* **38**:444-449.
103. Hornby SB, Evans GP, Hornby SL, Pataki A, Glatt M, Green JR 2003 Long-term zoledronic acid treatment increases bone structure and mechanical strength of long bones of ovariectomized adult rats. *Calcif Tissue Int* **72**:519-527.

104. Horwitz M, Stewart A, Greenspan SL 2000 Sequential parathyroid hormone/alendronate therapy for osteoporosis--robbing Peter to pay Paul? *J Clin Endocrinol Metab* **85**:2127-2128.
105. Iida-Klein A, Lu SS, Cosman F, Lindsay R, Dempster DW 2007 Effects of cyclic vs. daily treatment with human parathyroid hormone (1-34) on murine bone structure and cellular activity. *Bone* **40**:391-398.
106. Ikeda S, Tsurukami H, Ito M, Sakai A, Sakata T, Nishida S, Takeda S, Shiraishi A, Nakamura T 2001 Effect of trabecular bone contour on ultimate strength of lumbar vertebra after bilateral ovariectomy in rats. *Bone* **28**:625-633.
107. Ikeda T, Yamaguchi A, Yokose S, Nagai Y, Yamato H, Nakamura T, Tsurukami H, Tanizawa T, Yoshiki S 1996 Changes in biological activity of bone cells in ovariectomized rats revealed by in situ hybridization. *J Bone Miner Res* **11**:780-788.
108. Ito M, Nishida A, Nakamura T, Uetani M, Hayashi K 2002 Differences of three-dimensional trabecular microstructure in osteopenic rat models caused by ovariectomy and neurectomy. *Bone* **30**:594-598.
109. Ito M 2005 Assessment of bone quality using micro-computed tomography (micro-CT) and synchrotron micro-CT. *J Bone Miner Metab* **23**:115-121.
110. Iwamoto J, Takeda T, Ichimura S, Sato Y, Yeh JK 2003 Comparative effects of orchidectomy and sciatic neurectomy on cortical and cancellous bone in young growing rats. *J Bone Miner Metab* **21**:211-216.
111. Iwaniec UT, Moore K, Rivera MF, Myers SE, Vanegas SM, Wronski TJ 2007 A comparative study of the bone-restorative efficacy of anabolic agents in aged ovariectomized rats. *Osteoporosis International* **18**:351-362.
112. Iwata K, Li J, Follet H, Phipps RJ, Burr DB 2006 Bisphosphonates suppress periosteal osteoblast activity independently of resorption in rat femur and tibia. *Bone* **39**:1053-1058.
113. Jacobsson M, Jonsson A, Albrektsson T, Turesson I 1985 Alterations in bone regenerative capacity after low level gamma irradiation. A quantitative study. *Scand J Plast Reconstr Surg* **19**:231-236.
114. Jankovich JP 1972 The effects of mechanical vibration on bone development in the rat. *Journal of Biomechanics* **5**:241-248.
115. Jarvinen TL, Kannus P, Sievanen H, Jozsa L, Heinonen OJ, Vieno T, Jarvinen M 2001 Effects of remobilization on rat femur are dose-dependent. *Scand J Med Sci Sports* **11**:292-298.
116. Jayasinghe JA, Jones SJ, Boyde A 1994 Three-dimensional photographic study of cancellous bone in human fourth lumbar vertebral bodies. *Anat Embryol (Berl)* **189**:259-274.
117. Jee WS 2001 Integrated bone tissue Physiology: Anatomy and Physiology. In: Cowin SC (ed.) *Bone Mechanics Handbook*, second ed. CRC Press, pp. 1-68.
118. Jee WS, Yao W 2001 Overview: animal models of osteopenia and osteoporosis. *J Musculoskelet Neuronal Interact* **1**:193-207.
119. Jensen KS, Mosekilde L, Mosekilde L 1990 A model of vertebral trabecular bone architecture and its mechanical properties. *Bone* **11**:417-423.

120. Jerome CP, Burr DB, Van Bibber T, Hock JM, Brommage R 2001 Treatment with human parathyroid hormone (1-34) for 18 months increases cancellous bone volume and improves trabecular architecture in ovariectomized cynomolgus monkeys (*Macaca fascicularis*). *Bone* **28**:150-159.
121. Jiang SD, Dai LY, Jiang LS 2006 Osteoporosis after spinal cord injury. *Osteoporos Int* **17**:180-192.
122. Jiang SD, Shen C, Jiang LS, Dai LY 2007 Differences of bone mass and bone structure in osteopenic rat models caused by spinal cord injury and ovariectomy. *Osteoporos Int* **18**:743-750.
123. Jilka RL 2007 Molecular and cellular mechanisms of the anabolic effect of intermittent PTH. *Bone* **40**:1434-1446.
124. Ju YI, Sone T, Okamoto T, Fukunaga M 2008 Jump exercise during remobilization restores integrity of the trabecular architecture after tail suspension in young rats. *J Appl Physiol* **104**:1594-1600.
125. Judex S, Boyd S, Qin YX, Miller L, Muller R, Rubin C 2003 Combining high-resolution micro-computed tomography with material composition to define the quality of bone tissue. *Curr Osteoporos Rep* **1**:11-19.
126. Judex S, Chung H, Torab A, Xie L, Rubin CT, Donahue LR, Xu S 2005 Micro-CT induced radiation does not exacerbate disuse related bone loss. in proceedings of the 51st Annual Meeting of the Orthopaedic Research Society, Washington D.C.
127. Judex S, Boyd S, Qin YX, Turner S, Ye K, Muller R, Rubin C 2003 Adaptations of trabecular bone to low magnitude vibrations result in more uniform stress and strain under load. *Ann Biomed Eng* **31**:12-20.
128. Judex S, Donahue LR, Rubin C 2002 Genetic predisposition to low bone mass is paralleled by an enhanced sensitivity to signals anabolic to the skeleton. *FASEB J* **16**:1280-1282.
129. Judex S, Lei X, Han D, Rubin C 2007 Low-magnitude mechanical signals that stimulate bone formation in the ovariectomized rat are dependent on the applied frequency but not on the strain magnitude. *J Biomech* **40**:1333-1339.
130. Kalu DN 1991 The ovariectomized rat model of postmenopausal bone loss. *Bone Miner* **15**:175-191.
131. Kannus P, Sievanen H, Jarvinen TL, Jarvinen M, Kvist M, Oja P, Vuori I, Jozsa L 1994 Effects of free mobilization and low- to high-intensity treadmill running on the immobilization-induced bone loss in rats. *J Bone Miner Res* **9**:1613-1619.
132. Kasukawa Y, Miyakoshi N, Itoi E, Tsuchida T, Tamura Y, Kudo T, Suzuki K, Seki A, Sato K 2004 Effects of h-PTH on cancellous bone mass, connectivity, and bone strength in ovariectomized rats with and without sciatic-neurectomy. *J Orthop Res* **22**:457-464.
133. Ke HZ, Jee WS, Zeng QQ, Li M, Lin BY 1993 Prostaglandin E2 increased rat cortical bone mass when administered immediately following ovariectomy. *Bone Miner* **21**:189-201.
134. Keaveny TM 2001 Strength of trabecular bone. In: Cowin SC (ed.) *Bone Mechanics Handbook*, second ed. CRC Press.

135. Keaveny TM, Donley DW, Hoffmann PF, Mitlak BH, Glass EV, San Martin JA 2007 Effects of teriparatide and alendronate on vertebral strength as assessed by finite element modeling of QCT scans in women with osteoporosis. *J Bone Miner Res* **22**:149-157.
136. Keaveny TM, Pinilla TP, Crawford RP, Kopperdahl DL, Lou A 1997 Systematic and random errors in compression testing of trabecular bone. *J Orthop Res* **15**:101-110.
137. Keaveny TM, Guo XE, Wachtel EF, McMahon TA, Hayes WC 1994 Trabecular bone exhibits fully linear elastic behavior and yields at low strains. *J Biomech* **27**:1127-1129.
138. Keaveny TM, Wachtel EF, Ford CM, Hayes WC 1994 Differences between the tensile and compressive strengths of bovine tibial trabecular bone depend on modulus. *J Biomech* **27**:1137-1146.
139. Khosla S, Riggs BL, Atkinson EJ, Oberg AL, McDaniel LJ, Holets M, Peterson JM, Melton LJ, III 2006 Effects of sex and age on bone microstructure at the ultradistal radius: a population-based noninvasive in vivo assessment. *J Bone Miner Res* **21**:124-131.
140. Kimmel DB, Bozzato RP, Kronis KA, Coble T, Sindrey D, Kwong P, Recker RR 1993 The effect of recombinant human (1-84) or synthetic human (1-34) parathyroid hormone on the skeleton of adult osteopenic ovariectomized rats. *Endocrinology* **132**:1577-1584.
141. Kippo K, Hannuniemi R, Isaksson P, Lauren L, Osterman T, Peng Z, Tuukkanen J, Kuurtamo P, Vaananen HK, Sellman R 1998 Clodronate prevents osteopenia and loss of trabecular connectivity in estrogen-deficient rats. *J Bone Miner Res* **13**:287-296.
142. Kippo K, Hannuniemi R, Lauren L, Peng Z, Isaksson P, Virtamo T, Osterman T, Pasanen I, Sellman R, Vaananen HK 1997 Clodronate prevents bone loss in aged ovariectomized rats. *Calcif Tissue Int* **61**:151-157.
143. Kishi T, Hagino H, Kishimoto H, Nagashima H 1998 Bone responses at various skeletal sites to human parathyroid hormone in ovariectomized rats: effects of long-term administration, withdrawal, and readministration. *Bone* **22**:515-522.
144. Kitauchi T, Yoshida K, Yoneda T, Saka T, Yoshikawa M, Ozono S, Hirao Y 2004 Association between pentosidine and arteriosclerosis in patients receiving hemodialysis. *Clin Exp Nephrol* **8**:48-53.
145. Klinck RJ, Boyd SK 2006 The effects of radiation on ovariectomized mice as a function of genetic strain by in vivo micro-computed tomography. Transactions of the 28th annual meeting of the ASBMR, Philadelphia, PA, USA.
146. Klinck RJ, Campbell GM, Boyd SK 2008 Radiation effects on bone architecture in mice and rats resulting from in vivo micro-computed tomography scanning. *Med Eng Phys*.
147. Kneissel M, Boyde A, Gasser JA 2001 Bone tissue and its mineralization in aged estrogen-depleted rats after long-term intermittent treatment with parathyroid hormone (PTH) analog SDZ PTS 893 or human PTH(1-34). *Bone* **28**:237-250.
148. Kobayashi M, Hara K, Akiyama Y 2002 Effects of vitamin K2 (menatetrenone) on calcium balance in ovariectomized rats. *Jpn J Pharmacol* **88**:55-61.
149. Komm BS, Bodine PVN 2001 Regulation of bone cell function by estrogens. In: Marcus R, Feldman D, Kelsey J (eds.) *Osteoporosis*, 2 ed., vol. 1. Academic Press, pp. 305-338.

150. Laib A, Barou O, Vico L, Lafage-Proust MH, Alexandre C, Ruegsegger P 2000 3D micro-computed tomography of trabecular and cortical bone architecture with application to a rat model of immobilisation osteoporosis. *Med Biol Eng Comput* **38**:326-332.
151. Laib A, Hauselmann HJ, Ruegsegger P 1998 In vivo high resolution 3D-QCT of the human forearm. *Technol Health Care* **6**:329-337.
152. Laib A, Hildebrand T, Hauselmann HJ, Ruegsegger P 1997 Ridge number density: a new parameter for in vivo bone structure analysis. *Bone* **21**:541-546.
153. Laib A, Kumer JL, Majumdar S, Lane NE 2001 The temporal changes of trabecular architecture in ovariectomized rats assessed by MicroCT. *Osteoporos Int* **12**:936-941.
154. Laib A, Ruegsegger P 1999 Calibration of trabecular bone structure measurements of in vivo three-dimensional peripheral quantitative computed tomography with 28-microm-resolution microcomputed tomography. *Bone* **24**:35-39.
155. LaMothe JM, Hamilton NH, Zernicke RF 2005 Strain rate influences periosteal adaptation in mature bone. *Med Eng Phys* **27**:277-284.
156. Lane NE, Kumer JL, Majumdar S, Khan M, Lotz J, Stevens RE, Klein R, Phelps KV 2002 The effects of synthetic conjugated estrogens, a (cenestin) on trabecular bone structure and strength in the ovariectomized rat model. *Osteoporos Int* **13**:816-823.
157. Lane NE, Thompson JM, Haupt D, Kimmel DB, Modin G, Kinney JH 1998 Acute changes in trabecular bone connectivity and osteoclast activity in the ovariectomized rat in vivo. *J Bone Miner Res* **13**:229-236.
158. Lane NE, Yao W, Kinney JH, Modin G, Balooch M, Wronski TJ 2003 Both hPTH(1-34) and bFGF increase trabecular bone mass in osteopenic rats but they have different effects on trabecular bone architecture. *J Bone Miner Res* **18**:2105-2115.
159. Lecoq B, Potrel-Burgot C, Granier P, Sabatier JP, Marcelli C 2006 Comparison of bone loss induced in female rats by hindlimb unloading, ovariectomy, or both. *Joint Bone Spine* **73**:189-195.
160. Lewiecki EM, Watts NB 2008 Assessing response to osteoporosis therapy. *Osteoporos Int* **19**:1363-1368.
161. Lewiecki EM 2008 Prevention and Treatment of Postmenopausal Osteoporosis. *Obstetrics and Gynecology Clinics of North America* **35**:301-315.
162. Li M, Liang H, Shen Y, Wronski TJ 1999 Parathyroid hormone stimulates cancellous bone formation at skeletal sites regardless of marrow composition in ovariectomized rats. *Bone* **24**:95-100.
163. Li M, Mosekilde L, Sogaard CH, Thomsen JS, Wronski TJ 1995 Parathyroid hormone monotherapy and cotherapy with antiresorptive agents restore vertebral bone mass and strength in aged ovariectomized rats. *Bone* **16**:629-635.
164. Li M, Shen Y, Qi H, Wronski TJ 1996 Comparative study of skeletal response to estrogen depletion at red and yellow marrow sites in rats. *Anat Rec* **245**:472-480.
165. Lin BY, Jee WS, Chen MM, Ma YF, Ke HZ, Li XJ 1994 Mechanical loading modifies ovariectomy-induced cancellous bone loss. *Bone Miner* **25**:199-210.

166. Linde F 1994 Elastic and viscoelastic properties of trabecular bone by a compression testing approach. *Dan Med Bull* **41**:119-138.
167. Lindsay R, Cosman F 2001 Estrogens and osteoporosis. In: Marcus R, Feldman D, Kelsey J (eds.) *Osteoporosis*, 2 ed., vol. 2. Academic Press, pp. 577-602.
168. Lindsay R, Scheele WH, Neer R, Pohl G, Adami S, Mautalen C, Reginster JY, Stepan JJ, Myers SL, Mitlak BH 2004 Sustained vertebral fracture risk reduction after withdrawal of teriparatide in postmenopausal women with osteoporosis. *Arch Intern Med* **164**:2024-2030.
169. Lindsay R, Zhou H, Cosman F, Nieves J, Dempster DW, Hodsmann AB 2007 Effects of a one-month treatment with PTH(1-34) on bone formation on cancellous, endocortical, and periosteal surfaces of the human ilium. *J Bone Miner Res* **22**:495-502.
170. Lindsay R, Cosman F, Zhou H, Bostrom MP, Shen VW, Cruz JD, Nieves JW, Dempster DW 2006 A Novel Tetracycline Labeling Schedule for Longitudinal Evaluation of the Short-Term Effects of Anabolic Therapy With a Single Iliac Crest Bone Biopsy: Early Actions of Teriparatide. *J Bone Miner Res* **21**:366-373.
171. Little DG, McDonald M, Sharpe IT, Peat R, Williams P, McEvoy T 2005 Zoledronic acid improves femoral head sphericity in a rat model of perthes disease. *J Orthop Res* **23**:862-868.
172. Little DG, Smith NC, Williams PR, Briody JN, Bilston LE, Smith EJ, Gardiner EM, Cowell CT 2003 Zoledronic acid prevents osteopenia and increases bone strength in a rabbit model of distraction osteogenesis. *J Bone Miner Res* **18**:1300-1307.
173. Liu XS, Sajda P, Saha PK, Wehrli FW, Bevil G, Keaveny TM, Guo XE 2008 Complete volumetric decomposition of individual trabecular plates and rods and its morphological correlations with anisotropic elastic moduli in human trabecular bone. *J Bone Miner Res* **23**:223-235.
174. Lyles KW, Colon-Emeric CS, Magaziner JS, Adachi JD, Pieper CF, Mautalen C, Hyldstrup L, Recknor C, Nordsletten L, Moore KA, Lavecchia C, Zhang J, Mesenbrink P, Hodgson PK, Abrams K, Orloff JJ, Horowitz Z, Eriksen EF, Boonen S 2007 Zoledronic acid and clinical fractures and mortality after hip fracture. *N Engl J Med* **357**:1799-1809.
175. Macneil JA, Boyd SK 2007 Improved reproducibility of high-resolution peripheral quantitative computed tomography for measurement of bone quality. *Med Eng Phys*.
176. Mashiba T 2008 Assessment of bone quality. *Bone quality and osteoporosis treatment. Clin Calcium* **18**:300-307.
177. McCombs JS, Thiebaud P, Laughlin-Miley C, Shi J 2004 Compliance with drug therapies for the treatment and prevention of osteoporosis. *Maturitas* **48**:271-287.
178. McCubbrey DA, Cody DD, Peterson EL, Kuhn JL, Flynn MJ, Goldstein SA 1995 Static and fatigue failure properties of thoracic and lumbar vertebral bodies and their relation to regional density. *J Biomech* **28**:891-899.
179. Melton LJ, III, Riggs BL, van Lenthe GH, Achenbach SJ, Muller R, Bouxsein ML, Amin S, Atkinson EJ, Khosla S 2007 Contribution of in vivo structural measurements and load/strength ratios to the determination of forearm fracture risk in postmenopausal women. *J Bone Miner Res* **22**:1442-1448.

180. Meng XW, Liang XG, Birchman R, Wu DD, Dempster DW, Lindsay R, Shen V 1996 Temporal expression of the anabolic action of PTH in cancellous bone of ovariectomized rats. *J Bone Miner Res* **11**:421-429.
181. Miller MA, Bare SP, Recker RR, Smith SY, Fox J 2008 Intratrabecular tunneling increases trabecular number throughout the skeleton of ovariectomized rhesus monkeys treated with parathyroid hormone 1-84. *Bone* **42**:1175-1183.
182. Misof BM, Roschger P, Cosman F, Kurland ES, Tesch W, Messmer P, Dempster DW, Nieves J, Shane E, Fratzl P, Klaushofer K, Bilezikian J, Lindsay R 2003 Effects of intermittent parathyroid hormone administration on bone mineralization density in iliac crest biopsies from patients with osteoporosis: a paired study before and after treatment. *J Clin Endocrinol Metab* **88**:1150-1156.
183. Miyakoshi N, Sato K, Abe T, Tsuchida T, Tamura Y, Kudo T 1999 Histomorphometric evaluation of the effects of ovariectomy on bone turnover in rat caudal vertebrae. *Calcif Tissue Int* **64**:318-324.
184. Mori S, Burr DB 1993 Increased intracortical remodeling following fatigue damage. *Bone* **14**:103-109.
185. Mori S, Harruff R, Ambrosius W, Burr DB 1997 Trabecular bone volume and microdamage accumulation in the femoral heads of women with and without femoral neck fractures. *Bone* **21**:521-526.
186. Moriyama I, Iwamoto J, Takeda T, Toyama Y 2002 Comparative effects of intermittent administration of human parathyroid hormone (1-34) on cancellous and cortical bone loss in tail-suspended and sciatic neurectomized young rats. *J Orthop Sci* **7**:379-385.
187. Mosekilde L 1999 <http://www.lab.anhb.uwa.edu.au/mb140/MoreAbout/bonedynamics.html>.
188. Mosekilde L, Danielsen CC, Sogaard CH, McOsker JE, Wronski TJ 1995 The anabolic effects of parathyroid hormone on cortical bone mass, dimensions and strength--assessed in a sexually mature, ovariectomized rat model. *Bone* **16**:223-230.
189. Mosekilde L, Danielsen CC, Sogaard CH, Thorling E 1994 The effect of long-term exercise on vertebral and femoral bone mass, dimensions, and strength--Assessed in a rat model. *Bone* **15**:293-301.
190. Mosekilde L, Sogaard CH, McOsker JE, Wronski TJ 1994 PTH has a more pronounced effect on vertebral bone mass and biomechanical competence than antiresorptive agents (estrogen and bisphosphonate)--assessed in sexually mature, ovariectomized rats. *Bone* **15**:401-408.
191. Mosekilde L, Thomsen JS, McOsker JE 1997 No loss of biomechanical effects after withdrawal of short-term PTH treatment in an aged, osteopenic, ovariectomized rat model. *Bone* **20**:429-437.
192. Mosekilde L, Tornvig L, Thomsen JS, Orhii PB, Banu MJ, Kalu DN 2000 Parathyroid hormone and growth hormone have additive or synergetic effect when used as intervention treatment in ovariectomized rats with established osteopenia. *Bone* **26**:643-651.
193. Mosley JR, Lanyon LE 1998 Strain rate as a controlling influence on adaptive modeling in response to dynamic loading of the ulna in growing male rats. *Bone* **23**:313-318.

194. Mulder L, Koolstra JH, Van Eijden TM 2004 Accuracy of microCT in the quantitative determination of the degree and distribution of mineralization in developing bone. *Acta Radiol* **45**:769-777.
195. Muller R, Ruegsegger P 1997 Micro-tomographic imaging for the nondestructive evaluation of trabecular bone architecture. *Stud Health Technol Inform* **40**:61-79.
196. Neer RM, et al. 2001 Effect of parathyroid hormone (1-34) on fractures and bone mineral density in postmenopausal women with osteoporosis. *New Engl J Med* **344**:1434-1441.
197. New SA 2001 Exercise, bone and nutrition. *Proc Nutr Soc* **60**:265-274.
198. Nissenson RA 2001 PTH and PTH-related protein. In: Marcus R, Feldman D, Kelsey J (eds.) *Osteoporosis*, second ed., vol. 1. Academic Press, pp. 221-246.
199. Nozaka K, Miyakoshi N, Kasukawa Y, Maekawa S, Noguchi H, Shimada Y 2008 Intermittent administration of human parathyroid hormone enhances bone formation and union at the site of cancellous bone osteotomy in normal and ovariectomized rats. *Bone* **42**:90-97.
200. Odgaard A, Gundersen HJ 1993 Quantification of connectivity in cancellous bone, with special emphasis on 3-D reconstructions. *Bone* **14**:173-182.
201. Oxlund BS, Ortoft G, Andreassen TT, Oxlund H 2003 Low-intensity, high-frequency vibration appears to prevent the decrease in strength of the femur and tibia associated with ovariectomy of adult rats. *Bone* **32**:69-77.
202. Oxlund H, Andreassen TT 2004 Simvastatin treatment partially prevents ovariectomy-induced bone loss while increasing cortical bone formation. *Bone* **34**:609-618.
203. Oxlund H, Dalstra M, Ejersted C, Andreassen TT 2002 Parathyroid hormone induces formation of new cancellous bone with substantial mechanical strength at a site where it had disappeared in old rats. *Eur J Endocrinol* **146**:431-438.
204. Pan B, To LB, Farrugia AN, Findlay DM, Green J, Gronthos S, Evdokiou A, Lynch K, Atkins GJ, Zannettino ACW 2004 The nitrogen-containing bisphosphonate, zoledronic acid, increases mineralisation of human bone-derived cells in vitro. *Bone* **34**:112-123.
205. Pan Z, Jee WSS, Ma YF, McOsker JE, Li XJ 1995 Intermittent treatments of prostaglandin E2 plus risedronate and prostaglandin E2 alone are equally anabolic on tibial shaft of ovariectomized rats. *Bone* **17**:S291-S296.
206. Parfitt AM 1990 Bone-forming cells in clinical conditions. In: Hall BK (ed.) *Bone*. Volume 1. *The Osteoblast and Osteocyte*. Telford Press and CRC Press, Boca Raton, FL.
207. Parfitt AM, Drezner MK, Glorieux FH, Kanis JA, Malluche H, Meunier PJ, Ott SM, Recker RR 1987 Bone histomorphometry: standardization of nomenclature, symbols, and units. Report of the ASBMR Histomorphometry Nomenclature Committee. *J Bone Miner Res* **2**:595-610.
208. Pattin CA, Caler WE, Carter DR 1996 Cyclic mechanical property degradation during fatigue loading of cortical bone. *J Biomech* **29**:69-79.
209. Perez-Lopez FR 2004 Postmenopausal osteoporosis and alendronate. *Maturitas* **48**:179-192.
210. personal communication with Judex S 2007 .

211. Pinkerton JV, Dalkin AC 2007 Combination therapy for treatment of osteoporosis: A review. *Am J Obstet Gynecol* **197**:559-565.
212. Prince R, Sipos A, Hossain A, Syversen U, Ish-Shalom S, Marcinowska E, Halse J, Lindsay R, Dalsky GP, Mitlak BH 2005 Sustained nonvertebral fragility fracture risk reduction after discontinuation of teriparatide treatment. *J Bone Miner Res* **20**:1507-1513.
213. Qin YX, Rubin CT, McLeod KJ 1998 Nonlinear dependence of loading intensity and cycle number in the maintenance of bone mass and morphology. *J Orthop Res* **16**:482-489.
214. Rapillard L, Charlebois M, Zysset PK 2006 Compressive fatigue behavior of human vertebral trabecular bone. *J Biomech* **39**:2133-2139.
215. Recker R, Masarachia P, Santora A, Howard T, Chavassieux P, Arlot M, Rodan G, Wehren L, Kimmel D 2005 Trabecular bone microarchitecture after alendronate treatment of osteoporotic women. *Curr Med Res Opin* **21**:185-194.
216. Recker RR, Delmas PD, Halse J, Reid IR, Boonen S, Garcia-Hernandez PA, Supronik J, Lewiecki EM, Ochoa L, Miller P, Hu H, Mesenbrink P, Hartl F, Gasser J, Eriksen EF 2008 Effects of intravenous zoledronic acid once yearly on bone remodeling and bone structure. *J Bone Miner Res* **23**:6-16.
217. Reddy JN 1993 *An introduction to the Finite Element Method*, second ed. McGraw-Hill, New York, NY, USA.
218. Reeve J, Davies UM, Hesp R, McNally E, Katz D 1990 Treatment of osteoporosis with human parathyroid peptide and observations on effect of sodium fluoride. *Br Med J* **301**:314-318.
219. Reid IR, Brown JP, Burckhardt P, Horowitz Z, Richardson P, Trechsel U, Widmer A, Devogelaer JP, Kaufman JM, Jaeger P, Body JJ, Brandi ML, Broell J, Di Micco R, Genazzani AR, Felsenberg D, Happ J, Hooper MJ, Ittner J, Leeb G, Mallmin H, Murray T, Ortolani S, Rubinacci A, Saaf M, Samsioe G, Verbruggen L, Meunier PJ 2002 Intravenous zoledronic acid in postmenopausal women with low bone mineral density. *N Engl J Med* **346**:653-661.
220. Rhee Y, Won YY, Baek MH, Lim SK 2004 Maintenance of increased bone mass after recombinant human parathyroid hormone (1-84) with sequential zoledronate treatment in ovariectomized rats. *J Bone Miner Res* **19**:931-937.
221. Rietbergen Bv, Eckstein F, Koller B, Huiskes R, Baaijens FPT, Ruesegger P 1999 Feasibility of micro-FE analyses of human bones. In: Middleton J, Jones ML, Shrive NG, Pande GN (eds.) *Computer Methods in Biomechanics and Biomedical Engineering*. Gordon and Breach Science Publishers.
222. Rietbergen Bv, Muller R, Ulrich D, Ruesegger P, Huiskes R 1999 Tissue stresses and strain in trabeculae of a canine proximal femur can be quantified from computer reconstructions. *J Biomech* **32**:443-451.
223. Rietbergen Bv, Weinans H, Huiskes R, Odgaard A 1995 A new method to determine trabecular bone elastic properties and loading using micromechanical finite-element models. *J Biomech* **28**:69-81.
224. Riggs BL, Melton LJ 1995 The worldwide problem of osteoporosis: Insights afforded by epidemiology. *Bone* **17**:S505-S511.

225. Riggs BL, Melton Iii LJ, Robb RA, Camp JJ, Atkinson EJ, Peterson JM, Rouleau PA, McCollough CH, Bouxsein ML, Khosla S 2004 Population-based study of age and sex differences in bone volumetric density, size, geometry, and structure at different skeletal sites. *J Bone Miner Res* **19**:1945-1954.
226. Rittmaster RS, Bolognese M, Ettinger MP, Hanley DA, Hodsman AB, Kendler DL, Rosen CJ 2000 Enhancement of bone mass in osteoporotic women with parathyroid hormone followed by alendronate. *J Clin Endocrinol Metab* **85**:2129-2134.
227. Rosen CJ 2005 Clinical practice. Postmenopausal osteoporosis. *N Engl J Med* **353**:595-603.
228. Rubin C, Recker R, Cullen D, Ryaby J, McCabe J, McLeod K 2004 Prevention of postmenopausal bone loss by a low-magnitude, high-frequency mechanical stimuli: a clinical trial assessing compliance, efficacy, and safety. *J Bone Miner Res* **19**:343-351.
229. Rubin C, Turner AS, Bain S, Mallinckrodt C, McLeod K 2001 Anabolism. Low mechanical signals strengthen long bones. *Nature* **412**:603-604.
230. Rubin C, Turner AS, Mallinckrodt C, Jerome C, McLeod K, Bain S 2002 Mechanical strain, induced noninvasively in the high-frequency domain, is anabolic to cancellous bone, but not cortical bone. *Bone* **30**:445-452.
231. Rubin C, Turner AS, Muller R, Mittra E, McLeod K, Lin W, Qin YX 2002 Quantity and quality of trabecular bone in the femur are enhanced by a strongly anabolic, noninvasive mechanical intervention. *J Bone Miner Res* **17**:349-357.
232. Rubin C, Xu G, Judex S 2001 The anabolic activity of bone tissue, suppressed by disuse, is normalized by brief exposure to extremely low-magnitude mechanical stimuli. *FASEB J* **15**:2225-2229.
233. Rubin CT, Lanyon LE 1985 Regulation of bone mass by mechanical strain magnitude. *Calcif Tissue Int* **37**:411-417.
234. Russell RGG 2006 Ibandronate: Pharmacology and preclinical studies. *Bone* **38**:S7-S12.
235. Saito M 2008 Assessment of bone quality. Effects of bisphosphonates, raloxifene, alfacalcidol, and menatetrenone on bone quality: collagen cross-links, mineralization, and microdamage. *Clin Calcium* **18**:364-372.
236. Saito M, Mori S, Mashiba T, Komatsubara S, Marumo K 2008 Collagen maturity, glycation induced-pentosidine, and mineralization are increased following 3-year treatment with incadronate in dogs. *Osteoporos Int*.
237. Sato M, Ma YL, Hock JM, Westmore MS, Vahle J, Villanueva A, Turner CH 2002 Skeletal efficacy with parathyroid hormone in rats was not entirely beneficial with long-term treatment. *J Pharmacol Exp Ther* **302**:304-313.
238. Sato M, Vahle J, Schmidt A, Westmore M, Smith S, Rowley E, Ma LY 2002 Abnormal bone architecture and biomechanical properties with near-lifetime treatment of rats with PTH. *Endocrinology* **143**:3230-3242.
239. Sato M, Zeng GQ, Turner CH 1997 Biosynthetic human parathyroid hormone (1-34) effects on bone quality in aged ovariectomized rats. *Endocrinology* **138**:4330-4337.
240. Scales WE, Kluger MJ 1987 Effect of antipyretic drugs on circadian rhythm in body temperature of rats. *Am J Physiol* **253**:R306-R313.

241. Schaffler MB, Radin EL, Burr DB 1990 Long-term fatigue behavior of compact bone at low strain magnitude and rate. *Bone* **11**:321-326.
242. Sellmeyer DE, Black DM, Palermo L, Greenspan S, Ensrud K, Bilezikian J, Rosen CJ 2007 Heterogeneity in skeletal response to full-length parathyroid hormone in the treatment of osteoporosis. *Osteoporos Int* **18**:973-979.
243. Shahar R, Zaslansky P, Barak M, Friesem AA, Currey JD, Weiner S 2007 Anisotropic Poisson's ratio and compression modulus of cortical bone determined by speckle interferometry. *J Biomech* **40**:252-264.
244. Shen V, Birchman R, Liang XG, Wu DD, Lindsay R, Dempster DW 1997 Prednisolone alone, or in combination with estrogen or dietary calcium deficiency or immobilization, inhibits bone formation but does not induce bone loss in mature rats. *Bone* **21**:345-351.
245. Shen V, Birchman R, Wu DD, Lindsay R 2000 Skeletal effects of Parathyroid Hormone infusion in ovariectomized rats with or without estrogen repletion. *J Bone Miner Res* **15**:740-746.
246. Sheng ZF, Dai RC, Wu XP, Fang LN, Fan HJ, Liao EY 2007 Regionally specific compensation for bone loss in the tibial trabeculae of estrogen-deficient rats. *Acta Radiol* **48**:531-539.
247. Shiraki M 2003 Concurrent or sequential treatment for osteoporosis with PTH and alendronates. *Clin Calcium* **13**:54-58.
248. Slovik DM, Neer RM, Potts JTJ 1981 Short-term effects of synthetic human parathyroid hormone-(1-34) administration on bone mineral metabolism in osteoporotic patients., **68** ed., pp. 1261-1271.
249. Sogaard CH, Mosekilde L, Thomsen JS, Richards A, McOsker JE 1997 A comparison of the effects of two anabolic agents (fluoride and PTH) on ash density and bone strength assessed in an osteopenic rat model. *Bone* **20**:439-449.
250. Sornay-Rendu E, Boutroy S, Munoz F, Delmas PD 2007 Alterations of cortical and trabecular architecture are associated with fractures in postmenopausal women, partially independent of decreased BMD measured by DXA: the OFELY study. *J Bone Miner Res* **22**:425-433.
251. Sosa HM, Diez PA 2007 Parathyroid hormone in the treatment of osteoporosis. *An Med Interna* **24**:87-97.
252. Stepan JJ, Burr DB, Pavo I, Sipos A, Michalska D, Li J, Fahrleitner-Pammer A, Petto H, Westmore M, Michalsky D, Sato M, Dobnig H 2007 Low bone mineral density is associated with bone microdamage accumulation in postmenopausal women with osteoporosis. *Bone* **41**:378-385.
253. Stumpf UC, Kurth AA, Windolf J, Fassbender WJ 2007 Pregnancy-associated osteoporosis: an underestimated and underdiagnosed severe disease. A review of two cases in short- and long-term follow-up. *Adv Med Sci* **52**:94-97.
254. Takano Y, Tanizawa T, Mashiba T, Endo N, Nishida S, Takahashi HE 1996 Maintaining bone mass by bisphosphonate incadronate disodium (YM175) sequential treatment after discontinuation of intermittent human parathyroid hormone (1-34) administration in ovariectomized rats. *J Bone Miner Res* **11**:169-177.

255. Tanizawa T, Yamamoto N, Takano Y, Mashiba T, Zhang L, Nishida S, Endo N, Takahashi HE, Fujimoto R, Hori M 1998 Effects of human PTH(1-34) and bisphosphonate on the osteopenic rat model. *Toxicol Lett* **102-103**:399-403.
256. Theriault RL 2003 Zoledronic acid (Zometa) use in bone disease. *Expert Rev Anticancer Ther* **3**:157-166.
257. Thomas T 2006 Intermittent parathyroid hormone therapy to increase bone formation. *Joint Bone Spine* **73**:262-269.
258. Thompson DD, Simmons HA, Pirie CM, Ke HZ 1995 FDA guidelines and animal models for osteoporosis. *Bone* **17**:S125-S133.
259. Thomsen JS, Ebbesen EN, Mosekilde L 2002 Age-related differences between thinning of horizontal and vertical trabeculae in human lumbar bone as assessed by a new computerized method. *Bone* **31**:136-142.
260. Tou JC, Foley A, Yuan YV, Arnaud S, Wade CE, Brown M 2007 The effect of ovariectomy combined with hindlimb unloading and reloading on the long bones of mature Sprague-Dawley rats. *Menopause*.
261. Trebacz H 2001 Disuse-induced deterioration of bone strength is not stopped after free remobilization in young adult rats. *J Biomech* **34**:1631-1636.
262. Trebacz H 2003 Changes in bone strength during convalescence after immobilization induces bone loss--experiment with adult rats. *Chir Narzadow Ruchu Ortop Pol* **68**:197-201.
263. Turner CH 2002 Biomechanics of bone: determinants of skeletal fragility and bone quality. *Osteoporos Int* **13**:97-104.
264. Turner CH, Forwood MR, Rho JY, Yoshikawa T 1994 Mechanical loading thresholds for lamellar and woven bone formation. *J Bone Miner Res* **9**:87-97.
265. Turner RT 1999 Mechanical signaling in the development of postmenopausal osteoporosis. *Lupus* **8**:388-392.
266. Turner RT, Lotinun S, Hefferan TE, Morey-Holton E 2006 Disuse in adult male rats attenuates the bone anabolic response to a therapeutic dose of parathyroid hormone. *J Appl Physiol* **101**:881-886.
267. Turner RT, Riggs BL, Spelsberg TC 1994 Skeletal effects of estrogen. *Endocr Rev* **15**:275-300.
268. Turner RT, Vandersteenhoven JJ, Bell NH 1987 The effects of ovariectomy and 17 beta-estradiol on cortical bone histomorphometry in growing rats. *J Bone Miner Res* **2**:115-122.
269. Turner RT, Evans GL, Lotinun S, Lapke PD, Iwaniec UT, Morey-Holton E 2007 Doseresponse effects of intermittent PTH on cancellous bone in hindlimb unloaded rats. *J Bone Miner Res* **22**:64-71.
270. Tuukkanen J, Wallmark B, Jalovaara P, Takala T, Sjogren S, Vaananen K 1991 Changes induced in growing rat bone by immobilization and remobilization. *Bone* **12**:113-118.
271. Un K, Bevill G, Keaveny TM 2006 The effects of side-artifacts on the elastic modulus of trabecular bone. *J Biomech* **39**:1955-1963.

272. Uusi-Rasi K, Semanick LM, Zanchetta JR, Bogado CE, Eriksen EF, Sato M, Beck TJ 2005 Effects of teriparatide [rhPTH (1-34)] treatment on structural geometry of the proximal femur in elderly osteoporotic women. *Bone* **36**:948-958.
273. Valenta A, Roschger P, Fratzl-Zelman N, Kostenuik PJ, Dunstan CR, Fratzl P, Klaushofer K 2005 Combined treatment with PTH (1-34) and OPG increases bone volume and uniformity of mineralization in aged ovariectomized rats. *Bone* **37**:87-95.
274. van RB, Huiskes R, Eckstein F, Rueggsegger P 2003 Trabecular bone tissue strains in the healthy and osteoporotic human femur. *J Bone Miner Res* **18**:1781-1788.
275. Verhulp E, Rietbergen BV, Huiskes R 2004 A three-dimensional digital image correlation technique for strain measurements in microstructures. *J Biomech* **37**:1313-1320.
276. Verhulp E, van RB, Huiskes R 2008 Load distribution in the healthy and osteoporotic human proximal femur during a fall to the side. *Bone* **42**:30-35.
277. Waarsing JH 2006 Exploring bone dynamics by in-vivo micro-CT imaging. Erasmus Medical Center, Rotterdam, Netherlands.
278. Waarsing JH, Day JS, van der Linden JC, Ederveen AG, Spanjers C, De Clerck N, Sasov A, Verhaar JAN, Weinans H 2004 Detecting and tracking local changes in the tibiae of individual rats: a novel method to analyse longitudinal in vivo micro-CT data. *Bone* **34**:163-169.
279. Waarsing JH, Day JS, Weinans H 2005 Longitudinal micro-CT scans to evaluate bone architecture. *J Musculoskelet Neuronal Interact* **5**:310-312.
280. Waarsing JH, Day JS, Verhaar JAN, Ederveen AGH, Weinans H 2006 Bone loss dynamics result in trabecular alignment in aging and ovariectomized rats. *J Orthop Res* **24**:926-935.
281. Waarsing JH, Day JS, Weinans H 2004 An improved segmentation method for in vivo microCT imaging. *J Bone Miner Res* **19**:1640-1650.
282. Waarsing JH, van der Linden JC, Weinans H 2007 After ovx, bone adaptation is regulated by mechanical stimuli, but bone loss is not. in proceedings of the 53rd Annual Meeting of the Orthopaedic Research Society, San Diego, CA.
283. Washimi Y, Ito M, Morishima Y, Taguma K, Ojima Y, Uzawa T, Hori M 2007 Effect of combined humanPTH(1-34) and calcitonin treatment in ovariectomized rats. *Bone* **41**:786-793.
284. Weinbaum S, Cowin SC, Zeng Y 1994 A model for the excitation of osteocytes by mechanical loading-induced bone fluid shear stresses. *J Biomech* **27**:339-360.
285. Westerlind KC, Wronski TJ, Ritman EL, Luo ZP, An KN, Bell NH, Turner RT 1997 Estrogen regulates the rate of bone turnover but bone balance in ovariectomized rats is modulated by prevailing mechanical strain. *Proc Natl Acad Sci U S A* **94**:4199-4204.
286. Wolff J 1982 *Das Gesetz der Transformation der Knochen*, first ed. Verlag von August Hirschwald, Berlin.
287. Wronski TJ, Dann LM, Horner SL 1989 Time course of vertebral osteopenia in ovariectomized rats. *Bone* **10**:295-301.

288. Wronski TJ, Dann LM, Scott KS, Cintron M 1989 Long-term effects of ovariectomy and aging on the rat skeleton. *Calcif Tissue Int* **45**:360-366.
289. Wronski TJ, Yen C-F 1994 Anabolic effects of parathyroid hormone on cortical bone in ovariectomized rats. *Bone* **15**:51-58.
290. www.ats.ucla.edu/stat/spss/library/comp_repeated.htm 2008 Comparing strategies of analyzing repeated measures data. UCLA Academic Technology Services.
291. www.nof.org. National Osteoporosis Foundation 2008 .
292. Xie L, Donahue LR, Rubin C, Judex S 2006 Doubling the bouts or acceleration magnitude may increase the efficacy of low level vibrations in the growing skeleton. in proceedings of the 51st annual meeting of the ORS, Chicago, IL, p. 1622.
293. Xie L, Rubin C, Judex S 2008 Enhancement of the adolescent murine musculoskeletal system using low-level mechanical vibrations. *J Appl Physiol* **104**:1056-1062.
294. Xie L, Jacobson JM, Choi ES, Busa B, Donahue LR, Miller LM, Rubin CT, Judex S 2006 Low-level mechanical vibrations can influence bone resorption and bone formation in the growing skeleton. *Bone* **39**:1059-1066.
295. Yang J, Pham SM, Crabbe DL 2003 Effects of oestrogen deficiency on rat mandibular and tibial microarchitecture. *Dentomaxillofac Radiol* **32**:247-251.
296. Yao W, Cheng Z, Koester KJ, Ager JW, Balooch M, Pham A, Chefo S, Busse C, Ritchie RO, Lane NE 2007 The degree of bone mineralization is maintained with single intravenous bisphosphonates in aged estrogen-deficient rats and is a strong predictor of bone strength. *Bone* **41**:804-812.
297. Yerramshetty JS, Akkus O 2008 The associations between mineral crystallinity and the mechanical properties of human cortical bone. *Bone* **42**:476-482.
298. Yoshida S, Yamamuro T, Okumura H, Takahashi H 1991 Microstructural changes of osteopenic trabeculae in the rat. *Bone* **12**:185-194.
299. Yuan ZZ, Jee WS, Ma YF, Wei W, Ijiri K 1995 Parathyroid hormone therapy accelerates recovery from immobilization-induced osteopenia. *Bone* **17**:219S-223S.
300. Zanchetta JR, Bogado CE, Ferretti JL, Wang O, Wilson MG, Sato M, Gaich GA, Dalsky GP, Myers SL 2003 Effects of teriparatide [recombinant human parathyroid hormone (1-34)] on cortical bone in postmenopausal women with osteoporosis. *J Bone Miner Res* **18**:539-543.
301. Zeng QQ, Jee WS, Bigornia AE, King JG, Jr., D'Souza SM, Li XJ, Ma YF, Wechter WJ 1996 Time responses of cancellous and cortical bones to sciatic neurectomy in growing female rats. *Bone* **19**:13-21.
302. Zhang KQ, Chen JW, Li QN, Li GF, Tian XY, Huang LF, Bao LH, Wang ML 2002 Effect of intermittent injection of recombinant human parathyroid hormone on bone histomorphometry of ovariectomized rats. *Acta Pharmacol Sin* **23**:659-662.
303. Zhou H, Iida-Klein A, Lu SS, Ducayen-Knowles M, Levine LR, Dempster DW, Lindsay R 2003 Anabolic action of parathyroid hormone on cortical and cancellous bone differs between axial and appendicular skeletal sites in mice. *Bone* **32**:513-520.

Dankwoord

De afgelopen vier jaar heb ik met veel plezier aan mijn promotie gewerkt. Daarbij heb ik natuurlijk heel veel steun en hulp van mensen om me heen gehad. Bert, ik heb altijd veel gehad aan onze meetings, jouw input en ook praktische hulp. Bedankt voor de mogelijkheid om naar zoveel congressen te gaan en voor het mede mogelijk maken van mijn jaar in Boston. Rik, bedankt voor de vrijheid die je me hebt gegeven en voor de publiekelijke support wanneer nodig. Keita, thanks so much for your input and feedback in the last half year, you've been a great help. Mary, thanks a lot for having me in your lab, your feedback on several of my studies and for introducing me to the world of clinicians and pharmaceuticals. Thanks to the Orthopedic Biomechanics Laboratory, Beth Israel Deaconess Medical Center and Harvard Medical School for my one year visit.

Veel mensen om mij heen hebben geholpen met brainstormen over mijn onderzoek en met het maken van nieuwe apparatuur of onderdelen. Collega's uit onze groep (Jasper, René, Lieke, Peter, Lars), het was gezellig en ook nuttig om af en toe bij te kletsen. Verschillende studenten in Eindhoven en Boston hebben mij geholpen verder te komen met mijn onderzoek. Floor, Ellemiek, Rianne en Anthal, bedankt. Thanks to Michal and Neil for your help. Thanks to Juerg Gasser, for your ever so kind and knowledgeable feedback and help. Jo, heel erg bedankt voor al je zorgen voor de proefdieren en voor de rust, die je altijd had. Leonie, jij ook bedankt voor de zorgen voor de proefdieren. Elise Morgan and Zack Mason, thanks for helping me out with fatigue testing. Tom, bedankt voor je hulp bij Matlab. Marius en zijn team van de werkplaats in N-laag, heel erg bedankt voor jullie hulp.

Zonder al mijn gezellige collega's van vloer 4 in W-hoog en uit Boston was mijn promotietijd natuurlijk nooit zo leuk geweest! Vooral mijn kamergenoten van 4.11, ik heb met heel veel plezier elke dag met jullie gedeeld. Voornamelijk met Mirjam, Lisette, Karlien, Martijn en Rolf heb ik veel tijd doorgebracht. Ik zal jullie missen! Many thanks to John, my Boston roomy, for your kind help with practical things in the lab and life in Boston in general, and for taking me on your sailing trips. Esther and Olivier, thanks for being such a good friend. Thanks to the Boston colleagues for the great time.

Elma, Marleen, Hanneke, Charlotte en Rianne, ik ben nog steeds heel blij met jullie als vriendinnen, ondanks dat we steeds verder uit elkaar wonen! Bedankt voor de support wanneer nodig. Marleen, super dat je mijn paranimf bent! Elma, bedankt voor al je steun, telefoontjes, kaartjes en kado'tjes, ook toen het minder met me ging. Jammer dat je er vandaag niet bij kunt zijn... ik kom je snel opzoeken! Hally en

Elsbeth, we kennen elkaar al ZO lang en nog steeds is het erg leuk om elkaar te zien. Esther en Rachel, onze gezellige afspraakjes samen blijven we doen. Hopelijk ben jij er Floor, ook binnenkort weer vaker bij. Kaai, Noek en Suus, onze nichtjesavonden zijn altijd erg leuk geweest. Mirjam, Chantal, Wouter, Ewout en Carlo, tennissen met jullie was altijd ontzettend gezellig en ontspannend. Harvard a cappella group and Boston Chorus, it was such an honor and pleasure to sing with you! I still miss singing with you. Mirjam, Lisette, Karlien, Angelique en Debbie, de maandelijkse etentjes zijn erg leuk en gezellig om contact met elkaar te houden.

Mam, bedankt voor al je vertrouwen en steun; in goede en minder goede tijden ben je er steeds voor me geweest. Je bent altijd zo enthousiast en geïnteresseerd geweest voor en in alle spannende dingen die op mijn pad kwamen! Pap, jij ook bedankt voor je support! Onze jaarlijkse vakanties zijn altijd erg leuk om met zijn allen bij elkaar te zijn. Fleur en Bas, ik ben erg blij met jullie, bedankt voor de fijne momenten samen. Fleur, super dat je mijn paranimf bent! Valerie, wat fantastisch om nog zo'n lief, klein zusje te hebben, je hebt voor veel afleiding gezorgd! Lieve Chris, bedankt voor al je hulp, peptalks, begrip, vertrouwen, liefde en gezelligheid!

Curriculum Vitae

Julienne Brouwers werd op 23 oktober 1980 geboren in Delft. Na een paar jaar in het westen en in Engeland te hebben gewoond, verhuisde zij naar het oosten van het land waar ze basisonderwijs en vervolgens het Gymnasium aan het Jacobus College te Enschede volgde. Na de middelbare school ging zij in 1998 Biomedische Technologie studeren aan de Technische Universiteit Eindhoven. Tijdens haar studie liep zij stage in het Orthopaedic Biomechanics Laboratory aan de University of California, Berkeley in de Verenigde Staten. Daar werkte ze aan de ontwikkeling van computermodellen om de sterkte van wervelschijven in patiënten met osteoporose te voorspellen. Tijdens haar afstudeerwerk ontwikkelde zij een model om botgroei vanuit de groeischijf te beschrijven. Na haar Master of Science te hebben behaald in 2004, besloot zij in dezelfde vakgroep haar promotieonderzoek te starten. Als onderdeel van haar promotie, heeft zij een jaar onderzoek gedaan in de Verenigde Staten, ditmaal in het Beth Israel Deaconess Medical Center, verbonden met Harvard Medical School in Boston.

